MRC Mammalian Genetics Unit

UNIVERSITY OF OXFORD

The role of ZNRF3 in testis determination

A thesis presented for the degree of Doctor of Philosophy (DPhil)

St Edmund Hall, University of Oxford

Abigail Lucy Harris

Mammalian Genetics Unit, MRC Harwell Institute

Department of Biochemistry, University of Oxford

Supervisors:

Dr Andy Greenfield

Professor Lynne Cox

Trinity Term 2017

Word Count: 43,271

Abstract

In mammals, the presence or absence of *SRY* primarily determines whether the gonad will develop as a testis or an ovary – a process known as sex determination. Downstream of *SRY*, the testis and ovarian pathways diverge and mutually antagonise each other to ensure a robust switch in gonadal fate. One such interaction is well characterised in mice, between the ovary-promoting gene, *Wnt4* and the testis-determining gene, *Fgf9*. The mutual repression of these two genes has recently been shown to be crucial for mouse sex determination. However, there is currently little evidence for how this interaction between the male and female pathways, and others required for sex determination, may be controlled at the molecular level.

Differences/disorders of sex development (DSDs) are a group of rare human conditions in which chromosomal and anatomical sex are discordant. Exome screens of DSD patients exhibiting gonadal dysgenesis can be used to identify candidate genes. In one such screen, 2 independent mutations were found in *ZNRF3.* ZNRF3 is a WNT-signalling antagonist which functions by downregulating the number of Frizzled receptors available on the plasma membrane. WNT4 is expressed in pregranulosa cells and plays a key role in ovarian development through promotion of β-catenin-dependent gene transcription. This thesis demonstrates that *Znrf3* plays an important role in testis determination in the mouse. *Znrf3* is required to suppress the ovarian-pathway, and when removed from the testis causes partial or full XY sex reversal associated with ectopic activation of WNT/ β-catenin signaling. Moreover, use of a sensitized genetic background allows generation of sex-reversed XY female mice carrying a single copy of a *Znrf3* null allele. ZNRF3 may therefore play a key role in mediating the mutually antagonistic interactions between the testis and ovarian pathways, in both mice and in humans.

Acknowledgements

First, I would like to thank my supervisor, Dr Andy Greenfield for the excellent support you have provided throughout my D.Phil. You have provided me with and guided me through an excellent PhD project, and have taught me what it means to be a good scientist. Thank you in particular for your help and guidance in the writing of this thesis.

Thanks must also go to the wonderful members of the Sexual Development group. Nick Warr has been instrumental in my development in the lab, and has often been a sounding-board for many ideas or problems. Thanks to Pam Siggers for sharing her wealth of knowledge about sexual development, and to Gwenn for teaching me cell-sorting and qRT-PCR. Special thanks also go to current and former students in the lab. Huge thanks go to Catherine Livermore who has helped me sustain a positive attitude in the worst of times, and has put up with me as her messy next-bench neighbour for several years. Maddy Pope was always willing to help in times of need and has been a supportive figure, even after leaving the lab. Thank you also to Joel May and Dani Sagar who have provided moral (and edible) support throughout my time in the lab. I'd also like to thank other members of the Development lab, in particular, Becca Walker, Jenny Keynton, Hannah Farley and Rosie Little who, along with the rest of the students at Harwell, have made it a fantastic 4 years!

I am extremely grateful for the support that MRC Harwell has provided. The Core services have been excellent, in particular the Histology team and Protein Core. My sincere gratitude also goes to the Mary Lyon Centre and all of its staff. Special thanks go to Sara Wells, Jackie Harrison, and Alison Gallop for your incredible knowledge of my colonies and for caring for all our mice. Thanks also goes to Jeremy Sanderson, for passing on a small fraction of your immense knowledge of microscopy and imaging, and also for your personal support in times of stress. Also thank you to the Molecular and Cellular Biology team for succeeding in producing my CRISPR/Cas9 mice, and to the Genotyping core.

Thank you to my wonderful family who have been so supportive, and have always been there for me in my times of need. Particular thanks go to my partner, Gavin. You have provided continual support, advice, encouragement and a steadfast belief in my abilities. Without you, I would not have had the brilliant opportunities MRC Harwell has provided, and I would not be the person I am today.

Finally, thank you to the Medical Research Council for funding this DPhil.

Table of contents

Abstract **3**

Acknowledgements **5**

Table of contents **7**

List of figures **13**

List of tables **15**

Abbreviations **17**

Tail Somite staging of embryos **19**

Chapter 1: Introduction **21**

1.0 MAMMALIAN SEX DETERMINATION AND THE BIPOTENTIAL GONAD 21

1.0.1 Early development of the gonad *21*

1.0.2 Cell types in the gonad: Common Origins *23*

1.0.3 SRY, SOX9, and testis determination *28*

1.0.4 The ovarian pathway *32*

1.0.5 Mutually antagonistic pathways *34*

1.1 WNT-SIGNALLING 35

1.1.1 Canonical WNT-signalling *36*

1.1.2 Non-Canonical WNT-signalling *38*

1.2 WNT-SIGNALLING IN THE MAMMALIAN GONAD 40

1.2.1 WNT4 ..... *40*

1.2.2 β-catenin *42*

1.2.3 R-spondin1 ..... *43*

1.2.4 Other WNT-signalling mutant gonadal phenotypes in mice *46*

1.3 MUTUALLY ANTAGONISTIC PATHWAYS: FGF9 AND WNT4 49

1.4 ZNRF3 AND RNF43 51

1.4.1 ZNRF3 and RNF43 are antagonists of WNT-signalling *51*

1.4.2 Structure *52*

1.4.3 ZNRF3-dependent WNT-signalling antagonism is R-spondin-sensitive *52*

1.4.4 The ZNRF3/R-spondin/LGR complex *53*

1.5 DIFFERENCES/DISORDERS OF SEX DEVELOPMENT 55

1.5.1 Exome sequencing to identify novel DSD genes *56*

1.5.2 Mouse Models of DSDs *57*

1.6 AIMS OF THESIS 59

Chapter 2: Materials and methods **61**

2.1 UNIVERSAL SOLUTIONS 61

2.2 MOUSE LINES AND GENOTYPING 61

2.2.1 Chromosomal sexing *61*

2.2.2 Znrf3^{flox} and Rnf43^{flox} *62*

2.2.3 Znrf3^{del} and Rnf43^{del} *62*
2.2.4 Znrf3$^{flox/flox}$, Ubiq-Cre-ERT2 ..... *63*
2.2.5 Znrf3^{R749G} *63*
2.2.6 B6.Y^{AKR} *64*
2.2.7 Gadd45g *64*
2.2.8 Sf1-EGFP *65*
2.3 TISSUE COLLECTION AND PROCESSING 65
2.3.1 WMISH *65*
2.3.2 qRT-PCR *66*
2.3.4 Staging embryos *66*
2.3.5 Immunohistochemistry *66*
2.3.5.1 Wax sections: Adult gonads 66
2.3.5.2 Wax sections: Embryonic gonads 66
2.3.5.3 Fresh Frozen sections: Embryonic gonads 66
2.3.6 Protein extraction for Western Blot *67*
2.3.7 Fluorescence-activated cell sorting (FACS) *67*
2.3.7.1 Theory 67
2.3.7.2 Tissue processing 68
2.4 EXPRESSION ANALYSES 69
2.4.1 Wholemount in-situ hybridisation (WMISH) *69*
2.4.1.1 RNA-probe synthesis 69
2.4.1.2 WMISH PROTOCOL 71
2.4.2 Immunofluorescence *73*
2.4.2.1 Protocol 1: SRY, SOX9 antibodies 73
2.4.2.2 Protocol 2: FOXL2, AMH antibodies 73
2.4.2.3 Protocol 3: PECAM, frozen sections 74
2.4.3 qRT-PCR *74*
2.4.3.1 RNA/DNA extraction 74
2.4.3.2 Reverse transcription 75
2.4.3.3 PCR Reaction 75
2.4.3.4 qRT-PCR Primer pairs 77
2.4.4 Optical Projection Tomography (OPT) *78*
2.4.4.1 Embedding and clearing 78
2.4.4.2 Calibration and Scanning 79
2.4.4.3 Reconstruction and Post-processing 79
2.4.5 Western Blot analysis *80*

Chapter 3: Characterisation of *Znrf3* and *Rnf43* expression in the embryonic mouse gonad..... 81
3.1. INTRODUCTION 81
3.1.1 Protein structure and isoforms *81*
3.1.2 Cell sorting rationale *84*
3.1.3. Aims *84*
3.2. RESULTS 86
3.2.1 Expression of Znrf3 and Rnf43 in the embryonic mouse gonad *86*
3.2.2 Expression of Znrf3 in a known sex-reversing mutant: Gadd45g *92*
3.2.3 Protein studies *94*
3.3 DISCUSSION 96

3.3.1 Znrf3, but not Rnf43, expression can be detected in the embryonic gonad at the sex-determining stage ... *96*
3.3.2 Sexually Dimorphic expression of Znrf3 ... *97*
3.3.3 Limitations of Microarray data ... *100*
3.3.4 Znrf3 expression in Gadd45g-null gonads ... *101*
3.3.5 How is Znrf3 transcriptionally regulated in the gonad? ... *102*
3.3.5.1 A direct role for SOX9? ... 102
3.3.5.2 Feedback loop ... 104
3.3.4 ZNRF3: detecting the protein ... *104*
3.3.6 Summary and further questions ... *105*

Chapter 4: The role of ZNRF3 in sex determination ... **107**
4.0 INTRODUCTION ... 107
4.0.1 Using gain- and loss-off-function alleles ... *107*
4.0.2 Analysing Primary Sex Reversal ... *109*
4.0.3 Rationale for using a sensitised background, B6.Y^{AKR} ... *111*
4.0.4 Compensation by homologous proteins ... *111*
4.0.5 Maintenance of testicular fate in the adult gonad ... *112*
4.0.6 Aims ... *114*
4.1. RESULTS ... 115
4.1.1 Generation of Znrf3 and Rnf43 null embryos ... *115*
4.1.2 Znrf3-null gonads show partial XY male-to-female sex reversal ... *119*
4.1.3 Loss of Znrf3 on B6.Y^{AKR} leads to full XY male-to-female gonadal sex reversal ... *122*
4.1.5 Stra8 expression in Znrf3 null gonads ... *123*
4.1.6 Loss of one allele of Znrf3 causes a range of sex reversal phenotypes in B6.YAKR adults ... *124*
4.1.7 Loss of Rnf43 does not affect primary sex determination ... *128*
4.1.8 Rnf43+/- B6.YAKR adults are phenotypically normal ... *129*
4.1.9 Loss of one copy of Rnf43 on a Znrf3-null B6 background does not significantly exacerbate the sex reversal phenotype ... *130*
4.1.10 Deletion of Znrf3 in the adult mouse testis has no phenotypic effect ... *133*
4.1.11 Summary of Results: Znrf3 is a testis-determining gene ... *136*
4.2. DISCUSSION ... 138
4.2.1 Znrf3 is a testis-determining gene ... *138*
4.2.2 The Znrf3 null allele ... *139*
4.2.3 Loss of Znrf3 on a sensitised background mimics human DSDs ... *140*
4.2.4 Variable penetrance of the sex reversal phenotypes ... *141*
4.2.5 A role for Znrf3 in germ cells? ... *141*
4.2.6 Rnf43 does not play a role in sex determination. ... *142*
4.2.7 Znrf3 does not play a role in maintaining testicular fate ... *143*

Chapter 5: Molecular Phenotyping of the *Znrf3*-null gonad ... **145**
5.0. INTRODUCTION ... 145
5.0.1. Aims ... *146*
5.1. RESULTS ... 147
5.1.1 Sry expression analysis ... *147*

5.1.2 Sox9 expression analysis *147*
5.2.3 Analysis of canonical WNT-signalling *151*
5.2.4 Ovarian marker gene expression *153*
5.2.5 Fgf9 expression *157*
5.2.6 Sf1, Wt1 and Oct4 expression *158*
5.2.6 Znrf3 expression *161*
5.2.7 Results Summary *162*
5.2. DISCUSSION 163
5.2.1 Znrf3 acts downstream of Sry *163*
5.2.2 Loss of Znrf3 promotes canonical WNT-signalling and Wnt4 expression in the XY gonad *164*
5.2.3 WNT/β-catenin signalling and Sox9 ..... *166*
5.2.4 WNT/β-catenin signalling and Wnt4 expression *167*
5.2.4 Other ovarian genes are upregulated in the Znrf3-null gonad *167*
5.2.5 Mutual antagonism: FGF9 and WNT4 ..... *168*
5.2.6 Znrf3 is upregulated in the Znrf3$^{-/-}$ gonad *170*
5.2.8 Concluding Remarks *170*

Chapter 6: Recapitulating a human *ZNRF3* mutation in the mouse 173
6.1 INTRODUCTION 173
6.1.1 Human mutations in ZNRF3 ..... *173*
6.1.2 CRISPR/Cas9 technology *175*
6.1.3 Strategy for generating mZnrf3 mutations *177*
6.2 RESULTS 178
6.2.1 Generation of the Znrf3^{R749G} allele *178*
6.2.2 Znrf3^{R749G} does not cause sex reversal in mice *179*
6.2.3 Znrf3^{R749G} does not cause sex reversal on a sensitised genetic background *183*
6.2.4 The Znrf3^{R749G} allele on a Znrf3-null background *184*
6.3 DISCUSSION 186
6.3.1 The R749G mutation does not cause a phenotype in mice *186*
6.3.1.1 Hypothesis 1: The R768G mutation disrupts hZNRF3 function, but R749G does not disrupt mZNRF3 187
6.3.1.2 Hypothesis 2: The R768G and R749G have equivalent disruptive effects in human and mouse ZNRF3, respectively 188
6.3.1.3 Hypothesis 3: Neither R768G, nor R749G, are causative 189
6.3.2 ZNRF3 evolutionary conservation: the 29nt deletion allele *190*
6.3.4 The unfolded protein response *191*
6.3.5 Genetic Background *192*
6.3.6 Limitations of CRISPR/Cas9 ..... *193*
6.3.7 Summary: The R749G mutation does not cause a phenotype in mice *194*

Chapter 7: Discussion 195
7.0 OVERVIEW 195
7.1 ZNRF3 AND THE TESTIS-DETERMINING PATHWAY 195
7.1.1 ZNRF3 regulates mutually antagonistic relationships in the embryonic gonad *196*
7.1.2 RSPO1 regulates WNT-signalling in the developing gonad through ZNRF3 ..... *197*
7.1.3 Summary: a model for the function of ZNRF3 in the testis-determining pathway *198*
7.2 WNT/β-CATENIN SIGNALLING AND SOX9 200

7.3 GENETIC BACKGROUND 201
7.4 VARIABILITY OF GONADAL PHENOTYPES 202
7.5 A ROLE FOR ZNRF3 IN GERM CELLS? 204
7.7 ALTERNATIVE MECHANISMS OF ZNRF3/RNF43 AND RSPO1 FUNCTION? 207
7.7.1 Rnf43 can suppress WNT/β-catenin signalling downstream of β-catenin 208
7.7.2 The role of Rspondins 209
7.8 DIFFERING ROLES OF ZNRF3 AND RNF43 211
7.9 GENOMIC CONTEXT: *KREMEN1* 212
7.10 THE USE OF MICE IN THE STUDY OF HUMAN DISEASE 213
7.11 FUTURE WORK 214
7.11.1 Further assessing expression of Znrf3: single cell transcriptomics 214
7.11.2 A role for Znrf3 in adults 215
7.11.4 The role of other WNT-ligands in the gonad 216
7.11.5 Investigating non-canonical WNT signalling 217
7.11.6 Frizzled Receptors 218
7.12 CLOSING REMARKS 219
References 221
Appendix 244

List of figures

Figure i. Tail somite staging of mouse embryos.	19
Figure 1.1 Position of the developing urogenital ridge in the 10.5 dpc embryo.	22
Figure 1.2 Cell types in the developing testis and ovary at 14.5 dpc.	24
Figure 1.3 The testis and ovarian pathways.	28
Figure 1.4 Summary of canonical WNT-signalling.	37
Figure 2.1 *Sf1*-eGFP gating for FACs.	68
Figure 2.2 OPT embedding of WMISH gonads.	78
Figure 3.1 Protein structure of ZNRF3.	84
Figure 3.2 Schematic showing the exon structure of *Znrf3* and the position of primers and probes used in this thesis.	85
Figure 3.3 *Znrf3* is expressed in the mouse gonad during the critical sex determining period.	89
Figure 3.4 *Znrf3*, but not *Rnf43*, can be detected in the mouse embryonic gonad.	91
Figure 3.5 Expression of *Znrf3* in the *Sf1-eGFP* positive cells.	93
Figure 3.6 Expression of *Znrf3* in *Gadd45g*-null gonads.	95
Figure 3.7 Western Blots using purified in-house antibodies.	97
Figure 3.8 Location of putative SOX9-binding sites near *Znrf3*.	105
Figure 4.1 Allele structure for *Znrf3* and *Rnf43*.	117
Figure 4.2 Gross embryonic and adult phenotypes of $Znrf3^{+/-}$ and $Znrf3^{-/-}$ mice.	120
Figure 4.3 Sex reversal phenotype in XY $Znrf3^{-/-}$ gonads.	123
Figure 4.4 Sex reversal phenotype in B6.Y^{AKR} $Znrf3^{+/-}$ and $Znrf3^{-/-}$ embryos.	125
Figure 4.5 *Stra8* expression in *Znrf3*-null gonads.	126
Figure 4.6 Sex reversal phenotype in adult B6.Y^{AKR} $Znrf3^{+/-}$ mice.	129
Figure 4.7 Histological analysis of adult B6.Y^{AKR} $Znrf3^{+/-}$ gonads.	130
Figure 4.8 WMISH analysis of 14.5 dpc *Rnf43*-null gonads.	131
Figure 4.9 WMISH analysis of B6.Y^{AKR} *Rnf43*-null gonads.	132
Figure 4.10 *Sox9* and *Stra8* expression in compound *Znrf3/Rnf43* mutant gonads	135
Figure 4.11 Tamoxifen dosing of adult $Znrf3^{flox}$ mice.	136
Figure 4.12 Analysis of $Znrf3^{flox/flox}$ adult mice.	138
Figure 4.13 Expression of $Znrf3^{del}$ and $Znrf3^{flox}$ transcripts in the adult gonad.	139
Figure 5.1 *Sry* expression in the $Znrf3^{-/-}$ gonad.	153
Figure 5.2 *Sox9* expression in $Znrf3^{-/-}$ gonads.	154
Figure 5.3 Expression of *Axin2* and *Lef1* in the $Znrf3^{-/-}$ gonad.	156
Figure 5.4 Expression of *Wnt4* in the $Znrf3^{-/-}$ gonad.	159
Figure 5.5 Expression of *Rspo1* and *Foxl2* in $Znrf3^{-/-}$ gonads.	160
Figure 5.6 Expression of *Fgf9* in the *Znrf3*-null gonad.	162
Figure 5.7 Expression of *Sf1*, *Wt1* and *Oct4* in the *Znrf3*-null gonad.	164
Figure 5.8 Expression of *Znrf3* in the $Znrf3^{-/-}$ gonad.	165
Figure 6.1 Position of two mutations in human *ZNRF3*.	178
Figure 6.2 Generation of the $Znrf3^{R749G}$ allele.	182

Figure 6.3 Analysis of *Znrf3*$^{R749G/R749G}$ embryos and adults.	185
Figure 6.4 29-nucleotide deletion allele of *Znrf3*.	187
Figure 6.5 Optical Project Tomography (OPT) scans of *Sox9* expression.	188
Figure 6.6 Analysis of adult *XY*^{AKR} *Znrf3*$^{R749G/R749G}$ reproductive tracts.	189
Figure 6.7 Analysis of the *Znrf3*^{R749G} allele on the *Znrf3* null background.	190
Figure 7.1 Models for the function of ZNRF3 in the sex determining pathway.	204
Figure 7.2 Reinforcement of cell fate in the gonad.	210
Figure S1. Cell lineage map of Single Cell Transcriptomic data.	249
Figure S2. Needleman-Wunsch alignment of mouse ZNRF3 and RNF43.	253
Figure S3. *Sox9* and *Foxl2* expression in adult *Znrf3*$^{flox/flox}$, *Ubiq-ERT2-Cre* mice.	255
Figure S4. Ratio of *Znrf3*^{flox} and *Znrf3*^{del} alleles in tamoxifen treated adult *Znrf3*$^{flox/flox}$, *Ubiq-ERT2-Cre* mice.	256
Figure S5. Sex reversal phenotype in XY *Znrf3*$^{-/-}$ gonads (early backcross).	257
Figure S6. Super Top-flash (STF) assay in HEK293T cells.	259
Figure S7. Anogenital distances and testis weights of *Znrf3*$^{R749G/R749G}$ B6 and B6.Y^{AKR} mice.	260
Figure S8. Alternative views of OPT visualisation of WMISH gonads showing *Sox9* expression.	261
Figure S9. Immunohistochemical analysis of expression of PECAM.	262
Figure S10. Total number of each age in tail somites (ts).	262

List of tables

Table i. Number of tail somites corresponding to each stage (dpc)	19
Table 1.1 Major components of the β-catenin destruction complex, and their roles.	38
Table 1.2 Examples of WNT molecules and their roles in gonadal development.	40
Table 1.3 Summary of mouse mutant phenotypes in the WNT-signalling pathway	45
Table 2.1 List of universal solutions	61
Table 2.2 Primers for gel-based genotyping assays	64
Table 2.3 List of primers used to generate WMISH probes and product sizes.	70
Table 2.4 Further details, WMISH probe synthesis	71
Table 2.5 List of primers used for qRT-PCR.	77
Table S1. List of P-values: *Znrf3* expression.	249
Table S2. Predicted weights of mutant and wild-type ZNRF3.	250
Table S3. List of P-values: *Gadd45g* null tissue.	251
Table S4. Total numbers of *Znrf3*$^{-/-}$, *Znrf3*$^{+/-}$ and *Znrf3*$^{+/+}$ embryos.	254
Table S5. List of P-values: Adult *Znrf3*$^{+/-}$ B6.Y^{AKR} anogenital distance and testis weights.	254
Table S6. List of P-values: Adult *Znrf3*$^{flox/flox}$, *Ubiq-ERT2-Cre* mice.	256
Table S7. List of P-values: 11.5 dpc and 12.5 dpc XY and XX *Znrf3*$^{+/+}$, and *XY Znrf3*$^{-/-}$ gonads.	258
Table S8. List of P-values: Anogenital distances and testis weights of *Znrf3*$^{R749G/R749G}$ B6 and B6.Y^{AKR} mice.	260

Abbreviations

AIS	Androgen insensitivity syndrome
ALC	Adult Leydig Cells
AMH	Anti-Müllerian Hormone
bp	Base pairs
Cas9	CRISPR associated, 9
CD	Campomelic dysplasia
cDNA	Complementary DNA
CGD	Complete gonadal dysgenesis
ChIP	Chromatin Immunoprecipitation
Ct	Cycle threshold
CKO	Conditional Knockout
CRISPR	Clustered Regularly Interspaced Short Palindromic Repeat
crRNAs	CRISPR RNAs
Dhh	Desert Hedgehog
DIG	Digoxygenin
DKO	Double Knockout
DMRT1	Double-sex and Mab-3 related Transcription factor 1
dpc	Days *post coitum*
d*pp*	Days *post partum*
DSD	Difference/Disorder of sex development
dsDNA	Double-stranded DNA
EDU	5-ethynyl-2'-deoxyuridine
eGFP	Enhanced GFP
EMT	Epithelial-to-mesenchymal transition
FACs	Fluorescence-associated cell sorting
FGF9	Fibroblast Growth factor 5
FISH	Fluorescence *in situ* hybridisation
FLB	Forelimb bud
FLC	Foetal Leydig cell
FOXL2	Forkhead Box L2
Fst	Follistatin
Fu1/2	Furin 1/2 domain
Fzd	Frizzled
GD	Gonadal Dysgenesis
gDNA	Genomic DNA
GFP	Green fluorescent protein
GOF	Gain-of-function
HDR	Homology directed repair
HE	Hindgut endoderm
H&E	Haematoxylin and Eosin
Het	Heterozygote

HF	Heart field
HLB	Hindlimb bud
Hom	Homozygote
HPRT1	Hypoxanthine phosphoribosyl transferase 1
Ihh	Indian Hedgehog
K_d	Dissociation Constant
LOF	Loss-of-function
MAPK	Mitogen activated protein kinase
N	Notochord
NHEJ	Non-Homologous End Joining
OPT	Optical Projection tomography
PA-domain	Protease-associated domain
PAM	Protospacer adjacent motif
PCR	Polymerase chain reaction
PFA	Paraformaldehyde
PGC	Primordial Germ cell
PK	Proteinase K
qRT-PCR	Quantitative reverse transcription PCR
RNA-seq	RNA sequencing
RNF43	Ring finger protein 43
RSPO	R-spondin
RT	Room temperature
SD	Standard deviation
SEM	Standard error of the mean
SFRP1/2	Secreted Frizzled-Related Protein 1/2
SF1	Steroidogenic factor 1
sgRNA	Single guide RNA
siRNA	Small interfering RNA
SOX9	SRY-box 9
SRY	Sex determining region Y
ssDONS	Single-stranded DNA oligonucleotides
TDF	Testis-determining factor
TES	Testis-specific enhancer of *Sox9*
TESCO	Testis-specific enhancer of *Sox9* Core
tracrRNA	Trans-activating crRNA
ts	Tail somites
TSS	Transcriptional start site
UGR	Urogenital ridge
UTR	Untranslated region
WMISH	Wholemount *in situ* hybridisation
WNT	Wingless-related integration site
WT	Wild-type
WT1	Wilms tumour suppressor 1
ZNRF3	Zing and Ring finger protein 3

Tail Somite staging of embryos

Throughout this thesis, the age of embryos will be described using "days post coitum" (dpc) and the number of tail somites for embryos between 11.0 dpc and approximately 12.5 dpc. This section aims to briefly orientate the reader.

Somites are blocks of tissue which form either side of the neural tube. They form in a regular fashion, which in the mouse, corresponds to approximately one every 2 hours (P. P. L. Tam 1981). This allows for staging to be carried out that is precisely accurate to within this short period of time. In embryos aged between 11.0 dpc and 12.5 dpc, somites are clearly visible in the tail region of the embryo. Somites posterior to the hindlimb of the embryo are therefore used to accurately stage the embryo (**Fig. i**).

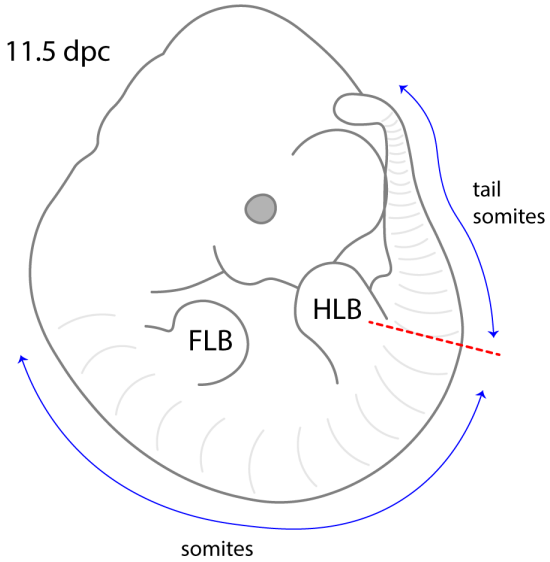

Figure i. Tail somite staging of mouse embryos. Somites that are posterior to the Hindlimb bud (HLB) are counted as tail somites. The diagram shows an 11.5 dpc embryo.

A guide to the relationship between the number of tail somites and the stage (dpc) of the embryo is briefly detailed below (**table i**).

Stage	11.0 dpc						11.5 dpc					
Tail somite number	9	10	11	12	13	14	15	16	17	18	19	20
Stage	**12.0 dpc**						**12.5 dpc**					
Tail somite number	21	22	23	24	25	26	27	28	29	30	31	32

Table i. Number of tail somites corresponding to each stage (dpc)

Chapter 1: Introduction

1.0 Mammalian sex determination and the bipotential gonad

In order to reproduce sexually, individuals must develop as either a male or a female. The term 'sexual development' encompasses the entire process of developing these specific characteristics, from fertilisation to reaching sexual maturity. In mammals, chromosomal sex is determined at fertilisation: the egg can either receive an X or a Y chromosome from the sperm and the resulting zygote will be XX or XY, respectively. When the gonad initially develops, its sexual fate is undetermined. At this stage, XX and XY gonads are morphologically and transcriptionally indistinguishable. Subsequently Primary Sex Determination usually leads to XY individuals developing testes and XX individuals, ovaries. The production of testosterone and Anti-Müllerian Hormone (AMH) by the testis then determines the internal and external sexual anatomy of males; their absence results in female structures (Swain and Lovell-Badge 1999).

1.0.1 Early development of the gonad

In mice, the urogenital system forms from the intermediate mesoderm just before 10 days post coitum (dpc). A thickening of the epithelial layer on the ventral surface of the mesonephros gives rise to the gonadal ridge. Cells in the newly formed coelomic epithelium proliferate and undergo an epithelial-to-mesenchymal transition (EMT). These cells migrate to form the body of the genital ridge, and will constitute some of the somatic cell lineages of the gonad.

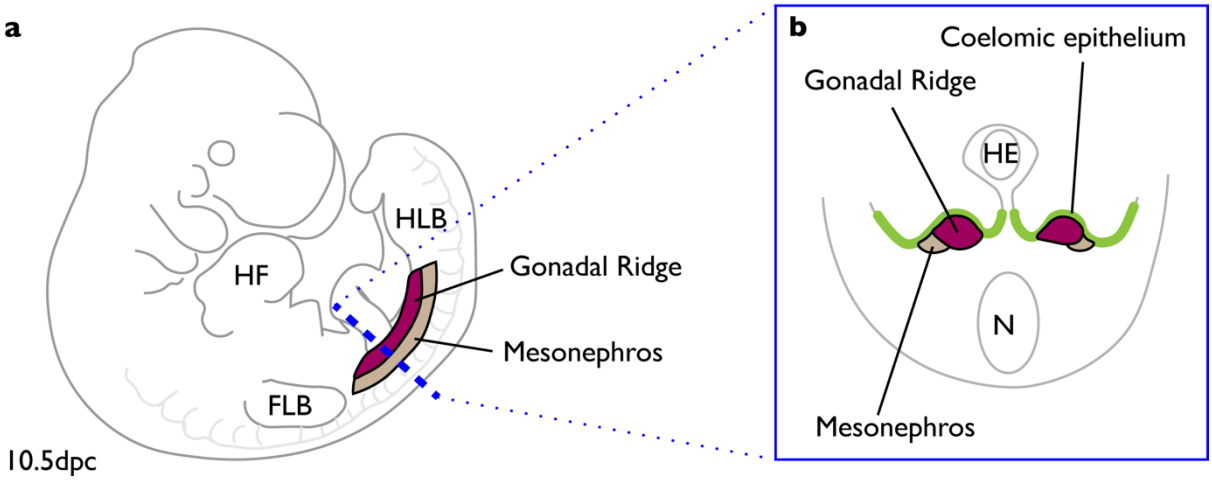

Figure 1.1 Position of the developing urogenital ridge in the 10.5 dpc embryo. The position of the gonadal ridge (red) and mesonephros (taupe) running along the dorsal body wall is shown in **(a)**. HF = Heart field, HLB = hindlimb bud, FLB = forelimb bud. The blue box **(b)** shows a cross section of the developing urogenital ridge, shown in in **(a)** using a blue dashed line. The gonadal ridge arises from a thickening of the coelomic epithelium (green) on the ventromedial surface of the mesonephros. N= notochord, HE = hindgut endoderm.

The genetic network which regulates this initial step in gonad formation has been well characterised through the use of mouse knockout models. Steroidogenic factor 1, (SF1, also known as NR5A1) is a nuclear receptor, and lies at the centre of this network. Gonads and adrenal glands are completely absent from *Sf1*$^{-/-}$ mice (X Luo, Ikeda, and Parker 1994). The genetic cascade which results in wildtype *Sf1* expression includes the genes *Wt1*, *Lhx9*, *Gata4* and *Cbx2*. *Wt1* null mice fail to form gonads or kidneys (Kreidberg et al. 1993) and *Lhx9* null mice have impaired gonad formation and importantly, fail to express *Sf1* (Westphal et al. 2000). WT1 and LHX9 cooperatively bind to the *Sf1* promoter to switch on its expression (Wilhelm and Englert 2002). When *Gata4* is conditionally deleted after 8.75 dpc, gonadal ridge formation is affected and expression of *Lhx9* and *Sf1* is reduced (Hu, Okumura, and Page 2013). *Cbx2* (also known as *M33*) null mice also have retarded gonadal ridge formation (Katoh-Fukui et al. 1998) and show reduced *Gata4*, *Lhx9* and *Sf1* expression (Katoh-Fukui et al. 2012). Therefore, these genes and several others that may yet be

undiscovered, play a crucial role in correctly regulating the expression of *Sf1*, which ultimately leads to the timely development of the early gonad.

After formation of the gonad, it is initially bipotential: it has the potential to become a testis or an ovary regardless of the sex chromosome complement. XY and XX gonads are transcriptionally indistinguishable until around 11.2 dpc (Nef et al. 2005; Munger et al. 2013) and morphologically indistinguishable until approximately a day later. Discussion of the developmental switch which leads to either testis or ovary formation is discussed below.

1.0.2 Cell types in the gonad: Common Origins

The gonad is made up of several cell types: supporting, steroidogenic, germ, and endothelial. Some of these lineages arise from the genital ridge, whereas others migrate into the gonad from elsewhere in the embryo, reviewed in Svingen and Koopman (2013). Each is bipotential and differentiates accordingly after primary sex determination. Subsequently, the gonad undergoes some major morphological changes that organise the different cell lineages into a characteristic pattern. This is detailed in **Fig. 1.2**, but will not be discussed further.

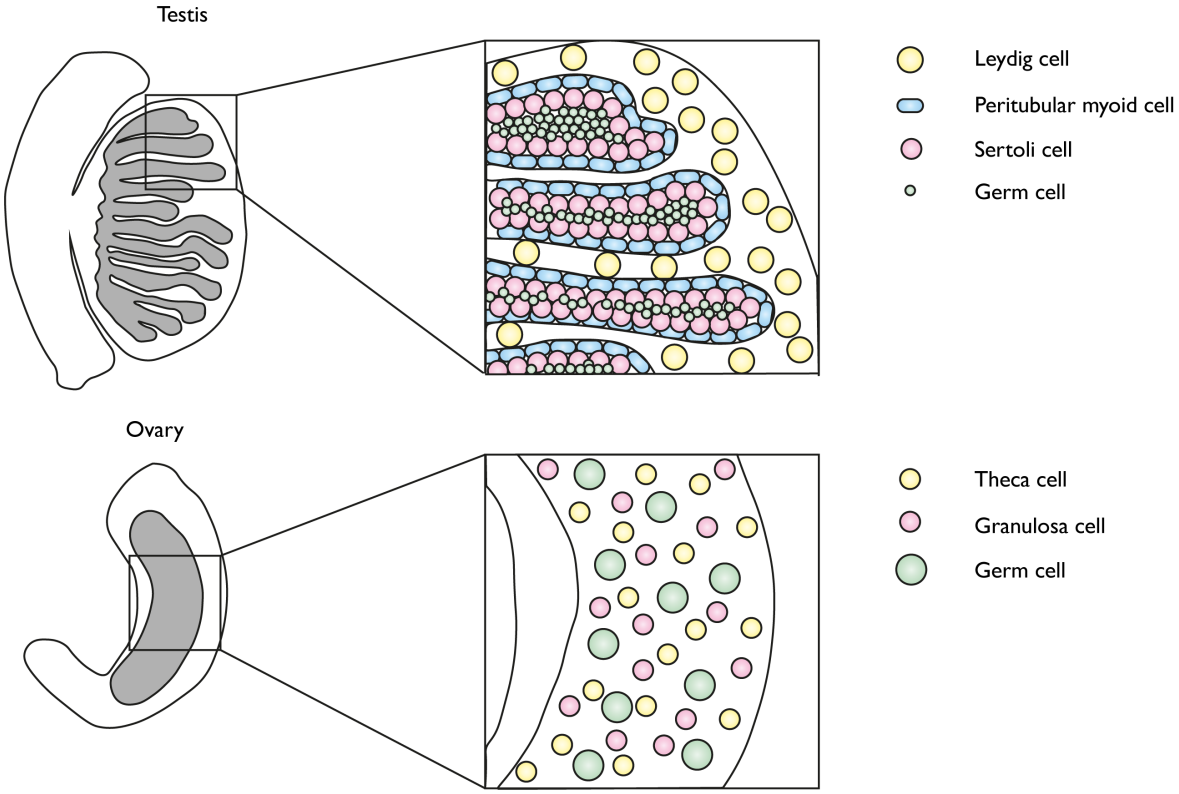

Figure 1.2 Cell types in the developing testis and ovary at 14.5 dpc. Leydig and theca cells (yellow) are a somatic cell lineage and are hormone producing. Sertoli and granulosa cells (pink) are somatic, and comprise the supporting cell lineage. Germ cells (green) will develop into spermatogonia in the testis, and ova in the ovary. Peritubular myoid cells (blue) are present only in the testis. Testes at this stage have an organised cord structure which consists of germ cells (green) surrounded by supporting Sertoli cells (pink), and a layer of Peritubular myoid cells. The interstitial Leydig cells (yellow) are excluded from the testis cord. Ovaries at this stage are relatively unstructured at the gross morphological level, and theca (yellow), granulosa (pink) and germ cells (green) are randomly distributed. Reviewed in Svingen and Koopman (2013).

The supporting cell lineage, which is somatic, is the sex-determining lineage of the gonad. In the testis, supporting cell precursors cells will differentiate into Sertoli cells, and in the ovary, into granulosa cells. In the adult testis, Sertoli cells control the microenvironment around germ cells, and allow them to mature into spermatozoa (M. D. Griswold 1998). In the ovary, granulosa cells surround the maturing oocyte and are responsible for the conversion of androgens to estradiol during folliculogenesis (Garzo and Dorrington 1984). Experiments using an *Sry* transgene suggest that Sertoli cells and granulosa cells are derived from the same population of somatic cell precursors (Albrecht and Eicher 2001). It is

important to note, however, that not all somatic cells in the early gonad are destined to become supporting cells; some will become steroidogenic cells or other interstitial cell-types.

Lineage tracing has shown that supporting cells originate in the coelomic epithelium and migrate into the body of the gonad in both sexes (Karl and Capel 1998). In chimeric gonads made up of XX and XY cells, a testis will be formed if more than 20% cells are XY. XX or XY cells can contribute to most cell lineages in the resulting testis regardless of their sex chromosome complement (Burgoyne et al. 1988). However, the supporting cell lineage in a XX/XY chimera will almost exclusively consist of XY cells (Burgoyne et al. 1988; Palmer and Burgoyne 1991). These experiments were the first to highlight the significance of the somatic cell lineage for testis determination, and indicates that the signal for male development may arise in the supporting cell lineage before being transmitted to the other lineages of the gonad. The nature of this signal will be discussed further in the following sections of this chapter (see section 1.0.4 - SRY, SOX9, and testis determination).

Primordial Germ cells (PGCs) will develop to form the gametes required for sexual reproduction. In mammals, PGCs arise in the extra-embryonic mesoderm at the base of the definitive primitive streak, at around 7.25 dpc (Ginsburg, Snow, and McLaren 1990). They migrate into the gonad, arriving between 10 dpc and 11.5 dpc. Once the germ cells arrive in the gonad they begin to differentiate into oocytes or prospermatogonia. There is evidence that the process of differentiation begins in the testis as early as 12.5 dpc: germ cells removed from the testis before, but not after, this time point can develop as oocytes in the correct context (A. McLaren and Southee 1997; Adams and McLaren 2002; Chuma and Nakatsuji 2001). Interestingly, the same is not true for XX germ cells at the same stage: they

can develop as either oocytes or spermatozoa when removed from the gonad at 12.5 dpc (Adams and McLaren 2002). Germ cells in the ovary begin to enter meiosis between 13.5 dpc and 15.5 dpc and arrest at prophase I (Anne McLaren 2000; Peters 1970). At the same time in the testis, XY germs cells cease proliferating and do not undergo meiosis, pausing as prospermatogonia. One key molecule in regulating this process is Retinoic acid (RA), which controls whether germ cells enter meiosis (J. Bowles 2006; Koubova et al. 2006). *Cyb26b1,* which encodes an enzyme which catabolises RA into inactive metabolites, is expressed in a testis-specific fashion at 13.5 dpc thereby ensuring RA activity in the ovary alone (Josephine Bowles, Bullejos, and Koopman 2000; Menke and Page 2002). This results in the sex-specific entry of XX germ cells into meiosis at this stage in gonadal development. In mammals, germ cells do not play a role in primary sex determination. It is well established that XY gonads depleted of germ cells can correctly specify the Sertoli cell fate and form testis cords (Buehr et al. 1993). Similarly, when germ cells are absent from the XX gonad, granulosa cells correctly express ovarian markers such as *Foxl2* (Maatouk et al. 2012).

The steroidogenic cell lineage is responsible for producing hormones during embryonic development and in adulthood. In the embryo, they are required for patterning the secondary sexual characteristics such as external genitalia, and internal reproductive tracts. In the ovary, steroidogenic precursors differentiate into theca cells. Theca cells are recruited to the developing ovarian follicle, and produce the androgen precursor that will be converted into oestrogen by the granulosa cells (Edson, Nagaraja, and Matzuk 2009). They arise mainly from a *Wt1*-positive cell population in the gonad, but a small contribution to the population is also made by Gli1-positive cells which migrate from the mesonephros (C.

Liu et al. 2015). Desert Hedgehog (*Dhh*) and Indian Hedgehog (*Ihh*) signalling, produced by surrounding granulosa cells, are key in theca cell development (C. Liu et al. 2015).

In the testis, the steroidogenic cells develop as Leydig cells which are located outside of the testis cords, in the interstitium, and produce androgens. Androgen production is critical for the formation of the male external genitalia, the Wolffian duct, and also for testicular descent (S. L. Griswold and Behringer 2009; Klonisch, Fowler, and Hombach-Klonisch 2004). In both rodents and humans there are two populations of Leydig cells: an embryonic or infantile population, and an adult population. In rats and mice, fetal Leydig cells (FLCs) are replaced soon after birth by adult Leydig cells (ALCs) (Roosen-Runge and Anderson 1959). In humans however, infantile Leydig cells (ILCs) are replaced with ALCs a few weeks after birth. In mice, fetal Leydig cells are specified at around 12.5 dpc when cords begin to form. The precise origins of both FLCs and ALCs in the gonad are currently undetermined, although it is likely that they come from multiple sources (reviewed in (Wen, Cheng, and Liu 2016)). It is also unknown whether the embryonic and adult lineages arise from the same precursor population. As in the ovary, DHH is crucial for specifying the steroidogenic cell fate. *Dhh* knockout gonads show significant reduction in numbers of FLCs at 13.5 dpc (H. H.-C. Yao, Whoriskey, and Capel 2002). DHH signalling from pre-Sertoli cells occurs through the Patched1 receptor and upregulates Sf1 and P450 Side Chain Cleavage enzyme expression to specify the Leydig cell fate (Yao, Whoriskey, and Capel 2002; Barsoum et al. 2009).

The cell lineages described above make up the main body of the gonad, and have been shown to have common origins in the testis and the ovary. However, several other cell types are also present and will be detailed briefly. The endothelial cell lineage is crucial for the developing structure of the testis. They arise from the mesonephros, migrate through the

body of the testis to form the coelomic vessel on the surface of the mesonephros. They also play a role in the developing testis cords of the testis. Peritubular myoid cells form the outer layer of the testis cord, but their origin is thus far unknown, partly owing to the lack of a reliable marker.

1.0.3 SRY, SOX9, and testis determination

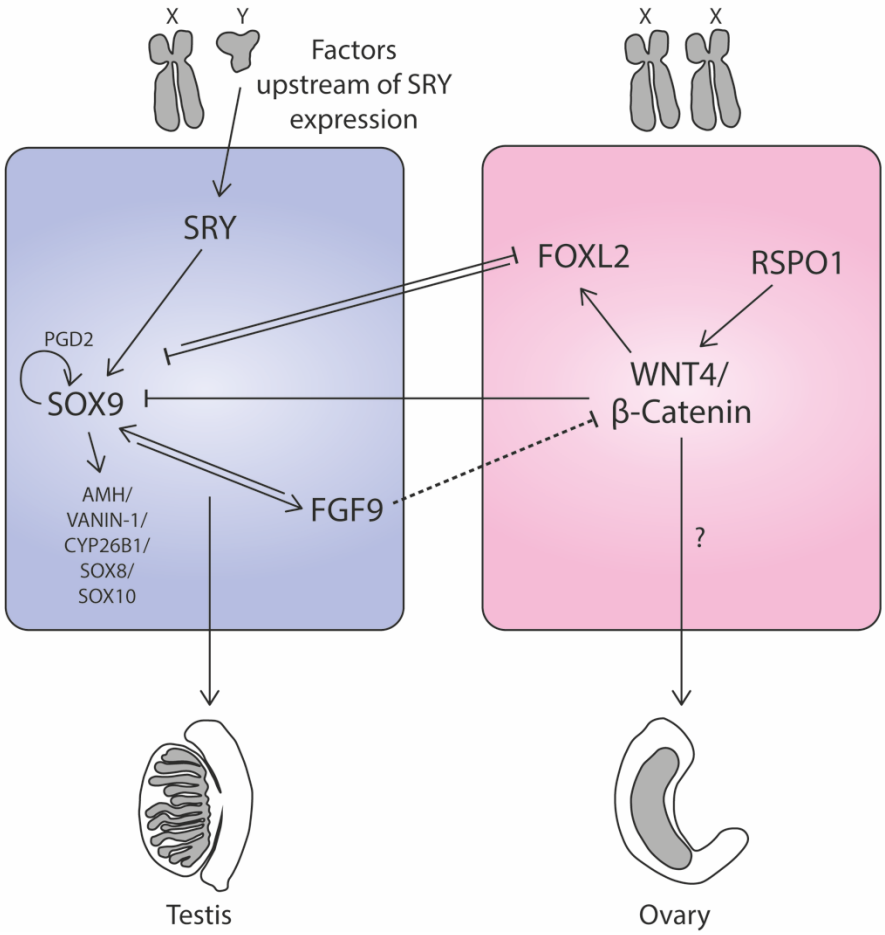

Figure 1.3 The testis and ovarian pathways. A summary of the key players involved in the development of the testis (purple) and the ovary (pink). Briefly, an XY individual carries a copy of SRY on the Y chromosome. This upregulates *SOX9* expression, which then acts upregulate downstream genes such as FGF9, and also to maintain its own expression. In an XX individual, where no SRY is present, ovarian genes such as *FOXL2*, *RSPO1* and *WNT4* predominate. There are mutually antagonistic interactions between these two pathways, for example between *SOX9* and *WNT4*, and *FOXL2* and *SOX9*. This diagram does not comprehensively cover all known interactions, and relies mainly on genetic studies, rather than known physical mechanistic interactions.

In mammals, the developmental switch between a testicular or ovarian fate is primarily determined by the presence or absence of the gene *SRY*, which is located on the Y-chromosome. The first evidence for the Y-chromosome's role in male sex determination was the discovery that the chromosomal complement of patients with Klinefelter's syndrome, who are male, is XXY (Jacobs and Strong 1959; Harnden and Stewart 1959). Subsequently, DNA hybridisation experiments were used to show the presence of small overlapping fragments of the Y-chromosome in 27 XX male individuals (Vergnaud et al. 1986), defining the region of the Y-chromosome on which the so-called Testis-determining Factor (*TDF* in humans, *Tdy* in mice) must lie. Further studies identified *SRY* as the *TDF/Tdy* in mice, and in humans (Gubbay et al. 1990; Sinclair et al. 1990). *SRY* expression was shown to be male-specific across a range of species, and was detected in testes, but not ovaries, in humans (Sinclair et al. 1990). Furthermore, the generation of a male XX mouse carrying an *Sry* transgene showed that *SRY* was sufficient for male sex determination. Although infertile, transgenic XX mice have testes and male external genitalia, indicating full sex reversal (Koopman et al. 1991).

As previously described, the supporting cell lineage is the sex-determining lineage in the gonad. In mice, *Sry* is expressed in XY supporting cells briefly between 10.5 dpc and 12.5 dpc. *Sry* must reach a threshold level of expression during this critical period for male sex determination to occur (Hiramatsu et al. 2008). Mutations which delay its expression, or reduce total levels of SRY, can therefore prevent the male pathway from being established, for example in *Gadd45g*-null mice (Warr et al. 2012; Johnen et al. 2013; Gierl et al. 2012). *Sry* expression begins at the centre of the gonad and spreads to the poles (Bullejos and Koopman 2005). This spatial expression profile therefore sensitises the poles of the gonad

to XY sex reversal. SRY is a transcription factor that contains a high-mobility group (HMG)-box. It initiates testis determination by acting on a related gene, *Sox9*. SRY binds a gonad-specific enhancer, TESCO (Testis-specific Enhancer of *Sox9* core), to activate its transcription. In order to bind and activate, SRY must cooperate with SF1, restricting the expression of *Sox9* to Sertoli cells (Sekido and Lovell-Badge 2008).

The role of SOX9 in sexual development is well defined in both humans and mice. Evidence for a role in sexual development even extends to vertebrates which do not have a copy of *SRY,* such as chickens (Kent et al. 1996). *SOX9* was first identified as a potential testis-determining gene in humans. Campomelic dysplasia is a disease characterised by defects in long bone formation amongst other skeletal defects, and a proportion of patients show male-to-female sex reversal (Unger, Scherer, and Superti-Furga 1993). Campomelic dysplasia was shown to be caused by mutations in *SOX9* (Foster et al. 1994). Furthermore, a case of female-to-male sex reversal was linked to a duplication of *SOX9* (Huang et al. 1999).

Subsequently, studies confirmed that *Sox9* is both necessary and sufficient for testis-determination in mice. Conditional deletion of *Sox9* in the mouse XY gonad at the critical sex determination period causes complete XY male-to-female sex reversal. These XY *Sox9* null gonads are phenotypically female, and express female marker genes such as *Wnt4* (F. Barrionuevo et al. 2006). Conversely, ectopic *Sox9* expression in the XX gonad causes female-to-male sex reversal. A *Sox9* transgene driven by the regulatory regions of *Wt1* was sufficient to cause the development of testes in XX mice. These XX testes express *Amh* and form testis cords. However, the cords are somewhat disorganised due to the absence of germ cells in the gonad. The male ducts are formed correctly, indicating the presence of

functional Sertoli cells (Vidal et al. 2001). This shows that *Sox9* is sufficient to drive testis determination in mice, even in the absence of *Sry*.

Although the role of *Sox9* in testis determination is well characterised, the direct downstream targets of this transcription factor are poorly understood. SOX9 binds to thousands of sites in the genome in the context of the embryonic gonads, many of which are genes that have a well-defined role in testis determination, for example *Dhh, Fgf9* and *Amh* (Rahmoun et al. 2017). Despite this comprehensive list of binding sites, it cannot be determined from these data whether genes are up- or downregulated as a direct result of this binding. Furthermore, the chromatin immunoprecipitation (ChIP) experiment may have missed weaker binding sites which may be equally important in testis determination. Therefore, although it is clear that SOX9 is a dominant player in the pro-testis pathway, the direct consequences of its presence on the transcriptional landscape of the Sertoli cell is not fully understood. *Sox9* expression is maintained in the gonad far beyond the critical window in which *Sry* is expressed. After SRY levels have fallen, a positive feedback loop subsequently maintains high levels of *Sox9* in Sertoli cells: SOX9 binds its own enhancer, together with SF1, to activate transcription (Sekido and Lovell-Badge 2008), and activity is maintained by Fibroblast Growth Factor 9 (FGF9).

FGF9 is initially detected in the gonad of both sexes at 11.5 dpc. Subsequently, it is down-regulated in XX gonads but maintained in XY gonads. By 12.5 dpc, FGF9 is seen on the surface of the gonad furthest from the mesonephros, and in the centre of cords (Kim et al. 2006). This sexually dimorphic pattern of expression is maintained at 13.5 dpc. FGF9 is not expressed in germ cells. *Fgf9*-null mice show full male-to-female sex reversal (Colvin et al. 2001). The role of FGF9 in the gonad is to maintain, but not initiate, *Sox9* expression in XY

Sertoli cells; *Sox9* is initially expressed in XY *Fgf9*-null gonads at around 11.5 dpc but is lost before 12.5 dpc (Kim et al. 2006). This loss of *Sox9* is due to the somatic cells of the gonad aborting the testis-determining pathway and switching on the ovarian pathway instead: loss of *Fgf9* does not increase the number of apoptotic cells in the gonad, so *Sox9* positive cells are not lost through cell death. *Wnt4*, an ovarian marker gene, can be detected at 12.5 dpc as *Sox9* expression is being lost. Cell and organ culture experiments have shown that exogenous FGF9 protein has the ability to directly upregulate expression of *Sox9* in the XX gonad (Colvin et al. 2001; Kim et al. 2006; Bogani et al. 2009).

The other lineages of the testis, including Leydig cells and germ cells, are thought to be masculinised by the signals from Sertoli cells, as previously described. During development, the XY gonad undergoes male-specific structural changes which results in the testis being morphologically distinct from the ovary around 48 hours after initial *SRY* expression. Cord structure is visible from about 12.25 dpc and cords are formed in part by the migration of endothelial cells from the mesonephros (Combes et al. 2009).

1.0.4 The ovarian pathway

For many years, the ovarian (female) pathway of development was thought of as the default pathway in the sense that, in the absence of SRY, the bipotential gonad would develop an ovarian fate. Indeed, there is some evidence that the bipotential gonad may be primed for the ovarian fate before sex determination (S. Jameson, Lin, and Capel 2012). The idea of a default pathway derives from the work of Alfred Jost, who removed the gonads from rabbit embryos to establish that phenotypic sex development is always female in the absence of gonads due to the absence of androgens: so his experiments are not strictly relevant to gonad development. Nevertheless, the identification of human XX males carrying mutations

in *RSPO1* and *WNT4* (Parma et al. 2006; Mandel et al. 2008), whilst crucially lacking *SRY*, indicated that the female pathway may play a more active role in sex determination. Although poorly defined in comparison with the testis-determining pathway, the key components in the genetic pathway in mice are understood to be the *Rspo1/Wnt4* pathway and *Foxl2*. Knocking out *Rspo1, Wnt4* or *Foxl2* causes partial female-to-male sex reversal. Both *Rspo1*$^{-/-}$ and *Wnt4*$^{-/-}$ mice develop a male-specific coelomic vessel, and delayed testis cords (Chassot et al. 2008; Vainio et al. 1999). Gonadal phenotypes of these mutants will be described in further detail below (see **section 1.2 - WNT-signalling in the mammalian gonad**).

Forkhead Box L2 (*Foxl2*) encodes a forkhead transcription factor. Expression can be detected as early as 12 dpc in the embryonic ovary. *Foxl2*$^{-/-}$ ovaries appear histologically normal at birth and only show a defect at two days (Ottolenghi et al. 2005), suggesting that it may not play a role in primary sex determination. However, after birth, granulosa cells are unable to mature leading to the breakdown of oocytes (Schmidt et al. 2004). FOXL2 is required for maintenance of ovarian fate of supporting cells (Uhlenhaut et al. 2009). On a molecular level, FOXL2 has been shown to directly regulate *Cyp19a1*, an enzyme which is responsible for the last step in the biosynthesis of oestrogen (Fleming et al. 2010; Pannetier et al. 2006). FOXL2 also regulates expression of follistatin (Fst). Loss of FST in mice appears to phenocopy *Foxl2* null gonads, perhaps suggesting that Fst is the primary target of FOXL2 (Yao et al. 2004).

Double knockouts have also been generated to investigate the consequence of losing both of these ovarian pathways. XX *Foxl2*$^{-/-}$, *Rspo1*$^{-/-}$ double knockouts (DKOs) develop a gonadal phenotype earlier in development and show a greater number of steroidogenic cells compared to *Rspo1* single knockouts (Auguste et al. 2011). Similarly, losing *Foxl2*

exacerbates the phenotype of *Wnt4* null gonads. Some male-specific genes such as *Dmrt1*, *Dmrt3*, *Ptdgs* and *Gdnt* are upregulated in the XX embryonic gonad only in *Foxl2*$^{-/-}$, *Wnt4*$^{-/-}$ mice, but are never detected in embryonic gonads when *Foxl2* or *Wnt4* are lost individually. *Foxl2*$^{-/-}$ gonads do express *Dmrt1* and *Sox9* but only one week postnatally. Furthermore, *Rspo1* expression appears to be independent of *Foxl2*, but *Foxl2* expression depends somewhat on the presence of RSPO1 (Auguste et al. 2011).

This, together with the delayed phenotypic consequence of loss of *Foxl2* alone suggests that *Foxl2* may be downstream of *Rspo1*/*Wnt4* signalling in the ovary. On the other hand, the fact that loss of *Foxl2* on an *Rspo1* or *Wnt4*-null background appears to sensitise the gonad to masculinisation is particularly intriguing, given that deleting *Foxl2* alone does not appear to have any effect on the embryonic gonad. *Wnt4*/*Rspo1* and *Foxl2* pathways may therefore synergise in the embryonic gonad to determine ovarian fate. The loss of *Foxl2* alone is not sufficient to cause primary sex reversal, perhaps due to compensation driven by the *Rspo1*/*Wnt4* pathway.

Therefore, the female pathway actively promotes the ovarian fate, and the loss of key genes in the ovarian network can lead to masculinisation of the gonad, even in the absence of any "male" genes (e.g. *Sry* or *Sox9*).

1.0.5 Mutually antagonistic pathways

Consistent with the idea that the female pathway plays an active role in sex determination, a mechanism of mutual antagonism between the ovarian and testis-determining pathways is now well defined. Components of the testis pathway have been shown to repress components of the ovarian pathway, and vice versa. This antagonism is played out both transcriptionally and post-transcriptionally. This mutual antagonism has been shown to be

critical in the sex determination pathway; indeed, it underlies the phenomenon of gonadal sex reversal.

An example of this is the antagonism between the *Rspo1*/*Wnt4*/β-catenin pathway and *Sox9*. *Wnt4* null XX gonads are masculinised and crucially transiently express *Sox9* (further described in Section 1.2.1 – WNT4), suggesting a repressive role for *Wnt4* in the ovary (Kim et al. 2006). Furthermore, there is convincing evidence that β-catenin, which is stabilised as a result of canonical WNT-signalling, is able to bind the enhancer of *Sox9* and inhibit its transcription (Bernard et al. 2012b). Conversely Wnt4 is expressed in sex-reversed XY *Sox9* null gonads (F. Barrionuevo et al. 2006). However, the mechanism in this case is unknown. FGF9 and WNT4 have also been shown to have a mutually repressive interaction, which will be discussed in detail below.

Antagonism between the two sex determining pathways is well characterised genetically, but currently there is minimal molecular evidence for direct inhibition. From this, we can conclude that there are proteins that actively repress the testis or ovarian pathway which play a key role in primary sex determination.

1.1 WNT-signalling

The WNT-signalling pathway constitutes a large proportion of the known pro-ovarian gene network. This section will outline the basic principles of the signalling pathway and describe the key components which will be critical for understanding this thesis. The WNT-signalling pathway is divergent and highly diverse. It has been implicated in an array of different systems; from cell polarisation to whole organ patterning, reviewed in (Logan and Nusse 2004). It is also an important signalling pathway in cell proliferation and is often deregulated

in cancer. WNT proteins are secreted glycosylated proteins that can act in a cell autonomous or on neighbouring cells. This well conserved signalling network can be segregated into two interdependent pathways: Canonical and Non-canonical, which will be detailed further below.

1.1.1 Canonical WNT-signalling

Canonical WNT-signalling ultimately results in the stabilisation of β-catenin, which is translocated to the nucleus and binds TCF/LEF. These co-transcription factors bind DNA and displace repressive Groucho proteins, activating the transcription of many downstream genes. The pathway is summarised below in **Fig. 1.4**. When a Frizzled receptor is unbound by a WNT molecule, the destruction complex (**Table 1.1**) is assembled. Therefore, when WNT molecules are absent, β-Catenin is phosphorylated by CK1 and ubiquitinated by β-TrCP. Ubiquitinated β-Catenin is then degraded via the proteasome.

Conversely, when a WNT molecule binds the Frizzled/LRP5/6 complex, Dishevelled (DVL) and AXIN are sequestered at the plasma membrane. AXIN is deactivated and Dishevelled activated by phosphorylation. Dishevelled inhibits GSK-3β, thereby stabilising β-catenin through the inhibition of its degradation. Some common downstream targets include *Axin2* and *Lef1* which are both often used as markers of canonical WNT-signalling (Jho et al. 2002; Filali et al. 2002).

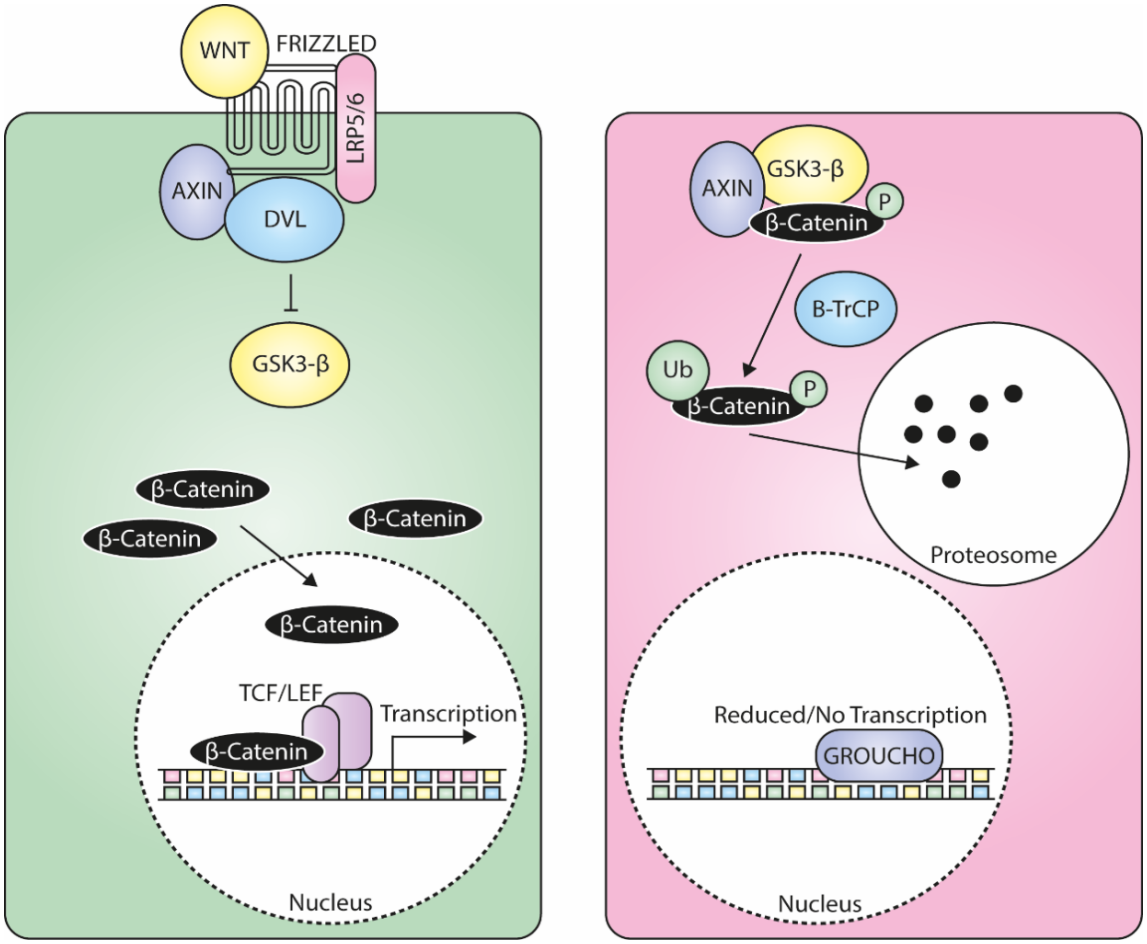

Figure 1.4 Summary of canonical WNT-signalling. When external WNT-molecules are present (**green**), WNT binds to the frizzled receptor, AXIN is sequestered at the plasma membrane alongside Dishevelled (DVL) and LRP5/6. This inhibits the formation of the destruction complex and therefore, the phosphorylation of β-catenin by GSK3-β. β-catenin therefore translocates into the nucleus and binds TCF/LEF to activate transcription. When no external WNT is present (**pink**), the destruction complex (see **table 1.1**) is assembled and β-catenin is phosphorylated by β-TrCP, and degraded in the proteasome. Groucho binds TCF/LEF binding sites on the DNA and inhibits transcription of target genes.

Destruction Complex component	Acronym	Role
AXIN	-	Scaffolding protein which binds other proteins in the complex, and β-catenin
Adenomatous Polyposis Coli	APC	Precise role is unknown
Glycogen Synthase Kinase 3 beta	GSK3-β	Phosphorylates β-catenin
Casein Kinase 1	CK1	Primes β-catenin for phosphorylation by GSK3, through phosphorylation of Ser45
Protein Phosphatase 2A	PP2A	Precise role is unknown

Table 1.1 Major components of the β-catenin destruction complex, and their roles. Adapted from (Kimelman and Xu 2006).

1.1.2 Non-Canonical WNT-signalling

Non-canonical WNT-signalling encompasses all WNT-driven pathways that are independent of β-catenin. Non-canonical signalling is involved in many aspects of vertebrate development, as well as playing a role in the maintenance of stem cells and in diseases such as cancer (Sugimura and Li 2010). Similar to canonical WNT-signalling, these pathways also require Frizzled receptors. The pathway diverges at Dishevelled (DVL) through the use of different domains of the protein: DIX, PDZ and DEP (Habas and Dawid 2005). When activated, the DIX and PDZ domains bind to Axin, which inhibits the destruction complex and leads to beta-catenin stabilisation, as described above. The DEP and PDZ domains collaborate to activate the small GTPases involved in non-canonical signalling (described below) (Sheldahl et al. 2003).

The PCP pathway was first identified in the fruitfly *Drosophila melanogaster* where it was shown to play a role in aligning the hairs on the imaginal wing disk (Gubb and García-Bellido 1982; Wong and Adler 1993). It is now implicated in many different processes involving coordinated cell extensions and movements within the same plane or cell polarisation, for

example roles in neural tube closure, gastrulation and stereocilia orientation. Briefly, Flamingo can recruit one of two transmembrane proteins; Frizzled (Fzd) or Van Gogh (Walck-Shannon and Hardin 2013). Fzd then recruits Dishevelled (Dsh), and signalling through this arm of the pathway is promoted by the cytoplasmic protein, Diego. If instead Van Gogh is present, Prickle is recruited. Prickle also inhibits signalling through the Fzd/Dsh/Diego pathway by competing with Diego for binding (Jenny et al. 2005). Van Gogh/Prickle and Fzd/Dsh/Diego are often located in opposing domains of the cell due to robust feedback mechanisms. The activated PCP pathway acts via small GTPases, RhoA and Rac1, to activate the JNK pathway (reviewed in (Schlessinger, Hall, and Tolwinski 2009)). This leads to rearrangements in the cytoskeleton but can also affect gene expression.

Another non-canonical WNT-pathway that has been well defined is the WNT/Ca^{2+} pathway. The activated Frizzled receptor cooperates with the co-receptor Ror1/2 to activate phospholipase C (PLC). PLC produces inositol 1,4,5-trisphosphate (IP_3) and diacyl glycerol (DAG) from phosphatidylinositol 4,5-bisphosphate (PIP2). IP_3 causes release of Calcium from the endoplasmic reticulum (ER), which in turn activates DAG. IP_3 also activates Calcineurin (Cn) and Cam kinase 3 (CamKII). Cn is responsible for activating a transcription factor, NFAT, which is able to translocate into the nucleus. CamKII activates TAK1 and NLK in the MAP-Kinase pathway and interestingly, antagonises the canonical signalling pathway (Ishitani et al. 2003). Activated DAG promotes Protein Kinase C activity (Sheldahl et al. 2003), which in turn activates NFkB and CREB. These transcription factors also translocate into the nucleus to regulate gene expression (Kohn and Moon 2005).

1.2 WNT-signalling in the mammalian gonad

There is strong evidence that *Wnt4*, β-catenin and R-*Spondin1* are required for the early development of the gonad in both humans and mice, and that they promote the ovarian pathway in the context of the mouse gonad. Various other WNT-signalling molecules have also been detected in the adult and embryonic gonad. Extensive profiling has not been carried out in the mouse embryonic gonad. However, analysis of the testes and ovaries of new-born pups shows expression of many non-canonical WNTs in the gonad, for example, WNT5a/b, WNT6 and WNT11. Expression of canonical WNTs such as WNT1, WNT3 and WNT8b is comparatively low (Kimura et al. 2006). Further evidence for expression of WNT signalling molecules in the mammalian gonad is summarised in the table below:

WNT molecule	Expression pattern	Reference
WNT1	Mouse: Post-meiotic germ cells in the testis, mouse	(Shackleford and Varmus 1987)
WNT3	Human: Adult testis	(Katoh 2001)
WNT4	Mouse: Somatic cells, female-specific	(Vainio et al. 1999; Jeays-Ward, Dandonneau, and Swain 2004)
WNT5a	Mouse: XY-specific expression in the testis, from e12.5 onwards	(Chawengsaksophak et al. 2012)
WNT7a	Mouse: Müllerian duct	(McMahon and Parr 1998)

Table 1.2 Examples of WNT molecules and their roles in gonadal development.

1.2.1 WNT4

WNT4 is the only WNT molecule thus far to be identified as critical for primary sex determination in mice and humans. Several human DSD patients have been identified with mutations in *WNT4*. Duplications in the region of Chromosome 1 carrying *WNT4* have been

associated with ambiguous genitalia in 46,XY patients (Elejalde et al. 1984; Wieacker et al. 1996). Furthermore, (Brian K. Jordan et al. 2001) confirmed that one of these patients did indeed have a duplication of the *WNT4* locus. Loss-of-function mutations have also been found in a consanguineous family where 3 aborted foetuses were analysed. At least one of these foetuses was shown to have a normal 46,XX karyotype and importantly, an absence of SRY, but histologically normal testes. The causative mutation was shown to reside in *WNT4* (Mandel et al. 2008).

Evidence for the importance of WNT4 in ovarian development also comes from studies in mice. *Wnt4* is expressed in both XY and XX mice as the gonad forms at around 10 dpc and is then upregulated in XX gonads as sex determination begins at around 11.5 dpc. It is maintained in the mesonephric mesenchyme of both sexes (Kim et al. 2006). Within the gonad itself, *Wnt4* is detected specifically in somatic cells and is maintained in the ovary throughout embryonic development (Vainio et al. 1999). Transcriptional targets of canonical WNT-signalling, such as *Axin2*, are also activated in a female-specific fashion and in the somatic cell lineage (Chassot et al. 2008).

Wnt4 plays a role in female fate specification in the mouse gonad. *Wnt4* $^{-/-}$ XX gonads are partially masculinised (Kim et al. 2006). They are more rounded than wildtype ovaries and are closely associated with a fat body, which is more typical of a testis. Ectopic expression of genes associated with male steroidogenesis is detected in the XX mutant gonad, including *3β-HSD* and *P450c17*. Activation of this pathway may explain the presence of the Wolffian duct in mutant XX mesonephroi. Despite a masculinised appearance and activation of a male biosynthetic pathway, *Wnt4* null embryonic gonads are correctly positioned, and external genitalia are normal at birth indicating that this female-to-male sex reversal is not complete.

XY *Wnt4* null gonads are unaffected: expression of *Dhh*, *3β-HSD*, and *Shh* is unaltered (Morel 1997).

1.2.2 β-catenin

As previously described, β-catenin is the primary target of canonical WNT-signalling. It is encoded by the gene *Ctnbb1*. Ablation of β-catenin in the somatic cell lineage of the mouse gonad, using *Sf1-Cre*, causes partial female-to-male sex reversal in a similar fashion to *Wnt4*-null gonads. Wolffian duct derivatives usually only seen in wildtype XY animals are present in the XX mutants, but external genitalia are indistinguishable from wildtype XX mice. Furthermore, as with wildtype ovaries, mutant XX gonads are located near the kidneys, and do not descend as in wildtype XY mice. XX *Sf1-Cre*, β-cat$^{flox/-}$ gonads also do not activate *Sox9* or *Fgf9*, which together with their positioning, suggests primary sex determination is hardly disrupted (Lui et al. 2009).

If removal of *Wnt4* or β-catenin from the gonad is sufficient to cause partial female-to-male sex reversal, it follows that activation of WNT-signalling may generate the opposite phenotype: male-to-female sex reversal. Maatouk et al. (2008) stabilised β-catenin specifically in the somatic cell lineage of the gonad. The *Ctnbb1$^{lox(ex3)}$* allele has LoxP sites flanking the 3rd exon of β-catenin. Exon 3 contains residues that are phosphorylated to direct its degradation. Therefore, when the LoxP sites are recombined, a stabilised form of β-catenin is expressed (Harada et al. 1999) and canonical WNT-signalling is upregulated. When this recombination is driven by *Sf1-Cre*, male-to-female sex reversal is seen in mice. At 3 weeks, XY β-cat$^{fl.ex3/+;}$ Sf1-cre external genitalia are indistinguishable from wildtype XX littermates. Gross morphology of the XY mutant reproductive tracts is also feminised: they have a uterus and vagina, and the gonads are positioned near the kidneys. Despite the

internal and external similarity to female anatomy, adult and embryonic gonads show significant histological differences from wildtype ovaries. Embryonic XY β-cat$^{fl.ex3/+}$; *Sf1-cre* gonads resemble wildtype testes in size and maintain a coelomic vessel. However, testis cord structure is completely absent. β-catenin stabilisation allows initial upregulation of *Sox9* and *AMH* but inhibits their maintenance. Therefore, stabilisation of β-catenin in the XY somatic cell lineage is sufficient to cause partial male-to-female sex reversal by inhibiting the maintenance of Sertoli cell fate.

1.2.3 *R-spondin1*

R-spondin1 (*Rspo1*) agonises WNT-signalling by allowing Frizzled receptors to accumulate on the plasma membrane (Hao et al. 2012). RSPO1 was first implicated in human sexual development when it was identified as the cause of female-to-male sex reversal in a large consanguineous Italian family (Parma et al. 2006). Through mapping, a homozygous single-nucleotide insertion was identified in exon 36 which results in a frameshift, and therefore a truncated protein. Due to the WNT-signalling agonising effect of R-spondin1, we might expect the sexual development phenotype of an *Rspo1* null mouse to be similar to the Wnt4 knockout mouse described above. Indeed, XX *Rspo1* null mice have masculinised external genitalia and internal reproductive tracts (A. Chassot et al. 2008). Adult gonads resemble small testes, and contain regions of cord structure alongside regions containing ovarian follicles. Female-specific genes, such as *Follistatin* (*Fst)* are downregulated. Male-specific genes, such as *Ptdgs*, *Sox9* and *AMH*, alongside genes involved in the testosterone biosynthesis (*Cyp11α1* and *Hsd17β3*), can be detected in XX mutant gonads. Sex reversal is not complete, however, and XX *Rspo1*$^{-/-}$ somatic cells partially retain an ovarian identity. Female markers *Foxl2* and *Bmp2* can still be detected in the gonad, as in *Wnt4*$^{-/-}$ gonads.

Intriguingly, canonical WNT-signalling appears to be more severely affected in *Rspo1*$^{-/-}$ gonads compared to *Wnt4*$^{-/-}$ gonads where residual canonical transcriptional target activation is detected. This suggests that *Rspo1* may be acting on other WNT-signalling pathways that are thus far not known to play a role in sexual development.

In summary, WNT-signalling, and in particular the Wnt4/β-catenin pathway, has been shown to play a major role in ovary development. However, even in the most severe cases, sex-reversal is not complete. This may suggest some redundancy in the pathway. In the case of the *Wnt4* null phenotype, the lack of full sex reversal could be due to other WNT molecules acting redundantly. However, this logic does not hold for the β-catenin stabilisation model. Perhaps the stabilisation was not complete, or sufficient, or perhaps other non-canonical pathways could lead to a partial rescue of the sex-reversal phenotype.

Alternatively, WNT signalling may synergise with other signalling pathways/molecules to effect ovary development. The absence of early XX gonadal sex reversal may also simply reflect a more complex set of cellular and molecular mechanisms at play during ovary development than in testis development.

Mutant		Reference	Effect on WNT-signalling	Phenotype
Wnt4 null	global	(Vainio et al. 1999)	↓ (Wnt4-specific only)	Partial female-to-male sex reversal XX mutant: no Müllerian duct, persistent Wolffian duct, coelomic vessel present ectopic expression of male steroidogenesis genes ovaries correctly positioned, but more rounded
β-catenin null	*Sf1-Cre*	(C.-F. Liu et al. 2009)	↓ canonical WNT-signalling	Partial female-to-male sex reversal XX mutant: XX external genitalia unaffected Wolffian duct derivatives present: epididymis and vas deferens no *Sox9* or *Fgf9* activation
β-catenin stabilisation	*Sf1-Cre*	(Maatouk et al. 2008)	↑ canonical WNT-signalling	Male-to-female sex reversal XY mutants: uterus and vagina external genitalia indistinguishable from XX WT ovarian positioning of gonads, but coelomic vessel present rapid decrease in *Sox9* expression from 11.5 dpc onward
Rspo1 null	global	(A. Chassot et al. 2008)	↓	Partial female-to-male sex reversal XX mutants: masculinised external genitalia Wolffian duct derivatives present: vas deferens, small seminal vesicles adult ovotestis histology: some cord structure, some ovarian follicles *FoxL2* and *Bmp2* still detected

Table 1.3 Summary of mouse mutant phenotypes in the WNT-signalling pathway

1.2.4 Other WNT-signalling mutant gonadal phenotypes in mice

Several other molecules which play a role in canonical and non-canonical WNT-signalling have been analysed for gonadal phenotypes in the mouse. These included WNT molecules, as well as modifiers of WNT signalling. Two examples of cases where a gonadal phenotype is detected include mice lacking *Wnt5a* and Secreted Frizzled-related proteins 1 and 2 (*Sfrp1*, *Sfrp2*) double knockout mice.

SFRP1 and SFRP2 are antagonists of WNT-signalling (Jones and Jomary 2002; Kawano and Kypta 2003). They are secreted by the cell and compete with WNT-ligands for Frizzled receptor binding, to downregulate WNT-signalling (S. Wang et al. 1997; Leyns et al. 1997; Dann et al. 2001). When these two related proteins are knocked out individually in mice, there is minimal phenotypic impact. *Sfrp1*$^{-/-}$ animals are viable and fertile, and *Sfrp2*$^{-/-}$ animals occasionally have syndactyl but are otherwise unaffected.

Doubly homozygous mice die at around 16.5 dpc and have a gonadal phenotype. XY mutants have significantly smaller testes compared to wildtype littermates as adults. In XY *Sfrp1*$^{-/-}$, *Sfrp2*$^{-/-}$ embryos, gonads are closely associated with the kidneys compared to wildtypes which are located more posteriorly in the embryo. Embryonic testes are significantly smaller, and have fewer cords. However, there is good evidence that all of the requisite cell lineages are correctly determined in the double knockout testis: robust *Sox9* expression shows the presence of somatic cells which have correctly undergone sex determination; 3β-HSD can be detected at 13.5 dpc indicating functioning steroidogenic cells; *Oct4* expression levels were similar in mutants compared to wildtype indicating the presence of germ cells. Furthermore, *Jag1* was detected indicating the presence of the male-specific coelomic vessel. There are also no significant differences in proliferation at 11.5 dpc, and migration

of endothelial cells from the mesonephros is not effected. However, the region of the gonadal ridge which expresses *Sf1* is markedly reduced at 10.5 dpc (Warr et al. 2008). Taken together, this indicates that *Sfrp1* and *Sfrp2* are not required for primary sex determination. However, they may be involved in the early patterning of the gonadal ridge, and transabdominal descent of the testis to the correct position during embryonic development.

Interestingly, *Wnt5a*-null gonads phenocopy the *Sfrp1*$^{-/-}$, *Sfrp2*$^{-/-}$ mutant phenotype. *Wnt5a* signals through the previously described non-canonical WNT-signalling pathway (Oishi et al. 2003; Schambony and Wedlich 2007). In contrast to *Wnt4*, *Wnt5a* is expressed in a male-specific fashion from 12.5 dpc onwards. Its absence from the gonad at the point of primary sex determination is good evidence that it is not required for this process. Interestingly, expression appears to be highest in the ventral portion of the gonad, furthest from the mesonephros, and is concentrated outside of the testis cords (Chawengsaksophak et al. 2012). Testes are small and are incorrectly positioned at 15.5 dpc (Warr et al. 2008). Levels of *Sox9* and *Amh* expression were no different in the *Wnt5a*$^{-/-}$ gonads compared to wildtype controls, and gross structures such as testis cords and the coelomic vessel are unaffected (Chawengsaksophak et al. 2012). However, there is a significant reduction in the number of germ cells in mutant gonads. No significant difference in proliferation or apoptosis is detected in *Wnt5a*$^{-/-}$ mutant gonads. Germs cells are also correctly specified at 7.5 dpc. The germ cell phenotype is instead due to defective migration of primordial germ cells (PGCs) into the gonad. Ectopic germ cells can be detected in the gut mesenchyme and the skin (Chawengsaksophak et al. 2012).

This evidence appears to suggest that only specific WNT molecules play a role in primary sex determination. It also implies that WNT-signalling, and more specifically non-canonical

WNT-signalling, may be involved in other morphological processes during testis development such as germ cell migration, and testicular descent. Another hypothesis, however, is that there is major redundancy in these pathways and other related molecules are able to compensate for the loss of another. Phenotypes may only be detected when multiple players in the pathways are eliminated.

1.3 Mutually Antagonistic Pathways: FGF9 and WNT4

As previously described, *Fgf9* is a pro-testis gene which, when disrupted, causes male-to-female sex reversal. *Wnt4* is a pro-ovarian gene. Recently, it has been shown that *Wnt4* and *Fgf9* sit in opposing pathways and act to supress each other. The relationship between FGF9 and WNT4 has been thoroughly scrutinised recently in genetic studies which utilise a mouse double knockout. The first evidence for a mutually repressive interaction was the observation that both genes were reciprocally upregulated in the knockout of the other gene: *Wnt4* expression is upregulated in *Fgf9*-null testes at e12.5 in the mouse, but is not present in wildtype littermates and FGF9 protein levels are increased in *Wnt4*-null gonads compared to wildtype (Colvin et al. 2001; Kim et al. 2006).

One striking hypothesis is that *FGF9* acts as a pro-testis gene solely through the suppression of WNT4. If this is the case, FGF9 should not be required in the context of a testis when no WNT4 is present to be downregulated. XY *Fgf9*$^{-/-}$ mice are fully sex reversed and upregulate several ovarian genes including *Wnt4*, *Rspo1* and *Foxl2* (Colvin et al. 2001; Jameson, Lin, and Capel 2012); levels of expression in XY *Fgf9*-null gonads are comparable to XX wildtype ovaries. Deleting *Wnt4*, to generate *Fgf9*$^{-/-}$, *Wnt4*$^{-/-}$ double knockouts, rescues the sex reversal phenotype. These *Fgf9* and *Wnt4* null gonads express male-specific SOX9, which is seen only sporadically in *Fgf9* nulls, and AMH, which is never detected in *Fgf9*$^{-/-}$ gonads. Deleting *Wnt4* also rescues the *Fgf9* null ovarian morphology, and double knockouts form testis cords containing correctly specified male germ cells. Leydig cells are also detected using the marker 3β-HSD. In this way, removing *Wnt4* on an *Fgf9* null background fully rescues the male-to-female sex reversal phenotype, suggesting that the primary role of FGF9 is to downregulate *Wnt4* (Jameson, Lin, and Capel 2012).

Interestingly, the same is not true for the reverse situation. When XX *Fgf9*$^{-/-}$, *Wnt4*$^{-/-}$ gonads are generated, a coelomic vessel and ectopic steroidogenic cells can still be detected similar to XX *Wnt4* null gonads (Jameson, Lin, and Capel 2012). However, as previously described, WNT4 does act indirectly to downregulate FGF9 protein levels, as shown by elevated FGF9 in *Wnt4*$^{-/-}$ gonads (Kim et al. 2006). Therefore, the role of *Wnt4* in the ovary extends beyond just suppression of FGF9.

Both WNT4 and FGF9 are secreted signalling molecules that have never been reported to physically interact, and therefore it is unlikely that this repressive interaction is direct. It is therefore likely that there are genes that are currently unknown in the sex determining pathway which may bridge this molecular gap. For example, a gene which was upregulated by FGF9 signalling, directly or indirectly, and which acted to antagonise WNT-signalling could mechanistically explain this genetic antagonism.

1.4 ZNRF3 and RNF43

1.4.1 ZNRF3 and RNF43 are antagonists of WNT-signalling

ZNRF3 (Zinc and Ring Finger protein 3) and *RNF43* (Ring Finger protein 43) are two homologous genes that were identified in a primary tissue microarray screen. Both were found to positively correlate with *AXIN2* mRNA, which is down-stream of canonical WNT-signalling. Furthermore, *Znrf3* and *Rnf43* expression was stimulated in mouse embryonic fibroblasts when cultured in Wnt3a-conditioned medium. ZNRF3 and RNF43 are both localised to the plasma membrane and are E3-Ubiquitin ligases (Hao et al. 2012). There is strong evidence that both proteins act to downregulate WNT-signalling by ubiquitinating Frizzled (FZD) receptors and removing them from the cell surface.

ZNRF3. Hao et al. (2012) showed that *ZNRF3* knockdown by siRNA increased levels of Myc-FZD4, Myc-FZD5, Myc-FZD8, and endogenous FZD6 on the plasma membrane. Conversely, a decrease of surface Myc-FZD8 was seen in cells overexpressing wildtype ZNRF3. Levels of a non-ubiquitinatable form of FZD4, in which all intracellular lysines have been mutated to alanines, were not increased upon *ZNRF3* siRNA knockdown. Together, this evidence suggests ZNRF3 removes FZD receptors from the plasma membrane, and that ubiquitination is critical for this process.

RNF43. (Koo et al. 2012) showed that a SNAP-tagged FZD5 receptor was lysosomally degraded in an RNF43-dependent manner; FZD5 colocalised with lysosomal marker CD63 upon *RNF43* expression. Furthermore, inhibiting lysosomal function leads to an accumulation of ubiquitinated FZD5, suggesting turnover of the protein was being prevented. Turnover of the FZD5 was increased in vitro upon co-expression of *RNF43*. This

was measured by a decreased level of mature, glycosylated FZD5, while the immature form of the protein remained constant. Increased turnover was not detected when a non-ubiquitinatable form of FZD5 was used, suggesting ubiquitination is critical for this process. A functioning RING finger domain of RNF43 was also required (Koo et al. 2012).

In this way, ZNRF3/RNF43 desensitise the cell to WNT ligands by removing Frizzled receptors from the plasma membrane. ZNRF3 and RNF43 are commonly part of a negative feedback loop in the WNT-signalling pathway and act to maintain steady-state levels of Frizzled receptors on the cell surface.

1.4.2 Structure

ZNRF3 and RNF43 are structurally similar proteins. As previously described, both are membrane bound, and have an intracellular ring finger domain which is responsible for their E3-Ubiquitin ligase function (Hao et al. 2012). A crystal structure has been solved for the ectodomains of ZNRF3 and RNF43, although the internal region has not been well characterised (Zebisch and Jones 2015). Further discussion of the structure of the two proteins can be found in Chapter 3.

1.4.3 ZNRF3-dependent WNT-signalling antagonism is R-spondin-sensitive

ZNRF3 and RNF43 appear to be the primary targets of R-spondin proteins. A mutant form of ZNRF3 is able to suppress Wnt-signalling but cannot bind RSPO proteins. When this mutant protein was introduced in vitro on a *Znrf3* null background, RSPO2 was unable to stimulate Wnt-signalling activity, suggesting ZNRF3 is the primary target (Xie et al. 2013). Significantly for this thesis, RSPO1 has been shown to agonise WNT-signalling in the context of the gonad.

As discussed previously, XX *Rspo1*$^{-/-}$ gonads show partial female-to-male sex reversal (Chassot et al. 2008) and so ZNRF3, one of the primary targets of R-spondins, may also play a role in sex determination.

1.4.4 The ZNRF3/R-spondin/LGR complex

ZNRF3/RNF43 forms a ternary complex with an R-spondin and LGR4/5. The complex is endocytosed, removing ZNRF3/RNF43 from the membrane. This releases the inhibition on WNT-signalling by allowing the plasma membrane to be repopulated with frizzled receptors.

Several studies have analysed the interactions within the complex for both ZNRF3 and RNF43. Both proteins appear to interact in a similar way despite low sequence homology of the ectodomains (~40%, (Xie et al. 2013)). R-spondins act as a bridge between ZNRF3/RNF43 and LGR receptor. ZNRF3 interacts modestly with RSPO1 alone (Kd = 0.8uM, surface plasma resonance, (Xie et al. 2013)). Similarly, the RNF43/RSPO1 interaction was also measured to be weak (7-10uM, Isothermal titration calorimetry). However, the interaction between RNF43 and a pre-formed complex of Rspo1/LGR5 is comparatively strong (0.5uM, (Chen et al. 2013)). Rspo1 and LGR4/5 interaction is also very strong (0.008uM, (Xie et al. 2013)). Taken together, these data suggest that R-spondins are complex assemblers.

In R-spondins, the Furin domains are the critical regions for interaction within the complex. The Furin domain 1 (Fu1) of RSPO1 interacts with ZNRF3, and Furin domain 2 (Fu2) with LGR4/5. Different R-spondins have different affinities for ZNRF3, RSPO2 having the strongest (Zebisch and Jones 2015). Both of these domains are required for R-spondin to activate Wnt-signalling (Xie et al. 2013), suggesting the formation of the ternary complex is critical for the ubiquitination abilities of ZNRF3/RNF43. RSPO1 binds to RNF43 through a “met” domain which protrudes from the ectodomain of RSPO1. A shallow groove in the PA domain of

RNF43 accepts and binds to the “met” domain. Sequence similarity between PA domains suggests ZNRF3 may interact in a similar way (Chen et al. 2013). One interesting difference between ZNRF3 and RNF43 is the propensity for ZNRF3 to form a complex with a 2:2:2 stoichiometry in solution (Zebisch and Jones 2015). The phenomenon was detected for RNF43 (Chen et al. 2013), but not in conditions that were deemed physiologically relevant.

1.5 Differences/disorders of Sex Development

The term Differences (or disorders) of Sex Development (DSDs) encompasses a wide range of congenital conditions which are defined by a discrepancy between a patient's chromosomal, gonadal or anatomical sex (Hughes et al. 2006). An epidemiological study in Germany found the incidence of ambiguous genitalia at birth as approximately 2:10,000 (Thyen et al. 2006). However, DSDs in patients can be identified at birth or later in life, when puberty does not progress as expected and therefore DSDs may be as common as 1:1000 (Ostrer 2014). Furthermore, DSDs vary greatly in their severity: from minor abnormalities in genitalia to the complete absence of gonads, which often makes it difficult to appropriately classify.

DSDs can be classified in the following groups: Sex Chromosome DSDs; 46,XY DSDs; and 46,XX DSDs, reviewed in Hughes et al. (2006). Sex Chromosome disorders comprise cases where chromosome numbers are abnormal, including Turner syndrome (45,X), Klinefelter syndrome (47,XXY), as well as chimeric disorders (45,X/46,XY or 46,XX/46,XY). 46,XY and 46,XX patients, on the other hand, have a normal complement of 46 chromosomes. In these cases, DSDs can be further classified based on whether the gonadal or anatomical abnormalities are due to a failure of primary sex determination, or a failure to produce or respond to specific sex hormones as in Androgen insensitivity disorder (AIS). In AIS, patients carry a mutation in the androgen receptor. They undergo normal primary sex determination, develop testes and produce androgen, but develop female anatomical characteristics as they are unable to respond to the androgens produced. This thesis will focus on Disorders of Sexual Development caused by abnormalities in primary sex determination, specifically 46,XY gonadal dysgenesis (GD) and 46,XX testicular DSD.

1.5.1 Exome sequencing to identify novel DSD genes

The exome can be defined as the subset of the genome which is protein coding. In some cases, this definition is extended to include genomic regions which code for non-coding RNA elements, such as micro-RNA or long intergenic non-coding RNA. Exome sequencing is a method which uses a targeted approach to identifying mutations within this portion of the genome. This method can be used to identify novel mutations in Mendelian disorders.

The most common method of exome capture is the aqueous-phase, capture-by-hybridisation method reviewed in (Bamshad et al. 2011). Briefly, genomic DNA (gDNA) is randomly sheared and an adaptor-labelled library is generated. In order to enrich for exonic DNA, biotinylated RNA or DNA fragments are used as baits. After hybridisation, streptavidin is used to pull down these fragments which are then amplified and sequenced. Mapping of the fragments to a reference is followed by analysis to identify potentially pathogenic mutations. Mutations which may be of interest can then be narrowed down using a range of techniques. Discrete filtering can eliminate common polymorphisms that have been identified in publicly available databases, as these are unlikely to be causative given that they are identified in unaffected individuals. Use of pedigree information, for example, sequencing parent-child trios can be effective. Furthermore, when screening an affected population, individuals can be pre-eliminated if they carry a mutation in a known causative gene which increases the likelihood of a novel finding. After filtering has been applied, further analysis of individual mutations allows us to predict the likelihood that it is deleterious to the protein product and therefore whether it may be pathogenic.

One obvious limitation of using exome screening as a method for gene discovery is the inability to pick up mutations outside of the protein coding regions of the genome. However,

despite only 2% of the genome predicted to be coding, exome screening is able to successfully identify between 25% and 50% of likely-causative mutations in patients with an unknown genetic disorder (Yang et al. 2013; Beaulieu et al. 2014). Cases in which potentially causative mutations were not found could be due to mutations lying outside of the coding genome, but could also be due to the technical limitations of exome sequencing. Because this technique relies on an enrichment process, it is limited by the design of the bate fragments: there may be protein coding regions that have not been identified so far, or baits may be incorrectly designed or inefficient. Other technical limitations include the quality of sequencing, and the ability to align these sequences to the reference.

Two mutations in *ZNRF3* were identified in an exome screen of 46,XY DSD patients. One mutation is shared by two sex-reversed (46,XY) sisters (R768G), and the second was found in an unrelated patient (S554N). Details of the extent of the disruption to testis and sexual development in these women is limited, as is the mode of transmission from the parents. The S554N mutation is in an XY female with gonadal dysgenesis (failure of testis development). The two 46,XY sisters with the R768G mutation are not well clinically defined. Both mutations were predicted to be deleterious to the protein structure when modelled in silico. One of the point mutations identified, (S554N), causes a Serine to be replaced by an Asparagine residue. However, in the mouse an Asparagine is already present at this locus. Further discussion of these mutations can be found in Chapter 6.

1.5.2 Mouse Models of DSDs

The genetic pathways which control primary sex development are well conserved in mammals, including importantly the role of *SOX9* and *SRY* (Nef and Vassalli 2009; da Silva et al. 1996; A Swain and Lovell-Badge 1999). As exemplified in the previous sections, mice have

been widely used to investigate mechanisms in mammalian sex determination. The majority of models used are global knockouts, conditional deletions in the somatic cell lineage of the gonad or transgenic overexpression models. Furthermore, forward genetic screens have been used in some cases as a method for gene discovery (Bogani et al. 2009; Siggers et al. 2014). Subsequently, these genes have sometimes been shown to also play a role in human testis development, although not always. However, there are some limitations to the use of mice, and several key differences have been identified between these two mammals. One example is the fact that the expression of *Sry* in the mouse is transient, and the timing of expression is critical for testis determination. On the other hand, human *SRY* is expressed throughout gonad development and adulthood (Clépet et al. 1993). Furthermore, some genes when removed cause XY sex reversal in mice, but not in humans. For example, *Map3k4* is required for testis determination in mice (Bogani et al. 2009), but no mutations have ever been reported in human 46,XY DSD patients.

Many cases of human DSDs have been shown to be highly dependent on the genetic background of the individual. For example, there have been cases reported whereby heterozygous XY female individuals have inherited a mutation in *SRY* from their heterozygous fathers (Chen et al. 2015). We are able to model this background-dependency in mice using inbred mouse strains which are sensitive to XY male-to-female sex reversal. The most commonly used strain in the field is C57BL/6J (B6J). These mice show higher levels of expression of female genes which may explain this sensitivity (Munger et al. 2009; Correa et al. 2012). Sensitivity to XY sex reversal can be increased even further in strains that carry a Y-chromosome from a *Mus domesticus* strain on a congenic B6J background, generated through many generations of backcrossing with B6J females. For example, XY B6J.Y^{AKR} mice

develop small testes due to transient ovotestis development (Washburn and Eicher 1989). Whilst they do not exhibit sex reversal in the wild-type state, further mutation of a gene functioning in testis determination can readily illicit gonadal sex reversal. In contrast, B6J.Y^{POS} mice develop either ovaries or ovotestes without any further mutations being required (Eicher et al. 1982).

Therefore, the mouse is an excellent tool for modelling human DSDs, showing conserved genetic pathways, and the ability to model the complexities of variable genetic backgrounds, with variable sensitivity to sex reversal, which are likely the norm in the outbred human genome.

1.6 Aims of thesis

Given the importance of mutual antagonism between the testis-determining pathway and the ovarian pathway, it is likely that there are undiscovered proteins, directly responsible for this process, which are critical for primary sex determination. *ZNRF3* is an excellent candidate for a new testis-determining gene, which could act to repress ovary-promoting WNT-signalling in the testis. This thesis therefore ultimately aims to analyse the role of *ZNRF3* in the testis-determining pathway through phenotypic analysis of mice carrying a *Znrf3* null allele on distinct genetic backgrounds, and by reproducing a potentially pathogenic human mutation in the mouse using CRISPR/Cas9 technologies.

Chapter 2: Materials and methods

2.1 Universal solutions

Reagent	
BABB	2 parts benzyl benzoate: 1 part benzyl alcohol
NTMT	100mM NaCl, 100mM Tris-HCL (pH9.5), 50mM $MgCl_2$, 0.1% Tween-20 in H_2O
PBT	PBS + 0.1% Tween-20
TBS	50mM Tris-HCl pH7.5, 150nM NaCl
TBST	50mM Tris-HCl pH7.5, 150nM NaCl, 0.1% Tween-20
PBSTx	PBS + 0.1% Triton X100
WMISH Prehybridisation Solution	50% formamide, 5X SSC, 0.1% Tween, 50ug/ml Heparin
WMISH Hybridisation solution	50% formamide, 5X SSC, 0.1% Tween, 50ug/ml Heparin, 100ug/ml yeast RNA, 100ug/ml salmon sperm DNA
WMISH Solution 1	50% formamide, 2XSSC, 1% SDS in H_2O
SSC (20x)	3mM NaCl, 300mM sodium citrate in water. pH7.2 with 3M citric acid.

Table 2.1 List of universal solutions

2.2 Mouse lines and genotyping

Mouse work was approved by the local AWERB and carried out under the Home Office Project License number 30/2877. Colonies were maintained by the staff of Mary Lyon Centre (MLC). Genotyping was either carried out using a Gel-based assay, myself, or by the Harwell Genotyping, Expression and Mutation Screens (GEMS) core facility.

2.2.1 Chromosomal sexing

All embryos were genotyped using a previously described PCR assay (Bogani et al. 2009). Lines which potentially sex reverse were genotyped by the Harwell GEMS core facility, using a copy-caller assay for *Sry*.

2.2.2 *Znrf3*^{flox} and *Rnf43*^{flox}

Male mice carrying *Znrf3* and *Rnf43* conditional alleles were a kind gift from Hans Clevers (Utrecht). They were reported to be on B6 but the extent of this was unclear. Males were culled, and their sperm used for in vitro fertilisation (IVF) of B6J oocytes, as part of the Mary Lyon Centre (MLC) quarantine procedure. The resulting F_1 animals were heterozygous for one or both of the alleles. Subsequent breeding segregated the two alleles. Initially, genotyping was carried out using a gel-based assay (Johan van Es, Hans Clevers, Utrecht), using primers designed around the LoxP sites (**Table 2.2**). Due to the size of the LoxP insertion, the mutant band was larger than the wild-type band. Embryos were also genotyped using this assay. Once established, the colony was genotyped by the Harwell GEMS core facility (Ramakrishna Kurapati, Deen Quwailid).

2.2.3 *Znrf3*^{del} and *Rnf43*^{del}

A proportion of the in vitro fertilised eggs (described above) were treated with soluble Cre [Excellgen] in order to immediately recombine the LoxP sites and generate heterozygous null animals in the F_1 generation. Embryos generated by IVF were washed in DMEM [Gibco] twice. Embryos were transferred into 0.6% HTN Cre in DMEM, and incubated at 37^{o}C (5% CO2) for 40 min. An excess of high calcium HTF medium (HTF) was then added to the embryos. Embryos were washed twice in HTF before being transferred into recipient females.

Soluble Cre-derived embryos were screened for null alleles, *Znrf3*$^{+/del}$ and *Rnf43*$^{+/del}$. *Znrf3*$^{+/del}$ alleles were detected in the F_1 generation. However, no *Rnf43* conditional alleles successfully recombined. F_1 *Rnf43*$^{+/flox}$ animals were instead crossed to a constitutively

active Cre line [C57BL/6NTac-Tg(ACTB-cre)^{3Mrt}/H] to generate null alleles in the following (F_2) generation.

Initially, genotyping was carried out using a gel-based assay. In both cases, 3 primers were used; the forward and reverse primers used to genotype the flox allele (described above); an alternative reverse primer which anneals in the deleted region. Differing band sizes indicate the presence of a wild-type or mutant allele (**Table 2.2**). Once established, the colony was genotyped by the Harwell GEMS core facility (Ramakrishna Kurapati, Deen Quaileed).

2.2.4 *Znrf3*$^{flox/flox}$, Ubiq-Cre-ERT2

Znrf3$^{flox/+}$ mice were crossed to B6.Cg-Tg(UBC-cre/ERT2)1Ejb/2J (referred to as Ubiq-Cre-ERT2 in this thesis) mice to generate *Znrf3*$^{flox/+}$, Ubiq-Cre-ERT2 studs. Ubiq-Cre-ERT2 mice express Cre-ERT2 under the control of a human ubiquitin C promoter (Ruzankina et al. 2007). *Znrf3*$^{flox/+}$, UBC-Cre-ERT2 studs were then crossed to *Znrf3*$^{flox/+}$ females to generate *Znrf3*$^{flox/flox}$, Ubiq-Cre-ERT2 males. Males were given 0.2mg Tamoxifen [Sigma] at a concentration of 20mg/ml in corn oil, for 5 days at 8-10 weeks, by oral gavage. Males were culled 60 days later, and tissue collected.

Mice were genotyped by the Harwell GEMS core facility and genotype was confirmed upon death by the previously described gel-based assays.

2.2.5 *Znrf3*^{R749G}

Znrf3-R749G mice carry a point mutation on a B6J background, which alters amino acid 749 in the mouse protein from Arginine to Glycine. Generation of *Znrf3*-R749G mice is detailed further in **Chapter 6**. Genotyping was carried out by the Harwell GEMS core facility.

2.2.6 B6.Y^{AKR}

B6.Y^{AKR} mice carry a Y chromosome derived from a *Mus domesticus strain*, AKR. All other chromosomes are B6. The line was maintained by crossing fertile B6.Y^{AKR} males to B6J females.

2.2.7 *Gadd45g*

Gadd45g knockout mice, as described in (Hoffmeyer et al. 2001), were a kind gift from P. Trainor (Stowers Institute for Medical Research, Kansas, USA). The allele was generated by replacing the majority of the coding region of endogenous *Gadd45g* with a Neomycin-resistance cassette. The line was maintained as heterozygotes, and intercross timed-mates were used to generate homozygote embryos.

Genotyping assay	Primers	Product sizes
Znrf3	Fw: CACACCCTGACCCTACGAA Rv: TTACCACACCCATACCCAACT Alt Rv: GTGGGCCATACTTCAAGGGAT	*Znrf3*^{WT} = 324bp *Znrf3*^{flox} = 405bp *Znrf3*^{del} = 205bp
Rnf43	Fw: GAAGCAGACAATGAAGCGAAT Rv: TAGTGCCCCACAGAGGACA Alt: CTATTGGCTGGTGGGTGGAG	*Rnf43*^{WT} = 284bp *Rnf43*^{flox} = 345bp *Rnf43*^{del} = 301bp
Gadd45g (Warr et al. 2012)	Fw: CTTGCAAAACCACACTGCTC Rv: TGGTCTGATCGACTTGGTGA Alt: GCCTAGGCCTTCCTGTGCTA	*Gadd45g*^{WT} = 217bp *Gadd45*^{del} = 120bp
XY sexing (Bogani et al. 2009)	Fw: TGGATGGTGTGGCCAATG Rv: TGGATGGTGTGGCCAATG	X-chromosome = 253bp Y-chromosome = 335bp

Embryos were genotyped using a gel-based PCR assay. 3 primers were used; the forward primer is common to both WT and mutant alleles; one reverse primer anneals to the Neomycin-resistance cassette; an alternative reverse primer anneals to the endogenous sequence. Differing band sizes are detected depending on the presence of the wild-type or null allele (Table 2.2).

Table 2.2 Primers for gel-based genotyping assays

2.2.8 *Sf1*-EGFP

Sf1-EGFP mice were a kind gift from J. Bowles and P. Koopman (Beverdam and Koopman 2006). Further details are described in **Chapter 3**. Adult mice were genotyped by the Harwell GEMS core facility.

2.3 Tissue collection and processing

For embryo dissection, timed mates were set up between mice and vaginal plugs checked the following morning. 12 noon on the day a plug was identified was considered to 0.5 dpc. Pregnant females were culled by cervical dislocation (Schedule One) and the uterus removed after confirmation of death. Embryos older than 14.0 dpc were removed from the uterus and decapitated immediately. Embryos were dissected in ice-cold PBS under a Nikon SMZ800 dissection microscope, and urogenital ridges or individual gonads were collected. For collection of adult gonads and reproductive tracts, mature adult mice were culled by cervical dislocation. Whole reproductive tracts were dissected and photographed, before gonads were removed and processed further.

2.3.1 WMISH

UGRs or individual gonads were dissected under a Nikon SMZ800 microscope in ice cold PBS. Dissected embryonic gonads were placed into a 4% PFA solution in PBS, and fixed overnight at 4 ^{o}C. The tissue was then washed with PBS twice (5 min) before being dehydrated using a methanol (MeOH) series: 1x 25% MeOH/PBS, 1x 50% MeOH/PBS, 1x 75% MeOH/PBS, 2x 100% MeOH. Tissue was then stored at -20 ^{o}C in 100% MeOH.

2.3.2 qRT-PCR

UGRs were dissected in ice cold PBS. A needle was used to separate the gonad from the mesonephros, which was discarded. Tissue was snap-frozen on dry ice, and stored at -80^{o}C.

2.3.4 Staging embryos

11.5 and 12.5 dpc embryos were staged by counting somites posterior to the hindlimb, as described previously. Embryos with >30ts were staged using morphological characteristics under the guidance of the Theiler staging method.

2.3.5 Immunohistochemistry

2.3.5.1 Wax sections: Adult gonads

Adult gonads were dissected and placed on ice, before being weighed. Testes or ovaries were placed in Bouins fixative for 4 hours, before being halved with a sharp scalpel. Testes were left in Bouins for a further 2 hours, before being washed in 70% EtOH and transferred into 70% until further processing by the MRC Harwell histology team.

2.3.5.2 Wax sections: Embryonic gonads

Dissected UGRs or embryonic gonads were placed into a 4% PFA solution in PBS, and fixed overnight at 4 ^{o}C. Gonads were processed into Paraffin Wax by the MRC Harwell Histology Team (Adele Austin and Caroline Barker). Tissue was embedded by me, and 8 μm sections were cut and placed on a slide.

2.3.5.3 Fresh Frozen sections: Embryonic gonads

Dissected gonads were fixed overnight in PFA at 4^{o}C. Tissue was then washed once in 60% sucrose solution and were incubated overnight at 4^{o}C in sucrose solution. The following day,

gonads were embedded in Optimal cutting temperature compound (OCT) and orientated appropriately. The OCT plug was frozen on dry ice and stored at -80^{o}C until further processing.

2.3.6 Protein extraction for Western Blot

Tissues (whole embryonic heads, livers, kidneys, testes) were manually homogenised in RIPA buffer supplemented with protease inhibitor (Complete EDTA-free protease inhibitor [Roche]) using a polypropylene pestle. Samples were centrifuges for 15 min, 10,000xg, at 4 ^{o}C. The supernatant was transferred to a clean microcentrifuge tube, and placed on ice.

A Bradford assay was carried out to determine the concentration of the sample. A standard set of concentrations was prepared using BSA (1.4; 1.0; 0.5; 0.25; 0.125; 0.0625; 0 mg/ml). 5µl of sample was added to a 96-well plate, followed by 250µl Bradford Reagent [Sigma]. Samples were incubated the reagent on a shaking platform, before absorbance at 595nm was measured.

2.3.7 Fluorescence-activated cell sorting (FACS)

2.3.7.1 Theory

FACs is a specialised form of flow cytometry. A cell suspension is passed in front of a laser, as a stream of droplets, with each droplet containing a small number of cells. Light is transmitted through the droplet, and the scattering used to determine its size and fluorescence. The instrument applies an appropriate charge to the droplet of interest, and electrostatic deflection is used to sort the droplet into the correct collection tube. In this thesis, this technique was used in this way to collect a population of eGFP-expressing, single

cells. Both eGFP-positive and eGFP-negative cells were collected by setting up the appropriate gates, as shown in Fig. 2.1.

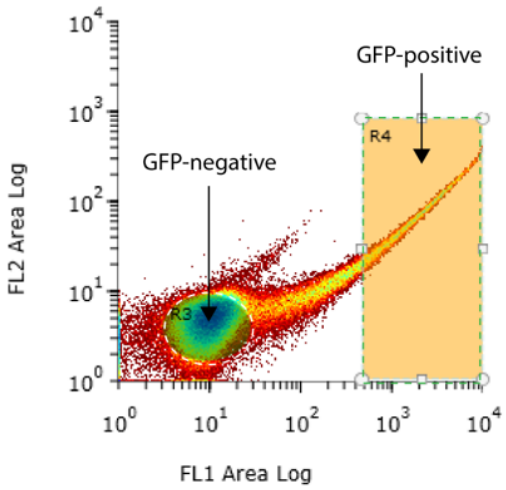

Figure 2.1 *Sf1*-eGFP gating for FACs. EGFP positive population (orange shaded area), and EGFP negative population (blue shaded area).

2.3.7.2 Tissue processing

FACs required a single-cell suspension from the gonad. Embryos were collected and removed from the uterus and amniotic sac, as previously described. Embryos were immediately screened for the presence of eGFP using a fluorescence microscope [Nikon SMZ1500, with HPX120C laser]. All eGFP-positive embryos and 2-3 eGFP-negative embryos were brought forward for processing.

Embryo heads were removed and a small piece of tissue placed in a 96 well PCR plate for genotyping. Embryos were placed in the corresponding well in a 12-well tissue culture plate in PBS. Chromosomal sex genotyping was carried out concurrently with aging of the embryos and dissections of the UGR (urogenital ridge). UGRs were stored in 12-well plates, in the dark, on ice. When genotyping results were available, the gonads and mesonephroi

were dissected away from the UGR, and were appropriately pooled in experimental groups. Between 1 and 4 pairs of gonads and mesonephroi were pooled per tube with minimal PBS.

250ul of 0.25% Trypsin in PBS was added to each tube of tissue and incubated at 37^{o}C for 5 min. 25ul FBS was added and mixed by tapping 10 times, to stop the reaction. 500ul ice cold PBS was added, and the tissue sedimented by spinning at 4^{o}C, 1700rpm for 10min. Supernatant was discarded and 500ul fresh PBS added. The pellet was resuspended by passing through pipette tips of decreasing sizes (P1000, P200) ten times. Finally, the tissue was passed through a 23G needle, using a 1ml syringe, six times. The suspension was passed through a Celltrics 30um filter [Sysmex] into a round-bottom flow cytometry tube (Falcon), and the filter washed with 250ul PBS. Cells were sorted immediately. Cells were then sorted using an S3 cell sorter [Biorad] using the gating previously describe.

2.4 Expression analyses

2.4.1 Wholemount in-situ hybridisation (WMISH)

2.4.1.1 RNA-probe synthesis

A region of the gene of interest between 600-900bp was amplified using standard PCR, and purified using a “QIAquick PCR purification kit” [QIAGEN]. PCR product was then ligated into pGEM-T vector [Promega]. 150ng of PCR product was incubated overnight at 4 ^{o}C using standard reaction detailed in kit.

Probe name	Description	Primers	Product size
Znrf3 (long)	recognises transcripts 1 and 2	*znrf3*_prblng1_fw AGACAATACCCAGCGTCACA *znrf3*_prblng4_rv GAATAATGGGGATGCGCTGG	996bp
Znrf3-001	recognises transcript 1 only	Fw: CTGCCTGGCTAGAAAACCAT Rv: AAGCATCAGTCCTGTGTGGA	647bp
Znrf3-002	recognises transcript 2 only	Fw: AGCAAAGTCCTGACAGAGGT Rv: TGTGATAAAGGGGGCAGCAA	636bp
Znrf3-003	recognises transcript 3 only	Fw: TGTGTTGTCCTGTCTGTGCT Rv: AGGTTGGAGAAACCAGACTTT	214bp

Table 2.3 List of primers used to generate WMISH probes and product sizes.

The following day, Subcloning Efficiency™ DH5α™ Competent E-coli Cells [Life Technologies] were transformed. Cells were defrosted for 15 min on ice. 50µl of cells were added to 2µl of ligation reaction, and the tube gently flicked to mix, before being incubated on ice for 20 min. Cells were heat shocked for 20sec at 42 ^{o}C before being incubated on ice for 2 min. 1ml of Lysogeny broth (LB) was added to the cells, and then incubated at 37 ^{o}C with shaking for 1 hour. 20µl and 200µl was then spread on an LB/agar plate with 100µg/ml ampicillin, and incubated overnight at 37 ^{o}C.

The following day, colonies were picked and grown overnight at 37 ^{o}C with shaking in 3ml of LB. A small volume was used for sequencing the following day in to determine the orientation of ligation into the vector. Cells were grown overnight at 37 ^{o}C with shaking in 30ml of LB, and the plasmid purified the following day using the standard protocol provide with the QIAGEN Plasmid Midi Kit.

Plasmid DNA was cut with the appropriate enzyme to generate an antisense template for generation of a sense RNA probe. Linearised Plasmid DNA was transcribed with T7 or SP6

(Table 2.4) such that the digoxygenin(DIG)-labelled RNA probe was complimentary to the endogenous mRNA of the gene of interest.

Probe name	Vector	Enzyme	RNA polymerase transcription	Reference
Sox9	pBluescript II KS(-)	HindIII	T7	Wright et al 1995
Stra8	pCR-BluntII-TOPO	HindIII	T7	Bogani et al 2009
Sry	pBluescript II KS(-)	SacI	T3	Bogani et al 2009
Lef1	Unknown	XbaI	T7	M.C. Chaboissier (Pers. Comms.)
Rnf43	pGemT	SpeI	T7	-
Znrf3-alltranscripts	pGemT	SacII	SP6	-
Znrf3-transcript1	pGemT	SacII	SP6	-
Znrf3- transcript2	pGemT	SacII	SP6	-
Znrf3- transcript3	pGemT	SacII	SP6	-
Axin2	pGemT	SacII	SP6	-

Table 2.4 Further details, WMISH probe synthesis.

2.4.1.2 WMISH protocol

Gonads were transferred into Netwell (Fisher) inserts in a 12-well tissue culture plate. Each net contained a similar number of gonads, and no more than 5 pairs in each well. Tissue was rehydrated using a methanol series, 5 min per wash: 1x 75% MeOH/PBS, 1x 50% MeOH/PBS, 1x 25% MeOH/PBS, and washed twice (5 min) in PBST (PBS + 1% Tween 20). Tissue was bleached in 6% H_2O_2 in PBST for 40 min, and washed 3 x PBST 5 min, before being digested in 10µg/ml proteinase K (Roche) in PBST for 15 min. The reaction was stopped with a 2mg/ml glycine wash, followed by 2 x 5 min PBST washes. Tissue was fixed for 20 min in 2mg/ml

glutaraldehyde in 4%PFA/PBST. After 2 x 5 min PBST washes, tissue was placed into prehybridisation solution (50% formaldehyde, 5X SSC, 1% Tween 20, 50µ/ml Heparin) at 70 ^{o}C for at least 1 hour. Probe was denatures for 10 min at 70^{o}C, then cooled on ice before 5µl/ml was added to Hybridisation solution (Prehybridisation solution + 5µl/ml Salmon Sperm DNA + 10µl/ml Yeast RNA). Tissue was incubated at 70^{o}C overnight in Hybridisation solution and probe.

The following day, tissue was washed in wash solution (25% formamide, 2X SSC, 1% SDS) 2 x 30 min at 70 ^{o}C, followed by 2 x 30 min at 65 ^{o}C. Following 3 x 5 min washes in 1X TBST (25mM Tris pH 7.5, 0.1% Tween, 14mM NaCl, 0.02mM KCl), tissue was pre-blocked in 10% Heat Inactivated Sheep Serum (HISS) in 1X TBST for at least 2.5hours at room temperature. Meanwhile, anti-digoxygenin antibody was prepared. Embryo powder was heat inactivated for 30 min at 70^{o}C in 1m 1X TBST before being pulsed down, and TBST removed. Embryo powder was resuspended in 1ml 1X HISS and 2.5µl anti-DIG-alkaline phosphatase conjugated fab fragments [Roche] per in situ well was added. Embryo powder solution was agitated on a rotator at 4 ^{o}C for at least 1 hour. Embryo powder was pulsed down and supernatant removed and added to the remaining 1X HISS to give a final concentration of 1µl/ml antibody, and tissue was incubated in this antibody solution overnight at 4^{o}C.

Tissue was washed the following day in 1X TBST for 3 x 5 min, followed by 6 x 1 hour at RT. Tissue was washed in NTMT (100mM NaCl, 100mM Tris-HCL (pH 9.5), 50mM MgCl2, 0.1% Tween 20 in H2O) for 3 x 10 min at RT before transferring to watch glasses that had been treated with Repel-cote. Tissue was incubated in alkaline phosphatase stain (20µl/ml NBT/BCIP [Roche] in NTMT) in the dark at RT until the stain had sufficiently developed. Tissue was then washed in NTMT for 3 x 10min, and left to whiten in PBST for up to 5 days

in the dark at RT, before being post-fixed in 4% PFA for 1 hour at RT. Samples were then stored in PBST at 4 °C.

After WMISH, tissue was photographed in PBST on 1% agarose/PBS using a Leica MZ16 dissection microscope with digital camera attached.

2.4.2 Immunofluorescence

All slides were imaged using a Zeiss LSM710 upright multiphoton microscope equipped with ZEN software. All steps were carried out at room temperature unless stated.

2.4.2.1 Protocol 1: SRY, SOX9 antibodies

Samples were placed in 1 x Declere in a steamer for 45 min to remove wax. Slides were transferred to fresh-boiled 1 x Declere to cool for 30 min. Slides were rinsed in ddH_2O, then 1x TBS, before being treated with 0.3% H_2O_2 in 1x TBS for 10 min. Samples were blocked for 1 hour in 2 % skim milk powder and 0.1% Triton in TBS, before being incubated with primary antibodies at a concentration of 1:100 in block overnight, at 4°C in a humidified chamber. The following day, slides were washed 4 time (5 min) in 1x TBS before being incubated with secondary antibodies (1:200) in block, for 1 hour at room temperature. Slides were washed 3 x 5 min in 1x TBS before being mounted in Antifade Mounting Medium with DAPI [Vectasheild].

2.4.2.2 Protocol 2: FOXL2, AMH antibodies

Samples were Declere treated as above. Slides were washed 4 times in 0.1% Triton in PBS (PBSTx) before being blocked for 1 hour at room temperature in 10% HISS/PBTx. Slides were then incubated with primary antibodies (1:100) in block, overnight at 4°C in a humidified chamber. The following day, slides were washed 3 times with PBS (5 min), and incubated

with secondary antibodies (1:200) in the dark for 1 hour, at room temperature. Slides were washed in 3 times in PBS (5 min) and incubated in 0.1% Sudan Black in 70% Ethanol for 5 mins, before being washed 3 times in PBS. Samples were mounted as above.

2.4.2.3 Protocol 3: PECAM, frozen sections

Slides were defrosted for 30 mins at room temperature, before being post-fixed in 4% PFA for 20 mins. Slides were rinsed with PBTx, washed 3 times in PBTx and then blocked for 1 hour in 10% HISS/PBTx at room temperature. Sample were incubated with primary antibodies (1:100) in 10% HISS/PBTx overnight at 4^{o}C in a humidified chamber. The following day, slides were washed 3 times in PBS (5 min) and re-blocked for 30 min in fresh 10% HISS/PBTx. Samples were then incubated with secondary antibodies (1:200) in block for 1 hour at room temperature. Slides were washed 3 times in PBS (5 min) before being mounted as above.

2.4.3 qRT-PCR

2.4.3.1 RNA/DNA extraction

For embryonic gonads and sorted cells, a RNeasy Plus Micro kit [Quiagen] was used. The standard protocol was used with the following modifications: (1) gonads or cell pellets were manually homogenised by vortexing for 15 seconds; (2) 10µl per 1ml β-mercaptoethanol was used for in the RLT lysis buffer to inhibit RNase activity in the sample; (3) carrier RNA was used after sample lysis; and (4) RNA was eluted in 16µl RNase-free water and passed through the column twice to maximise yield.

For MEFs, cells were pelleted for 10min at 1700rpm, and supernatant discarded. RNA was extracted using an RNeasy Plus Micro kit [Quiagen], using the standard protocol.

For adult testes, tissue was placed in lysis matrix D tubes [MP Biomedicals] and were homogenised for 30sec, at 4°C using a FastPrep FP120 cell disruptor [Qbiogene], in 350 µl RLT buffer. RNA extraction was then carried out using an RNeasy Micro kit and the standard protocol.

2.4.3.2 Reverse transcription

200ng of cDNA was synthesised from 220ng RNA using a High Capacity Transcription kit (Applied Biosystems) in a thermocycler at 37°C for 2 hours. cDNA was subsequently diluted 1:6 with water.

2.4.3.3 PCR Reaction

qRT-PCR was performed using the Fast SYBR® Green system. This system quantifies the concentration of a specific cDNA by measuring fluorescence as the SYBR® Green dye is incorporated into the double stranded DNA as it is amplified by a Taq polymerase.

A master mix (1x SYBR® Green Master Mix + 0.2µM each primer) was prepared, and 15µl added to each well of a Microamp fast optical reaction place (Applied Biosystems) followed by 5µl of cDNA. Each sample was analysed in duplicate. Real time PCR was performed using the 7500 Fast real time PCR system (Applied Biosystems).

The Cycle threshold (Ct) value for each sample was first calculated using the 7500 Fast system software, before being analysed in Microsoft Excel 2010. Relative expression levels were calculated using the comparative method, giving the ratio (R) of the Ct value of the target gene versus the endogenous and ubiquitously expressed gene, Hprt1 (equation 1). The standard error of the mean was calculated (equation 2).

Equation 1

$$\frac{2^{-\mathrm{Ct}_{\mathrm{target}}}}{2^{-\mathrm{Ct}_{\mathrm{endogenous}}}}$$

Equation 2

$$\frac{\mathrm{Standard\ Deviation}_{\mathrm{samples}}}{\sqrt{\mathrm{number\ of\ samples}}}$$

Primer pairs used were validated by generating a standard curve. A range of cDNA concentrations (30ng, 10ng, 1ng, 0.1ng, 0.01ng) from both male and female gonads was used, with three technical replicates. The standard curve was generated by plotting Ct over log of the cDNA concentration, and the gradient of the resulting linear regression was used to calculate the efficiency of the SYBR® Green assay (equation 3).

Equation 3

$$\left(10^{\left(-1/\mathrm{slope}\right)} - 1\right) \times 100$$

The optimal slope gradient is -3.32 which is equivalent to 100% efficiency. However, an assay with an efficiency of between 90 and 110% is acceptable.

2.4.3.4 qRT-PCR Primer pairs

Detects	Forward primer	Reverse Primer
*Znrf3*_qPCR_T1.9 (transcript 1)*	CACAACCCGGGAAGAGGAAC	GATGCCTGGGCCAGATCC
*Znrf3*_qPCR_T2.1 (transcript 2)*	TGACCATAGTATGATGCACCCA	TGGTCGATGGCTTCTGGATT
*Znrf3*_qPCR_T3.2 (transcript 3)*	GCCATCGACCAGCTAAACCA	TTCCTGTGCCATAGTTGAGC
Recognises all transcripts of mouse *Znrf3**	ACCATGTCTCACTGTCCTGG	TTCACATACACCACTGGCCT
Recognises all transcripts of mouse *Znrf3**	CAAGGCCAAGAGAGCAGTTC	GCACCCTTCACATACACCAC
Gadd45g	GGAGACCTGCATTGCATCCTCATTT	ACTCGGGAAGGGTGATGCTGG
Hprt1	CATTATGCCGAGGATTTGGAA	CACACAGAGGGCCACAATGT
Sry	TTATGGTGTGGTCCCGTGGT	GGCCTTTTTTCGGCTTCTGT
Sox9	AAGAAAGACCACCCCGATTACA	CAGCGCCTTGAAGATAGCATT
*Axin2**	AGTGCAAACTCTCACCCACC	TCGCTGGATAACTCGCTGTC
*Lef1**	GCGACTTAGCCGACATCAAG	AGGGTCCCTTGTTGTACAGG
*Wnt4**	GTCTTCGCCGTGTTCTCG	CTCAAGGTTCCGTTTGCACA
Rspo1	GCTCCAACTCTCGGAGACAC	GTCACTGTGCCCAGGTAGGT
Fgf9	AGTGGACTCTACCTCGGCAT	TTCTCTTGGAGTCCCGTCCT
Sf1	TTCGTCTGTCTCAAGTTCCTCATC	CCTTTACGAGGCTGTGGTTGTT
Wt1	AGGTTTTCTCGCTCAGACCA	CCTGGTGTGGGTCTTCAGAT
Oct4	CTCAGCCTTAAGAACATGTG	TTCTCTTGTCTACCTCCCTT

Table 2.5 List of primers used for qRT-PCR. Starred primers were newly designed and tested for this thesis.

Details of primer binding sites for *Znrf3* are detailed further in Chapter 3.

2.4.4 Optical Projection Tomography (OPT)

Following WMISH, gonads were stored in PBT at 4 ^{o}C until processing. Before embedding, tissue was washed 3 x 5min in ddH_2O at RT. Samples were imaged with a bespoke Optical Projection Tomography (OPT) scanner (M. D. Wong et al. 2013).

2.4.4.1 Embedding and clearing

10ml syringes were used as moulds as shown in Fig 2.2. Moulds were stabilised by standing in crushed ice. 1.5% Macrosieve low-melt agarose (Invitrogen) in ddH_2O was heated until fully dissolved. Agarose was allowed to cool before being filtered (0.2um, Thermo Fischer) directly into moulds, to a depth of approximately 2cm. Agarose was allowed to cool in the mould before a Pasteur pipette was used to transfer tissue with minimal liquid.

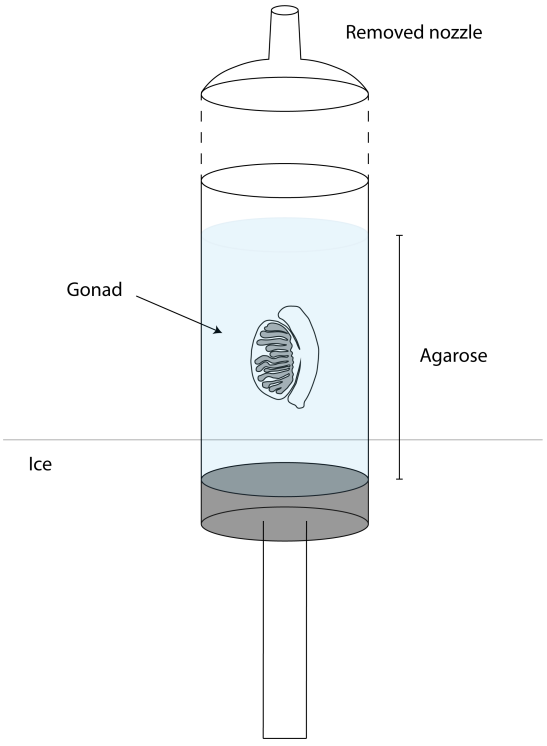

Figure 2.2 OPT embedding of WMISH gonads. A cut-off syringe with the nozzle removed was used as a mould. The syringe was stabilised on crushed ice. Liquid agarose was poured into the mould and the gonad orientated appropriately. After cooling, the plunger is depressed to eject the agarose plug.

Once fully cooled, agarose cylinders were ejected directly into 100% MeOH in a 50ml centrifugation tube. Cylinders were left on a rocker overnight. MeOH was removed, and replaced with fresh MeOH the following day, which was repeated as many times as necessary. Cylinders were monitored until fully dehydrated, when cylinders sink to the bottom of the tube.

Once dehydrated, MeOH was removed, and replaced with BABB (two parts benzyl benzoate and one part benzyl alcohol). Cylinders were placed on a rocker, and BABB replaced at least once until cylinders and tissue were fully cleared, and sank to the bottom of the tube. Tissue was monitored carefully to prevent staining from being removed by the BABB solution.

2.4.4.2 Calibration and Scanning

Fully cleared samples were briefly washed with 100% MeOH, and allowed to air-dry on Whatman lens cleaning tissue (Grade 105). Care was taken to minimise contact with the convex surface of the agarose cylinder. Once fully dried, superglue was used to secure the cylinder to a metal magnetic stub. The cylinder was left for 10 min to dry before being mounted in the OPT machine.

Stubs were adjusted so that the tissue of interest was at the centre of rotation. Tissue was scanned first with white light to identify areas WMISH stained, and then with Ultra Violet light to map the general morphology. A step size of 0.9 degrees was used resulting in a total of 400 images. A dark field was used to eliminate any background interference.

2.4.4.3 Reconstruction and Post-processing

Matlab was used to process the images received from the scanner before NRecon was used to reconstruct cross-sections of both the UV and white-light scans of the tissue samples. The

program was used to adjust for misalignment of the sample around the centre of rotation, and for movement of the sample in the x-axis during the scan. Ring artefacts were also minimised during processing in NRecon. The resulting images were further processed in Fiji (Fiji is Just Image J). UV scans were used to generate a threshold which represented the surface of the tissue. Manual correction of some artefactual errors in the scans were used at this point to generate a solid surface with no holes. White light scans were minimally processed, with some manual editing of large areas of dirt outside of the tissue. Fiji was used to align and render a 3D image of the UV and white light scans together. The threshold of the white light scan was manually adjusted to best represent the photograph of the original WMISH. The scan was then exported as a .gif file and can be viewed as a movie of one 360^{o} rotation.

2.4.5 Western Blot analysis

Lysates of known concentration were separated by SDS-PAGE on a 4-12% Bis-Tris gel [Life Technologies] in 1xMOPs buffer. Samples were run alongside a Precision Marker [Biorad] to allow estimation of molecular weights. Protein was then transferred to a nitrocellulose membrane using the iBlot dry electrotransfer system [Life technologies] by passing 20V across the stack for 7 min. The membrane was blocked in 5% skimmed milk powder in PBST. The membrane was then incubated with primary antibodies, diluted 1:250 in block, overnight, at 4^{o}C, on a rocker. Membranes were washed 4 x 5min in PBT at RT on a rocker, before being incubated with IR fluorophore-conjugated secondary antibodies (IRDye800, and IRDye700) for 1 hour, at RT. Membranes were washed 4 x 5min in PBT at RT on a rocker, and then dried. Imaging was carried out using an Odyssey infra-red imaging system [Li-COR Biosciences].

Chapter 3: Characterisation of *Znrf3* and *Rnf43* expression in the embryonic mouse gonad

3.1. Introduction

After the identification of mutations in *ZNRF3* in human DSD patients (see **Chapter 1, section 1.5.1**), it was first important to ascertain whether *Znrf3,* or its homologue *Rnf43,* were expressed in the mouse embryonic gonad. The absence of *Znrf3/Rnf43* from the early embryonic gonad would preclude either genes playing a role in primary sex determination in the mouse.

3.1.1 Protein structure and isoforms

As previously described, ZNRF3 and RNF43 are transmembrane Zinc Ring Finger proteins. The extracellular domain is well characterised, with crystal structures solved for both RNF43 and ZNRF3. However, the structure of the intracellular domain is currently unsolved and its functions, such as significant protein interactions, also remain unclear. Both proteins have a single transmembrane domain. The Ring Finger domain is intracellular/cytoplasmic. The extracellular domain is responsible for the interaction of these proteins with Rspondins and LGR5/6 (**Fig 3.1**).

The ectodomain of ZNRF3 has high structural homology with a Protease-Associated (PA) domain. This PA-fold is found in many proteases such as subtilases and Zn-containing metalloproteases, as well as catalytically inactive proteins such as the transferrin receptor

family (Mahon and Bateman 2000; Xinmei Luo and Hofmann 2001). The crystal structures also highlight the structural similarities between ZNRF3 and RNF43 ectodomains, despite the relatively low sequence homology (37%) (Peng et al. 2013).

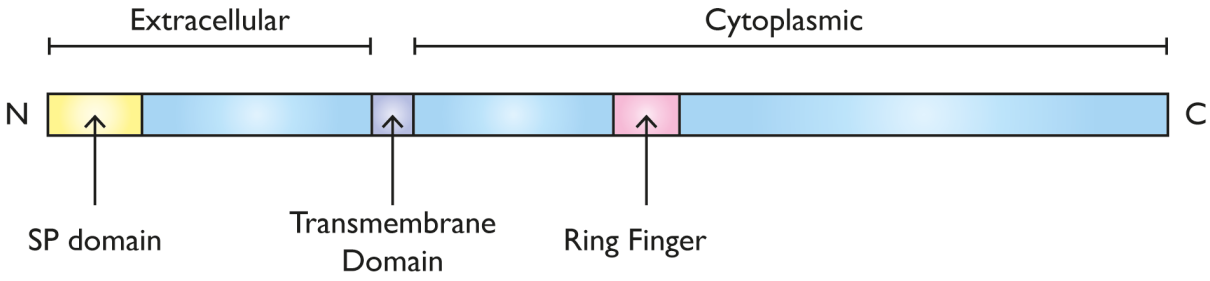

Figure 3.1 Protein structure of ZNRF3. ZNRF3 is a transmembrane protein. Identified domains are labelled on the figure. A predicted Signal Peptide (SP) domain is located at the N-terminus. The ring finger domain in located intracellularly.

There are three isoforms of the mouse and human *ZNRF3* transcript. In mice, transcripts 1 and 2 contain the exons which encode the Ring Finger domain, which is critical for ZNRF3's role in ubiquitination. Transcript 3 encodes an isoform which lacks the Ring Finger and transmembrane domain (**Fig. 3.2**). The specific qRT-PCR primers and WMISH probes used to detect these different isoforms in this chapter, are detailed below (**Fig. 3.2**).

The *Znrf3*-null allele (referred to as *Znrf3*^{del}*)* used in this thesis will be discussed further in the following chapter (**Chapter 4**). Briefly, the *Znrf3*^{del} is missing exon 7, which encodes half of the critical ring finger domain. This deletion also results in a frame shift and a truncated protein product. It is predicted to be a null allele.

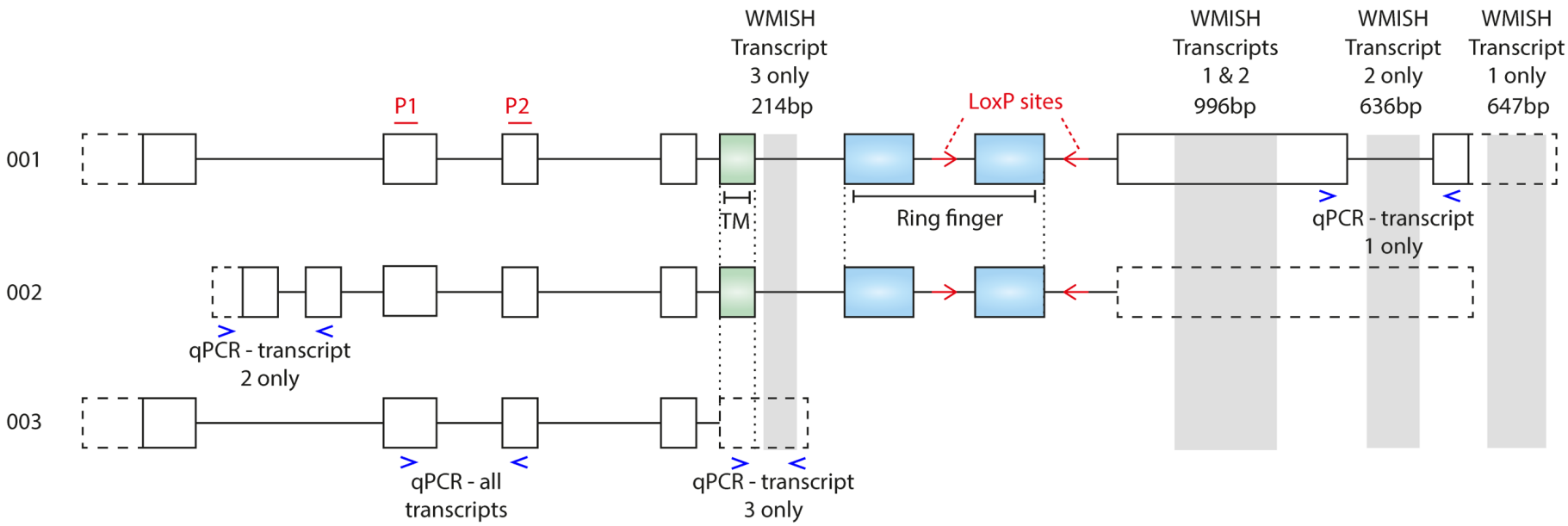

Figure 3.2 Schematic showing the exon structure of *Znrf3* and the position of primers and probes used in this thesis. *Znrf3* has 3 transcripts: transcript 1 (001), transcript 2 (002) and transcript 3 (003). Boxes represent exons, dashed boxes show untranslated regions (UTRs) and lines represent introns: not drawn to scale. Ring finger domain (blue) and transmembrane domain (green, TM) are shown. LoxP recombination sites are shown as red arrows. Positions of probes used for Wholemount In Situs (WMISH) are shown in grey. Position of qPCR primers are shown by blue arrows. Peptide sequences used to generate antibodies are shown in red; peptide 1 = P1; peptide 2 = P2.

3.1.2 Cell sorting rationale

The *Sf1-eGFP* transgenic mouse line can be used to enrich for the somatic cell lineages in both XX and XY gonads. *Sf1* (Steroidogenic Factor-1) is expressed in the gonad primordium in both sexes as early as 9dpc, until about 13.5 dpc when it cannot be detected in the XX gonad. It is expressed broadly, in both the pre-supporting cell lineage (pre-Sertoli and pre-granulosa cells), and in precursors which will become the steroidogenic cells (Leydig and theca cells) (Ikeda et al. 1994). In *Sf1-eGFP* transgenic mice, eGFP expression is driven by a 674bp (-590 to +85) region of the *Sf1* promoter, which includes both the LHX9 and WT1 binding sites (Beverdam and Koopman 2006). FACs sorting of eGFP positive cells was shown to enrich for supporting cells in both XX and XY gonads (Beverdam and Koopman 2006). The supporting cell precursors of the somatic cell lineage are the site of sex determination, and *Sf1*-positive somatic cells represent some degree of enrichment for these cells. Thus, a gene which plays a role in primary sex determination should be expressed in this *Sf1*-positive population of cells.

3.1.3. Aims

This chapter aims to investigate the expression of *Znrf3* and *Rnf43* in wild-type embryonic and adult gonads. Wholemount *in situ* hybridisation (WMISH) is used to examine expression in the gonad and mesonephros, and analyse the differing level of expression of the three transcripts of *Znrf3* in a semi-quantitative fashion. Further quantitative analyses address expression specifically in the somatic cell lineages of the gonad. This chapter will also describe attempts to examine the distribution of ZNRF3 protein in the embryonic gonad, using several antibodies. Finally, expression of *Znrf3* is examined in another sex-reversed

mouse model to further elucidate the potential relationship between *Znrf3* expression and the testis-determining genetic pathway.

3.2. Results

3.2.1 Expression of *Znrf3* and *Rnf43* in the embryonic mouse gonad

Previous transcriptomic studies have indicated the presence of *Znrf3* in the developing gonad. Microarray analysis (S. A. Jameson et al. 2012) detects *Znrf3* in a number of cell lineages of the embryonic gonad between 11.5 dpc and 13.5 dpc. These data suggest that *Znrf3* is expressed at higher levels in XY supporting cells compared to XX across all time points analysed (**Fig. 3.3a**). Expression is lower, and is not sexually dimorphic, in the other cell lineages of the gonad. *Rnf43* is also detected (**Fig. 3.3b**). Expression of *Rnf43* remains constant in all cell types over the period analysed, except for increased expression in XX stromal and supporting cells. Furthermore, single cell RNA-seq analyses (Serge Nef, Isabel Stevant – pers. comm.) (Stevant et al. 2017) detected *Znrf3* at low levels across all Sf1-positive cell lineages of the XY gonad from 10.5 dpc (**Fig. 3.3c**) but only detected *Rnf43* sporadically in a small number of cells (**Fig. 3.3d**); violin plots show the frequency of cells with different levels of expression. In 10.5 dpc progenitor cells and Sertoli cells, the modal expression level is between 3 and 4. However, in interstitial and fetal leydig cells, most cells express a low level of *Znrf3,* or show no expression (**Fig. 3.3e**). In contrast, *Rnf43* is expressed at very low levels in all cell types, with the vast majority of cells having no detectable expression. *Rnf43* is never detected in 10.5 dpc progenitor cells and fetal Leydig cells, but is sporadically seen at higher levels in interstitial and Sertoli cells (**Fig. 3.3f**).

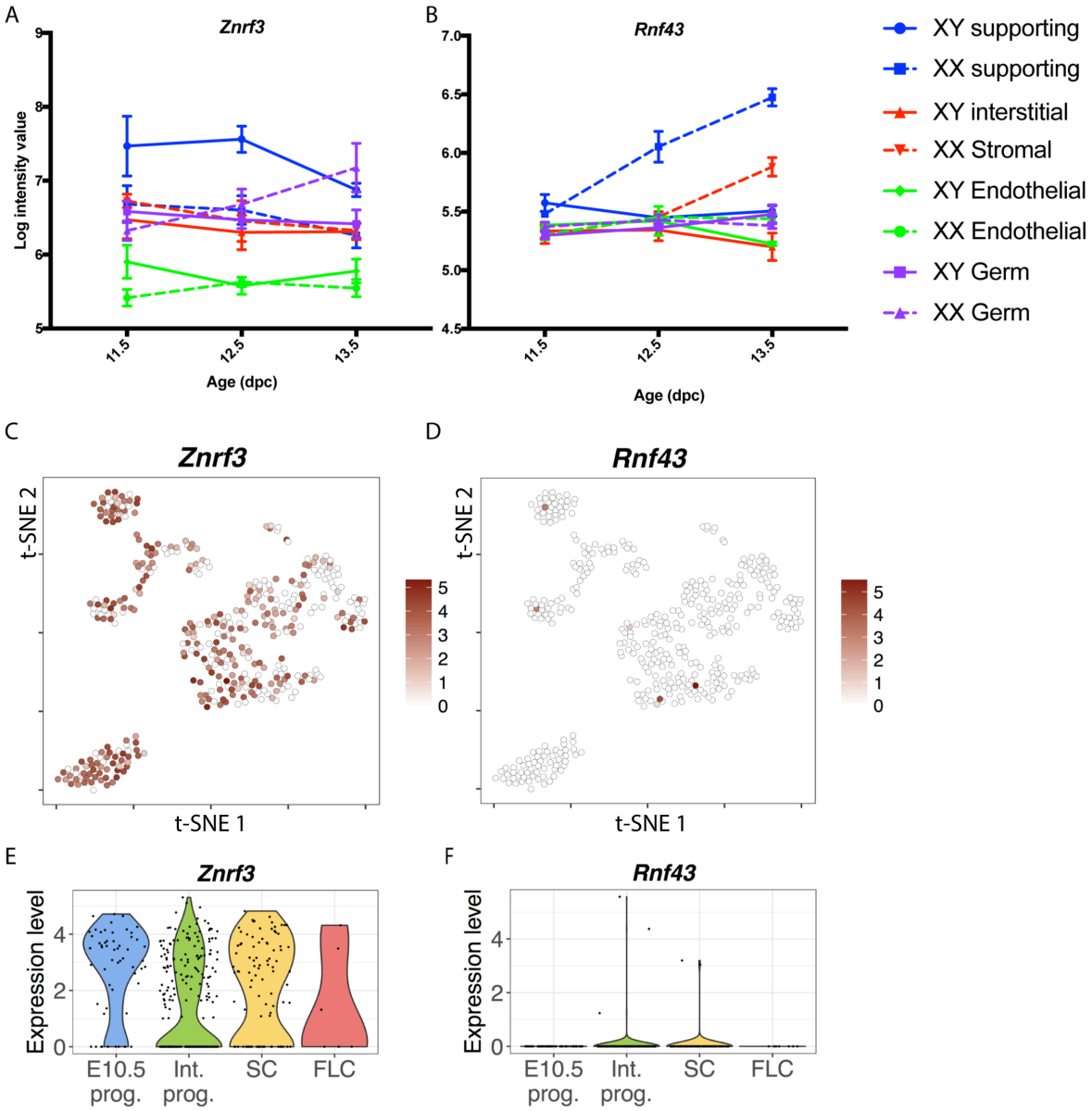

Figure 3.3 *Znrf3* is expressed in the mouse gonad during the critical sex determining period. Microarray studies (S. A. Jameson et al. 2012) shows expression of *Znrf3* **(a)** and *Rnf43* **(b)** in the supporting cell lineage (blue), the interstitial/stromal cell linage (red), the endothelial cell lineage (green) and in germ cells (purple), between 11.5 dpc and 13.5 dpc, in XX and XY gonads. Single cell RNA seq. data shows expression of *Znrf3* **(c)** and *Rnf43* **(d)** in single XY *Sf1*-positive cells from 10.5 dpc to 14.5 dpc gonads. Each circle represents an individual cell. A plot to show the cell lineage and the embryonic stage to which each of these cells belongs can be found in the appendix (Fig. S1)**.** Violin plots show the frequency of cells expressing low to high levels of *Znrf3* **(e)** and *Rnf43* **(f)**.

To confirm *Znrf3* expression in the embryonic gonad, Wholemount in situ Hybridisation (WMISH) studies were carried out on wild-type C57BL/6J (B6) urogenital ridges (UGRs) between 11.0 dpc and 13.5 dpc, using a probe which detects isoforms 1 and 2 (**Fig. 3.2**). Expression of *Znrf3* in wildtype UGRs appears to be low and essentially ubiquitous at all ages. Higher expression can be detected in the Wolffian duct, in the mesonephros. Wolffian duct expression is particularly pronounced at 11.5 dpc (**Fig. 3.4a**). Expression appears higher in the 11.5 dpc XY gonad compared to the XX. At later stages expression is somewhat concentrated in the testis cords in XY gonads, although low-level expression in the surrounding cells is also seen. When qRT-PCR was carried out, using primers which detect all transcripts, on whole sub-dissected gonads (mesonephros removed), no difference was seen between XX and XY gonads at 11.5, 12.5 or 13.5 dpc (**Fig. 3.4b**). This expression pattern was also seen with a separate pair of primers (data not shown) and confirmed in several subsequent experiments: no significant sexual dimorphism was ever detected. WMISH probes were also designed against the three transcript isoforms of *Znrf3*. Transcripts 1 and 2 were detected in the Wolffian ducts and in the testis cords of 12.5 dpc and 13.5 dpc XY gonads (**Fig. 3.4c**). Transcript 3 was not detected at any stage.

Rnf43 could not be detected in wildtype UGRs at 11.5 dpc confirming the results of the transcriptomic studies (**Fig. 3.4d**) and effectively excluding this gene from playing a role in mouse sex determination. Furthermore, attempts to design a qRT-PCR assay for *Rnf43* were unsuccessful and this experiment was discontinued due to time constraints. At this point, it was decided that the project should focus on *Znrf3* expression.

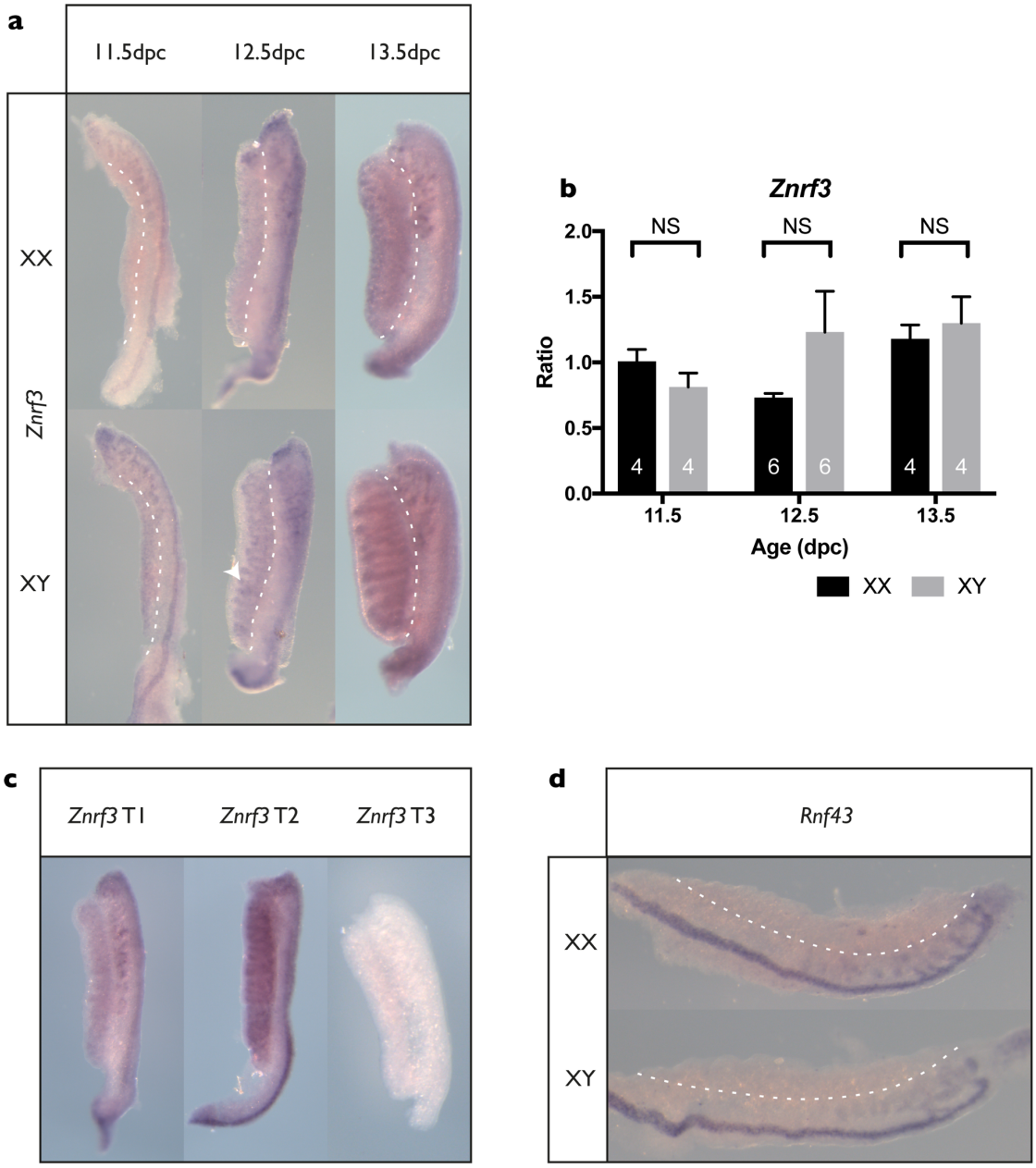

Figure 3.4 *Znrf3*, but not *Rnf43*, can be detected in the mouse embryonic gonad. WMISH was performed on XX and XY B6 gonads between 11.5 dpc and 12.5 dpc. Expression is concentrated in the testis cords at 12.5 and 13.5 dpc (white arrows). White dotted lines divide gonad (left) and mesonephros (right) **(a)**. qRT-PCR was performed on B6 11.5 dpc (17-18ts), 12.5 dpc (27-28ts) and 13.5 dpc sub-dissected gonads. Expression was calculated relative to *Hprt1* (ratio). Error bars show SEM. T-tests were performed with Welch's correction. Non-significant differences are signified by NS. Exact *P* values are detailed in the appendix (Table S1) **(b)**. WMISH was performed on XY gonads using probes specific for individual transcripts: 1 = *Znrf3* T1, 2 = *Znrf3* T2, 3 = *Znrf3* T3 **(c)**. WMISH with an *Rnf43* probe was performed on B6 11.5 dpc gonads. White dotted line divides gonad (upper) and mesonephros (lower) **(d).**

Sf1-eGFP cells were sorted from B6 gonad and mesonephros pairs at 11.5 dpc (17-18ts) using Fluorescence-Associated Cell Sorting (FACS) to allow for some degree of enrichment for supporting cell precursors. Cells were sorted into a GFP-positive population and a GFP-negative population. Cells from multiple cell sort experiments were pooled for each genotype (n=4 each genotype, with cells from 5-6 pairs of gonads pooled in each sample). Expression was analysed by qRT-PCR using primers which detect all three transcripts. We hypothesised that, by excluding cells from other lineages in the gonad and enriching for somatic cells, a sexually dimorphic expression pattern may be revealed.

As expected, *Sf1* expression is significantly higher in the GFP-positive population of cells in both sexes (Fig. 3.5a). To confirm the ability of this experiment to detect sexually dimorphic gene expression, *Sox9* was also analysed as a positive control. A significant difference was detected between XX GFP-positive and XY GFP-positive cells as expected. Interestingly, XX GFP-positive cells showed a significantly lower level of expression compared to either XX or XY GFP-negative cell populations (Fig. 3.5b).

When *Znrf3* expression was analysed, no significant difference was detected between XX and XY GFP-positive cell populations. There was also no significant difference between XY GFP-positive and -negative samples. However, there is significantly higher expression in XX GFP-positive cells when comparing to XX negative cells (Fig. 3.5c). Expression of *Znrf3* was also detected in the adult gonad. This data will be presented and discussed further in Chapter 4.

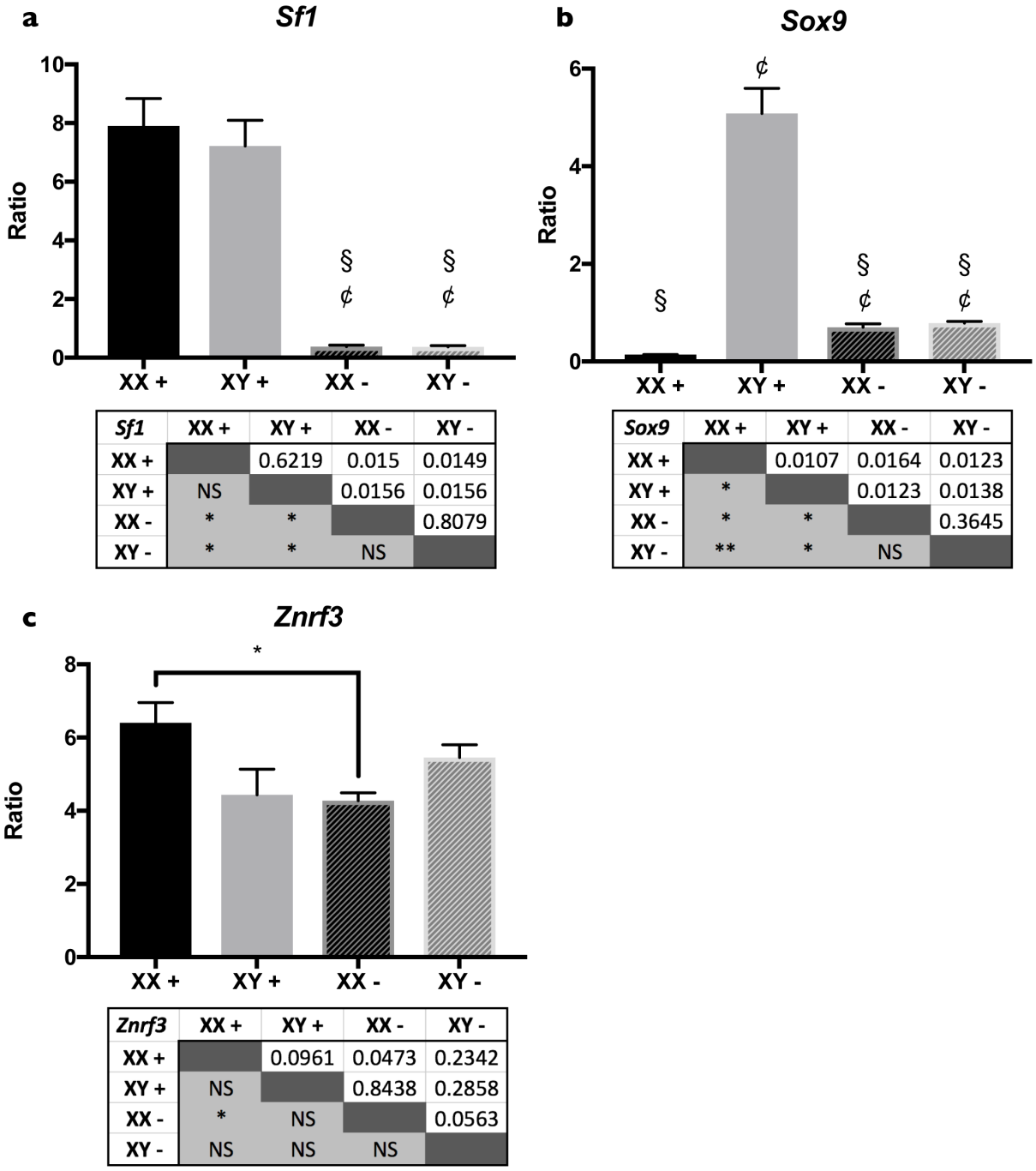

Sf1	XX +	XY +	XX -	XY -
XX +		0.6219	0.015	0.0149
XY +	NS		0.0156	0.0156
XX -	*	*		0.8079
XY -	*	*	NS	

Sox9	XX +	XY +	XX -	XY -
XX +		0.0107	0.0164	0.0123
XY +	*		0.0123	0.0138
XX -	*	*		0.3645
XY -	**	*	NS	

Znrf3	XX +	XY +	XX -	XY -
XX +		0.0961	0.0473	0.2342
XY +	NS		0.8438	0.2858
XX -	*	NS		0.0563
XY -	NS	NS	NS	

Figure 3.5 Expression of *Znrf3* in the *Sf1-eGFP* positive cells. Expression of *Sf1* **(a)**, *Sox9* **(b)**, and *Znrf3* **(c)** in populations of XX GFP-positive (XX +), XY GFP-positive (XY +), XX GFP-negative (XX -) and XY GFP-negative (XY -) cells sorted from C67B6/J semi-subdissected gonads at 11.5 dpc (17-18ts). Relative expression was calculated relative to *Hprt1* (ratio). Error bars show SEM. T-tests (two-tailed) were performed with Welch's correction. Significant results are signified by * = $P<0.05$, ** = $P<0.01$, and non-significant differences are signified by NS. Exact *P*-values are detailed in the corresponding tables below each graph. For **(a)** and **(b)** ¢ = significantly different from XX +, § = significantly different from XY +.

3.2.2 Expression of *Znrf3* in a known sex-reversing mutant: *Gadd45g*

Gadd45g null mice show complete XY male-to-female sex reversal on a B6 background (Warr et al. 2012). WMISH studies were attempted on *Gadd45g* null tissue. However, *Znrf3* expression was variable and weak, and data are not shown here. qRT-PCR was instead attempted on sub-dissected embryonic gonads to compare expression between wild-type gonads and those lacking *Gadd45g*.

Quantitative real-time PCR analysis was carried out on subdissected gonads at 11.5 dpc and 12.5 dpc. These data confirm that *Gadd45g* expression is significantly downregulated in *Gadd45g* null gonads at all ages, and in both sexes, except in XX 11.5 gonads (**Fig. 3.6a**). When comparing expression of *Znrf3* in wildtype and *Gadd45g*$^{-/-}$ gonads, no difference is seen in 11.5 dpc gonads of either sex, or in XX 12.5 dpc gonads (**Fig. 3.6b**). However, *Znrf3* expression is significantly reduced in XY Gadd45g$^{-/-}$ gonads compared to XY wild-type compared at 12.5 dpc. Interestingly expression in the XY *Gadd45*-null gonad is also significantly reduced compared to XX wild-type gonads. Primers were also designed to be specific for each of the 3 transcripts of *Znrf3* (**Fig. 3.6c, d, e**). Detected expression levels of each of the transcripts was very low compared to *Hprt1*. No significant difference in expression of any transcript was seen when comparing wild-type and *Gadd45g*$^{-/-}$ gonads.

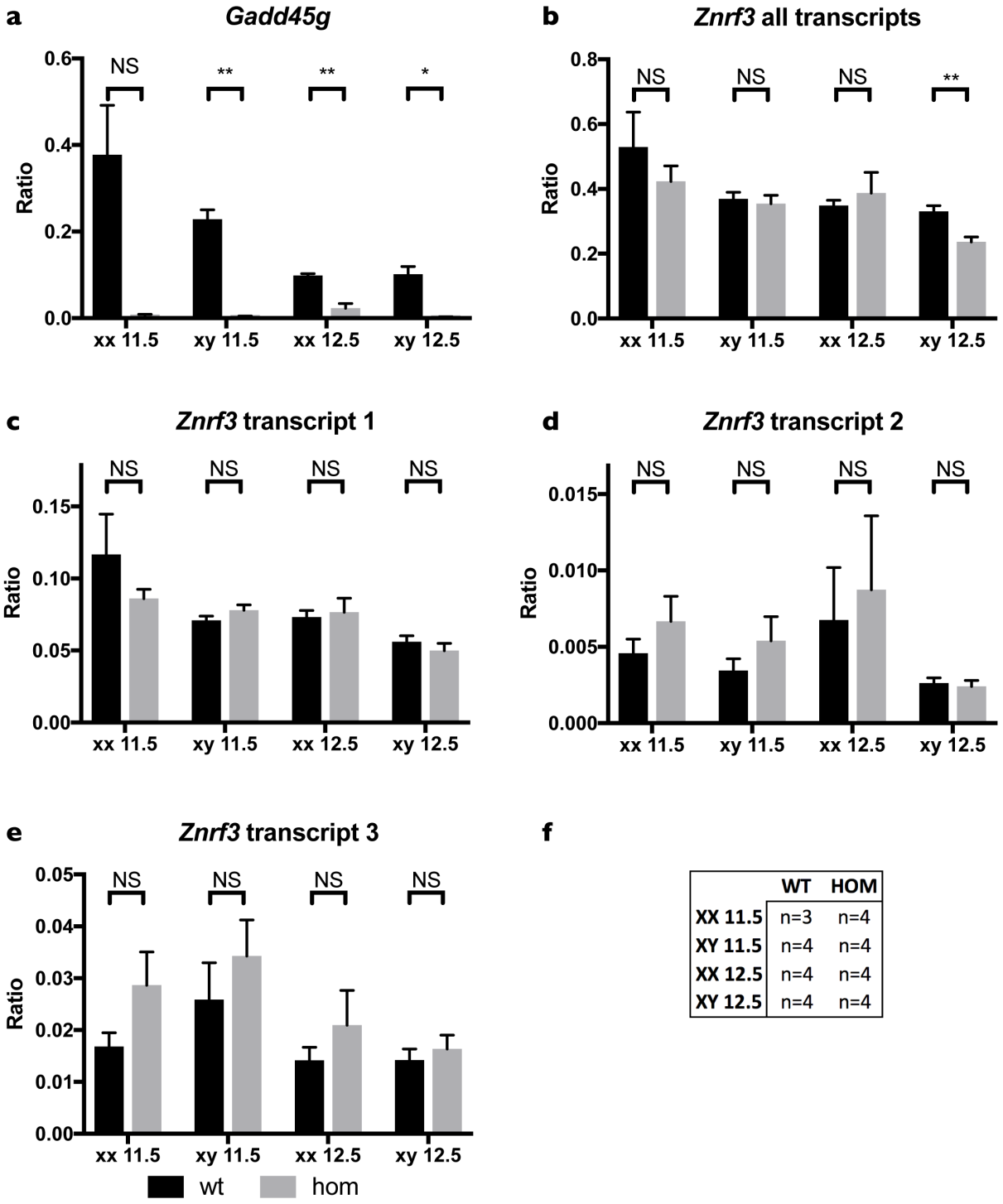

Figure 3.6 Expression of *Znrf3* in *Gadd45g*-null gonads. qRT-PCR was performed on wildtype (black) and *Gadd45*$^{-/-}$ (grey) subdissected gonads at 11.5 and 12.5 dpc. Expression of *Gadd45g* **(a)** and *Znrf3* (all transcripts) **(b)** was analysed. Expression of individual transcripts was also analysed: transcript 1 **(c)**, transcript 2 **(d)** and transcript 3 **(e)**. Expression was calculated relative to *Hprt1* (ratio). Error bars show SEM. T-tests (two-tailed) were performed with Welch's correction. Significant results are signified by * = P<0.05, ** = P<0.01, and non-significant differences are signified by NS. Exact P-values are detailed in the appendix (Table S3). N-numbers for each experimental group **(f)**.

3.2.3 Protein studies

Multiple commercial antibodies were tested for Western blot and immunohistochemistry studies without success (data not shown). Subsequently, an antibody was raised in rabbits against two peptides from mZNRF3 (**Fig. 3.2**). Two rabbits (rabbit 37, and rabbit 42) were injected with both peptides, and antibodies were purified from each rabbit using either peptide1 or peptide2. The MRC Harwell proteomics team (Chris Esapa and Helen Hilton) verified the specificity of these antibodies on Western Blot. HEK293T cells were transfected with a m*Znrf3-GFP* construct expressing a tagged ZNRF3 protein. Protein from lysed cells was run on a Western Blot and an antibody against GFP was used alongside each of the purified ZNRF3 antibodies. A band of the correct size was identified which was detected by both anti-ZNRF3 antibodies and anti-GFP antibody (data not shown).

Subsequently, these antibodies were tested to ascertain whether they could detect endogenous protein. Whole heads, livers, kidneys and gonads were collected from wildtype and *Znrf3*-null 14.5 dpc embryos. The mutant and wildtype protein differ significantly in molecular weight **(Table S2**) and antibodies raised against either peptide should be able to recognise both mutant and wildtype protein. Therefore, if the antibodies recognise endogenous ZNRF3, a band with a size difference in wildtype and *Znrf3*-null tissues should be detected. A band running at approximately the expected weight of ZNRF3 (~ 90 kDa) can be seen in all lanes **(Fig. 3.7).** However, this band cannot correspond to ZNRF3 because the band is also present in homozygote tissues, but a full-length product of this size cannot be generated in *Znrf3*$^{-/-}$ animals. Antibodies were also tested on frozen sectioned tissue using immunohistochemistry, but no specific signal was detected (data not shown).

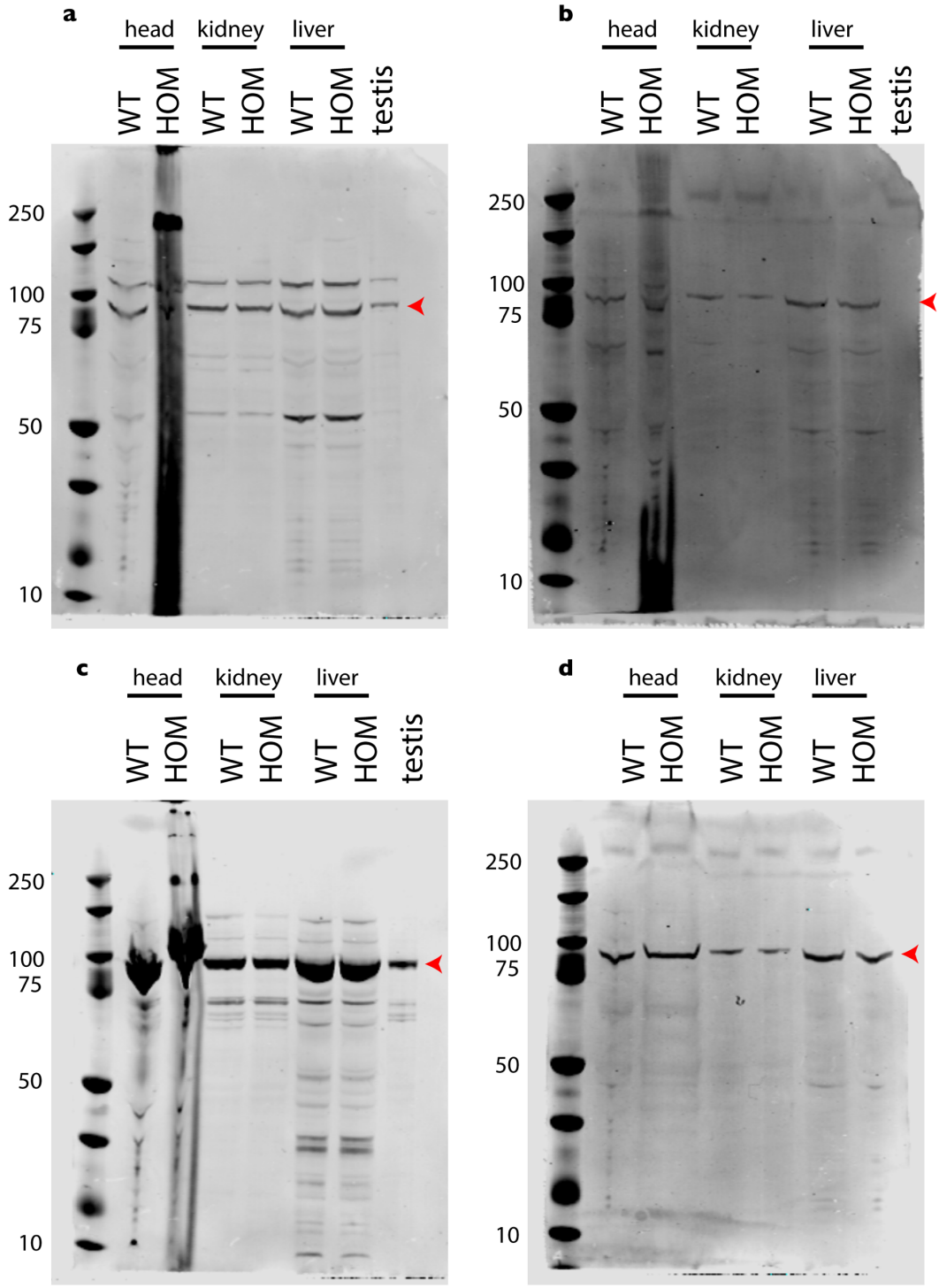

Figure 3.7 Western Blots using purified in-house antibodies. Western blots were run using tissue collected from 14.5 dpc embryos, including liver, kidney, whole heads and testis. The antibodies used were as follows: Rabbit 37, peptide 2 purified **(a)**, Rabbit 37, peptide 1 purified **(b)**, Rabbit 42, peptide 2 purified **(c)** and Rabbit 42, peptide 1 purified **(d)**. Red arrow shows presence of a band at approximately the expected weight of mZNRF3.

3.3 Discussion

3.3.1 *Znrf3*, but not *Rnf43*, expression can be detected in the embryonic gonad at the sex-determining stage

Several studies, including my own, show that *Znrf3* transcripts can be detected in the mouse embryonic gonad at the stage of primary sex determination. It appears to be present in all cell types of the gonad; it is also particularly abundant in the developing Wolffian duct of the adjacent mesonephros. Detection of *Znrf3* mRNA at the point of primary sex determination is good supporting evidence for a potential role in testis development. *Znrf3* could also be detected in *Sf1-eGFP*-positive cells, suggesting expression more specifically in the somatic cell lineage. In summary, *Znrf3* appears to be in the right place, at the correct time to be involved in primary sex determination.

Znrf3 expression in the embryonic gonad appears to be consistently low across all ages. WMISH experiments, despite several re-designs of the RNA-probe, required several days as opposed to several hours of staining. Although this analysis is not strictly quantitative and depends on the RNA-probe design and synthesis, it gives an indication of the lower levels of the transcript that may be present in the gonad compared to other regularly used probes, such as *Sox9.* Furthermore, the strong staining in the Wolffian duct could be used as an internal positive control. Expression in the gonad is comparatively weak in relation to this. On the other hand, *Znrf3* transcripts are sufficiently abundant to be detected in qRT-PCR experiments where the total amount of mRNA is often very low (200-220ng) due to the small size of the embryonic gonad. The low levels of expression detected in WMISH experiments may therefore be due to an artefact of probe design. However, the number of

sequence reads from *Znrf3* in single-cell RNAseq experiments is significantly lower than *Wt1* at the same stage, for example (Serge Nef & Isabelle Stevant, pers. comm.) (Stevant et al. 2017). If levels of *Znrf3* transcripts are in fact rare in the embryonic gonad, this may have implications for our ability to detect differential expression reliably and for mechanistic predictions and studies.

Rnf43 was not detected at significant levels in the embryonic gonad, either in our experiments or in independent transcriptomic studies. This effectively excludes *Rnf43* from playing a role in mouse testis determination, despite its high structural homology to ZNRF3. These data, combined with the positive identification of *Znrf3* in the gonad led us to focus effort and resources on investigating the role of *Znrf3* in testis determination. Therefore, the main body of this thesis will be centred on *Znrf3* and its function in the gonad.

3.3.2 Sexually Dimorphic expression of *Znrf3*

Many genes involved in sex determination are expressed at differing levels in the XX and XY gonad as early as 11.5 dpc: pro-testis genes *Sry* and *Sox9* are expressed exclusively in XY gonads at 11.5 dpc, whereas pro-ovarian *Wnt4* can only be detected in XX gonads (Sinclair et al. 1990; Kim et al. 2006). One notable exception to this is genes functioning upstream of *Sry*, such as *Map3k4* and *Gadd45g* (Gierl et al. 2012; Warr et al. 2012). This thesis hypothesises that *Znrf3* is a testis-determining gene, and therefore will be functioning in the developing gonad at the time of sex determination. Therefore, we might predict higher expression in the XY gonad compared to the XX gonad after *Sry* expression. If this is case, *Znrf3* could be positively transcriptionally regulated by a pro-testis factor or negatively regulated by a pro-ovarian factor. Indeed, sexually dimorphic expression was detected in previous transcriptomic studies (S. A. Jameson et al. 2012) and the WMISH data in this

chapter appear to confirm this. However, when quantitative (real-time) Reverse Transcription PCR (qRT-PCR) was performed on whole gonads, no difference was detected between XY and XX samples over multiple experiments.

As previously described, the supporting cell lineage is the critical cell lineage responsible for primary sex determination: *Sry* is expressed in these cells, and this initial switch is then relayed to the other cell types in the gonad (Burgoyne et al. 1988; Palmer and Burgoyne 1991). Therefore, we could hypothesise that *Znrf3* expression may only be sexually dimorphic in the supporting cell lineage, and not in others such as the germ cell or indeed other somatic cell lineages. The essentially ubiquitous expression of *Znrf3* throughout the gonad may be masking a subtle difference between XX and XY supporting cell precursors, particularly as *Znrf3* expression in the gonad appears to be low. This could explain why we are unable to detect a difference when RNA was extracted from whole gonad. Microarray data suggest that *Znrf3* expression is low and not sexually dimorphic in any cell lineages apart from supporting cells. However, even when the somatic cell lineage was enriched using FACs in this thesis, no significant difference could be detected between XX and XY GFP-positive populations of cells.

The expression of *Sf1* and *Sox9* seem to confirm that the experiment was sensitive enough to detect both differences in expression between the GFP-positive and -negative populations, and between XX and XY GFP-positive pools of cells. The difference in expression of *Sox9* between XX and XY at this stage is, in real terms, large whereas the difference detected by this experiment is significant, but only to P=0.05. This may indicate that this experiment is not sensitive enough to detect smaller differences in expression. The sensitivity of the assay is limited by the amount of tissue available for the experiment: each

pair of gonads yielded between 5,000 and 12,000 GFP-positive cells, from which only small amounts of RNA could be extracted. Due to the limited number of cells, samples from multiple experiments were pooled to obtain sufficient RNA concentrations to generate cDNA.

It is important to emphasise that the *Sf1-eGFP* population of cells is made up of the pre-Sertoli/pre-granulosa cell lineage as well as Leydig cell precursors, and possibly other somatic lineages. An attempt was made to collect only cells that were expressing high levels of *GFP* to enrich for the pre-Sertoli/granulosa cells (McClelland et al. 2015). However, this cut-off was arbitrary and it is therefore likely that the GFP-positive pools of cells comprised mixture of cell lineages. The microarray studies by Jameson et al. (2012) which indicate a sexually dimorphic pattern of expression use a *Sry-eGFP* reporter to collect supporting cells, which is a specific marker for this cell lineage. This may partially explain the discrepancy between the micro-array data and the data presented here.

Furthermore, by pooling cells from multiple gonads, the power of the experiment is reduced as we are unable to determine the contribution to the variance that individual pairs of gonads make. Finally, as previously described, expression of *Znrf3* appears to be very low in the gonad according to WMISH studies. Therefore, due to the low level of expression in a very small population of cells, a small but biologically relevant difference in the expression of *Znrf3* may have been missed.

Therefore, despite some evidence in the literature that expression of *Znrf3* is sexually dimorphic, this thesis was unable to convincingly recapitulate these results. However, these data do not eliminate the possibility that *Znrf3* is expressed at higher levels in the testis in the critical supporting cell lineage, as current methods may be insufficient to detect a subtle,

but biologically relevant difference. Moreover, significant sexually dimorphic expression may only be present in the very early gonad, prior to 11.5 dpc, and may have become less significant by 11.5 dpc. Assays prior to 11.5 dpc were not performed. Alternatively, or additionally, the main mode of regulation of ZNRF3 activity may not be transcriptional. For example, RSPO1 may regulate its activity in a sex-specific fashion, since its expression is higher in the XX gonad. This and other hypotheses for how ZNRF3 activity may be controlled in the developing testis will be discussed in Chapter 7.

3.3.3 Limitations of Microarray data

One important question for this thesis, is whether the microarray data for expression of *Znrf3* is reliable. Broadly, although the single-cell RNAseq only assayed expression in XY gonads, it is consistent with the microarray data. For example, the RNAseq data shows *Znrf3* expression decreasing between 11.5 dpc and 13.5 dpc in the cells identified as the pre-sertoli cell lineage, which is also seen in the supporting cell lineage in the microarray data. This supports the fact that the microarray data is accurate for *Znrf3.* However, there are disadvantages to using microarray chips for detecting differential expression. These issues stem from the use of a set of probes for each experiment. The use of probes can lead to issues such as cross-hybridisation (Slater et al. 2005). Furthermore, as probes must be designed, errors in detection due to alternative splicing and SNPs may occur (S. Zhao et al. 2014). In the case of detecting *Znrf3,* it is thus far unknown which of the three transcripts are expressed and which are important, and therefore the probes used to detect *Znrf3* may not be able to detect the functional transcript. Microarray methodologies are also particularly poor at detecting low level transcripts, in comparison to RNAseq, which may be relevant if *Znrf3* is expressed at a low level (S. Zhao et al. 2014). These limitations further

highlight the importance of recapitulating the sexually dimorphic expression detected by (S. A. Jameson et al. 2012).

3.3.4 *Znrf3* expression in *Gadd45g*-null gonads

Gadd45g functions upstream of *Sry* and regulates its expression through a Mitogen-Activated Protein Kinase (MAPK) cascade. XY *Gadd45g*$^{-/-}$ mice fully sex reverse and show delayed *Sry* expression which results in *Sox9* being absent from *Gadd45g*$^{-/-}$ gonads at 11.5 dpc (Warr et al. 2012; Johnen et al. 2013). Therefore, if *Znrf3* was transcriptionally regulated directly by *Sry* or *Sox9*, we might expect to see a difference in expression between XY wildtype and XY mutant gonads at the critical sex determining period. As expected, *Gadd45g* mRNA was significantly reduced in *Gadd45*$^{-/-}$ subdissected gonads. Furthermore, *Gadd45g* expression levels in the 12.5 dpc gonads are reduced compared to 11.5 dpc, which is consistent with WMISH data in (Warr et al. 2012). However, when levels of *Znrf3* transcripts were compared between *Gadd45g*-null and wildtype control gonads, no difference was detected at 11.5 dpc in either sex. This suggests that, at this stage, *Znrf3* expression is not being regulated by *Gadd45g*, or by *Sry* and *Sox9.*

By 12.5 dpc, the transcriptomes of the XX and XY gonad are beginning to diverge significantly (S. A. Jameson et al. 2012). *Wnt4* is strongly expressed in the XX gonad, and *Sox9* in the XY gonad. XY *Gadd45g* null gonads develop as ovaries, but at 12.5 dpc SOX9 can be detected a small number of cells (Johnen et al. 2013). Therefore, if *Znrf3* is positively regulated by the male pathway, we might expect *Znrf3* expression in an XY *Gadd45g*$^{-/-}$ gonad to be similar to levels in a wildtype XX gonad. Indeed, at 12.5 dpc *Znrf3* is significantly reduced in XY *Gadd45g*-null gonads compared to XY wildtype controls. However, interpretation of these results is complicated by the fact that no significant difference was seen between XX and XY

wildtype gonads at 12.5 dpc, confirming previous experimental results at this stage. This discrepancy indicates that the reduction in *Znrf3* expression in XY mutants cannot simply be explained by the biological sex of the gonads. Perhaps the loss of *Gadd45g* has a secondary effect, independent of the testis-determining pathway which causes *Znrf3* levels to be reduced?

We currently do not have enough information about *Znrf3* and its expression to fully understand these data. However, if time and resources permitted, this experiment could be repeated whilst being more selective about the ages of gonads used in the experiment. Furthermore, to reduce the impact of other cell lineages in the gonad, cell sorting using the *Sf1-eGFP* or more specific reporter lines line could be used to enrich for the somatic or supporting cell lineage. However, both experiments would be time-consuming, expensive and would require many mice.

3.3.5 How is *Znrf3* transcriptionally regulated in the gonad?

Notwithstanding microarray and WMISH data, the above qRT-PCR data suggest that *Znrf3* is not significantly sexually dimorphic in gonadal somatic cells at 11.5 dpc or beyond, and suggest that it is not transcriptionally regulated directly by SRY or SOX9. However, as previously described, *Znrf3* may only be regulated in the supporting cell lineage in a stage-specific fashion, and we may be unable to detect small differences in expression given the methodologies employed.

3.3.5.1 A direct role for SOX9?

Recently, a ChIP-seq data set has been published which details putative binding sites of SOX9 in a gonadal context. Binding sites proximal to *Znrf3* were identified in both bovine and mouse genomes (Rahmoun et al. 2017). This could suggest that SOX9 binds and activates,

or inhibits, *Znrf3* transcription in the XY gonad. In the bovine genome, the binding site was identified 9.9kbp away from the transcriptional start site (TSS) of *ZNRF3* (**Fig 3.8b)**. However, in the mouse, the binding site was 183.1kbp from the TSS of *Znrf3*, and is in fact closer to the TSS of *Kremen1* (**Fig 3.8a)**. *Kremen1* is another WNT-signalling antagonist, and its potential role in testis-determination will be discussed in **Chapter 7**.

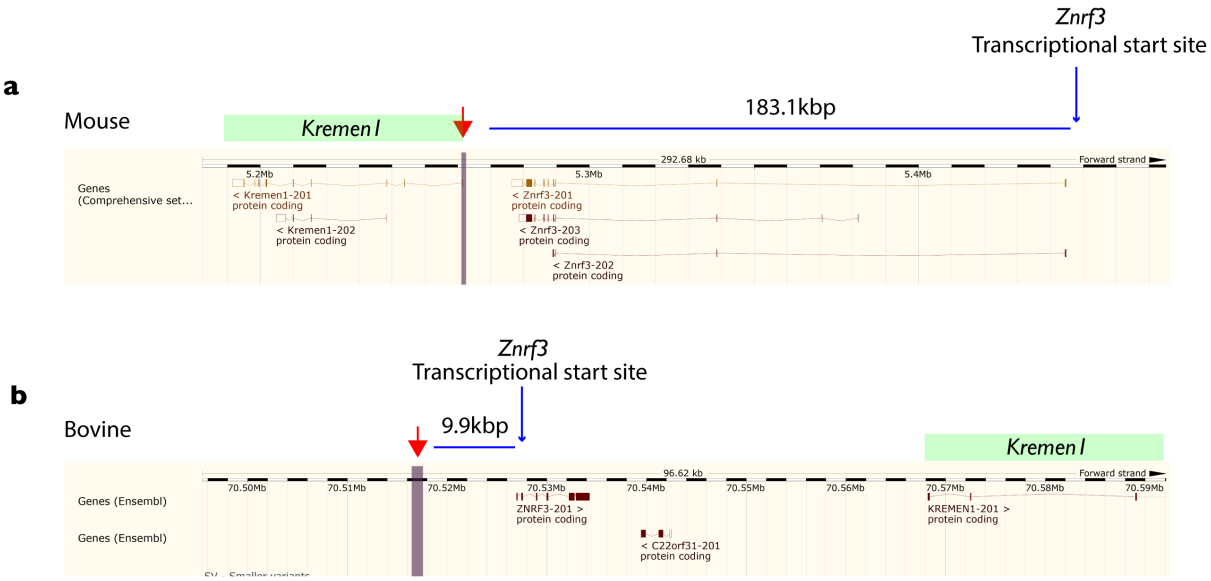

Figure 3.8 Location of putative SOX9-binding sites near *Znrf3*. Schematic showing location of *Znrf3* transcriptional start site (TSS), location of SOX9 binding site (highlighted in purple, and indicated by red arrow), location of *Kremen1* gene, and the distance of SOX9 binding from *Znrf3* TSS, in mouse **(a)** and bovine **(b)** genomes.

Other evidence in this thesis does not support a direct role for SOX9 in transcriptional regulation of *Znrf3* expression. For example, *Sox9* is strongly expressed in XY gonads, and is almost completely absent from XX gonads. If SOX9 was a strong positive regulator of *Znrf3* we might expect to see a similar ON/OFF pattern of expression in the developing gonads. Data in this chapter suggest *Znrf3* transcript levels are potentially only weakly sexually dimorphic in a stage- and cell lineage-specific fashion, even at 12.5 dpc when *Sox9* is strongly expressed in the XY gonad.

3.3.5.2 Feedback loop

Znrf3 and *Rnf43* are involved in a negative feedback loop: both are transcriptionally upregulated by elevated levels of canonical WNT-signalling. As previously described, they were identified in a human screen due to a positive correlation with *AXIN2* mRNA. But WNT-signalling levels are high in the XX gonad throughout gonadal development: thus, any enhanced expression of *Znrf3* in the XY supporting cell lineage is unlikely to be due to enhanced canonical WNT signalling and any suppression of *Znrf3* in the XX gonad is unlikely to be due to decreased canonical WNT signals. Sexually dimorphic expression in the manner suggested by microarray and WMISH data would have to rely on a regulatory network that was independent of any simple feedback mechanism and imposed differential expression. If such a mechanism to establish sexual dimorphism in *Znrf3* expression did exist, in the XY gonad, the upregulation by this mechanism would have to supersede the positive impact of the high WNT/β-catenin signalling which drives *Znrf3* expression in the XX gonad. Perhaps a more parsimonious explanation is that *Znrf3* is expressed equally in both sexes, and its activity is regulated post-transcriptionally.

3.3.4 ZNRF3: detecting the protein

Thus far, attempts to find a specific antibody which detects endogenous ZNRF3 protein has failed. Several commercial antibodies and in-house antibodies have been tested by Western blots and immunohistochemistry. Encouragingly, the homemade antibodies have been proven to detect an overexpressed form of the protein, which suggests they have some avidity for mouse ZNRF3. However, endogenous protein cannot be detected.

One hypothesis for this discrepancy is that the levels of ZNRF3 are too low to be detected. This is supported by WMISH studies where samples required 1-2 days of staining for a signal

to become apparent, suggesting low levels of transcript in the gonad. Furthermore, information on *Znrf3* expression in the mouse embryo is limited, and therefore, the tissues selected (gonad, kidney, liver, and whole heads) may not have been appropriate. The dynamic turnover of ZNRF3 could also make the protein hard to detect. ZNRF3 is removed from the plasma membrane in an Rspondin-dependent fashion (Hao et al. 2012). This active turnover of ZNRF3 molecules could mean that few molecules of ZNRF3 are present in the cell at one time. On the other hand, the in-house antibodies may in fact be detecting endogenous protein. In this case, the band seen in all lanes of the western blots may be obscuring the band which corresponds to ZNRF3.

Znrf3$^{-/-}$ tissue is an excellent negative control for Western Blot analysis. However, as we cannot preclude a truncated form of ZNRF3 being present in *Znrf3* null tissues, which our antibodies may still be able to recognise, it is more difficult to assess the specificity of these antibodies for immunohistochemistry. In this case strategies such as siRNA knockdown of *Znrf3* could be employed to generate a negative control. Alternatively, endogenous *Znrf3* could be tagged, which would preclude the requirement for an antibody, and furthermore, would allow us to carry out experiments such as live-imaging of ZNRF3 in the mouse gonad.

3.3.6 Summary and further questions

In summary, *Znrf3* is expressed in the gonad during the critical sex determining period in the mouse. This suggests that ZNRF3 could play a role in mammalian sex determination. Expression studies also provide some evidence that expression may be sexually dimorphic, showing upregulation in the XY gonad. However, this dimorphism, if present, is subtle and therefore may not be sufficient, on its own, to explain a role in the testis, and significantly reduced activity in the ovary. Furthermore, examining expression in a known sex-reversing

mutant suggests that *Znrf3* is not regulated directly by SRY or SOX9, at least at 11.5 dpc. Therefore, it is possible that ZNRF3 activity is regulated by other means.

Finally, *Rnf43* appears to be absent from the embryonic gonad, and cannot be detected in transcriptomic studies or by WMISH. This suggests that *Rnf43* is unlikely to play a role in mammalian sex determination.

Chapter 4: The role of ZNRF3 in sex determination

4.0 Introduction

In the previous chapter, it was shown that *Znrf3,* but not *Rnf43*, is present in the mouse embryonic gonad during the critical sex determination period. The evidence presented in Chapter 3, combined with the known role for *Znrf3* in antagonising canonical WNT signalling, a crucial component of the ovarian pathway, is sufficient to justify our investigation of this gene *in vivo*. This chapter will investigate the sexual development phenotype of *Znrf3*-null mice using a loss-of-function (LOF) allele which disrupts the critical Ring Finger domain.

4.0.1 Using gain- and loss-off-function alleles

A range of different tools can be used to study the function of a gene *in vivo* in the mouse. Genetic manipulations can be characterised by the effect they have on the function of the protein. Loss-of-function (LOF) mutations result in partial or complete loss of protein function, whereas gain-of-function (GOF) mutation results in an enhanced, or a new molecular function for the protein (Griffiths 2000). LOF mutations occur more frequently in nature than GOF mutations. They frequently act in a recessive manner, because a single copy of the wild-type allele is often sufficient to maintain wild-type function. This can sometimes be achieved through upregulation of the wild-type allele to sustain sufficient levels of a functional protein. However, LOF alleles can also act in a dominant or semidominant fashion and cause a phenotype in the heterozygous condition. This can be

due to haploinsufficiency, where the amount of wild-type protein falls below the threshold for normal function.

GOF alleles, on the other hand, mostly act in dominant fashion. The mutant protein can adopt an entirely new function (neomorphic), become dysregulated and overactive (hypermorphic) (Hawley and Walker 2003) or can act in a dominant negative fashion (Herskowitz 1987). For example, a neomorphic mutation may lead to a transcription factor binding and activating a different gene. A hypermorphic mutation may instead prevent the transcription factor from being post-translationally inhibited, leading to over activation of its downstream targets. In this case of a dominant-negative allele, a transcription factor could lose the ability to recruit the transcriptional machinery due to a GOF mutation, but retain the ability to bind DNA. By binding DNA at the target site, it could block wild-type transcription factors from binding here, thereby acting to inhibit rather than promote gene expression. Another commonly used GOF tool is transgenic overexpression of a gene. In this case, multiple copies of the gene of interest are inserted into the host genome, which leads to high levels of expression of the protein of interest (reviewed in (Lewandoski 2001)).

Both LOF and GOF mutations can be generated in mice, and can be useful tools for studying gene function. Global knockout models carry two LOF alleles in every cell. This means that the protein of interest is non-functional in all cell types and tissues. This can be advantageous if you wish to investigate multi-organ or multi-tissue disorders, but can result in lethality. Conditional knockout (CKO) mutants allow spatial or temporal specificity of gene knockout (Sauer 1987; Sauer and Henderson 1988; Orban, Chui, and Marth 1992; Friedel et al. 2011). This relies on the presence of a conditional allele: an allele with recombination sites, such as *LoxP* sites, flanking critical exons or the whole gene. A second component is

required to drive the recombination of these *LoxP* sites in a specific tissue and time. Cre protein, when expressed will cause the *LoxP* sites to recombine and excise the region they flank. Cre expression can be driven by an endogenous tissue-specific promoter (Orban, Chui, and Marth 1992). Alternatively, an inducible Cre allele can be used, where recombinase activity is dependent on the introduction of Tamoxifen (Zhang et al. 1996; Metzger et al. 1995; Feil et al. 1997; Feil et al. 1996). Tamoxifen is given to mice at specific time-points to induce recombination, and therefore inactivation of the allele, during embryonic development or adulthood. Furthermore, a conditional, tissue-specific allele can also be designed such that, upon tamoxifen exposure, the gene will only be inactivate in a specific tissue or set of tissues. Conditional alleles can therefore be used to analyse the effects of mutations that may be lethal in the homozygous state. Furthermore, they can be used to investigate tissue- or temporal-specific effects of the LOF of a gene.

4.0.2 Analysing Primary Sex Reversal

Disorders of Sex Development (DSDs) occur when chromosomal, gonadal or anatomical sex are atypical (Hughes et al. 2006). As previously described **(Chapter 1)**, DSDs can develop due to failures of multiple stages of sex development: failure to initially pattern the gonad; failure to maintain the sexual fate of the gonad; or a failure to produce or respond appropriately to androgens produced by the gonad. Some may be caused by an intrinsic failure of differentiation of internal or external genitalia (F. Zhao et al. 2017). Primary sex determination defects occur when the initial fate decision in the bipotential gonad is not made appropriately. Most frequently, in the case of an XY individual, this leads to the development of a dysmorphic testis or an ovotestis, which contains both testicular and

ovarian tissue. Rarely, complete primary sex reversal can occur whereby an XX individual develops a testis, or an XY individual develops an ovary.

This thesis will focus on cases where primary sex determination is affected. Several tools can be used to assess the extent of the sex reversal phenotype. As previously described, *Sox9* is both sufficient and necessary for testis determination, and is directly downstream of *Sry* in the testis-determining pathway (Sekido and Lovell-Badge 2008). Expression of *Sox9* can therefore be used to mark somatic (pre-Sertoli) cells which have initiated testis-determination. *Stra8* is a pre-meiotic germ cell marker, which is expressed in a female-specific pattern from 13.5 dpc in the mouse embryonic gonad (Kumar et al. 2011). Therefore, in this thesis *Sox9* and *Stra8* will be commonly used as markers of male and female gonad development, respectively. Analyses are carried out at 14.5 dpc after primary sex determination, when the testis and ovary have differentiated and when both *Stra8* and *Sox9* are strongly expressed in wild-type XX and XY gonads, respectively.

In the adult mouse, external genitalia can be assessed using an anogenital distance measurement which is greater in wild-type XY individuals than in XX. Furthermore, dissection of the internal reproductive system can identify any gross morphological differences, and histopathological studies, more subtle differences. Internal and external reproductive tract morphology develops as a response to hormones produced by the gonad. Therefore, abnormal morphology seen at this stage, but not in the embryonic gonad, may indicate a role for the gene in other aspects of sexual development. In this way, we can assess the point in sexual development which is affected.

4.0.3 Rationale for using a sensitised background, B6.Y^{AKR}

Our initial interest in ZNRF3 was in part due to the discovery of human DSD patients carrying mutations in *ZNRF3*. Most DSD human patients are heterozygous for causative deleterious mutations (Laino et al. 2014). Furthermore, the variability of the human genome within the population means that genetic background plays a significant role in the manifestation of DSDs in humans. In this case, homozygous null mice which carry two alleles of the non-functional protein may not be the most applicable model for human DSDs. As previously described, B6.Y^{AKR} male mice are sensitised to male-to-female sex reversal. This genetic background can therefore be used to mimic the potentially sensitised genome of individual human DSD patients, and may allow us to better model the human heterozygous condition.

4.0.4 Compensation by homologous proteins

There are many examples in genetic analyses in which the loss of function of one protein may be compensated for by the function of another, possibly similar, protein. This can often lead to the suppression of a phenotype, which may not be revealed until a double-knockout analysis is performed. For example, when deleted individually in the mouse, *Sfrp1* and *Sfrp2* show no gonadal phenotype. However, if both are simultaneously removed, small and abnormally positioned testes form (Warr et al. 2008). ZNRF3 and RNF43 share low sequence identity (29% - Needleman-Wunsch algorithm, see **Fig S2**), but are functional homologues of each other (Hao et al. 2012; Koo et al. 2012). Both proteins modulate WNT-signalling through ubiquitination of the Frizzled receptor. Therefore, the presence of one may be able to compensate for the absence of the other. This can be tested using compound mutants which lack functional copies of both genes.

4.0.5 Maintenance of testicular fate in the adult gonad

Although the initial developmental switch of sex determination is robust, it is now understood that the identity of the gonad as either a testis or an ovary is not irreversibly fixed. Ablation or ectopic expression of some genes, including *Foxl2, Dmrt1* and *Sox8/Sox9,* in the adult gonad can lead to a post-natal switch in identity.

FOXL2 is a transcription factor which is required for the suppression of the testis-determining pathway in the adult ovary. *Foxl2* null ovaries are normal during embryonic development, but transdifferentiate around birth when they begin to express male marker genes (Ottolenghi et al. 2005). Ablation of *Foxl2* in adults is sufficient to cause somatic cell reprogramming from the granulosa fate to the Sertoli cell fate (Uhlenhaut et al. 2009). Adult loss of *Foxl2* is also sufficient to begin to change the gross morphology of the gonad: XX mutant gonads develop seminiferous tubule structures (Uhlenhaut et al. 2009).

Dmrt1 is expressed in both the testis and the ovary until 13.5 dpc, when it is specifically downregulated in the XX gonad. It is not required for initial sex determination in mice but is necessary for the maintenance of Sertoli cell fate. XY *Dmrt1*$^{-/-}$ mice are born male, and have normal testes (Raymond et al. 2000) but undergo partial male-to-female sex reversal when adult. 4-weeks postnatally, XY null gonads show significant *Foxl2* expression (Matson et al. 2011). Deleting *Dmrt1* in XY adults using a tamoxifen-inducible Cre is sufficient to replicate this sex reversal phenotype. Cells resembling granulosa cells, which express both *Foxl2* and *Sox9,* and others that express *Foxl2* alone, can be detected 4 weeks after tamoxifen treatment (Matson et al. 2011). Therefore, *Dmrt1* is not necessary for initial testis determination, but is required for maintenance of testicular fate in adults.

Mice in which overexpression of *Dmrt1* is driven by *Sf1-Cre* in the somatic cell lineage of the XX gonad are born with ovaries (Lindeman et al. 2015), despite *Sf1-Cre* being active at around the time of primary sex determination (Bingham et al. 2006). Earlier activation of *Dmrt1*-overexpression at around 9.5 dpc by *Wt1-CreERT2* is also not sufficient to cause primary sex reversal (Lindeman et al. 2015). Lindeman et al., show that transdifferentiation of the somatic cell lineage from granulosa to Sertoli fate occurs in the adult. Sertoli-like cells expressing *Sox9* and GATA1 are seen, and there are significantly fewer *Foxl2*-positive cells in the XX mutant gonad, compared to wild-type control ovaries. Interestingly, nearly all the genes affected by a loss of *Foxl2* in the adult gonad change in the same direction when *Dmrt1* is postnatally ectopically expressed suggesting that ectopic *Dmrt1* may completely account for the *Foxl2*-loss phenotype, as described above. However, other studies disagree with this interpretation. (Zhao et al. 2015) show that when *Dmrt1* overexpression is driven in XX gonads by a *Wt1*-BAC transgene system, XX transgenic gonads show masculinisation at 14.5 dpc. This is perhaps due to differences in the level of overexpression in each model.

Similarly, *Sox9* and *Sox8* are required to maintain the testicular fate. *Sox9* and *Sox8* are highly homologous (67% homology, (Schepers et al. 2003)) and have been shown to function redundantly in the embryonic gonad (Chaboissier et al. 2004). Loss of *Sox8* alone does not cause a sex development phenotype, and mice are fertile with histologically normal embryonic testes and in the adult until p120, when some germ cells are seen to desquamate (Barrionuevo et al. 2016; Chaboissier et al. 2004). When *Sox9* is deleted in the adult gonad, on a *Sox8* null background, seminiferous tubules become disorganised and Sertoli cells begin to transdifferentiate into *Foxl2*-expressing granulosa-like cells. Furthermore, *Dmrt1* is

downregulated indicating that *Sox8/9* play a role in maintaining its expression in the adult gonad (Barrionuevo et al. 2016).

In summary, DMRT1 is required to constantly repress *Foxl2* in the adult testis and prevent transdifferentiation and *Sox8/9* are required to maintain *Dmrt1* expression. There is thus far no evidence in the literature that WNT-signalling is required in the adult ovary. Therefore, any role for ZNRF3 in opposing pro-ovarian WNT signals may be limited to the embryonic gonad. However, given that other testis-determining genes such as *Sox9* have been shown to play a dual role in primary sex determination and in maintenance, and given that the relevant mouse lines were available, a small cohort was bred to test this hypothesis.

4.0.6 Aims

This chapter will investigate the role of *Znrf3* and, despite the lack of expression detected in the previous chapter, *Rnf43* in mouse sex determination. It will present data from embryonic and adult gonads to assess the extent of sex reversal in *Znrf3*-null gonads. Furthermore, a sensitised background will be used to exacerbate the phenotype and model the sensitised genome of some human DSD patients. Finally, this chapter will assess the role of *Znrf3* in the adult testis through conditional deletion in adult mice.

4.1. Results

4.1.1 Generation of *Znrf3* and *Rnf43* null embryos

The following rederivation was managed by myself and carried out by the staff of the MRC Mary Lyon Centre, at Harwell.

Three conditional knockout (CKO) male mice were imported that harboured floxed alleles of both *Znrf3* and *Rnf43* (**Fig. 4.1**). Males were culled and sperm was taken for in vitro fertilisation of C57BL/6J (B6) wild-type eggs to generate heterozygote F1 animals. One cohort was re-derived after treating fertilised eggs with soluble Cre protein to immediately generate deletion alleles in the F0 generation. A second cohort was re-derived without soluble Cre and these conditional alleles were banked for future use in the frozen sperm archive. 40 pups were born in the untreated cohort and 24 pups in the soluble Cre-treated cohort. The $Znrf3^{flox}$ allele successfully recombined due to soluble Cre treatment and $Znrf3^{+/-}$ mice were generated. Successful deletion of the critical region was confirmed by sequencing (data not shown) and further breeding segregated the alleles. No recombined alleles were detected for *Rnf43*, and therefore $Rnf43^{+/flox}$ mice were crossed to a β-*actin-Cre* line which expresses Cre protein ubiquitously. Successful recombination of the allele in the following generation was confirmed by sequencing and further breeding segregated the alleles.

To generate homozygous null embryos, intercross matings were set up between $Znrf3^{+/-}$ or $Rnf43^{+/-}$ animals. By inspection, $Rnf43^{-/-}$ embryos show no gross morphological abnormalities (data not shown). $Znrf3^{-/-}$ embryos of both sexes were grossly normal but showed an eye development defect, visible from 12.5 dpc onwards in all null embryos (**Fig. 4.2a**). Rarely, this defect was also seen in $Znrf3^{+/-}$ embryos in a single eye, and in adults of

the same genotype (Fig. 4.2b, c). Some *Znrf3*$^{-/-}$ embryos also showed exencephaly and others craniofacial abnormalities (Fig. 4.2d).

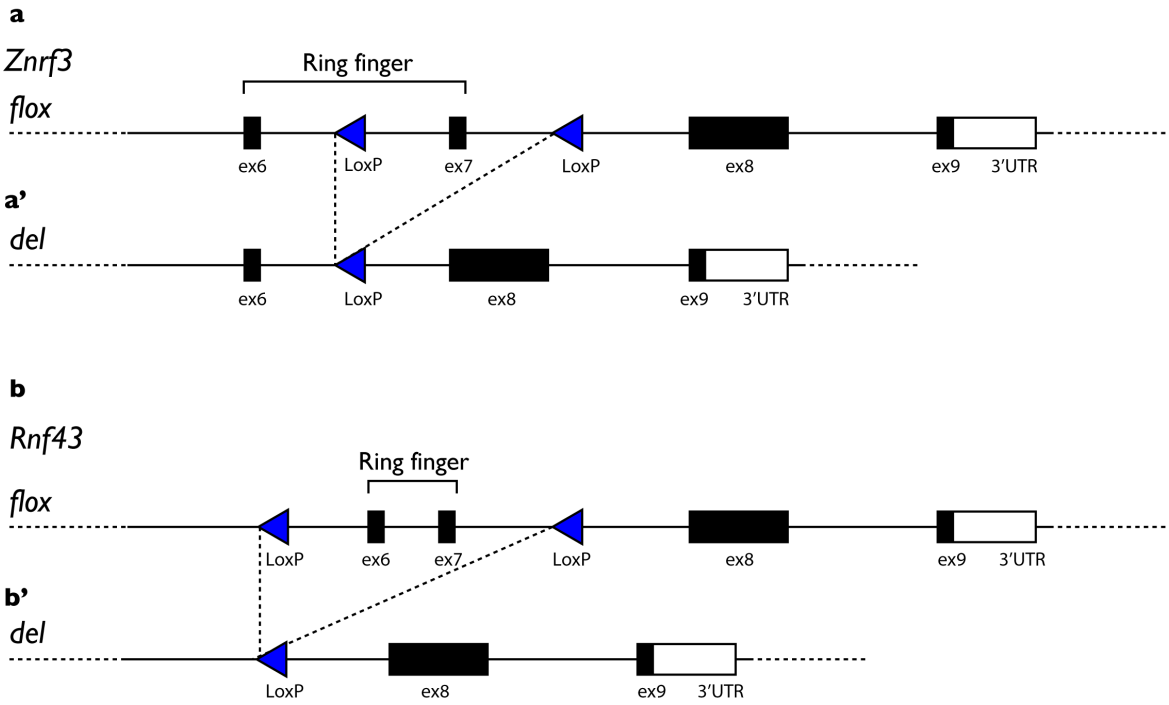

Figure 4.1 Allele structure for *Znrf3* and *Rnf43*. Not drawn to scale. The *Znrf3*^{flox} allele has LoxP sites flanking exon 7, one of the critical exons for the Ring Finger domain **(a).** After exposure to soluble Cre, these recombine to generate the *Znrf3*$^{-}$ allele **(a').** The *Rnf43*^{flox} allele has LoxP sites flanking exons 6 and 7 which together code for the Ring Finger domain **(b)**. When these mice were crossed to *actin-Cre* these recombined to generate the *Rnf43*$^{-}$ allele **(b').**

The total number of embryos of each genotype, between 11.5 and 16.5 dpc, was analysed using a Chi-squared test. When carried out on XY embryos, the observed numbers did not differ significantly from the expected Mendelian ratios (Chi-squared test, two tailed, p=0.4361). However, there was a significant difference when analysis was carried out on XX embryos (Chi-squared test, two tailed, p=0.0253). This is due to a decrease in XX *Znrf3*$^{-/-}$ embryos compared to the expected. Due to time constraints, this phenomenon was not investigated further.

It was reported in (Hao et al. 2012) that *Znrf3*$^{-/-}$ animals die around birth. Consistent with this, we found embryos of each genotype in the correct ratio at 18.5 dpc (Chi-squared test, two-tailed, p=0.6514, data not shown). Mice potentially carrying homozygote embryos were never allowed to litter down due to welfare concerns.

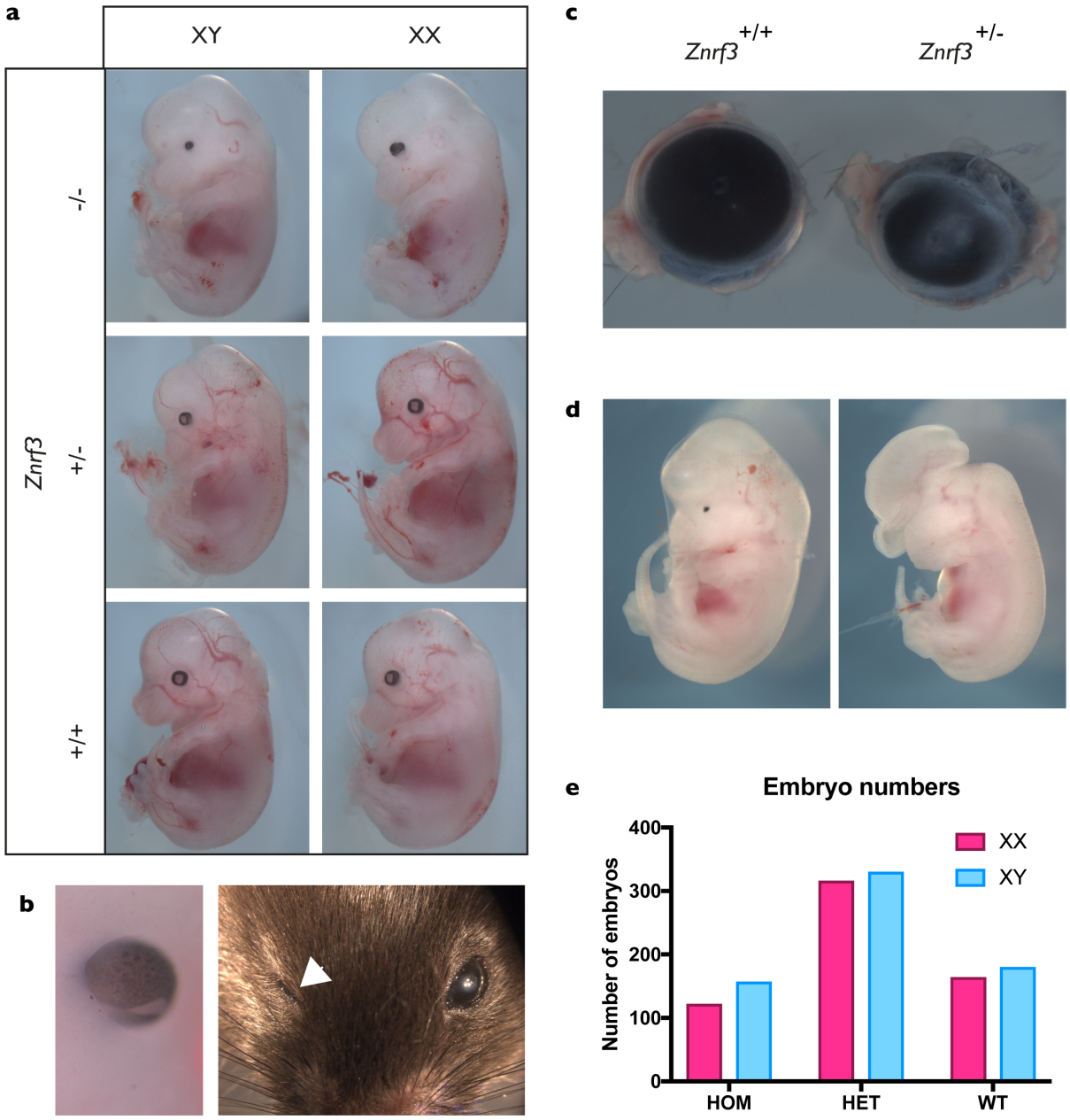

Figure 4.2 Gross embryonic and adult phenotypes of *Znrf3*$^{+/-}$ and *Znrf3*$^{-/-}$ mice. Whole embryos (13.5 dpc) **(a).** *Znrf3*$^{+/-}$ 14.5 dpc embryo (left) and adult (right) eye phenotype. White arrow indicates missing eye in the adult **(b)**. Dissected eyeballs from *Znrf3*$^{+/+}$ and *Znrf3*$^{+/-}$ adults **(c).** 13.5 dpc *Znrf3*$^{-/-}$ embryos with a severe eye phenotype (left) and exencephaly (right) **(d)**. Graph showing total number of *Znrf3*$^{-/-}$ (HOM), *Znrf3*$^{+/-}$ (HET) and *Znrf3*$^{+/+}$ (WT) embryos of each sex collected. Embryos were aged between 11.5 dpc and 16.5 dpc. A table of exact numbers can be found in the appendix (Table S4) **(e).**

4.1.2 *Znrf3*-null gonads show partial XY male-to-female sex reversal

WMISH was carried out on explanted gonads from mutant and control embryos using probes for two marker genes of testicular and ovarian fate. As previously described, *Sox9* is expressed in Sertoli and pre-Sertoli cells and labels supporting cells which have adopted the testicular fate. *Stra8* is a marker of pre-meiotic germ cells, and labels germ cells in an ovarian context. In wild-type XY 14.5 dpc gonads, *Sox9* expression was restricted to the testis cords. Some expression was also seen in the mesonephros. However, *Stra8* was not detected. In contrast, wild-type XX gonads at 14.5 dpc expressed *Stra8* along the length of the gonad and no *Sox9* expression was detected. XY *Znrf3*$^{+/-}$ gonads were comparable to wild-type controls. No *Stra8* expression was seen in any XY heterozygotes (n=6, two independent experiments) and *Sox9* WMISH revealed cord structure was well organised, and extended fully to the poles of the gonad (**Fig. 4.3a**).

XY *Znrf3*$^{-/-}$ gonads showed a range of abnormalities at 14.5 dpc, from full male-to-female sex reversal to minor disruptions to testis morphology. Some were elongated testes with cords extending along most of the length of the gonad, but with narrower and less well defined structure than controls (**Fig. 4.3a [1]**). Ovotestes were also seen, which showed *Sox9* expression in part of the gonad, sometimes associated with an attempt at testis cord formation (**Fig. 4.3a [2]**). Rarely, a gonad indistinguishable from an ovary was seen, with no *Sox9* expression detected (**Fig. 4.3a [3]**). When this was seen, the other gonad in the pair was often an ovotestis. XY *Znrf3*$^{-/-}$ gonads showed some sporadic *Stra8* expression. However, this was also highly variable, was excluded from testicular regions of ovotestes,

and was generally at a lower level when compared to wild-type XX littermate controls (**Fig. 4.3a**).

As confirmation of the phenotypes detected by WMISH, antibodies against FOXL2 and Anti-Mullerian hormone (AMH) were used on sections of 14.5 dpc gonads (**Fig. 4.3b**). A range of different XY *Znrf3*$^{-/-}$ gonads were chosen to reflect the variability in phenotype seen. AMH, a Sertoli cell marker, was concentrated in the testis cords of XY wild-type gonads and was never seen in XX wild-type ovaries (n=3). FOXL2, a granulosa cell marker, was detected in wild-type XX gonads, but never in wild-type XY testes. FOXL2 was detected in all XY null gonads (n=5). As expected, a range of different phenotypes were observed. Some mutant gonads predominantly expressed FOXL2, and others had widespread AMH expression and reasonably well defined cords. FOXL2 expression in XY *Znrf3*$^{-/-}$ gonads appeared to be focused in the region of the gonad adjacent to the mesonephros (**Fig. 4.3b**). Conversely, AMH expression was restricted to areas of cord formation; it was often concentrated in the centre of the gonad, and never at the extreme poles of the gonad. AMH-positive cells appeared to be preferentially found in the tissue furthest from the mesonephros (**Fig. 4.3b**).

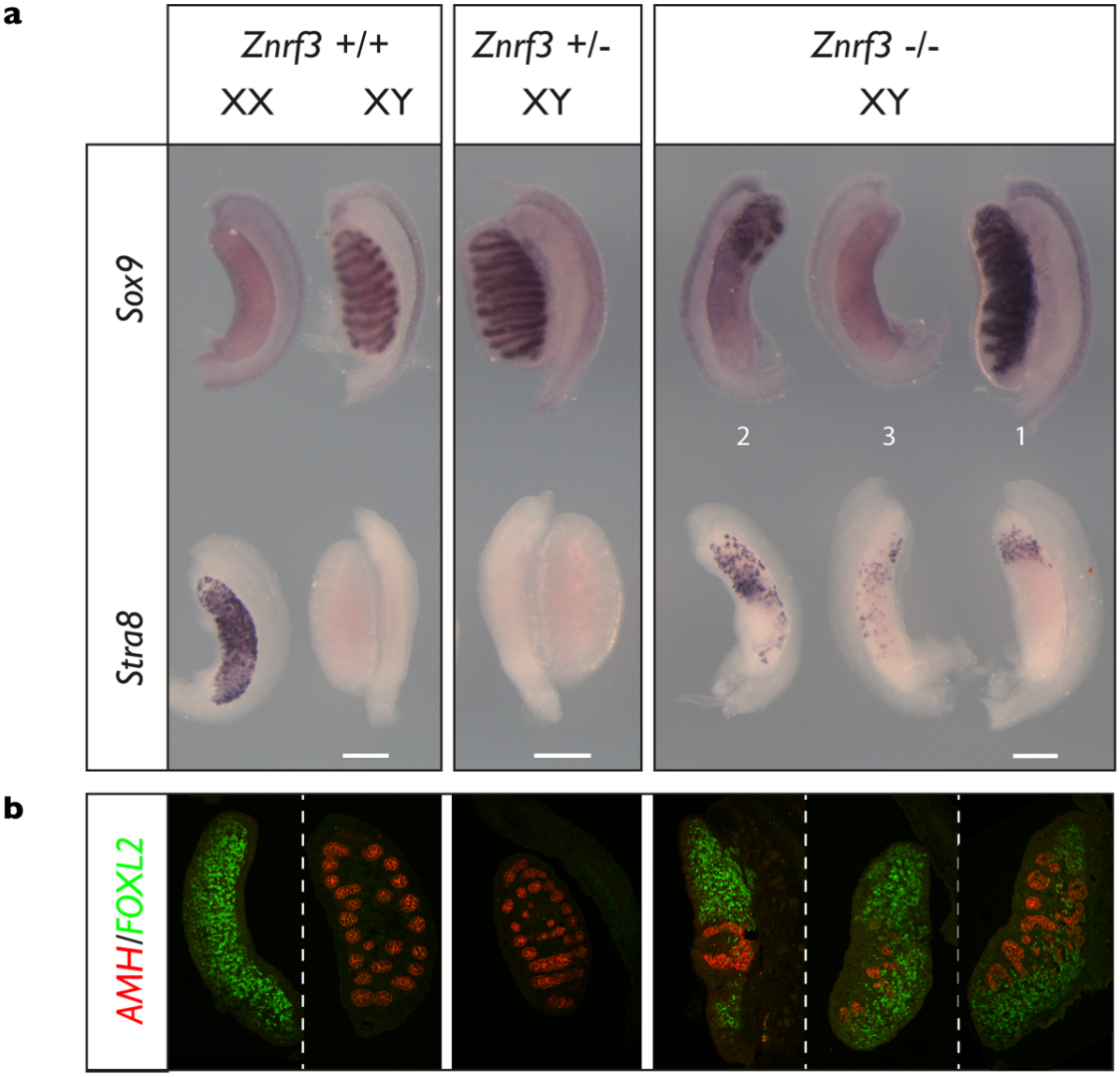

Figure 4.3 Sex reversal phenotype in XY *Znrf3*$^{-/-}$ gonads. WMISH was carried out on 14.5 dpc gonads. The top row shows expression of *Sox9* and the bottom row shows expression of *Stra8*. Scale bar 250μm **(a)**. Immunofluorescence staining was carried out using an anti-AMH (red) and an anti-FOXL2 antibody (green) on wax sections of 14.5 dpc gonads **(b)**.

4.1.3 Loss of *Znrf3* on B6.Y^{AKR} leads to full XY male-to-female gonadal sex reversal

The B6.Y^{AKR} line carries a Y-chromosome from a *Mus. domesticus* strain (AKR/J) on a congenic B6 background, and is sensitised to disruptions to testis determination. Wild-type B6.Y^{AKR} gonads develop as transient ovotestes, with a small area of ovarian tissue at the poles of the gonad, denoted by *Stra8* expression, visible at 14.5 dpc; these resolve during development to form hypoplastic testes with normal fertility. *Znrf3*$^{+/-}$ B6.Y^{B6} mice form normal testes (**Fig. 4.3a**) and are fertile. However, when just one copy of *Znrf3* was lost on B6.Y^{AKR}, partial and full sex reversal was seen at 14.5 dpc. Several heterozygous XY gonads showed *Stra8* expression along the length of the gonad and had an ovarian morphology (**Fig. 4.4a [1]**). Others were ovotestes, with central *Sox9* expression (**Fig. 4.4a [2, above]**) and expanded regions of *Stra8* expression at the poles compared to *Znrf3*$^{+/+}$ B6.Y^{AKR} gonads (**Fig. 4.4a [2, below]**). *Sox9* expression showed that, although it was expressed extensively in some XY gonads, testis cords have not formed (**Fig. 4.4a [3]**). When two copies of *Znrf3* were lost, all XY gonads showed full XY male-to-female sex reversal (n=5). XY^{AKR} *Znrf3* null gonads showed no *Sox9* expression and sporadic *Stra8* expression (**Fig. 4.4b**).

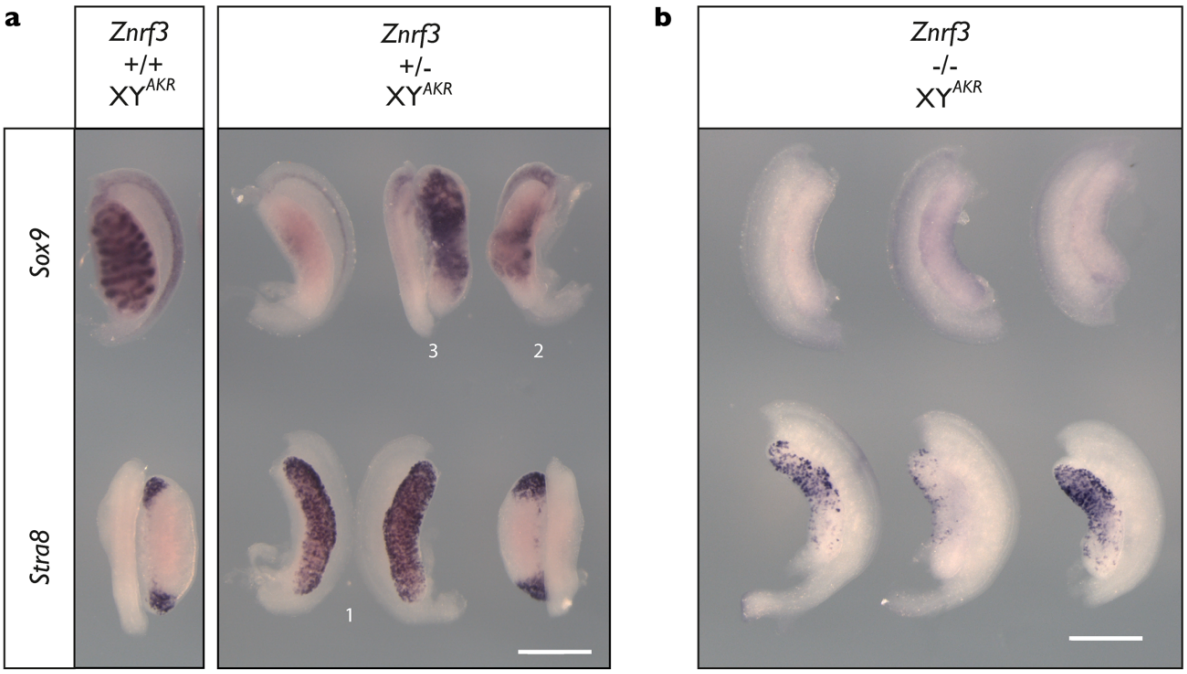

Figure 4.4 Sex reversal phenotype in B6.Y^{AKR} *Znrf3*$^{+/-}$ and *Znrf3*$^{-/-}$ embryos. WMISH was carried out on *Znrf3*$^{+/-}$ B6.Y^{AKR} **(a)** and *Znrf3*$^{-/-}$ B6.Y^{AKR} (in a separate experiment), 14.5 dpc gonads **(b).** Top row shows expression of *Sox9* and bottom row shows expression of *Stra8*. Scale bars 500μm.

4.1.5 *Stra8* expression in *Znrf3* null gonads

It was observed in previous experiments that *Stra8* expression in XY *Znrf3*-null gonads appeared to be reduced. WMISH was carried out on XX *Znrf3*$^{-/-}$ gonads: *Stra8* was significantly reduced compared to wild-type littermate controls, although variability in expression between embryos of the same genotype was significant (**Fig. 4.5**).

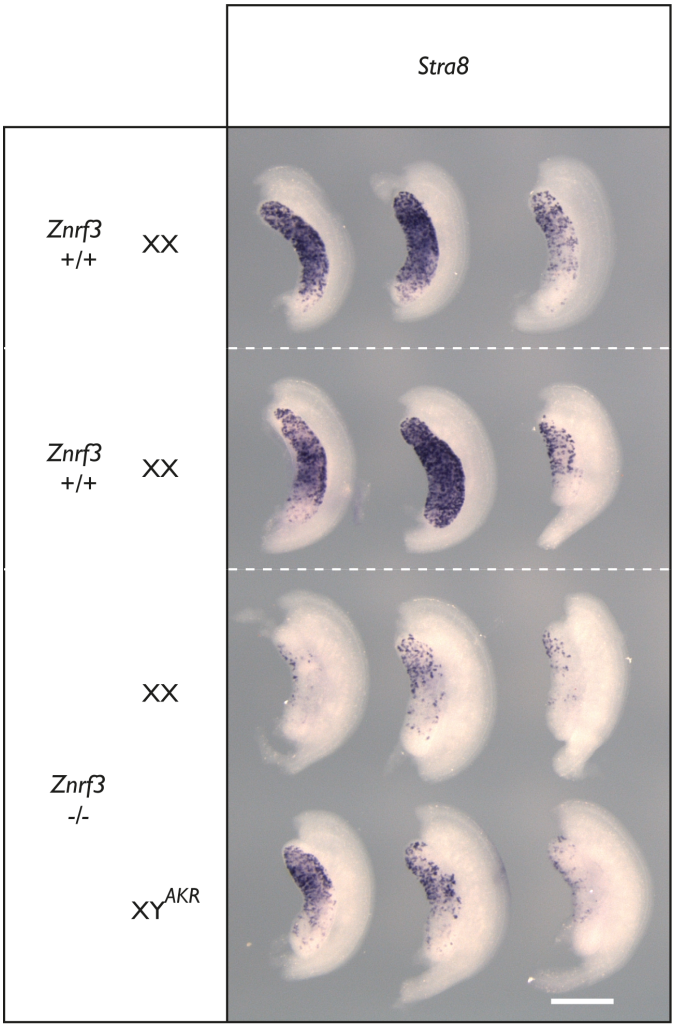

Figure 4.5 *Stra8* expression in *Znrf3*-null gonads. WMISH was carried out on wild-type XX (*Znrf3*$^{+/+}$), XX *Znrf3*$^{+/-}$, XX *Znrf3*$^{-/-}$ and XY^{AKR} *Znrf3*$^{-/-}$ gonads at 14.5 dpc. Scale bar = 500μm.

4.1.6 Loss of one allele of *Znrf3* causes a range of sex reversal phenotypes in B6.YAKR adults

Znrf3$^{-/-}$ mice die around birth. However, *Znrf3*$^{+/-}$ animals are viable. A cohort of B6.Y^{AKR} *Znrf3*$^{+/-}$ mice were aged to around 4 months, before being culled and dissected. *Znrf3*$^{+/-}$ B6.Y^{AKR} mice showed a range of sex reversal phenotypes. Ano-genital distance was significantly reduced when compared to wild-type XY^{AKR} mice, and was not significantly different from XX mice (**Fig. 4.6b**). 2 out 5 adults were fully sex reversed, and their internal

reproductive tracts were indistinguishable from a wild-type female littermate control (**Fig. 4.6a**). 3 out of 5 *Znrf3*$^{+/-}$ B6.Y^{AKR} mice had one small testis and either a contralateral ovary, an absent gonad, or unidentifiable mass of tissue. Of those which had a testis, the testicular weight was significantly reduced compared to B6.Y^{AKR} wild-type controls (**Fig. 4.6c**). Importantly, 2 of these adult XY *Znrf3*$^{+/-}$ B6.Y^{AKR} mice were able to successfully mate with an XX *Znrf3*$^{+/-}$ female to produce *Znrf3*$^{-/-}$ B6.Y^{AKR} embryos.

Adult gonads were sectioned and stained using Haematoxylin and Eosin (H&E) to examine gross morphology. Wild-type XY^{AKR} gonads (**Fig. 4.7a**) showed seminiferous tubules containing spermatids (**Fig. 4.7a'**). Wild-type ovaries (**Fig. 4.7b**) showed evidence of follicle formation (**Fig. 4.7b'**) and corpora lutea. *Znrf3*$^{+/-}$ XY^{AKR} adult gonads were either small testes (**Fig. 4.7c**) or ovary-like gonads (**Fig. 4.7d**). When testes were formed, seminiferous tubules were identified (**Fig. 4.7c'**) but regions of degrading tubules could also be seen (**Fig. 4.7c''**). These tubules showed complete loss of Leydig cells and spermatogonia, and were filled with cell debris, and some exfoliated cells were visible alongside mature spermatids (**Fig. 4.7c"**).

When a testis was not formed, the histology of the gonad formed was neither testicular or ovarian. Histology of gonads from the two XY females showed normal fallopian tube development (data not shown). The majority of the gonad was comprised of steroid producing interstitial cells, with characteristic finely granulated cytoplasm, and high pigmentation. Infoldings of the tissue appeared to be lined with Ovarian Surface Epithelium (OSE) (**Fig. 4.7d'**). No mature follicles were identified in either animal (n=2), but in one gonad a large cystic structure comprising proteinaceous material lined by cuboidal cells was seen (**Fig. 4.7d''**). This mass is structurally similar to a follicle which has ejected the ovum, and therefore could be evidence of functional ovum maturation.

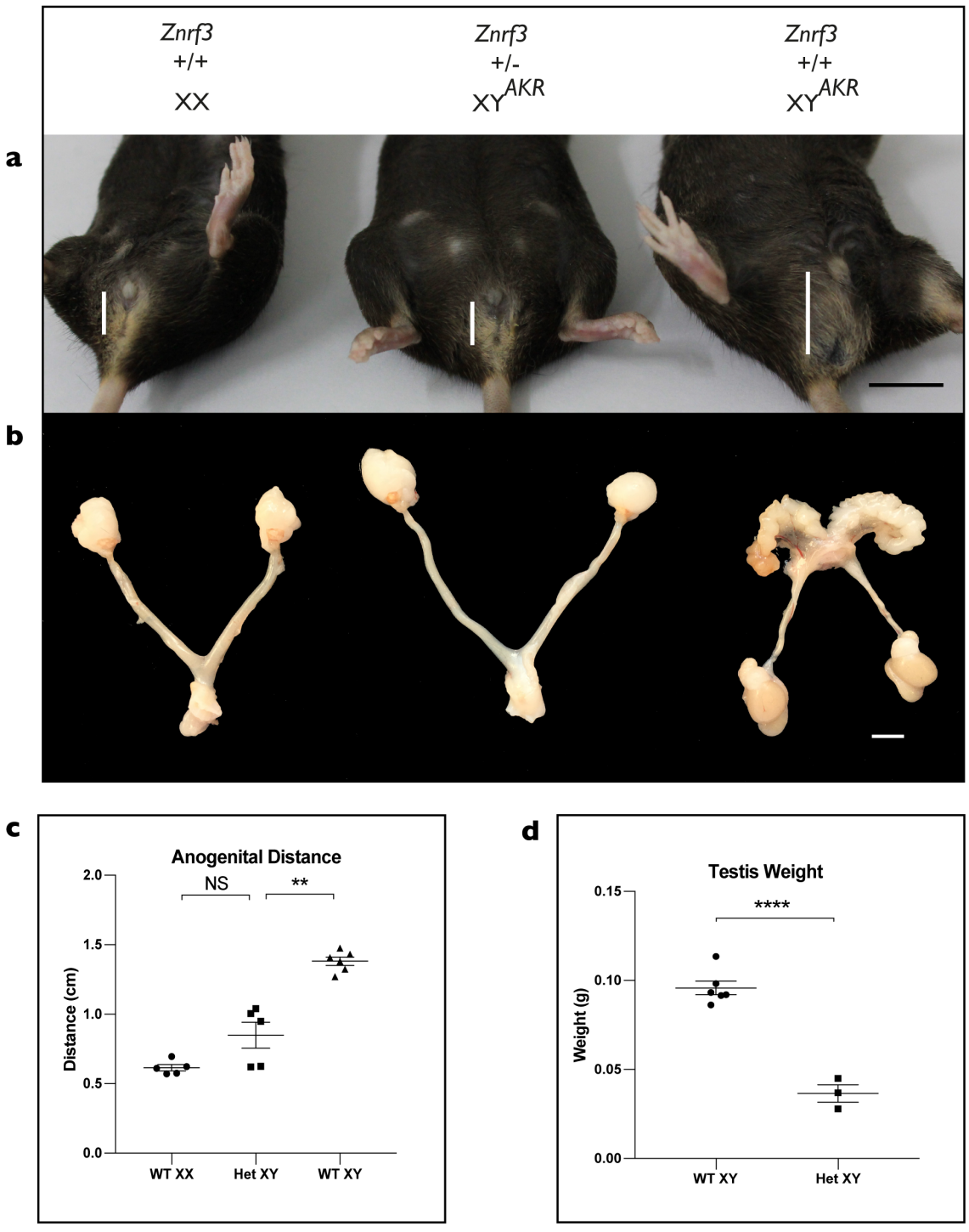

Figure 4.6 Sex reversal phenotype in adult B6.Y^{AKR} *Znrf3*$^{+/-}$ mice. External genitalia of *Znrf3*$^{+/-}$ B6.XY^{AKR} adult mice. White lines show approximate anogenital distances of mice shown. Scale bar: 1cm **(a)**. Internal reproductive tracts of above mice. Scale bar: 0.5cm **(b)**. Anogenital distances **(c)** and testis weights **(d)** were measured. Differences analysed by un-paired t-test, with Welch's correction. Error bars show SEM. T-tests (two-tailed) were performed with Welch's correction. Significant results are signified by * = P<0.05, ** = P<0.01, *** = P<0.001, **** = P<0.0001. Non-significant differences are signified by NS. Exact P-values are detailed in the appendix (Table S5).

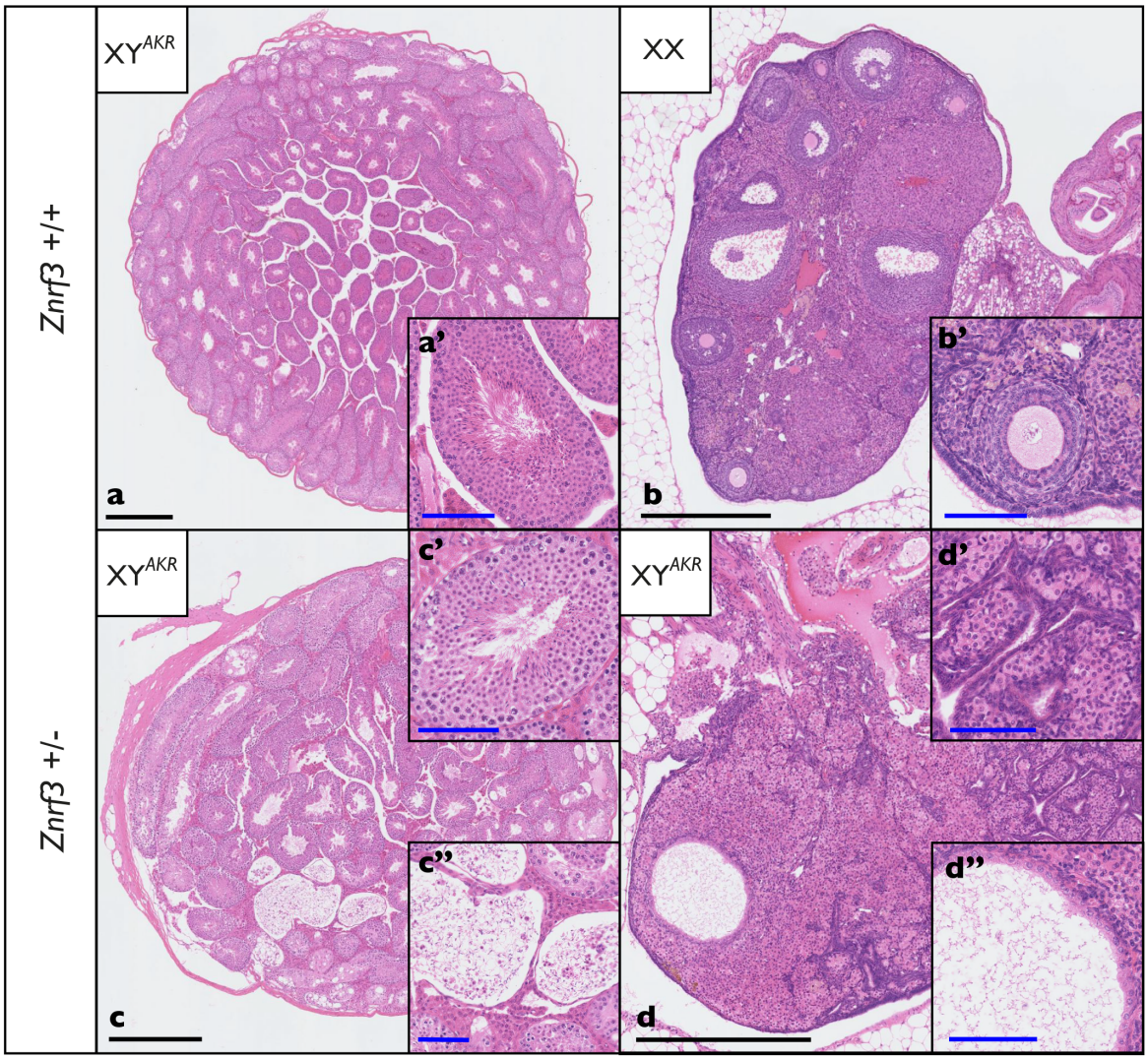

Figure 4.7 Histological analysis of adult B6.Y^{AKR} *Znrf3*$^{+/-}$ gonads. Haemolysin and Eosin (H&E)-stained sections of adult gonads. Wild-type **B6.Y^{AKR}** testis **(a)** shows evidence of well-formed seminiferous tubules containing spermatids **(a')**. XX wild-type ovary **(b)** showing evidence of follicle formation **(b')**. *Znrf3*$^{+/-}$ XY^{AKR} testis **(c)** showing some seminiferous tubules **(c')** and some areas of tubule degeneration **(c'')**. *Znrf3*$^{+/-}$ XY^{AKR} gonad **(d)** showing infolded tissue lined by an epithelial layer **(d')** and a large cystic structure **(d'')**. Scale bars: black = 500um, blue = 100um.

4.1.7 Loss of *Rnf43* does not affect primary sex determination

WMISH was carried out on 14.5 dpc gonads, using probes for *Sox9* and *Stra8* as described above. XY *Rnf43*$^{-/-}$ gonads were indistinguishable from wild-type littermate controls (**Fig. 4.8**). *Sox9* expression extended the length of the gonad, and testis cords were well organised. No *Stra8* expression was detected in any XY *Rnf43*$^{-/-}$ gonads (n=3). XX *Rnf43*$^{-/-}$ also appeared phenotypically normal when compared to wild-type controls. No *Sox9* expression was detected in any of the gonads analysed (n=3).

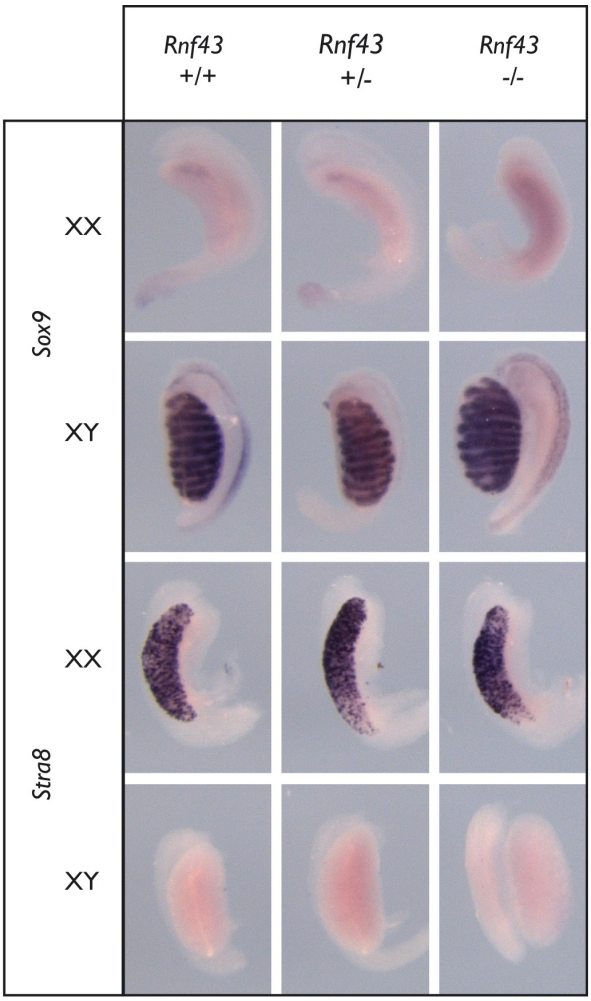

Figure 4.8 WMISH analysis of 14.5 dpc *Rnf43*-null gonads. XX and XY gonads were analysed by WMISH at 14.5 dpc. Expression of *Sox9* is shown in the top two rows and expression of *Stra8* in the bottom two rows.

Similarly, when *Rnf43* was deleted on a B6.Y^{AKR} background, no significant differences were seen compared to wild-type controls (**Fig. 4.9**). WMISH analysis of B6.XY^{AKR} *Rnf43*$^{-/-}$ gonads showed *Stra8* and *Sox9* expression as expected. *Stra8* expression at the poles was not significantly more extensive in *Rnf43* mutant gonads compared to wild-type controls (n=4, n=8), and testis cord structure was well defined in the centre of these gonads.

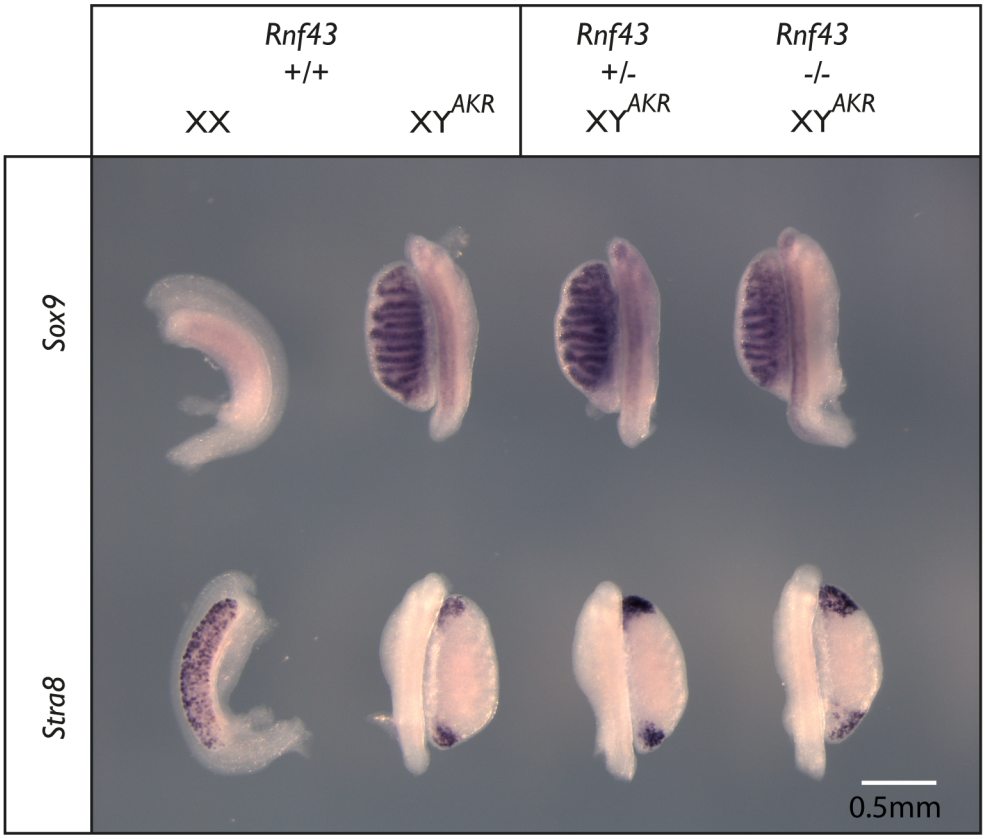

Figure 4.9 WMISH analysis of B6.Y^{AKR} *Rnf43*-null gonads. WMISH was carried out on XX and XY^{AKR} gonads at 14.5 dpc. *Sox9* expression is shown in the top row, and *Stra8* expression in the bottom row. Scale bar 500μm.

4.1.8 *Rnf43*+/- B6.YAKR adults are phenotypically normal

Small cohorts of XY *Rnf43*$^{+/-}$ B6.Y^{AKR} adults and controls (n=6, n=6) were culled at 2-4 months. No significant difference was seen in anogenital distance between heterozygous animals and wild-type controls. Reproductive tracts were grossly normal, and there was no

significant difference in testis weight between the two groups. H&E staining of sections of these gonads revealed no overt morphological differences, and *Rnf43*$^{-/+}$ B6.Y^{AKR} testes had seminiferous tubules throughout the gonad with visible spermatids present (data not shown).

4.1.9 Loss of one copy of *Rnf43* on a *Znrf3*-null B6 background does not significantly exacerbate the sex reversal phenotype

As previously described, *Rnf43* is a homologue of *Znrf3* and functions through the same mechanism to downregulate canonical WNT-signalling. Therefore, it is possible that *Rnf43* can compensate for the loss of *Znrf3* from the gonad. As in previous experiments, wild-type XY gonads showed *Sox9* expression in the testis cords (**Fig. 4.10a**) and no *Stra8* expression (**Fig. 4.10c**). Similarly, XY *Rnf43*-null gonads appeared phenotypically normal (**Fig. 4.10b, d**).

Previous experiments have shown that *Znrf3*$^{+/-}$ gonads are also phenotypically normal with no *Stra8* expression detected (**Fig. 4.3a**). When one (**Fig. 4.10e, g**) or two (**Fig. 4.10f, h**) copies of *Rnf43* were lost on this background, *Sox9* expression appeared normal, and both *Znrf3*$^{+/-}$, *Rnf43*$^{+/-}$ and *Znrf3*$^{+/-}$, *Rnf43*$^{-/-}$ XY gonads were able to form normal testis cords. When *Stra8* expression was analysed in these gonads, small patches of expression could be detected at the gonad-mesonephros border (**Fig. 4.10g', h'**). This was seen in multiple, but not in all, XY gonads of each genotype (1/5 *Znrf3*$^{+/-}$, *Rnf43*$^{+/-}$ and 4/5 *Znrf3*$^{+/-}$, *Rnf43*$^{-/-}$). Furthermore, *Stra8* expression was never detected in wild-type or *Rnf43*-null gonads. However, no *Znrf3*$^{+/-}$ gonads were included in this experiment for comparison, so we cannot rule out that this is a phenotype associated with losing one copy of *Znrf3* alone.

To analyse whether losing a copy of *Rnf43* can exacerbate the sex reversal phenotype seen in *Znrf3*-null gonads, XY *Znrf3*$^{-/-}$, *Rnf43*$^{+/+}$ gonads were compared to XY *Znrf3*$^{-/-}$, *Rnf43*$^{+/-}$ gonads. A range of phenotypes were seen in both groups. However, in general it appears there was greater expression of *Sox9* in the *Znrf3*-null gonads (**Fig. 4.10i**) compared to those which have additionally lost a copy of *Rnf43* (**Fig. 4.10k**). However, when the same comparison is made with the female marker *Stra8*, expression was not expanded when a copy of *Rnf43* is lost on the *Znrf3*-null background (**Fig. 4.10j & m**).

Two doubly homozygous (*Znrf3*$^{-/-}$, *Rnf43*$^{-/-}$) XY embryos were identified during tissue collection for this experiment. However, both embryos were dead and therefore were not included in the WMISH analysis. Both pairs of gonads were scored as ovotestes by morphology alone (data not shown), suggesting that even when both *Znrf3* and *Rnf43* are lost from the gonad, male-to-female sex reversal is often not complete.

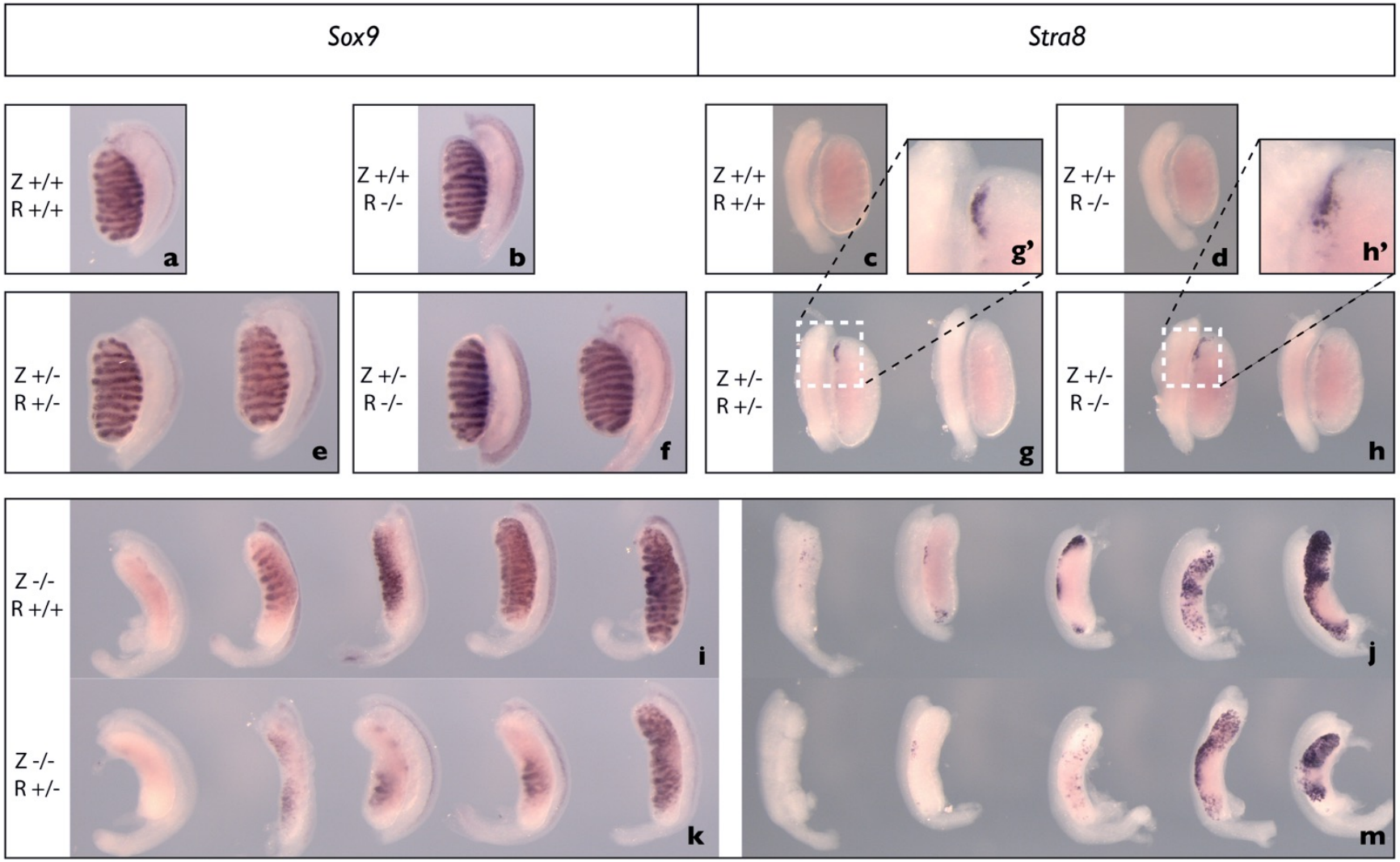

Figure 4.10 *Sox9* and *Sra8* expression in compound *Znrf3/Rnf43* mutant gonads. For full figure legend, please see the following page.

Figure 4.10 *Sox9* and *Stra8* expression in compound *Znrf3/Rnf43* mutant gonads. WMISH was carried out on XY gonads at 14.5 dpc. Expression of *Sox9* is shown in **(a, b, e, f, i, m)** and *Stra8* expression in **(c, d, g/g', h/h', j, m).** Wild-type gonads **(a, c)**, *Rnf43*-null gonads **(b, d)**, *Znrf3*$^{-/-}$, *Rnf43*$^{+/-}$ gonads **(e, g/g')**, and *Znrf3*$^{+/-}$, *Rnf43*$^{-/-}$ gonads **(f, h)** were analysed. **(g')** and **(h')** show an expanded section of the region highlighted by the white dotted box in **(g)** and **(h)** respectively. *Znrf3*$^{-/-}$ gonads **(i, j)** are compared to *Znrf3*$^{-/-}$, *Rnf43*$^{+/-}$ compound mutants **(k, m)**.

4.1.10 Deletion of *Znrf3* in the adult mouse testis has no phenotypic effect

In order to delete *Znrf3* from the adult gonad, *Znrf3*$^{flox/flox}$ mice were crossed to an inducible ubiquitous Cre line (*Ubiq-ERT2-Cre*) which can drive recombination of *LoxP* sites around exon7 of *Znrf3,* following exposure to Tamoxifen. *Znrf3*$^{flox/+}$, *Ubiq-ERT2-Cre* mice were then crossed to *Znrf3*$^{flox/+}$ mice, to generate *Znrf3*$^{flox/flox}$, *Ubiq-ERT2-Cre* mice. These mice, and *Znrf3*$^{+/flox}$, *Ubiq-ERT2-Cre* control adult mice were dosed with tamoxifen at 8 weeks. 12 weeks later, tissues were taken for analysis (Fig. 4.11).

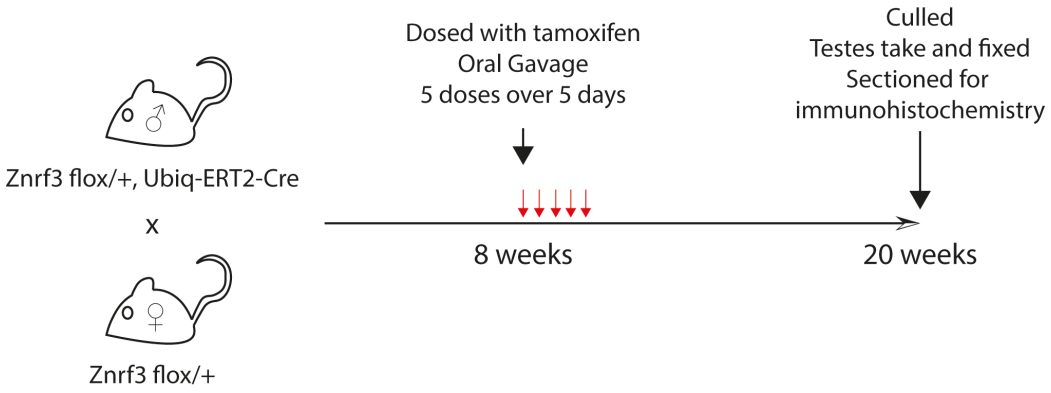

Figure 4.11 Tamoxifen dosing of adult *Znrf3*^{flox} mice. *Znrf3*$^{+/flox}$, *Ubiq-ERT2-Cre* mice were crossed to *Znrf3*$^{+/flox}$ mice to generate *Znrf3*$^{flox/flox}$, *Ubiq-ERT2-Cre* mice and *Znrf3*$^{+/flox}$, *Ubiq-ERT2-Cre* mice. Adults were treated with tamoxifen at 8 weeks, and tissues taken at 20 weeks.

As expected, deleting *Znrf3* from gonads at 8 weeks had no effect on the external genitalia of tamoxifen treated mice (Fig. 4.12 a-e). No differences between the internal reproductive tracts of experimental and control mice were observed (Fig. 4.12f-j), nor between the

internal structures of the testes (**Fig. 4.12k-p**). Tamoxifen-treated *Znrf3$^{flox/flox}$, Ubiq-ERT2-Cre* mice had well-formed seminiferous tubules with evidence of the presence of spermatids (**Fig. 4.12p**). Expression of *Sox9* and *Foxl2* was also analysed by qRT-PCR (**Fig. S3**). *Foxl2* expression was highly variable, and there was no significant difference between tamoxifen treated *Znrf3$^{flox/flox}$, Ubiq-ERT2-Cre* testes and wild-type. Similarly, there was also no significant difference in *Sox9* expression between these groups.

Analysis of the extent of recombination was carried out using qRT-PCR (**Fig. 4.13**). RNA was extracted from whole adult testes. One set of primers is specific for *Znrf3^{flox}* and *Znrf3^{WT}* transcripts (referred to as *Znrf3$^{flox/WT}$* transcripts). The second pair are specific for *Znrf3^{del}* transcripts. Together, these primers were used to measure the extent of deletion of *Znrf3* in the testis.

Znrf3$^{flox/flox}$, Ubiq-ERT2-Cre testes which were treated with tamoxifen expressed significantly more *Znrf3^{del}* transcript compared to *Znrf3$^{flox/flox}$, Ubiq-ERT2-Cre* testes which had not been treated with tamoxifen or compared to XY wild-type testes (**Fig. 4.13a**). Furthermore, *Znrf3$^{flox/flox}$, Ubiq-ERT2-Cre*, tamoxifen-treated mice expressed significantly less *Znrf3^{WT}* transcript than untreated mice or wild-type mice (**Fig. 4.13b**). The ratio of *Znrf3^{del}* transcripts to *Znrf3$^{flox/WT}$* was measured to be approximately 1:1 in *Znrf3$^{flox/flox}$, Ubiq-ERT2-Cre* tamoxifen treated testes, and approaching zero in both untreated testes, and in wild-types (**Fig. S4**).

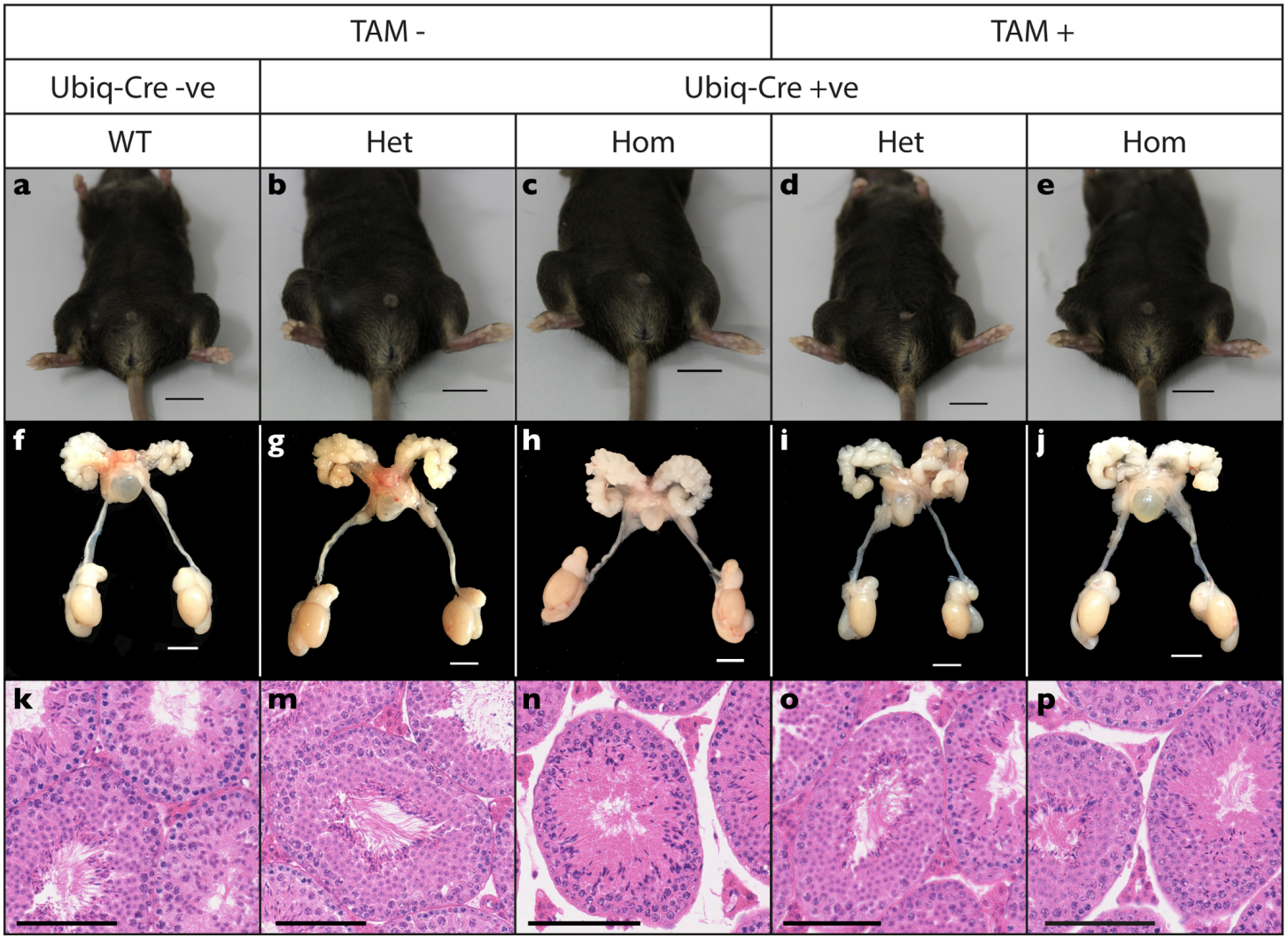

Figure 4.12 Analysis of *Znrf3*$^{flox/flox}$ adult mice. For figure legend, see following page.

Figure 4.12 Analysis of *Znrf3*$^{flox/flox}$ adult mice (previous page). Anogenital distances **(a-e)**, internal reproductive tracts **(g-j)** and histology of adult testes **(k-p)** of *Znrf3*$^{+/+}$ (WT), *Znrf3*$^{+/flox}$ (Het) and *Znrf3*$^{flox/flox}$ (Hom) mice, carrying (Ubiq-Cre +ve) or not carrying (Ubiq-Cre –ve) ERT2-Ubiq-Cre. Mice were treated with tamoxifen (TAM +) or were untreated (TAM -). Scale bars: 10mm **(a-e)**, 5mm **(f-j)**, and 100μm **(k-p)**.

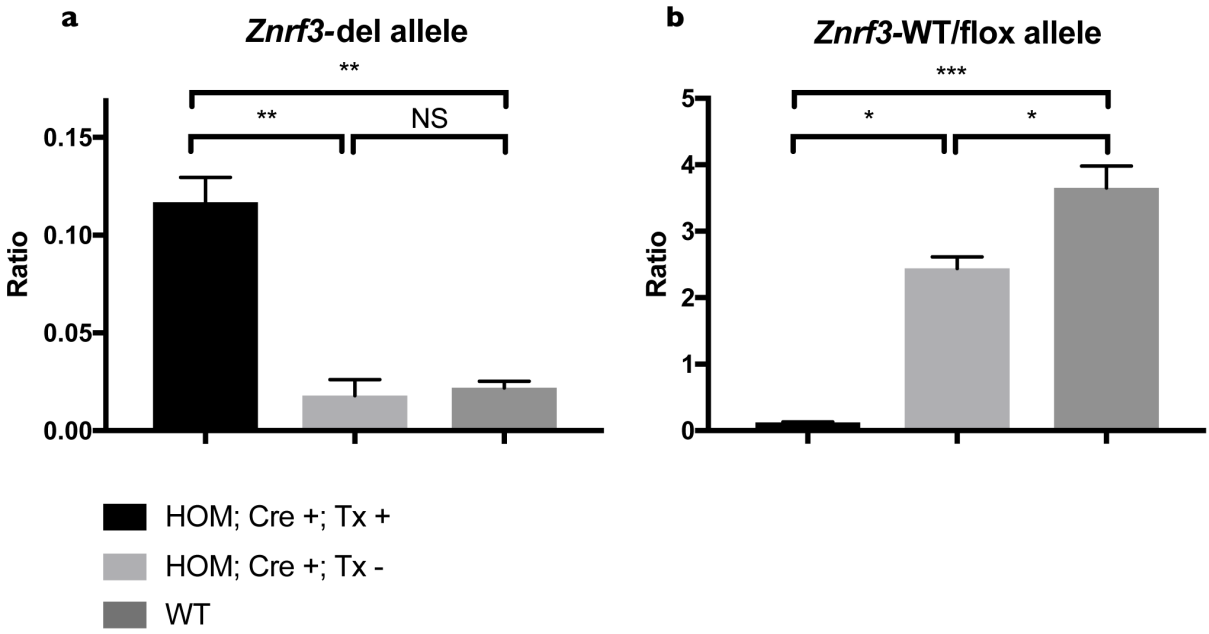

Figure 4.13 Expression of *Znrf3*^{del} and *Znrf3*^{flox} transcripts in the adult gonad. qRT-PCR was performed on adult testes (20 weeks) (n=2-6, each genotype) using primers specific for the recombined allele (*Znrf3*-del) **(a)** and for the wild-type or flox allele (*Znrf3*-WT/flox) **(b)**. Relative expression was calculated relative to *Hprt1* (ratio). Error bars show SEM. T-tests (two-tailed) were performed with Welch's correction. Significant results are signified by * = P<0.05, ** = P<0.01, *** = P<0.001. Non-significant differences are signified by NS. Exact P-values are detailed in the appendix (Table S6).

4.1.11 Summary of Results: *Znrf3* is a testis-determining gene

This chapter has demonstrated that *Znrf3* is a testis-determining gene in mice. When the Ring Finger domain of ZNRF3 is disrupted, XY embryos carrying two copies of this allele show partial-to-full XY gonadal sex reversal, and on a sensitised (B6.Y^{AKR}) background, consistently fully sex reverse. Moreover, phenotypic sex reversal of some XY *Znrf3* -/+ heterozygous adult mice is observed on this sensitised background. Deletion of a homologue of *Znrf3, Rnf43*, is

not sufficient to disrupt testis-determination and *Rnf43* does not appear to make a major contribution to the *Znrf3*-null phenotype. Despite the clear role of *Znrf3* in the embryonic testis, deletion in the adult does not appear to inhibit the maintenance of the testicular fate.

4.2. Discussion

4.2.1 *Znrf3* is a testis-determining gene

This chapter has demonstrated that *Znrf3* is required for normal mouse testis development. In the absence of *Znrf3*, the XY gonad commonly develops as an ovotestis, expressing both testicular and ovarian marker genes. Male-to-female sex reversal is not complete, and is highly variable, with some gonads developing testis cords whilst others develop an ovarian morphology and exhibit minimal expression of testicular markers such as *Sox9*. This indicates that in the absence of *Znrf3*, a significant, but variable proportion of the XY gonad assumes an ovarian fate.

As would be expected, the sex reversal phenotype of XY *Znrf3*$^{-/-}$ gonads has become more severe as the colony has been further backcrossed to the B6 background over 5-6 generations. Initial experiments revealed ovotestes with small areas of *Stra8* expression at the poles, and well-formed cords at the centre of the gonad (**Fig. S5**). However, gonads taken from later backcrosses, shown in **Fig. 4.3**, show a more ovarian morphology and a greater proportion of the gonad appears to express ovarian marker genes. Furthermore, ovarian tissue in later experiments is found throughout the gonad or restricted to one end of the gonad, rather than being found exclusively at the poles. This change in severity of phenotype is due to the sensitivity of the B6 genome to sex reversal. Therefore, as the embryos approach congenic B6, the balance in the gonad is tipped towards an ovarian fate, and a greater proportion of the gonad expresses female markers. Given that *Znrf3* is a potent WNT-antagonist, and given the known role of canonical WNT-signalling in the gonad, the most likely cause of this phenotype is the dysregulation of WNT signalling in the XY gonad.

4.2.2 The *Znrf3* null allele

As previously detailed, canonical WNT-signalling has been shown to be critical for the development of the ovary. Furthermore, over-stimulation of the canonical WNT-signalling pathway, through the stabilisation of β-catenin, has been shown to inhibit testis-determination. Therefore, it seems likely that the role of ZNRF3 is determined by its WNT-antagonising function.

The *Znrf3* null allele used in this thesis deletes exon 7 of the mouse *Znrf3* gene. Exon 7 codes for one half of the Ring Finger domain, which is responsible for ubiquitinating the frizzled receptor. This domain is critical for the WNT-antagonising function of ZNRF3. Deletion of exon 7 also causes a frame shift and a premature stop codon. However, in the absence of an antibody that detects endogenous protein, we are unable to determine whether the shortened version of the protein is present in the cell, or whether it is degraded through the unfolded protein response. Furthermore, the *Znrf3* transcripts may be degraded through nonsense mediated decay. If ZNRF3 protein is completely absent from the *Znrf3*$^{-/-}$ gonad, it is possible that its loss causes other effects alongside the dysregulation of WNT-signalling.

Generation of an allele of *Znrf3* which used a point mutation to disrupt the ring finger domain, but which left the rest of the protein intact, could be used to precisely assess the functional role of this domain. This allele could be used to test whether the ring finger alone was the critical in testis determination, but would not allow separation of the roles of the canonical and non-canonical pathways as both pathways signalling through the Frizzled Receptors, the targets of ZNRF3.

4.2.3 Loss of *Znrf3* on a sensitised background mimics human DSDs

As previously described, human DSD patients are frequently heterozygous for a causative mutation. Furthermore, it has been demonstrated that the genetic background of the individual is critical in whether sex reversal is seen, and the severity of the condition (Chen et al. 2015; Bouma et al. 2007; Bagheri-Fam et al. 2015). Some human genomes may be more sensitive to sex reversal for several reasons:

1) The individual may have a second mutation in a sex-determining gene. For example, a mutation in *SOX9,* which only causes a partial disruption to its DNA-binding efficiency, may only cause a sex reversal phenotype in the context of genome with a secondary mutation in a testis-determining gene downstream.
2) Alternatively, another gene may compensate for the effect of the causative mutation in an unaffected individual, but may also be disrupted in a DSD patient.
3) More broadly, the sensitised genetic background may be the result of the cumulative effect of many minimally-damaging single nucleotide polymorphisms (SNPs). This may result in a global up- or down-regulation of the testis or ovarian pathway, which primes the gonad for one fate. In this case, the mutation is more likely to be sufficient to tip the balance towards sex reversal.

Znrf3$^{+/-}$ B6.Y^{AKR} mice show partial and full sex reversal. This line may therefore be a good mouse model for human cases of DSD involving *ZNRF3*, and more broadly. The interaction of the Y^{AKR} sex chromosome with the B6 genome presumably mimics the genome of a human individual which may be sensitised to gonadal sex reversal. In both the mouse and the human, the inheritance of a single copy of a mutated testis-determining gene, such as

Znrf3, is sufficient in some cases to cause complete sex reversal. Despite full male-to-female sex reversal occurring in some *Znrf3*$^{+/-}$ B6.Y^{AKR} mice, others were fertile and able to produce litters of embryos. This variability models another aspect of human DSDS: unaffected parents can pass causative mutations to affected children (Chen et al. 2015). *Znrf3*$^{-/-}$ B6.Y^{AKR}, on the other hand, consistently fully sex reverse.

4.2.4 Variable penetrance of the sex reversal phenotypes

Znrf3-null embryos showed a range of phenotypes from near-complete sex reversal, to extensive expression of *Sox9* at 14.5 dpc. Furthermore, this variability is echoed in the phenotype of *Znrf3*$^{+/-}$ B6.Y^{AKR} mice, where some are fully sex reversed while others are fertile. One explanation for this variation is genetic background differences between embryos; another may be the consequences of stochastic events at the early stages of sex determination. This will be discussed further, in the context of additional experimental result, in **Chapter 7**.

4.2.5 A role for *Znrf3* in germ cells?

XY *Znrf3*-null gonads appear to express less *Stra8* than XX wild-type controls **(Fig. 4.5)**, even in gonads which appear to have fully sex reversed based on morphology and extensive expression of FOXL2. Furthermore, a reduction in *Stra8* expression is also seen in XX *Znrf3*-null gonads compared to XX wild-type littermates. *Stra8* is a pre-meiotic germ cell marker, and is expressed in an ovary-specific fashion in cells which are preparing to enter meiosis 1. A lack of *Stra8* expression could be explained by:

1) A reduction in the number of germ cells, either because fewer germ cells entering the gonad due to a defect in PGC migration from the base of the primitive streak;

2) A failure of germ cells to proliferate in the gonad or loss of germ cells by apoptosis;

3) A defect in the ability of *Znrf3*$^{-/-}$ germ cells to initiate meiosis;

4) A delay in global development of the gonad or whole embryo.

Normal development and specification of somatic cells in the XX or XY embryonic gonad does not require germ cells to be present (Buehr et al. 1993). Therefore, the presence of FOXL2 in the sex-reversed XY *Znrf3*-null gonads is still consistent with the hypothesis that germ cells are completely absent from the gonad or reduced in numbers, but not consistent with a major delay in the events of ovary development, such as granulosa cell commitment. The presence of germ cells will be assessed in **Chapter 5,** and the reduction in *Stra8* in the *Znrf3*-null gonad will be further discussed in **Chapter 7** in the light of these results.

4.2.6 *Rnf43* does not play a major role in sex determination

When *Rnf43* is deleted, XY gonads are indistinguishable from wild-type littermate controls. This indicates that *Rnf43* does not play a role in primary sex determination. *Rnf43* and *Znrf3* share only moderate sequence homology. However, crystal structures of the extracellular domain show a highly-conserved 3D protein structure (Peng et al. 2013). Whether this similarity extends to the intracellular domain of the proteins is unknown. Furthermore, both proteins bound RSPO1 in a cell-based binding assay through the same structural elements (Xie et al. 2013). However, as discussed in **Chapter 2**, *Rnf43* is not expressed in the gonad. Therefore, it is not surprising that disruption of *Rnf43* has no effect on testis determination: even if RNF43 is able to function in a similar way to ZNRF3, it is unlikely to do so in the context of the gonad, simply because it is not expressed in this tissue. However, the possibility exists that *Rnf43* is up-regulated in the embryonic gonad only when *Znrf3* is ablated.

4.2.7 *Znrf3* does not play a role in maintaining testicular fate

Many studies now indicate that the sexual fate of the testis is not fixed in adulthood in the mouse, and have shown that adult Sertoli cells are able to transdifferentiate into granulosa-like cells. Given the important role played by ZNRF3 in primary sex determination, its role in the adult was analysed. Results in this chapter suggest that ZNRF3 does not play a role in maintaining the fate of the testis in adulthood. When ZNRF3 was deleted from the gonad 8 weeks postnatally, no differences were seen between reproductive tracts of Tamoxifen-treated compared to untreated *Znrf3$^{flox/flox}$, ERT2-UBIQ-Cre* mice. Furthermore, no histological differences were seen. Analyses of FOXL2 expression by immunohistochemistry were attempted on sections of these adult gonads, but were unsuccessful.

Tamoxifen treatment allows CreERT2 to enter the nucleus; without tamoxifen, the Cre protein is still express, but cannot cause recombination of the *LoxP* sites as it is prevented from entering the nucleus (Robert Feil et al. 1997). Analysis of expression of *Znrf3^{del}* and *Znrf3^{flox}* transcripts in the adult mutant gonad reveals significant expression of the recombined allele, and low expression of the wild-type allele. This shows that tamoxifen treatment has successfully led to recombination in the adult testis, and therefore deletion of *Znrf3*. Furthermore, these data show that there is relatively little recombination occurring in the untreated *Znrf3$^{flox/flox}$, Ubiq-ERT2-Cre* testes. This suggests that in the context of the testes, Cre protein is only active when the testis is exposed to Tamoxifen.

However, it is difficult to assess from this experiment the precise extent of recombination. The two qRT-PCR assays used were not of equivalent efficiency, and therefore it is impossible to directly compare the levels of recombined transcripts with wild-type/flox transcripts. Therefore, it is possible that, despite tamoxifen treated *Znrf3$^{flox/flox}$, Ubiq-ERT2-*

Cre testes having significantly higher levels of recombined transcripts, this level of recombination could be biologically irrelevant.

XY *Znrf3*$^{+/-}$ embryonic testes are normal and adults are fertile. Therefore, we might only expect a phenotype in treated *Znrf3*$^{flox/flox}$, *Ubiq-ERT2-Cre* animals if greater than approximately 50% of *Znrf3* transcripts produced were recombined. Due to the experimental design, we are unable to calculate this figure precisely. Despite this, the fact that levels of wild-type/flox transcripts are over 30-fold higher in the WT adult testes than in the tamoxifen-treated *Znrf3*$^{flox/flox}$, *Ubiq-ERT2-Cre* testes, is good evidence that a significant proportion of *Znrf3* alleles are recombined. Critically, it is also impossible to assess the differences in ZNRF3 protein levels without a working antibody. If a Western Blot or Immunohistochemical analyses could confirm the absence of ZNRF3 protein in these animals, we could definitively rule out a role for ZNRF3 in the adult gonad.

In summary, *Znrf3* does not appear to play a role in maintaining testicular fate in the adult gonad; this observation is consistent with the absence of any report indicating a role for canonical WNT signalling in the adult ovary.

Chapter 5: Molecular Phenotyping of the *Znrf3*-null gonad

5.0. Introduction

In the previous chapter, *Znrf3* was demonstrated to be a new testis-determining gene. XY *Znrf3* null gonads show partial to near-complete male-to-female sex reversal. ZNRF3 may be acting at different points in the known sex-determining pathway. Some testis-determining genes act through the regulation of *Sry* and affect the level or timing of expression, for example GATA4 (Miyamoto et al. 2008). Some act directly on *Sox9*, and others act on pathways downstream. This chapter will attempt to address this question.

The most likely explanation for the role of *Znrf3* in testis determination is through the regulation of WNT-signalling. One WNT family member is particularly interesting in relation to sex determination, *Wnt4*. It plays a role in the ovarian pathway and when disrupted, causes partial female-to-male sex reversal in mice and humans (Mandel et al. 2008; Vainio et al. 1999).

The molecular mechanism through which ZNRF3 acts to down-regulate WNT-signalling is now well understood (Hao et al. 2012; Koo et al. 2012). It is also understood that canonical WNT-signalling is crucial for the development of an ovary (Vainio et al. 1999; Liu et al. 2009; Chassot et al. 2008). Furthermore, suppression of this signalling pathway in the XY gonad is required for proper testis development: the upregulation of canonical WNT-signalling through the stabilisation of β-catenin can cause partial male-to-female sex reversal

(Maatouk et al. 2008). Therefore, one important question is whether canonical WNT-signalling is indeed up-regulated in the absence of *Znrf3*, specifically in the context of the gonad at the sex-determining stage of development. It is also crucial to identify whether expression of *Wnt4*, a major player in the ovarian pathway, is affected. Finally, it must be determined whether this up-regulation of canonical WNT-signalling results in the upregulation of other ovarian genes in the gonad and the corresponding downregulation of testis-determining genes.

As previous described, *Wnt4* and *Fgf9* oppose each other in the developing gonad (Kim et al. 2006). Indeed, the role of *Fgf9* in the testis may primarily be to downregulate *Wnt4* in the testis. If WNT-signalling is promoted by the loss of *Znrf3* from the gonad, it follows that levels of *Fgf9* may decrease because of this mutual antagonism.

5.0.1. Aims

This chapter aims to analyse the expression of known sex-determining genes which may act downstream of *Znrf3* to further elucidate the role of *Znrf3* in testis determination. It will focus on determining whether WNT/β-catenin signalling is affected in the context of the developing XY mutant gonad at around the stage of sex determination (between 11.5 and 12.5 dpc), and whether this extends to an upregulation of the ovarian marker *Wnt4*. This chapter will assess the potential critical time in gonad development at which *Znrf3* is having an impact, and the origins of the phenotypic variability seen at 14.5 dpc (Chapter 4).

5.1. Results

5.1.1 *Sry* expression analysis

Sry is the dominant, Y-linked testis-determining gene (Gubbay et al. 1990; Sinclair et al. 1990). As previously detailed, the timely expression of SRY is critical for testis determination and a delayed or reduced level of SRY can prevent the male pathway from being established (Warr et al. 2012; Johnen et al. 2013; Gierl et al. 2012; Hiramatsu et al. 2008). For this reason, *Sry* expression was analysed in *Znrf3* null gonads. As expected, *Sry* is detected in XY wild-type gonads at 11.5 dpc (17ts) but not in XX gonads by Wholemount in situ hybridisation (WMISH). Levels in both XY *Znrf3*$^{+/-}$ and XY *Znrf3*$^{-/-}$ gonads appeared to be broadly similar. *Sry* expression in *Znrf3*-null gonads extends along the length of the gonad, although all gonads appear slightly thinner when compared to the wild-type (n=3) (**Fig. 5.1a**). qRT-PCR data from subdissected gonads (18ts) appears to confirm this WMISH data: no expression of *Sry* is detected in the XX gonad, and there is no significant difference in expression between wild-type and *Znrf3*$^{-/-}$ gonads (**Fig. 5.1b**).

5.1.2 *Sox9* expression analysis

Sox9 is both necessary and sufficient for testis development, as previously described (F. Barrionuevo et al. 2006; Vidal et al. 2001). At 11.5 dpc (17-18ts), *Sox9* expression is not detected in XX wild-type gonads, but is strongly expressed in XY wild-type gonads. In XY *Znrf3*$^{-/-}$ gonads, weak expression can be seen in the gonad, but it is often discontinuous and at a much lower level than XY controls (n=4,4) (**Fig. 5.2a**). qRT-PCR data show that *Sox9* expression is significantly reduced in the XY *Znrf3* null gonads, compared to XY wild-types, and not significantly higher than in XX wild-type gonads (**Fig. 5.2b**). A few hours later, at

around 12.0 dpc (20-21ts), *Sox9* expression appears stronger in the XY wild-type gonad and remains absent from the XX. At this time-point, expression is more variable in the XY *Znrf3*$^{-/-}$ gonads. Some gonads express *Sox9* along the length of the gonad, but at a lower level when compared to the XY wild-type control. Others have small regions of low expression, with areas where no expression can be detected (**Fig. 5.2a**). qRT-PCR data confirms the same pattern of expression at 12.5 dpc: XY *Znrf3*-null gonads have significantly lower *Sox9* expression that XY wild-type, but higher than XX wild-type gonads (**Fig. 5.2c**).

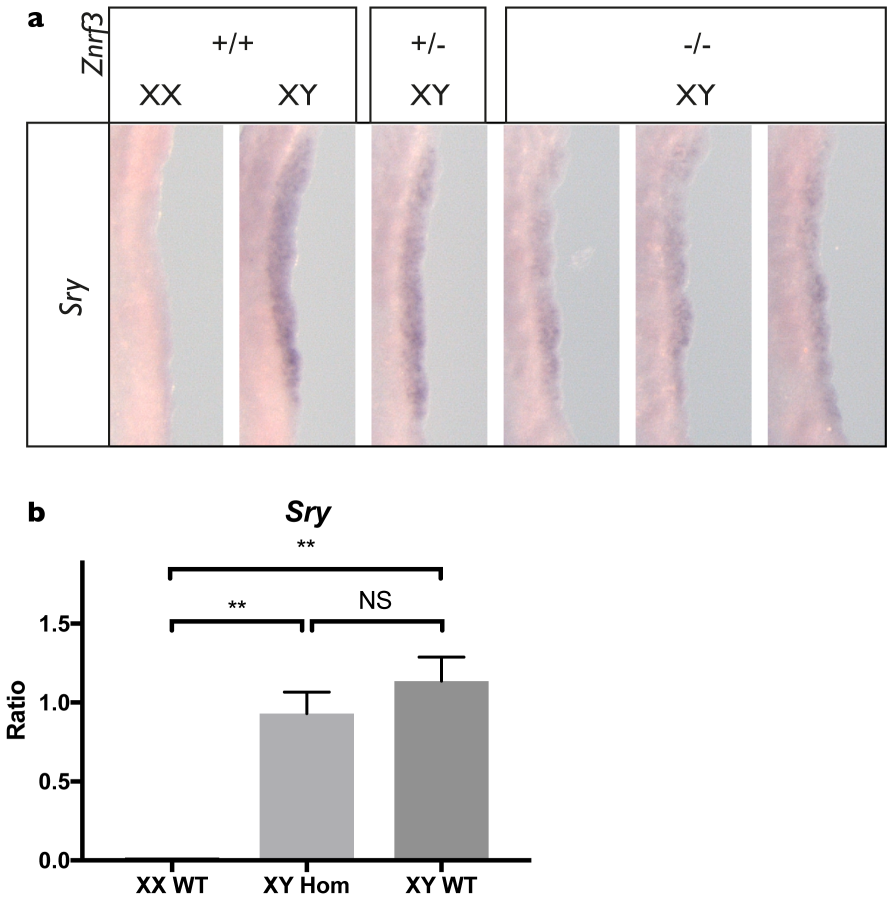

Figure 5.1 *Sry* expression in the *Znrf3*$^{-/-}$ gonad. *Sry* expression was analysed by WMISH on 11.5 dpc UGRs (17ts) **(a)**. qRT-PCR was performed on 11.5 dpc (18ts) XX wild-type (XX WT, n=2), XY wild-type (XY WT, n=4) and XY *Znrf3*$^{-/-}$ (XY Hom, n=4) sub-dissected gonads. Expression was calculated relative to *Hprt1* (ratio). Error bars show SEM. T-tests (two-tailed) were performed with Welch's correction. Significant differences are indicated by * = P<0.05, ** = P<0.01, *** = P<0.001, **** = P<0.0001. Non-significant differences are signified by NS. Exact P values are detailed in the appendix (Table S7) **(b)**.

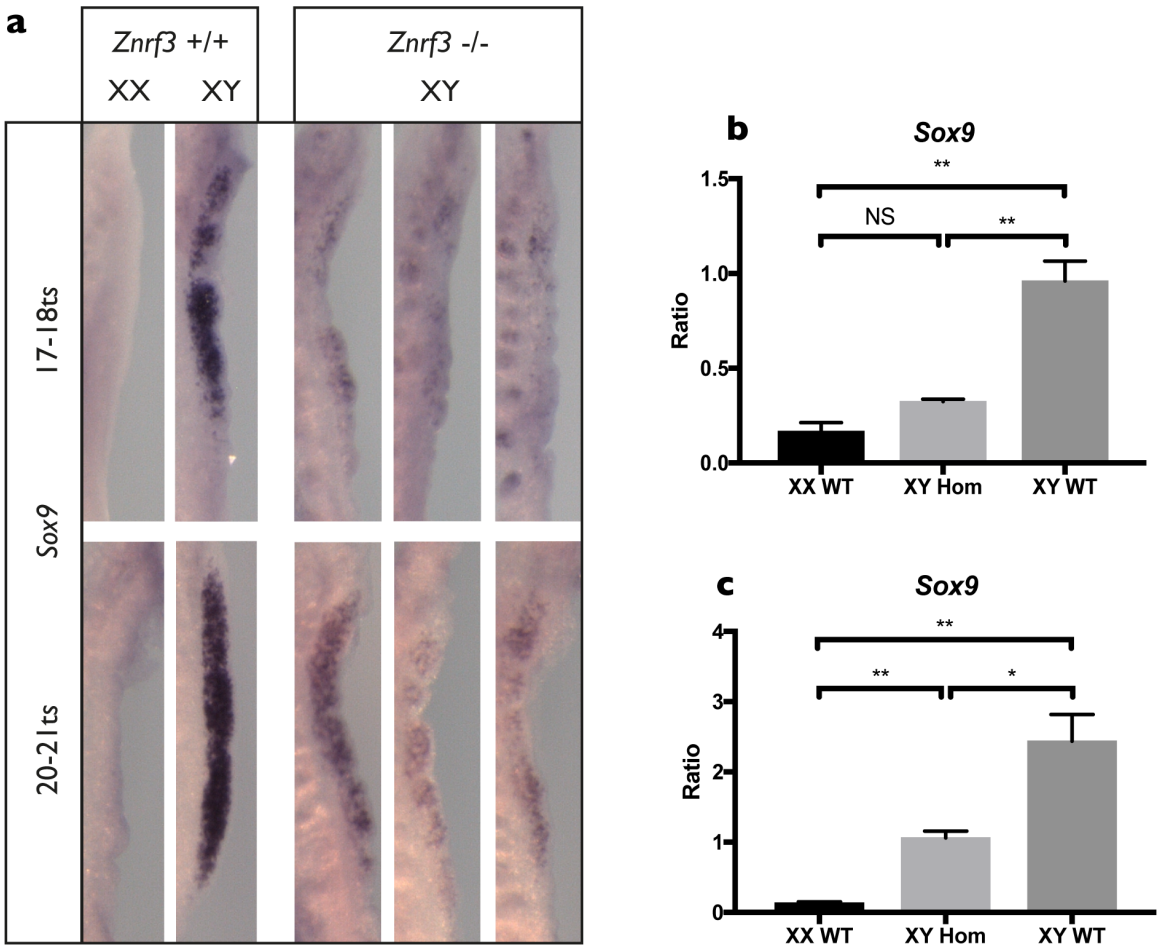

Figure 5.2 *Sox9* expression in *Znrf3*$^{-/-}$ gonads. WMISH was performed on 11.5 dpc gonads (17-18ts) (n=3, each genotype) and 12.0 dpc gonads (20-21ts) (n=3, each genotype) **(a)**. qRT-PCR was performed on 11.5 dpc (18ts) XX wild-type (XX WT, n=2), XY wild-type (XY WT, n=4) and XY *Znrf3*$^{-/-}$ (XY Hom, n=4) sub-dissected gonads **(b)**, and on 12.5 dpc (26-28ts) XX WT (n=3), XY WT (n=4) and XY Hom (n=4) sub-dissected gonads **(c)**. For qPCR results, expression was calculated relative to *Hprt1* (ratio). Error bars show SEM. T-tests (two-tailed) were performed with Welch's correction. Significant results are signified by * = $P<0.05$, ** = $P<0.01$, *** = $P<0.001$, **** = $P<0.0001$. Non-significant differences are signified by NS. Exact *P* values are detailed in the appendix (Table S7).

5.2.3 Analysis of canonical WNT-signalling

Lef1 and *Axin2* are genes downstream of β-catenin stabilisation, and therefore canonical WNT-signalling, and are routinely used as 'read-outs' or reporters of the activity of this signalling pathway (Chassot et al. 2008; Filali et al. 2002; Jho et al. 2002). The expression of *Lef1* was analysed in *Znrf3* null gonads at 11.5 dpc by WMISH. At 11.5 dpc (18ts), wild-type XX gonads express *Lef1* in the gonad, whereas expression cannot be detected in wild-type XY gonads. Significant expression is seen in *Znrf3*$^{-/-}$ XY gonads indicating an activation of canonical WNT-signalling (**Fig. 5.3a**). Expression levels of *Axin2* and *Lef1* were also analysed by qRT-PCR at 11.5 dpc. In both cases, expression was significantly higher in the XY *Znrf3*$^{-/-}$ gonad than XY wild-type, and not significantly different from the XX wild-type. As expected, *Lef1* expression is significantly higher in the XX compared to the XY wild-type. However, this sexual dimorphism is not seen in *Axin2* (**Fig. 5.3b and c**).

At 12.5 dpc there is high expression of *Lef1* in wild-type XX gonads of all genotypes, and no detectable expression in wild-type XY gonads by WMISH. However, high levels of *Lef1* are seen in XY *Znrf3*$^{-/-}$ gonads, and this expression extends along the entire length of the gonad. Levels of expression in all 4 XY *Znrf3* null gonads were similar. Expression of *Lef1* can also be seen in the mesonephros in all genotypes, which perhaps corresponds to the newly formed Müllerian ducts, and appears to be independent of sex or genotype (**Fig. 5.3d**). The gonadal expression patterns were confirmed by qRT-PCR. Both *Lef1* and *Axin2* levels are significantly higher in XX wild-type gonads compared to XY wild-types, where expression is minimal. XY *Znrf3*$^{-/-}$ gonads express *Lef1*/Axin2 at an intermediate level: expression is significantly greater than an XY wild-type, and significantly lower than an XX wild-type (**Fig. 5.3e and f**).

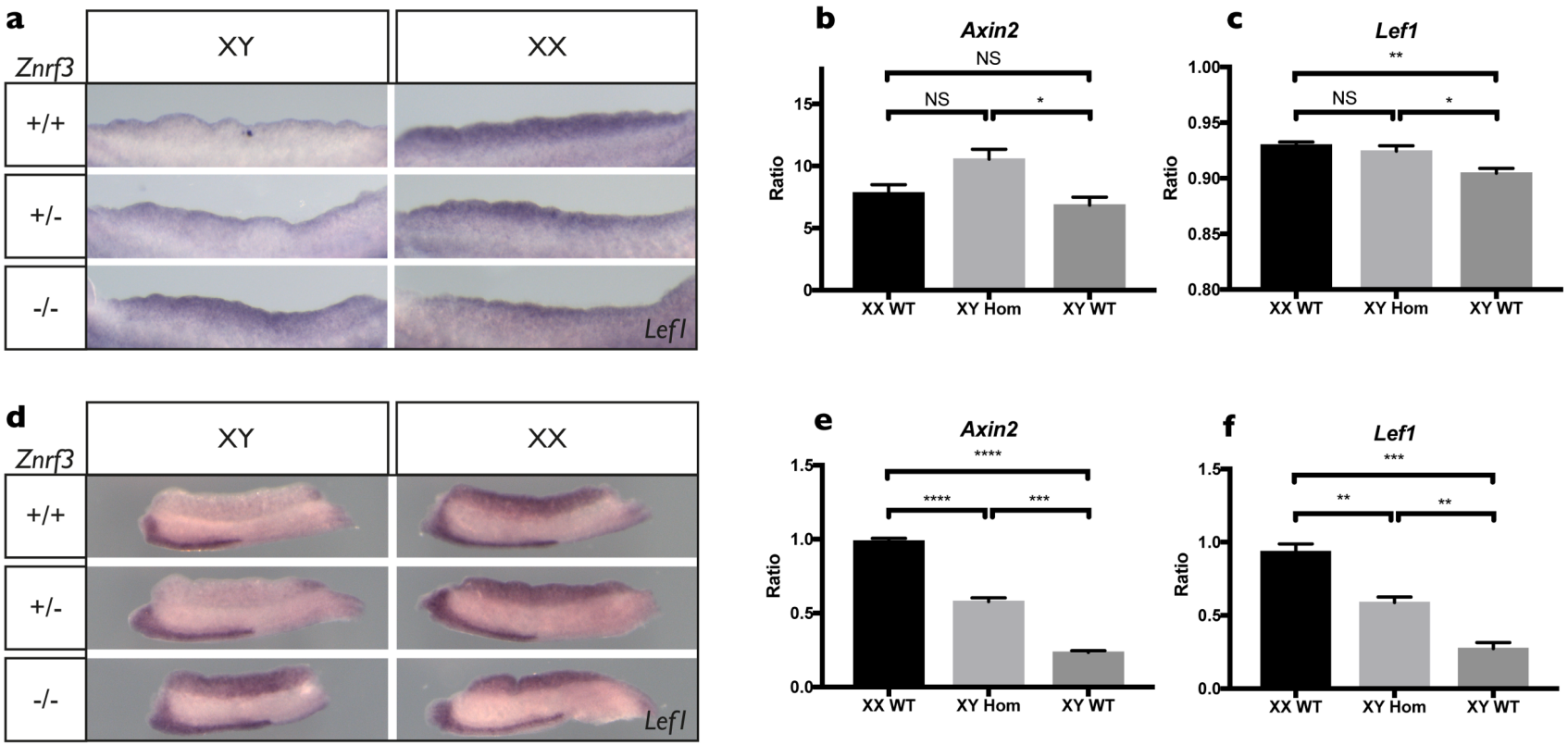

Figure 5.3 Expression of *Axin2* and *Lef1* in the *Znrf3*$^{-/-}$ gonad. For figure legend, please see following page.

Figure 5.3 Expression of *Axin2* and *Lef1* in the *Znrf3*$^{-/-}$ gonad (previous page) WMISH was performed on 11.5 dpc gonads (17-18ts) (n=3, each genotype) **(a)**. qRT-PCR was performed on 11.5 dpc (18ts) XX wild-type (XX WT, n=2), XY wild-type (XY WT, n=4) and XY *Znrf3*$^{-/-}$ (XY Hom, n=4) subdissected gonads for *Axin2* **(b)**, and *Lef1* **(c).** WMISH was performed on 12.5 dpc gonads (n=3-4, each genotype) to analyse *Lef1* expression **(d)**. qRT-PCR was also performed on 12.5 dpc (26-28ts) XX WT (n=3), XY WT (n=4) and XY Hom (n=4) sub-dissected gonads for *Axin2* **(e)** and *Lef1* **(f)**. For qPCR results, relative expression was calculated relative to *Hprt1* (ratio). Error bars show SEM. T-tests (two-tailed) were performed with Welch's correction. Significant results are signified by * = $P<0.05$, ** = $P<0.01$, *** = $P<0.001$, **** = $P<0.0001$. Non-significant differences are signified by NS. Exact *P* values are detailed in the appendix (Table S7).

5.2.4 Ovarian marker gene expression

Wnt4 is an ovarian gene which is initially expressed in both sexes, but which becomes restricted to the XX gonad at around the time of sex determination (Kim et al. 2006; Vainio et al. 1999). At 11.5 dpc, *Wnt4* expression is significantly increased in XY *Znrf3*$^{-/-}$ gonads compared to XY wild-type gonads. Expression levels are instead similar to XX wild-type gonads. As expected, *Wnt4* expression is significantly higher in XX wild-type compared to XY wild-type gonads (Fig. 5.4a). At 12.5 dpc, expression in XY *Znrf3* null gonads is significantly different from both XX and XY wild-types, with intermediate levels apparent. *Wnt4* expression is also significantly higher in XX wild-types compared to XY wild-types at this stage (Fig. 5.4a').

In order to allow some assessment of inter-sample and spatial variability, expression was further analysed by WMISH at 12.5 dpc. Strong expression is detected in wild-type XX gonads, with lower levels in the mesonephros (n=3) (Fig. 5.4b). In contrast, *Wnt4* is absent from the XY wild-type gonad, but can be detected more strongly in the mesonephros (n=4). In XY *Znrf3*$^{-/-}$ tissue, expression can be detected in both the gonad and mesonephros in all samples (n=4). However, the expression in the gonad is highly variable (Fig. 5.4b); expression along the length of the gonad [1]; expression in half of the gonad [2]; expression at the poles

but absent from the middle [3]; and expression only in cells close to the gonad-mesonephros border [4], are all observed. XY *Znrf3*$^{+/-}$ gonads show a similar expression pattern to wild-type littermates: no *Wnt4* expression is detected in the gonad, but significant expression is seen in the mesonephros. However, very small areas of *Wnt4* expression can be detected at the extreme poles in some (2/8 single gonads) *Znrf3*$^{+/-}$ gonads, which are never observed in any wild-type XY gonads (n=4) (**Fig. 5.4c**).

RSPO1 regulates the levels of ZNRF3 on the cell surface (Hao et al. 2012). *Rspo1* is expressed predominately in the supporting cell lineage, and is expressed at higher levels in XX supporting cells than XY, from 11.5 dpc to 13.5 dpc (Jameson et al. 2012). *Rspo1* expression levels were analysed by qRT-PCR in sub-dissected gonads. At 11.5 dpc (17ts) there is no significant difference in whole gonadal expression between XX and XY wild-type, consistent with published data (Parma et al. 2006), and levels of *Rspo1* are also not significantly different in XY *Znrf3* null gonads (**Fig. 5.5a**). However, by 12.5 dpc (26-27ts) expression has become sexually dimorphic: XX wild-type gonads express significantly more *Rspo1* than XY wild-type gonads, again consistent with published data (Parma et al. 2006). XY *Znrf3*$^{-/-}$ gonads have an intermediate phenotype with significantly less expression compared to an XX wild-type gonad, but significantly more compared to an XY wild-type (**Fig. 5.5a'**).

Another ovarian marker gene is *Foxl2,* which is a marker of granulosa cells (Ottolenghi et al. 2005). At 12.5 dpc (26-28ts) expression is sexually dimorphic in the wild-type gonads, with significantly higher expression in the XX gonads. Like *Rspo1* expression, the XY *Znrf3*$^{-/-}$ gonads express an intermediate level of *Foxl2* which is significantly different from both XX and XY wild-type controls (**Fig. 5.5b**).

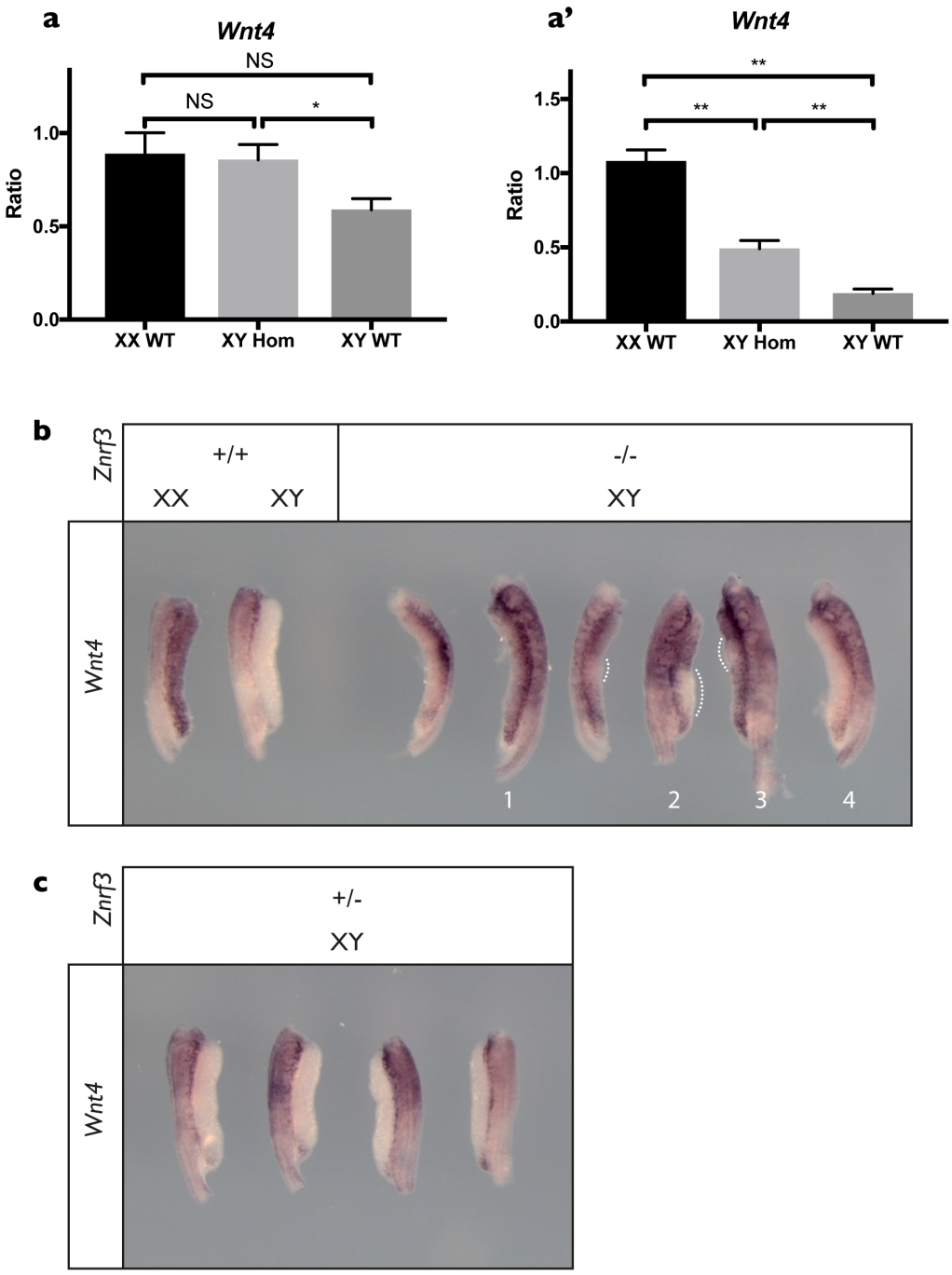

Figure 5.4 Expression of *Wnt4* in the *Znrf3*$^{-/-}$ gonad. qRT-PCR was performed on 11.5 dpc (18ts) XX wild-type (XX WT, n=2), XY wild-type (XY WT, n=4) and XY *Znrf3*$^{-/-}$ (XY Hom, n=4) sub-dissected gonads **(a)**, and on 12.5 dpc (26-28ts) XX WT (n=3), XY WT (n=4) and XY Hom (n=4) sub-dissected gonads **(a')**. WMISH was carried out on 12.5 dpc XX wild-type, XY wild-type and XY *Znrf3*$^{-/-}$ gonads **(b).** White dotted lines emphasize portions of the gonad with no *Wnt4* expression **(b).** WMISH was also carried out on XY *Znrf3*$^{+/-}$ gonads at 12.5 dpc. For qPCR results, relative expression was calculated relative to *Hprt1* (ratio). Error bars show SEM. T-tests (two-tailed) were performed with Welch's correction. Significant results are signified by * = P<0.05, ** = P<0.01, *** = P<0.001, **** = P<0.0001. Non-significant differences are signified by NS. Exact P values are detailed in the appendix (Table S7). WMISH was performed on 12.5 dpc gonads (26-28ts) (n=3-4, each genotype).

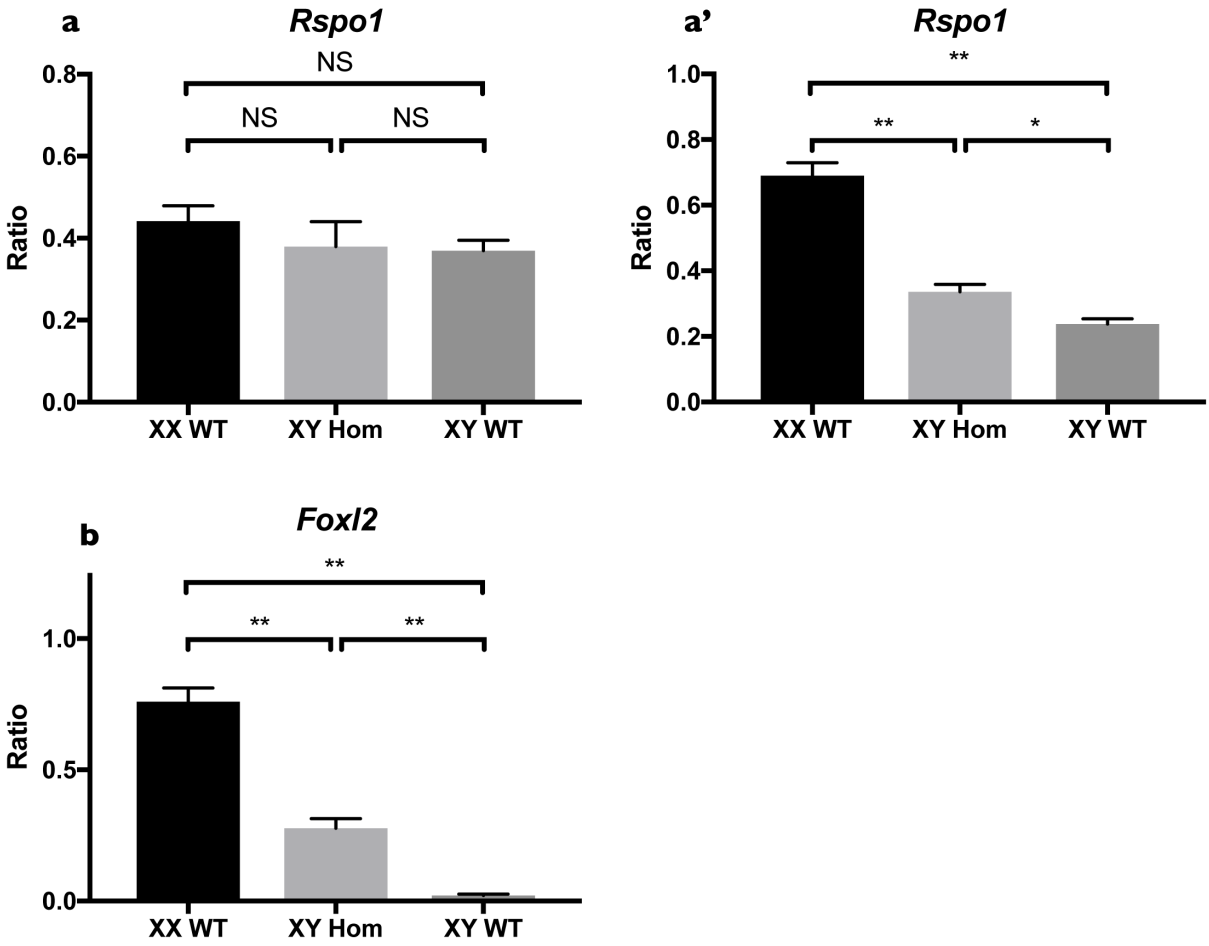

Figure 5.5 Expression of *Rspo1* and *Foxl2* in *Znrf3*$^{-/-}$ gonads. *Rspo1* expression was analysed by qRT-PCR at 11.5 dpc (18ts) XX wild-type (XX WT, n=2), XY wild-type (XY WT, n=4) and XY *Znrf3*$^{-/-}$ (XY Hom, n=4) subdissected gonads **(a)**, and at 12.5 dpc (26-28ts) XX WT (n=3), XY WT (n=4) and XY Hom (n=4) subdissected gonads **(a')**. *Foxl2* expression was analysed at 12.5 dpc (26-28ts) **(b).** For qPCR results, relative expression was calculated relative to *Hprt1* (ratio). Error bars show SEM. T-tests (two-tailed) were performed with Welch's correction. Significant results are signified by * = $P<0.05$, ** = $P<0.01$, *** = $P<0.001$, **** = $P<0.0001$. Non-significant differences are signified by NS. Exact *P* values are detailed in the appendix (Table S7).

5.2.5 *Fgf9* expression

Wnt4 and *Fgf9* oppose each during sex determination (Kim et al. 2006; S. Jameson, Lin, and Capel 2012). Given that loss of *Znrf3* causes an increase in canonical WNT-signalling in the gonad (see Fig. 5.3), we analysed whether *Fgf9* expression was downregulated in the XY *Znrf3*$^{-/-}$ gonad. qRT-PCR analysis was carried out on 11.5 dpc (17ts) subdissected gonads. *Sox9* expression levels were used as a control. XY wild-type and XX wild-type gonads show a significant difference in expression, as expected. Confirming previous experiments (see Fig. 5.2b), there is a significant difference between XY *Znrf3*-null gonads and XY wild-type controls (Fig. 5.6a). The actual observed difference in *Sox9* expression is lower, perhaps due to inter-experimental differences, or due to samples in the previous experiment being 1ts older. When *Fgf9* expression was analysed at 17ts, no significant differences in expression were seen between any genotype or sex. Two-way ANOVA on data including XX *Znrf3*$^{-/-}$ gonads showed no significant interaction and no contribution to the error by sex or genotype (data not shown). However, there does appear to be a trend towards an intermediate level of *Fgf9* in the XY *Znrf3*$^{-/-}$ null gonad. *Fgf9* WMISH experiments were not performed due to the quality of the probe and time constraints. Analysis of *Fgf9* expression by qRT-PCR at later stages was not attempted due to time constraints, but may have been more informative.

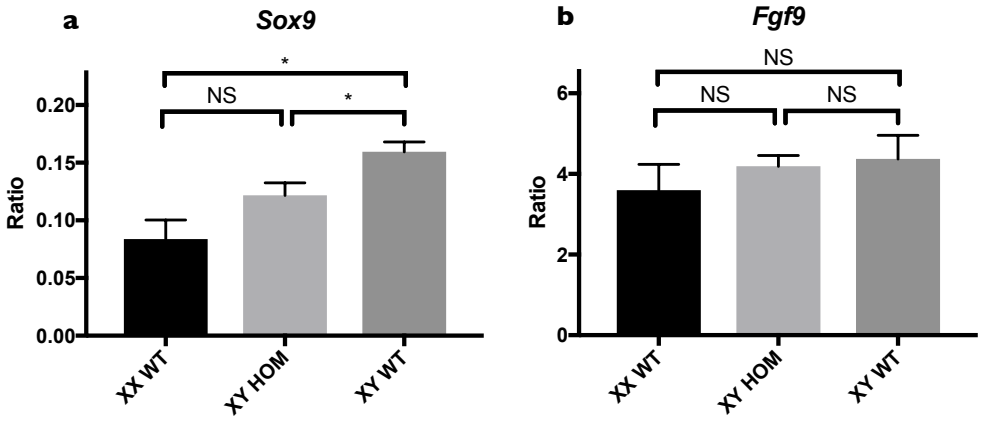

Figure 5.6 Expression of Fgf9 in the *Znrf3*-null gonad. qRT-PCR was performed on 11.5 dpc (17ts) XX wild-type (XX WT, n=4), XY wild-type (XY WT, n=4) and XY *Znrf3*$^{-/-}$ (XY Hom, n=4) subdissected gonads to analyse *Sox9* expression **(a)** and *Fgf9* expression **(b).** For qPCR results, relative expression was calculated relative to *Hprt1* (ratio). Error bars show SEM. T-tests (two-tailed) were performed with Welch's correction. Significant results are signified by * = *P*<0.05, ** = *P*<0.01, *** = *P*<0.001, **** = *P*<0.0001. Non-significant differences are signified by NS. Exact *P* values are detailed in the appendix (Table S7).

5.2.6 *Sf1, Wt1* and *Oct4* expression

Sf1, as previously described, is expressed in the somatic cell lineages, including supporting and interstitial cells and is critical for the initial formation of the gonadal ridge (X Luo, Ikeda, and Parker 1994). No significant difference in expression was detected by qRT-PCR at 11.5 dpc or 12.5 dpc between XY wild-type, XY *Znrf3*$^{-/-}$ or XX wild-type gonads (**Fig. 5.7a, a'**). *Wt1* is also critical for the initial gonadal development, and regulates the expression of *Sf1* in the somatic cells (Kreidberg et al. 1993; Westphal et al. 2000). qRT-PCR shows that *Wt1* is not significantly different between XY *Znrf3* null gonads and XY wild-type gonads at either 11.5 dpc or 12.5 dpc (**Fig. 5.7b, b'**). Together, this suggests that the early development and specification of the somatic cell lineages is unaffected by the loss of *Znrf3*.

Oct4 is a transcription factor which is expressed exclusively in primordial germ cells (PGCs) from around 7.5 dpc (Rosner et al. 1990; Schöler et al. 1990). No significant difference in

Oct4 expression was detected between XY *Znrf3* null, XY wild-type or XX wild-type gonads at 12.5 dpc (**Fig. 5.7c'**). This suggests that the loss of *Znrf3* does not affect the number of PCGs that are specified, or which enter the gonad. At 11.5 dpc, significantly higher expression was detected in the XY *Znrf3*$^{-/-}$ gonads compared to XY wild-types (**Fig. 5.7c**). This may be artefactual, but even if a true result, still suggests that *Znrf3* null gonads do not lack PGCs at this early stage. The potential role of *Znrf3* in germ cells will be discussed further in **Chapter 7**.

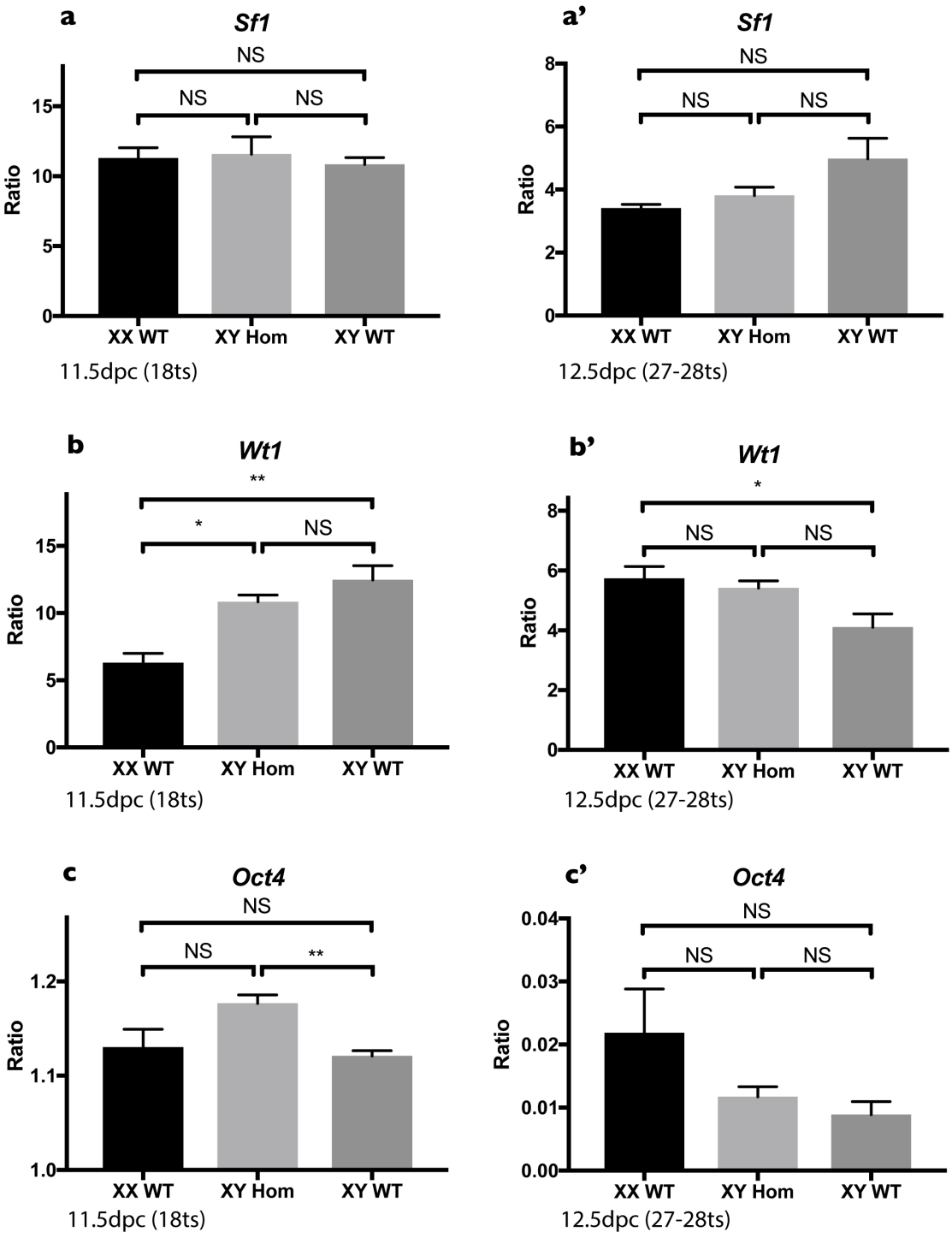

Figure 5.7 Expression of *Sf1*, *Wt1* and *Oct4* in the *Znrf3*-null gonad. qRT-PCR was performed on 11.5 dpc (18ts) XX wild-type (XX WT, n=2), XY wild-type (XY WT, n=4) and XY *Znrf3*$^{-/-}$ (XY Hom, n=4) subdissected gonads to analyse *Sf1* **(a),** *Wt1* **(b)** and *Oct4* **(c)** expression**.** qRT-PCR was also performed on 12.5 dpc (27-28ts) subdissected gonads (of each genotype) to analyse *Sf1* **(a'),** *Wt1* **(b')** and *Oct4* **(c')** expression**.** For qPCR results, expression was calculated relative to *Hprt1* (ratio). Error bars show SEM. T-tests (two-tailed) were performed with Welch's correction. Significant results are signified by * = *P*<0.05, ** = *P*<0.01, *** = *P*<0.001, **** = P<0.0001. Non-significant differences are signified by NS. Exact *P* values are detailed in the appendix (Table S7).

5.2.6 *Znrf3* expression

Znrf3 and *Rnf43*, whilst being WNT-antagonists, are in a negative feedback loop; both genes are transcriptionally upregulated as a result of canonical WNT-signalling (Hao et al. 2012). Given that the *Znrf3*$^{-}$ allele removes only exon 7, it is possible that a *Znrf3* transcripts are still present in the homozygous null gonad. qRT-PCR primers were therefore designed upstream of the excised region to detect both the *Znrf3*^{WT} and *Znrf3*$^{-}$ allele.

Znrf3 expression was analysed by qRT-PCR. At 11.5 dpc, levels are not significantly different between XX and XY gonads as seen in previous experiments. However, XY *Znrf3*$^{-/-}$ show significantly greater expression than both XX and XY wild-type controls (**Fig. 5.8a**). The following day, at 12.5 dpc, expression remains highest in XY *Znrf3*-null gonads. This is significantly higher than expression in XX wild-type controls, but not XY wild-type controls. This experiment also confirms previous results which show no difference between expression in XX and XY whole wild-type gonads (**Fig. 5.8a'**).

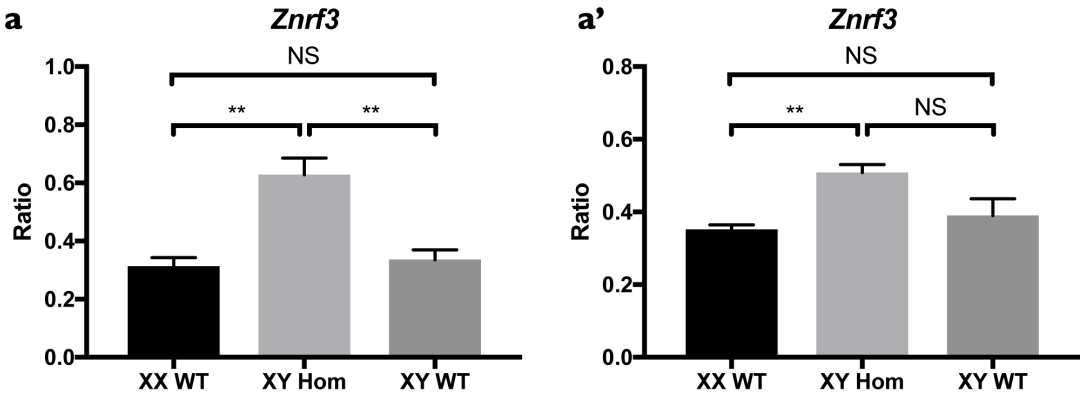

Figure 5.8 Expression of *Znrf3* in the *Znrf3*$^{-/-}$ gonad. qRT-PCR was performed on 11.5 dpc (18ts) XX wild-type (XX WT, n=2), XY wild-type (XY WT, n=4) and XY *Znrf3*$^{-/-}$ (XY Hom, n=4) subdissected gonads **(a)**, and on 12.5 dpc (26-28ts) XX WT (n=3), XY WT (n=4) and XY Hom (n=4) subdissected gonads **(a')**. For qPCR results, expression was calculated relative to *Hprt1* (ratio). Error bars show SEM. T-tests (two-tailed) were performed with Welch's correction. Significant results are signified by * = P<0.05, ** = P<0.01, *** = P<0.001, **** = P<0.0001. Non-significant differences are signified by NS. Exact P values are detailed in the appendix (Table S7).

5.2.7 Results Summary

In this chapter, the expression of genes in the testis-determining pathway has been analysed in mutant and wild-type gonads at the sex-determining stage of development. At the peak of *Sry* expression in the gonad, there is no detectable difference between XY wild-type and XY *Znrf3* null gonads. *Sox9* is significantly downregulated in the *Znrf3*-null gonad at 11.5 dpc. However, by about 12.0 dpc, Sox9 expression is more variable with some XY *Znrf3*$^{-/-}$ gonads show reasonable levels of *Sox9* expression, although not to the extent of the XY wild-type.

Genes downstream of canonical WNT-signalling are absent from XY wild-type gonads, and upregulated in XY *Znrf3*-null gonads at both 11.5 dpc and 12.5 dpc. *Wnt4* is also strongly expressed in the XY *Znrf3*$^{-/-}$ gonad at 12.5 dpc, although the pattern of expression is highly variable. Other ovarian pathway genes are also upregulated in the XY mutant gonad at 12.5 dpc, including *Rspo1* and *Foxl2.* Finally, levels of *Znrf3* transcript are increased in the mutant gonad at 11.5 dpc, but not at 12.5 dpc.

5.2. Discussion

5.2.1 *Znrf3* acts downstream of *Sry*

As previously described, *Sry* must be expressed at a threshold level, and in a critical developmental window, to initiate the cascade of expression of testis-determining genes downstream (Sekido and Lovell-Badge 2008; Hiramatsu et al. 2008). Loss of *Znrf3* from the XY gonad does not affect *Sry* expression at 11.5 dpc (18ts) confirmed by WMISH and quantitatively by qRT-PCR. This suggests that *Znrf3* does not act upstream of *Sry.* However, only gonads of 18ts were analysed in this experiment. This time point was chosen as it has been previously shown that the peak of *Sry* expression in C57BL6/J is at this stage (Hacker et al. 1995; Bullejos and Koopman 2005). If time and resources permitted, a fine-grained time-course of *Sry* expression would be carried out over the critical sex determination period. This might reveal more subtle differences in *Sry* expression.

Despite normal *Sry* expression being maintained in the XY *Znrf3*-null gonad, *Sox9* expression is severely affected. At 11.5 dpc (18ts), *Sox9* expression in XY *Znrf3*$^{-/-}$ gonads is not significantly different from XX wild-types. This is confirmed by WMISH which shows patchy, low expression, indicating that *Sry* expression at this point is sufficient to activate some expression of *Sox9*. By 20-21ts, *Sox9* expression in the XY wild-type gonad is strong and throughout the gonad. On the other hand, expression in the XY *Znrf3* null gonad is variable, both between gonads and within individual gonads. The difference between expression in XY wild-type and XY *Znrf3*$^{-/-}$, quantified by qRT-PCR, is still significant at this point, although the actual difference is reduced. This suggests that some gonads are able to upregulate *Sox9* to a more significant degree on a regional basis. This may be due to stochastic effects seen

at a cellular level involving the complex interaction between pro-testis factors (SRY, SOX9, FGF9) and pro-ovary factors (WNT/β-catenin, FOXL2).

5.2.2 Loss of *Znrf3* promotes canonical WNT-signalling and *Wnt4* expression in the XY gonad

Lef1 and Axin2 are direct downstream targets of canonical WNT-signalling (Filali et al. 2002; Jho et al. 2002). Through analysis of expression of these two genes, this chapter has presented evidence that canonical WNT-signalling is significantly upregulated in the *Znrf3*-null gonad, compared to wild-type. This difference appears to be more pronounced at 12.5 dpc than at 11.5 dpc. This correlates with the increase in sexually dimorphic expression of *Lef1* and Axin2 in wild-type gonads. Levels are consistently high in the XY *Znrf3*$^{-/-}$ null gonad, and based on WMISH data, *Lef1* expression can be detected throughout the gonad at both 11.5 dpc and 12.5 dpc. Interestingly, qRT-PCR data at 12.5 dpc suggests that levels of canonical WNT-signalling are intermediate when compared to XX and XY wild-types. The fact that levels of expression of *Axin2* and *Lef1* are still significantly lower than XX wild-type gonads may account somewhat for the phenotypic variability in the male-to-female sex reversal we see at 14.5 dpc, as previously described.

At 11.5 dpc, *Axin2* is not significantly sexually dimorphic, compared to *Lef1* which shows significantly greater expression in the XX gonad both in WMISH and qRT-PCR experiments. This may simply be an artefact owing to the smaller size of the 11.5 dpc gonad, cell type-specific variability in *Axin2* levels or the sensitivity of the *Axin2* primers. Alternatively, *Axin2* and *Lef1* could be differentially regulated and differentially effected by the loss of *Znrf3* at this time-point. However, by 12.5 dpc, *Lef1* and *Axin2* show a similar pattern of expression, suggesting a similar impact on phenotype at this stage.

WMISH shows that *Lef1* was also expressed in the mesonephros of both sexes, at 12.5 dpc. Expression was consistently detected from the anterior end of the mesonephros, to approximately midway down the length of the gonad. This most likely corresponds to the Müllerian Duct, which at this stage is elongating in both XX and XY mesonephroi, and will regress in XY embryos from around 15.5 dpc (Mullen and Behringer 2014). Therefore, it is not surprising that expression is similar in XX and XY embryos. However, expression was also not affected by the absence of *Znrf3*. In this case, we may have expected an expansion of the region in which *Lef1* is expressed in the absence of a WNT-antagonist, given that *Znrf3* is strongly expressed in the mesonephros at 12.5 dpc.

In contrast to the expression of *Lef1* in the gonad, which indicates that canonical WNT-pathway is activated throughout the whole gonad, *Wnt4* expression in *Znrf3*-null gonads is irregular and variable. Some areas of an XY *Znrf3*$^{-/-}$ gonad express *Wnt4*, while in an adjacent patch expression is completely absent. This variability echoes that seen at 14.5 dpc, and may also explain some of the unusual ovotesticular phenotypes observed, including gonads where *Sox9* expression and testis cords are limited to one pole of the gonad. Portions of the gonad expressing *Wnt4* may develop as ovarian tissue, and patches where *Wnt4* is absent, as testicular tissue.

Interestingly, WMISH data seem to suggest that tissue closest to the gonad-mesonephros border is more likely to express *Wnt4* in *Znrf3*-null gonads. For example, an XY *Znrf3*$^{-/-}$ gonad which is expressing very little *Wnt4* in the body of the gonad (**Fig. 5.4 [4]**) still expresses *Wnt4* in a thin band near the mesonephros. Furthermore, other gonads expressing *Wnt4* throughout the gonad seem to express the highest levels in this region. This medullary-cortical polarity of expression has been reported before, in Kim et al. (2006), who showed

that *Fgf9* is most highly expressed near the gonad surface, and *Wnt4* near the mesonephros at 11.5 dpc. The importance of this polarity of expression in the gonad is thus far not understood, in particular for phenotypes caused by loss of genes in the FGF9 or WNT4 pathways or sex reversal phenotypes more generally.

Significant *Lef1, Axin2* and *Wnt4* expression cannot be detected in XY *Znrf3*$^{+/-}$ gonads by qRT-PCR. This suggests that one copy of wild-type *Znrf3* is sufficient to suppress canonical WNT-signalling, and to prevent the activation of *Wnt4* in the XY gonad. This is consistent with the fact that *Znrf3*$^{+/-}$ gonads do not show a sex reversal phenotype at 14.5 dpc.

5.2.3 WNT/β-catenin signalling and *Sox9*

One significant question for this thesis is: how does elevated WNT/β-catenin signalling in the *Znrf3*-null gonad at 11.5 – 12.5 dpc result in reduced Sox9 expression at the same stages? This is the simplest explanation of the observed disruption to testis determination in mutants: *Znrf3* causes enhanced WNT/β-catenin signalling and this disrupts Sox9 expression. But how? There is good evidence in the literature that a mutually antagonistic relationship exists between canonical WNT-signalling and SOX9. For example, ectopic activation of the WNT/β-catenin signalling pathway directly inhibits the transcription of *Sox9* in ex vivo XY gonads, and interferes with the ability of SF1 to interact with and activate the *Sox9* enhancer, TESCO (Bernard et al. 2012b). Data presented in this chapter show that *Sox9* expression is significantly decreased in XY *Znrf3*-null gonads from 11.5 dpc onwards. The ability of WNT/β-catenin signalling to inhibit the initial upregulation of *Sox9* by SF1/SRY is consistent with these data. In addition to WNT/β-catenin signalling suppressing *Sox9* expression, SOX9 has also been shown to inhibit canonical WNT-signalling activity (Topol et

al. 2009a). The reciprocal interaction between SOX9 and WNT4 will be discussed further in Chapter 7.

5.2.4 WNT/β-catenin signalling and *Wnt4* expression

One other question is how an upregulation of canonical WNT-signalling results in strong *Wnt4* expression in the XY *Znrf3*-null gonad. There are many mechanistic examples of negative feedback loops in the regulation of WNT/β-catenin signalling in many systems and organisms (Jho et al. 2002; Leung et al. 2002; Niida et al. 2004; Zeng and Verheyen 2004; Chamorro et al. 2005). This includes the upregulation of WNT-antagonists ZNRF3/RNF43 in response to β-catenin stabilisation (Hao et al. 2012). However, there is little evidence in the literature which suggests that positive feedforward loops are common. One hypothesis which could explain these data is that activation of the WNT/β-catenin pathway leads to the inactivation of a repressor of *Wnt4*. This will be discussed in the context of the mutually antagonistic relationship which has been described between FGF9 and WNT4 below (section 5.2.5 – Mutual antagonism).

5.2.4 Other ovarian genes are upregulated in the *Znrf3*-null gonad

Rspo1 expression is not initially sexually dimorphic based on studies of the whole gonad at11.5 dpc and there is no significant difference in expression in XY *Znrf3*-null gonads compared to XX or XY controls. However, by 12.5 dpc, expression is significantly sexually dimorphic. Expression levels in the 12.5 dpc XY *Znrf3*$^{-/-}$ are closer to the XX wild-type gonad although still significantly higher. This intermediate expression of *Rspo1* supports the fact that, by 12.5 dpc, the XY *Znrf3*$^{-/-}$ gonad is partially sex reversed. *Rspo1* expression becomes upregulated in the XY *Znrf3*-null gonad only after primary sex determination. This may suggest that this is a secondary effect of the XY *Znrf3*-null gonad assuming the ovarian fate.

Alternatively, the assay used may not be sensitive enough to detect small differences between the XY wild-type and *Znrf3*-null gonads at this time-point, and furthermore, may be confounded by the presence of other cell lineages in the gonad. Microarray data shows *Rspo1* expression is significantly higher in XX pre-granulosa cells compared to XY pre-Sertoli cells when only the supporting cell lineage is analysed (S. A. Jameson et al. 2012). Therefore, it is possible that if we could analyse expression in supporting cell precursors alone, a significant difference may have been detected between XY *Znrf3*$^{-/-}$ and XY wild-type controls at this earlier time point.

Foxl2 is a transcription factor expressed in an ovary-specific fashion from at least 12.0 dpc (Ottolenghi et al. 2005). *Foxl2* does not appear to play a role in primary sex determination, and is considered to act at downstream of other ovarian pathway components such as *Wnt4* and *Rspo1*. *Foxl2* expression is significantly elevated in XY *Znrf3* null gonads compared to XY wild-type controls at 12.5 dpc. This suggests that the ovarian fate is well established in the XY *Znrf3* null gonad, at least in some somatic cells, as early as 12.5 dpc.

Taken together, expression profiles of *Rspo1* and *Foxl2* support data described earlier in this thesis, which suggests loss of *Znrf3* is having an early effect on sex determination. This is then canalised such that by 12.5 dpc, the XY *Znrf3*$^{-/-}$ gonad shows significantly different expression from both wild-type XX and XY gonads for a wide range of genes.

5.2.5 Mutual antagonism: FGF9 and WNT4

As previously described, the ovarian and testicular pathways antagonise each other, to ensure a robust switch in cell fate in an individual cell. One of the most well studied and convincing antagonistic interactions between a pair of genes during sex determination is between *Wnt4* and *Fgf9* (Kim et al. 2006). This chapter has demonstrated that WNT-

signalling is significantly upregulated in the XY *Znrf3*-null gonad compared to an XY wild-type. Given that *Wnt4* itself is also upregulated, we might expect that *Fgf9* levels would decrease as a result in the *Znrf3*-null gonad.

This chapter shows no significant differences in *Fgf9* expression between genotypes, although there is a non-significant trend for an intermediate level of *Fgf9* in the XY *Znrf3*$^{-/-}$ gonad compared to XX and XY wild-types. Interestingly, there is also no significant difference between wild-type XX and XY gonads. This can be explained by the fact that *Fgf9* expression is sexually dimorphic between 11.5 dpc and 13.5 dpc, but only in the supporting cell lineage, with significantly higher expression in pre-Sertoli cells compared to pre-granulosa cells. *Fgf9* expression in other cell lineages is low, and is not sexually dimorphic (S. A. Jameson et al. 2012). Expression of *Fgf9* in these other lineages may be masking this biologically relevant difference because whole gonads were used for qPCR experiments. Therefore, as has been stated elsewhere in this thesis, detection of a difference between XY *Znrf3*-null and XY wild-type gonads may be hindered by the presence of other expressing cell lineages in the gonad.

Interestingly, FGF9 is also able to upregulate *Znrf3* expression in the mouse gonad. In organ culture experiments, carried out by another member of the lab, XX wild-type gonads were cultured in the presence of high concentrations of FGF9 exogenous protein. WMISH showed that *Znrf3* is upregulated in those gonads treated with FGF9 compared to untreated control gonads (Pam Siggers, unpublished data). This demonstrates that, in an *ex vivo* context, FGF9 can directly or indirectly upregulate *Znrf3* expression. *Znrf3* may only be upregulated in the XY supporting cell lineage where *Fgf9* expression is highly sexually dimorphic.

5.2.6 *Znrf3* is upregulated in the *Znrf3*$^{-/-}$ gonad

In certain contexts, *Znrf3* and *Rnf43* are involved in a negative feedback loop with canonical WNT/β-catenin signalling (Hao et al. 2012). They are transcriptionally upregulated when WNT/β-catenin signalling is high, and act to antagonise it to modulate its level in the cell. Whether such feedback mechanisms are operative in the developing gonad, or whether other transcriptional control mechanisms over-ride them, remains to be discovered. This chapter has shown that *Lef1* and *Axin2* are significantly upregulated in the *Znrf3* null gonad. This increased canonical WNT-signalling therefore may drive *Znrf3* transcription in the gonad.

5.2.8 Concluding Remarks

This chapter aimed to characterise gene expression in the *Znrf3*-null gonad to further elucidate the role of *Znrf3* in mouse testis development and the basis of partial and variable gonadal sex reversal on the B6 background. Data have been presented that show that, whilst ZNRF3 acts downstream of *Sry*, it has a significant impact on *Sox9* expression even at 11.5 dpc. This suggests that *Znrf3* is playing a role early in the primary sex determination process. The significant reduction of *Sox9* expression in the XY *Znrf3*$^{-/-}$ gonad is associated with upregulation of the WNT/β-catenin signalling pathway, and *Wnt4*. This upregulation is detected as early as 18ts, with significantly higher expression of *Lef1* in the XY *Znrf3*$^{-/-}$ gonads compared to wild-type control. Furthermore, other markers of ovarian fate, such as *Rspo1* and *FoxL2* are upregulated in the XY *Znrf3* null gonad as early as 12.5 dpc.

The simplest interpretation of these data is a model in which loss of ZNRF3 causes elevated WNT/β-catenin signalling in the mutant XY gonad; these ectopic WNT signals then disrupt *Sox9* expression at 11.5 dpc. Consequently, activated ovarian pathway genes such as *Wnt4*

and *Foxl2* can drive granulosa fate, and ovarian fate more widely, in at least a subset of cells and regions. Variability in the degree of loss of *Sox9* and gain of *Wnt4* may depend on stochastic variability in expression levels at the earliest stages of sex determination and ultimately determine phenotypic variability observed at 14.5 dpc.

Chapter 6: Recapitulating a human *ZNRF3* mutation in the mouse

6.1 Introduction

This thesis has demonstrated that *Znrf3*-null mice show partial to full XY gonadal sex reversal, depending on genetic background, and therefore that ZNRF3 plays a key role in testis determination. Initial interest in the role of ZNRF3 was in part due to the identification of *ZNRF3* mutations in an exome screen of human DSD patients. Therefore, a key question is whether recapitulating these mutations in the mouse will lead to male-to-female gonadal sex reversal, as seen in the human patients.

6.1.1 Human mutations in *ZNRF3*

As previously described, two mutations were identified in an exome screen of DSD patients. Both are missense mutations causing amino acid substitutions in the intracellular domain of ZNRF3. The first mutation (S554N), detected in a case of 46,XY complete gonadal dysgenesis (CGD), causes a Serine residue to be substituted by an Asparagine. This mutation, in the context of the human protein, was predicted to be deleterious by prediction tools *Sift* and *Condel*, and probably damaging by *Polyphen*. The second (R768G), was identified in two sisters with 46,XY DSD, although clinical details were unavailable and CGD could not be confirmed. This causes an Arginine residue to be replaced with a Glycine residue. Again, R768G was predicted to be deleterious to the human protein structure by all 3 tools, apart from in the context of the longest isoform by *Sift*.

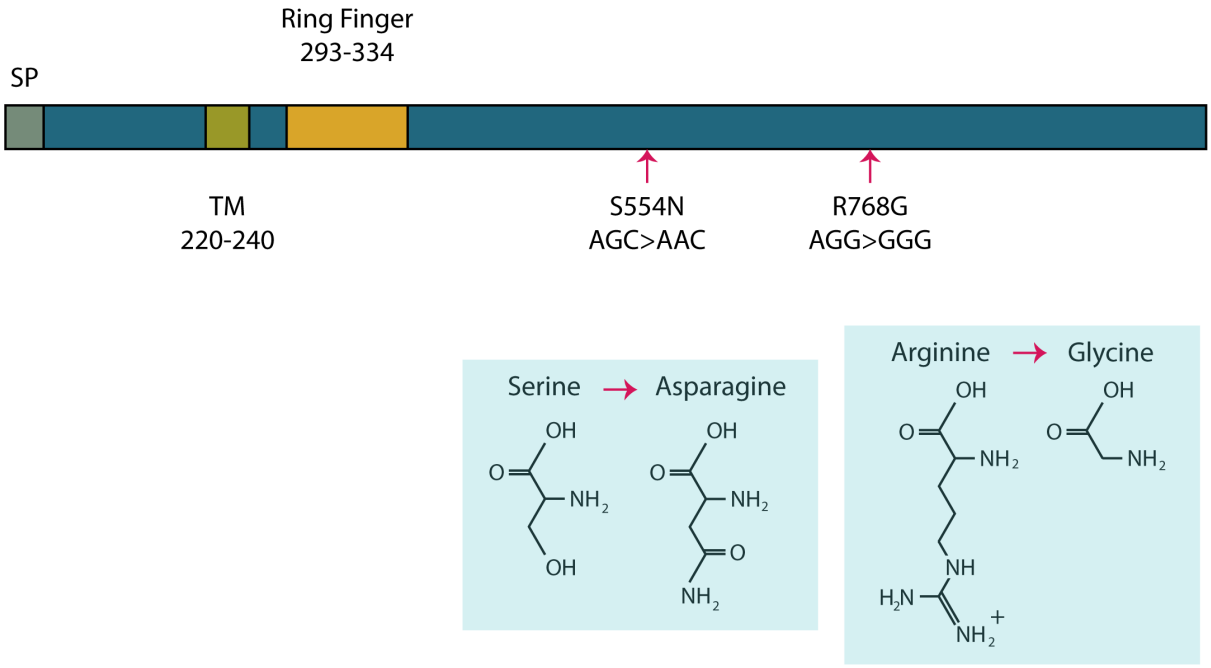

Figure 6.1 Position of two mutations in human *ZNRF3*. Two mutations were identified in an exome screen of human DSD patients: S554N and R768G. Amino acid structure of substitutions is shown in the blue box below each mutation. SP = Signal Peptide, TM = Transmembrane domain.

The effect of both mutations on protein function was analysed *in vitro* using a Super Top-Flash (STF) assay. Both S554N and R768G mutations were shown to significantly inhibit the WNT-antagonistic function of ZNRF3 in HEK293T cells (S. Corrochano, Pers. Comms, Fig. S6). This was confirmed in the KGN cell line, which originates from a human ovarian granulosa cell tumour (Anu Bashamboo, Pers. Comms.). These data suggest that both mutations could be pathogenic in the context of the human protein. Recently, a third mutation in *ZNRF3* has been identified, but has not yet been analysed *in vitro* for its potential effect on protein function. This provides further evidence for a role of ZNRF3 in human gonadal development. Together, this evidence was sufficient to justify investigation these mutations *in vivo*.

6.1.2 CRISPR/Cas9 technology

The use of CRISPR (clustered regularly interspaced palindromic repeats)/Cas9 (CRISPR-associated, 9) in genome editing has revolutionised our ability to efficiently and precisely generate mutations both *in vitro* and *in vivo*. Importantly for this thesis, CRISPR/Cas9 is now regularly being used to generate point mutations in the mammalian genome. The system is adapted from a type II CRISPR-Cas bacterial adaptive immune system.

CRISPRs are repeated sequences found in the bacterial genome, which originate from plasmid and viral genomes. CRISPRs were first identified in 1987 (Ishino et al. 1987). Subsequent studies identified similar repeats of bacteriophage-origin sequences in several bacterial and archaea genomes (Mojica et al. 2000; Bolotin et al. 2005; Pourcel, Salvignol, and Vergnaud 2005). Genetic manipulation of the number of spacers between CRISPR repeats, showed this correlated with resistance to bacteriophage (Barrangou et al. 2007). Barrangou et al. (2007) also showed that the CRISPR spacers were identical in sequence to the phage against which they provided resistance. This led to the hypothesis that the spacers constitute, in part, a prokaryotic immune system.

In the type II CRISPR system, used in this thesis, CRSIPR loci are transcribed and processed into shorter CRISPR RNAs (crRNAs). The crRNA binds a *trans*-activating crRNA (tracrRNA) (Deltcheva et al. 2011), and together are used to guide the Cas9 enzyme to a targeted cleavage site in the DNA (Jinek et al. 2012; Gasiunas et al. 2012). In prokaryotes, this system is, in this way, utilised to degrade invading pathogenic genetic material. The CRISPR/Cas9 system has therefore evolved to efficiently deliver the Cas9 enzyme to target sequences. Engineering of its components, including the Cas9 enzyme itself, allows us to target enzymatic activity to a precise location in any genome.

The most common use of CRISPR/Cas9 is in genome editing: the introduction of mutations into the genome of an organism, including point mutations or insertions and deletions (indels). In this case, the Cas9 enzyme is responsible for making a single- or double-stranded break at the target site (Garneau et al. 2010). Single guide RNAs (sgRNAs), which comprise an artificially fused form of the crRNA and tracrRNA, are used to target the Cas9 enzyme to the region of interest (Jinek et al. 2012). The only constraint is that the gRNA must end with a Protospacer Adjacent Motif (PAM) sequence which is dependent on the specific Cas9 used (Bolotin et al. 2005; Deveau et al. 2008). In the case of a *Streptococcus pyogenes* Cas9, used in this thesis, the specific PAM sequence is NGG (Jiang et al. 2013).

Once the Cas9 has been correctly targeted, the DNA is repaired by one of two endogenous pathways: the Non-Homologous End Joining (NHEJ) pathway (reviewed in (Lieber 2010)) or, with the aid of a DNA template for repair, the Homology-Directed Repair pathway (HDR). The NHEJ pathway frequently results in an insertion or deletion of sequence, an indel, at the site of the break (Bassing and Alt 2004). This can be useful in generating knockout alleles through deletions which result in a frame shift (Shalem et al. 2014). In contrast, repair through the HDR pathway can lead to the introduction of point mutations, and is most active in S phase, when DNA is replicated (Z. Mao et al. 2008). To introduce a point mutation using HDR and the CRISPR system, a DNA template containing the desired mutation is introduced, either as double-stranded DNA (dsDNA), or a single-stranded DNA oligonucleotides (ssDONs) (Song and Stieger 2017). The donor must contain homology arms complementary to the region of interest. The HDR pathway is then able to use the mutated template to repair the break, and will introduce the mutation into the repaired genomic DNA.

More recently, the CRISPR/Cas9 system has been further adapted for many applications. The critical aspect of the system is its ability to efficiently guide the CRISPR complex to a specific sequence. Therefore, by using enzymatically inactive forms of Cas9, effectively replacing the Cas9 enzyme with either another enzyme or, for example, with a fluorophore, the targeting system can be adapted for many other uses. Recently, the CRISPR system has been used to simultaneously and precisely label loci in live human cells, which provides an alternative to techniques such as Fluorescent In-situ Hybridisation (FISH) (Ma et al. 2015).

6.1.3 Strategy for generating *mZnrf3* mutations

Two mutations were identified at the start of this project as potentially causative in cases of human DSDs. For the S554N mutation, an Asparagine reside was already present in the equivalent position in the mouse protein. Therefore, a corresponding allele could not be generated in the mouse. The R768G mutation had a greater effect on ZNRF3 protein function *in vitro,* acting to enhance WNT/β-catenin activity above control levels (S. Corrochano, Pers. Comms., **Fig. S6**). Furthermore, the protein sequence is highly conserved between the human and mouse immediately around this amino acid (data not shown). Therefore, the R769G mutation was chosen to recapitulate in the mouse using CRISPR/Cas9. The allele generated with be referred to as $Znrf3^{R749G}$ in this thesis, due to the distinct amino acid numbering of the mouse ZNRF3 protein.

6.2 Results

6.2.1 Generation of the *Znrf3*^{R749G} allele

This work was carried out by the Molecular and Cellular Biology team, and the Microinjection/Quarantine team at the MRC Harwell Institute.

The *Znrf3*^{R749G} allele was generated by the Molecular and Cellular Biology team at MRC Harwell. Multiple injections were attempted, using alternative guide RNAs and donor oligos. Details of unsuccessful attempts will not be discussed further due to space constraints. The reagents used in the successful experiment are detailed in (**Fig. 6.2**). A single guide RNA was used (sgRNA), and the donor oligo contained two SNPs: one to generate the desired mutation, and a second silent mutations which alters the PAM sequence to prevent the Cas9 enzyme re-cutting after successful editing.

Figure 6.2 Generation of the *Znrf3*^{R749G} allele. Wildtype genomic sequence of target region is shown, with corresponding amino acids above. Residues to be mutated are surrounded by a solid black box. Cas9 was targeted using a single guide RNA (sgRNA), shown in the red box. Position of the desired mutation (adenine to guanine) shown by red arrow. Position of silent mutation (guanine to thymidine) is shown by a blue arrow. The position of the donor oligo sequence is highlighted in green. Substituted residues at point mutation in the donor oligo, at target sites are highlighted by a dashed box.

The sgRNA and Cas9 were introduced into 1-cell stage embryo by pronuclear injection, as purified mRNA. The donor oligo, injected at the same time, was synthesised and purified by

Polyacrylamide gel electrophoresis (PAGE) by *Integrated DNA technologies*. Embryos were then implanted, after 30 minutes' recovery, into pseudo-pregnant recipient females.

8 F1 pups were born, 3 of which carried alleles with the correct SNP, but interestingly, not the silent mutation (data not shown). Further analysis by sub-cloning of the PCR products confirmed the presence of the correct allele, and several others. The 3 mosaic females were bred with C57BL6/J (B6) males, and their offspring genotyped. Two of the three females successfully transmitted the correct SNP to the F2 generation. One of these females was used to establish a colony. A second mutation, which includes a 29-nucleotide deletion and the correct SNP, was generated by a previous injection. This allele, *Znrf3*^{del29nt}, will be described further below (**Fig. 6.4**), and was also selected to establish a small colony.

6.2.2 *Znrf3*^{R749G} does not cause sex reversal in mice

Znrf3$^{R749G/R749G}$ embryos looked morphologically normal (data not shown). XX and XY gonads were analysed at 14.5dpc by WMISH. XY and XX *Znrf3*$^{R749G/R749G}$ gonads are indistinguishable from wildtype controls. XY gonads express *Sox9*, and have well-formed, regular testis cords. *Stra8* was never seen in any XY *Znrf3*$^{R749G/R749G}$ gonad (n=4). Similarly, XX *Znrf3*$^{R749G/R749G}$ gonads were all morphologically normal, and expressed *Stra8* throughout the gonad (**Fig. 6.3a**).

Znrf3^{R749G} homozygotes survive until adulthood. Therefore, external and internal genitalia of *Znrf3*$^{R749G/R749G}$ XY animals were examined 6 weeks postnatally (**Fig. 6.3b**). There was no significant difference in anogenital distance or testis weights between XY *Znrf3*$^{R749G/R749G}$ animal and wildtype littermate controls (**Fig. S7a, c**). Similarly, internal reproductive tracts were indistinguishable from wildtype controls (**Fig. 6.3b**).

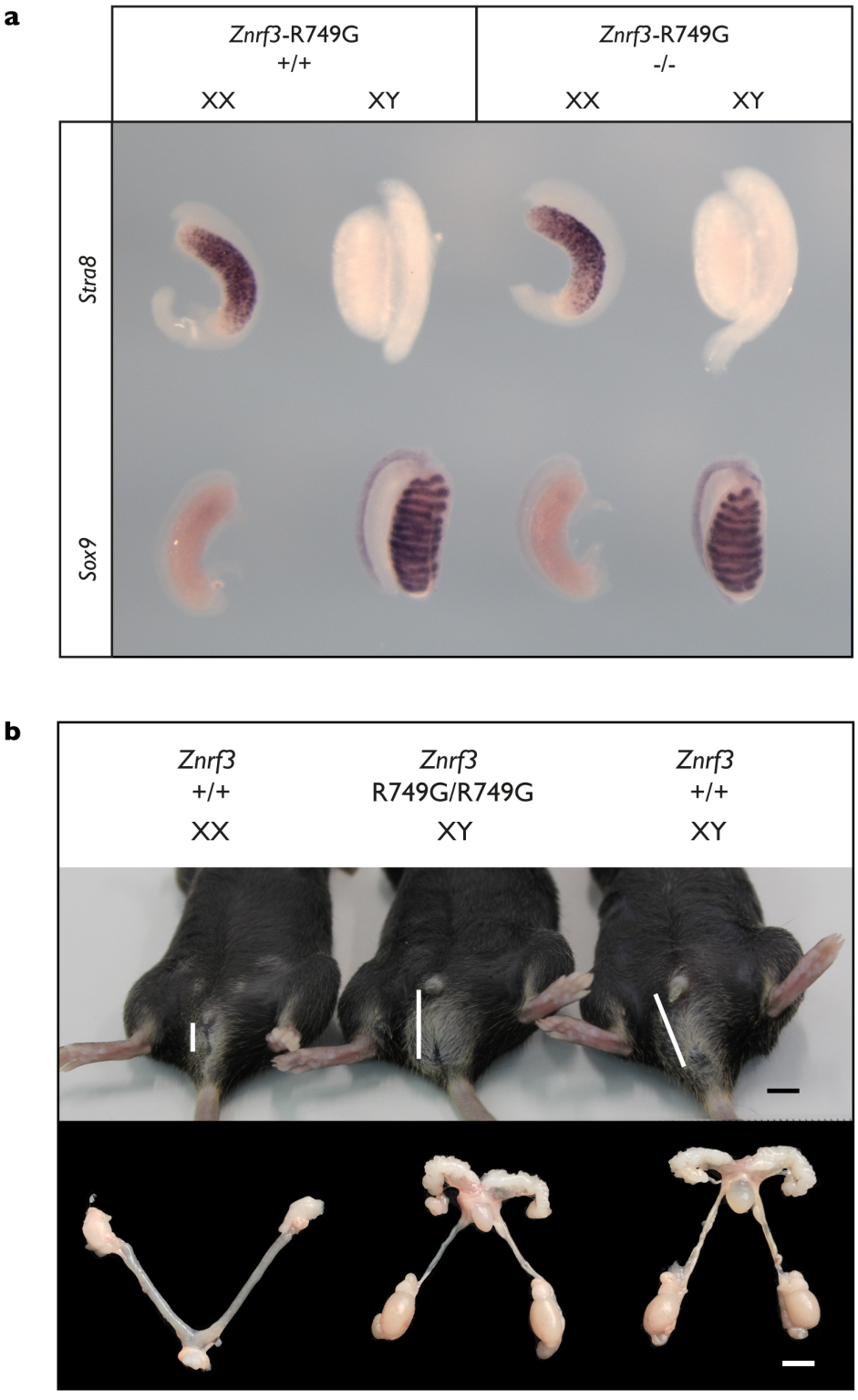

Figure 6.3 Analysis of *Znrf3*$^{R749G/R749G}$ embryos and adults. WMISH was carried out on XX and XY, *Znrf3*$^{+/+}$ and *Znrf3*$^{R749G/R749G}$ 14.5dpc gonads. Top row shows *Stra8* expression, and the bottom row shows *Sox9* expression **(a)**. Analysis of the reproductive tracts of adult mice were carried out. Top row shows anogenital distance of XX and XY *Znrf3*$^{+/+}$ and XY *Znrf3*$^{R749G/R749G}$ adults. Bottom row shows dissected reproductive tracts of the same mice **(b)**.

A second mutation was generated by CRISPR/Cas9 which causes a 29-nulceotide deletion at the C-terminus of the protein. This causes a frame shift and a premature stop codon, which removes amino acids 738-913 (**Fig. 6.4a**), including the amino acid which is substituted in the *Znrf3*^{R749} allele. Interestingly, *Znrf3*$^{del29nt/del29nt}$ gonads are also indistinguishable from wildtype controls. XY *Znrf3*$^{del29nt/del29nt}$ gonads express *Sox9* in well-formed cords, and never express *Stra8* (n=4). XX mutant gonads look morphologically normal, and express *Stra8* throughout the gonad (**Fig. 6.4b**). These WMISH gonads were also analysed using Optical Projection Tomography (OPT) which results in a reconstructed 3D image of the areas of stain (**Fig. 6.5**). This allows for visualisation of the 3D structure of the testis cord, and confirms that the organisation of the XY *Znrf3*$^{del29nt/del29nt}$ testis is normal.

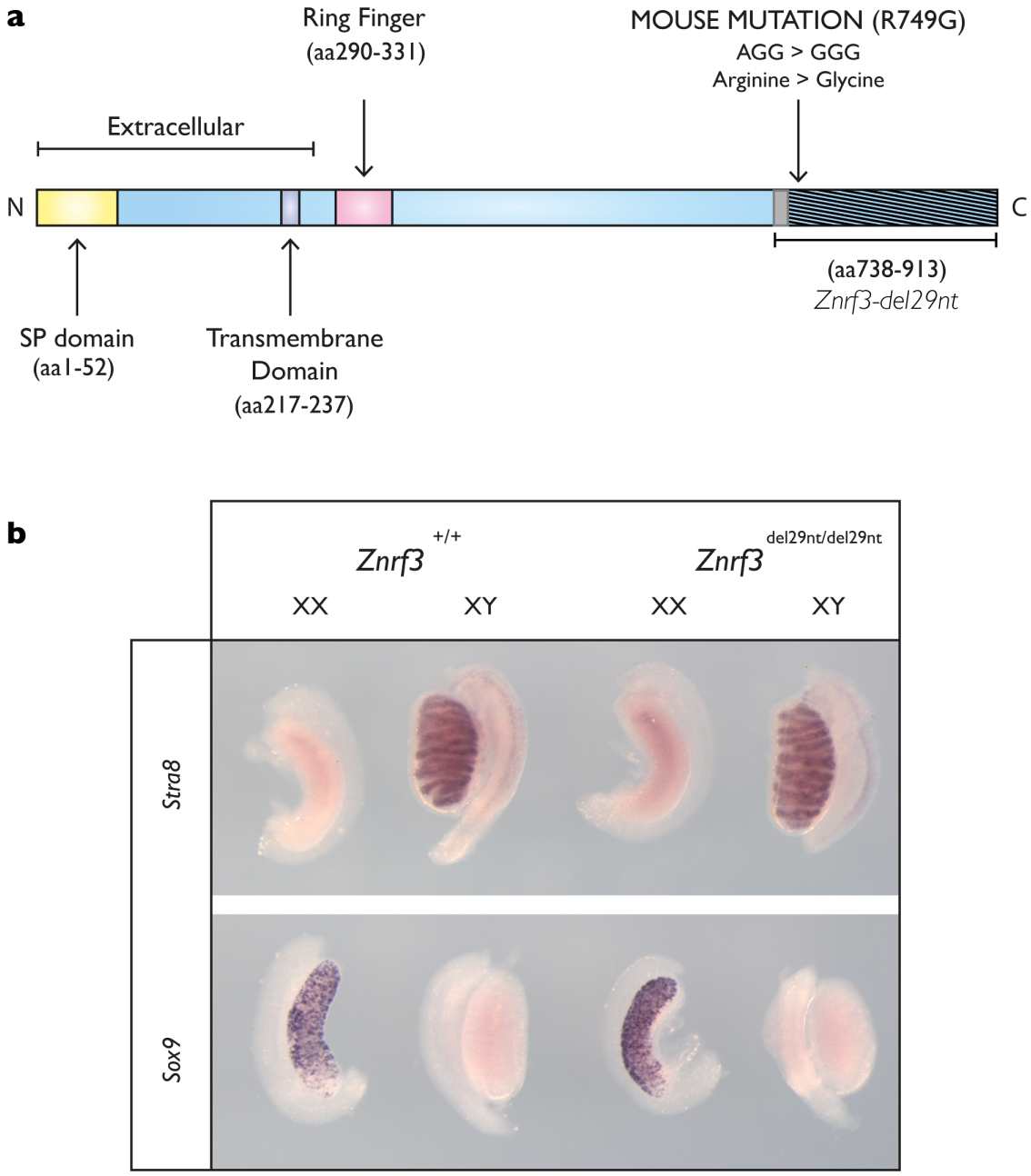

Figure 6.4 29-nucleotide deletion allele of *Znrf3*. Schematic demonstrating region missing from the mouse protein upon 29nt deletion **(a)** Diagram shows position of the R749G mutation. Grey region represents random amino acids generated by the frame shift before the STOP codon. Hatched area represents amino acids which are missing from the protein product. WMISH was carried out on XX and XY 14.5dpc gonads. Top row show *Stra8* expression, and the bottom row shows *Sox9* expression **(b)**.

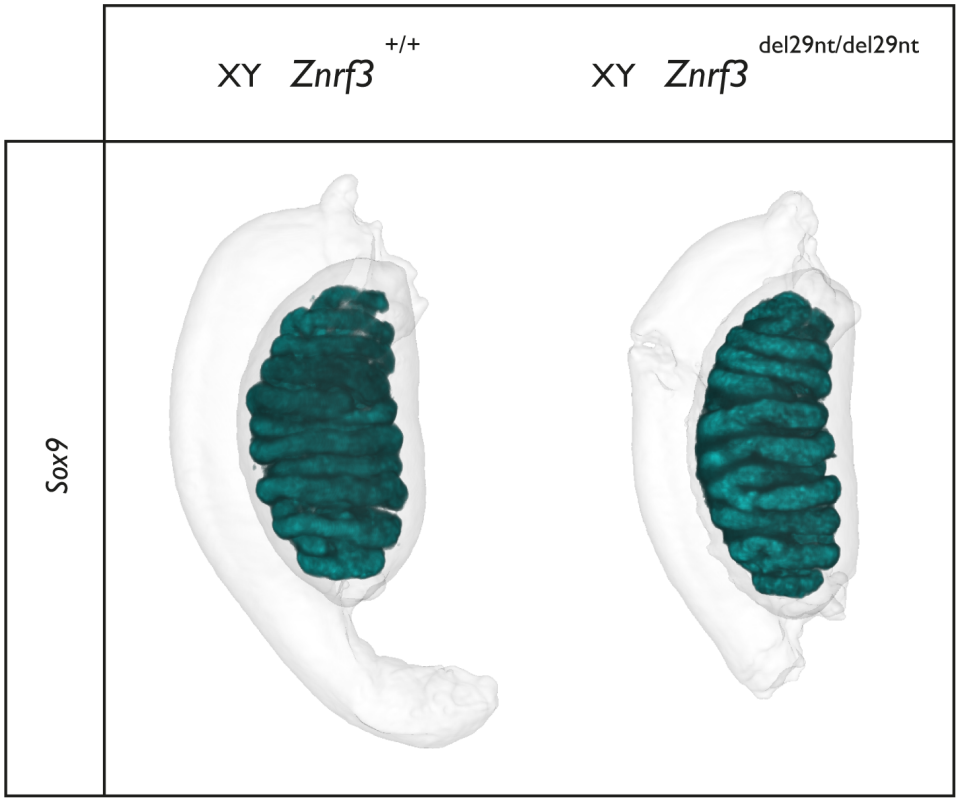

Figure 6.5 Optical Project Tomography (OPT) scans of *Sox9* expression. WMISH was carried out on 14.5 dpc XY *Znrf3*$^{+/+}$ and *Znrf3*$^{del29nt/del29nt}$ gonads to show *Sox9* expression. OPT scans were then carried out on WMISH-stained gonads to generate 3D reconstructions of expression. Details of the location of the movies of the 3D scans gonads can be found in the appendix (Fig S8).

6.2.3 *Znrf3*^{R749G} does not cause sex reversal on a sensitised genetic background

As previously described, B6.Y^{AKR} mice are particularly sensitive to XY male-to-female sex reversal. Therefore, to confirm that the *Znrf3*^{R749} allele does not cause even minor disruptions to testis determination, the mutation was homozygosed on this sensitised background. Adult XY^{AKR} *Znrf3*$^{R749G/R749G}$ mice appear phenotypically normal (**Fig. 6.6**). Anogenital distances or testis weights are not significantly different from wildtype age-matched controls (**Fig. S7b, c**). Due to time constraints testes were not processed for histological analysis.

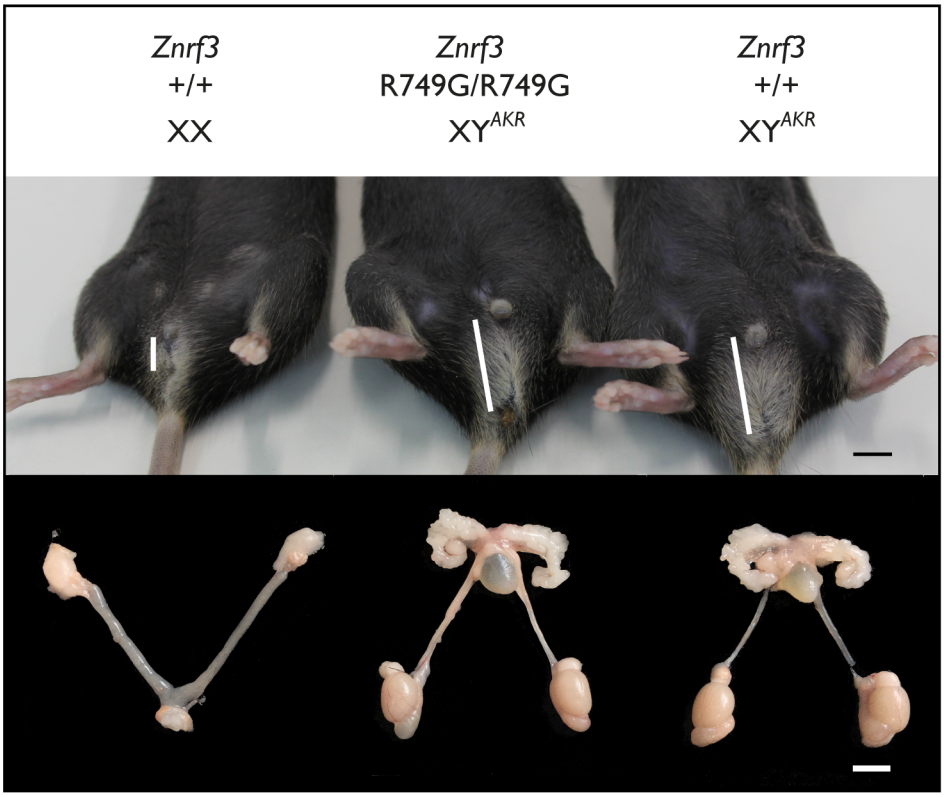

Figure 6.6 Analysis of adult *XY^{AKR} Znrf3$^{R749G/R749G}$* reproductive tracts. Analysis of the reproductive tracts of adult mice were carried out. Top row shows anogenital distance of XX and XY^{AKR} *Znrf3$^{+/+}$* and *XY^{AKR} Znrf3$^{R749G/R749G}$* adults. Bottom row shows dissected reproductive tracts of the same mice.

6.2.4 The *Znrf3^{R749G}* allele on a *Znrf3*-null background

To fully assess the pathogenicity of the R749G mutation, embryos carrying one *Znrf3^{R749G}* allele were analysed on the *Znrf3*-null background and *Znrf3$^{R749G/-}$* compound mutants were generated. As previously described, XY *Znrf3$^{+/-}$* gonads are indistinguishable from wildtype litter mate controls, but XY *Znrf3$^{-/-}$* gonads show significant disruptions to testis determination (**Chapter 4**). Therefore, it was hypothesised that, if the R749G mutation was damaging to ZNRF3 protein function, testis determination defects may be seen in the compound mutant. When 14.5dpc XY *Znrf3$^{R749G/-}$* gonads are analysed by WMISH, no sex reversal phenotype is seen. XY compound mutants express *Sox9* in well-formed testis cords, and no *Stra8* expression is detected in any gonads (n=4) (**Fig. 6.7**).

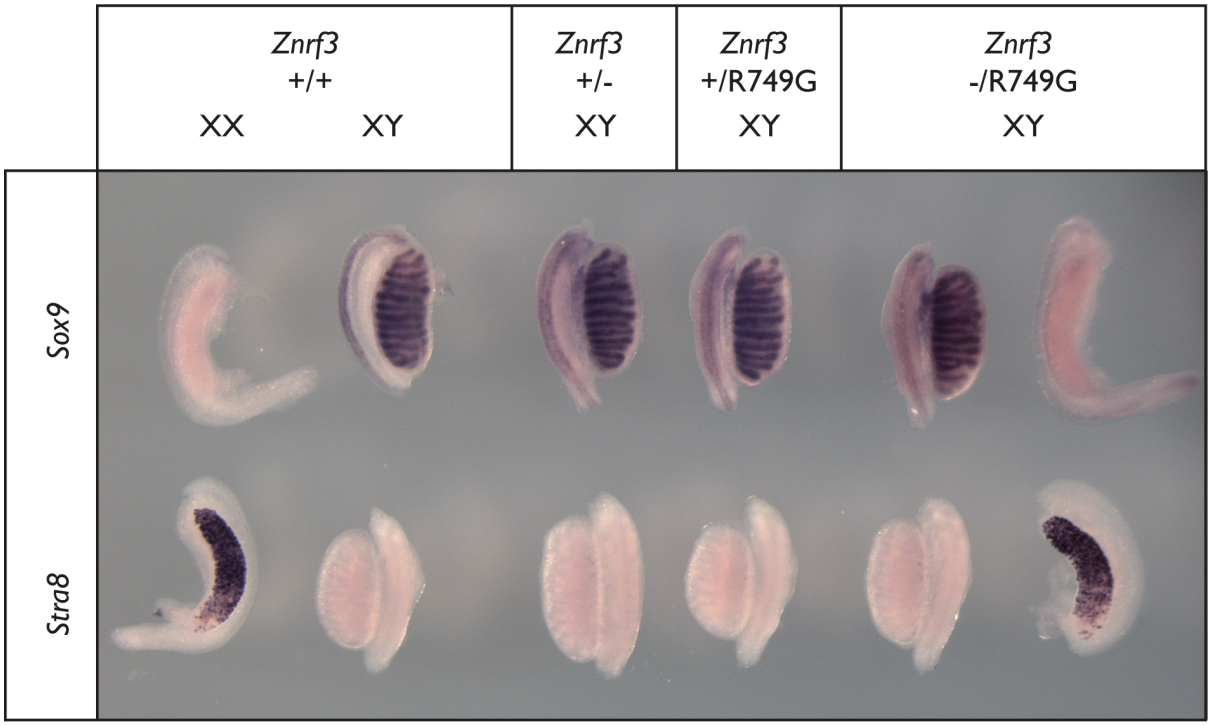

Figure 6.7 Analysis of the *Znrf3*^{R749G} allele on the *Znrf3* null background. 14.5dpc gonads were analyses by WMISH. Top row shows *Sox9* expression. Bottom row shows *Stra8* expression. Controls shown include XX and XY *Znrf3*$^{+/+}$, XY *Znrf3*$^{+/-}$ and *XY Znrf3*$^{+/R749G}$ gonads. XY and XX *Znrf3*$^{-/R749G}$ were also analysed.

6.3 Discussion

6.3.1 The R749G mutation does not cause a phenotype in mice

This chapter has demonstrated that mice carrying two copies of the *Znrf3*^{R749G} allele do not show any evidence of disruptions to testis determination, in contrast to the dramatic gonadal phenotype described in XY *Znrf3*-null mice. Even when the *Znrf3*^{R749G} allele is homozygosed on a XY sex reversal-sensitised background, B6.Y^{AKR}, no obvious phenotype is seen in embryos or in adult mice. Furthermore, *Znrf3*$^{R749G/R749G}$ mice do not show the eye phenotype seen in *Znrf3*-null mice. Taken together, these data suggest that the *Znrf3*^{R749G} allele produces a protein product which is sufficiently functional to have no obvious effects on embryos or adult mice. In contrast, as previously described, the equivalent mutation in the human protein (R768G) is shown to disrupt the WNT-antagonising abilities of ZNRF3 *in vitro.* Furthermore, the detection of the R768G mutation in two sex-reversed sisters is evidence that this amino acid substitution, in the context of the human ZNRF3 protein, may also have an effect *in vivo.*

Why therefore, do we see this apparent discrepancy between the effect of the R749G/R768G mutations in mice, and in humans? What, if anything, can we confer from lack of phenotype seen in mice? Three possible hypotheses, which are consistent with the data thus far, are described below:

1) The R768G mutation disrupts human ZNRF3 function, but R749G does not disrupt, or only has a very mild effect on, mouse ZNRF3;
2) The R768G and R749G have equivalent disruptive effects in human and mouse ZNRF3, respectively;

3) Neither R768G, nor R749G, are causative.

These three hypotheses will now be discussed in further detail, with a particular focus on the consequences for our understanding of the human R768G mutation.

6.3.1.1 Hypothesis 1: The R768G mutation disrupts hZNRF3 function, but R749G does not disrupt mZNRF3

Perhaps the simplest explanation for the absence of a phenotype in mouse embryos homozygous for the R749G mutation is that this amino acid substitution is not disruptive/pathogenic in the context of the mouse protein; nevertheless, R768G could still be disruptive in the context of the human protein. This would account for the fact that R768G disrupts hZNRF3 function *in vitro*, and is also consistent with it being the causative SNP in the two 46,XY DSD individuals identified. Furthermore, it is consistent with the fact that *Znrf3*$^{-/-}$ mice, that lack any ZNRF3 functionality, show a testis determination phenotype.

There is strong evidence that contextual differences between orthologous proteins from different species can have a profound effect on the impact of mutations on protein structure. Compensated pathogenic deviation (CPD) describes the phenomenon by which a point mutation may be pathogenic in one species but fixed in another. (Jordan et al. 2015) showed that between 3 and 9% of pathogenic mutations in humans are found as CPDs in other vertebrates. Furthermore, it was found that these SNPs were often compensated for by a single additional amino acid substitution elsewhere in the protein.

Therefore, a simple explanation, which is consistent with the data, is that the R749G mutation is compensated for by a secondary sequence variant, or variants, elsewhere in the mouse ZNRF3 protein. The absence of such compensating variants in human ZNRF3 would explain the disruptive effect of R768G. A similar explanation may account for the second

mutation identified in the exome screen (S554N): this is already present in the wildtype mouse protein, and may be compensated for in mZNRF3 in a similar way.

6.3.1.2 Hypothesis 2: The R768G and R749G have equivalent disruptive effects in human and mouse ZNRF3, respectively

A second possibility is that the R768G/R749G mutations disrupt the function of ZNRF3 to the same extent in both mouse and human proteins. In this case, differences in the biology of the human and the mouse gonad could explain the difference in phenotype. For example, the human developing XY gonad may be much more sensitive to elevated levels of WNT-signalling than the mouse gonad, or a compensatory mechanism, such as a secondary WNT-antagonist, may exist in the mouse but not human gonad. However, if this were the case, this compensatory antagonist could not be sufficient to compensate for the loss of function of ZNRF3 in *Znrf3*$^{-/-}$ mice.

There are several known differences in the biology and genetics of the developing human and mouse gonad. For example, some orthologous genes have been shown to have differing effects in mouse and human sex development. Examples include the genes *DAX1* and *MAP3K4/1*. In humans, a duplication of a region of the X chromosome containing *DAX1* is sufficient to cause XY male-to-female sex reversal in humans (Zanaria et al. 1994; Bardoni et al. 1994). Such a duplication is predicted to lead to an approximate 2-fold up-regulation of genes in the region, including *DAX1*. However, in mice, overexpression of *Dax1* alone, at five-fold the endogenous level, leads to delayed but normal testis determination (Amanda Swain et al. 1998). Only when *Dax1* is overexpressed on a background with a weak *Sry* allele (Swain et al, 1998) or a *Sox9*$^{+/-}$ background, is testis determination severely disrupted in mice (Ludbrook et al. 2012). In a second example, it has been shown that *Map3k4* is critical

for testis determination in mice (Bogani et al 2009), but no *MAP3K4* mutations have been reported in cases of 46,XY DSD in humans. However, mutations in the related human gene, *MAP3K1,* are associated with 46,XY DSD, including CGD (Pearlman et al. 2010); but mouse *Map3k1* is not required for testis determination (Warr et al. 2011). Both examples demonstrate that the human and mouse developing gonad have different sensitivities and thresholds in the context of loss- and gain-of-function of orthologous or paralogous genes. Such differences may account for the different impacts that mutations have on mouse and human sex determination. In more general terms, Georgi et al. (2013) demonstrated that more than 20% of genes which are absolutely essential in humans, are not essential in mice, highlighting that this phenomenon is not restricted to the context of the gonad.

Alternatively, the effect of the R768G mutation alone may not be sufficient to cause the DSD phenotype seen in the two sisters identified in the exome screen, even though it is disruptive. It is possible that we only see a phenotype in these individuals because they share a secondary mutation, one which sensitises them to sex reversal, or because their genomes are sensitised through the combinatorial effects of many partially disruptive SNPs.

6.3.1.3 Hypothesis 3: Neither R768G, nor R749G, are causative

Despite the convincing *in vitro* evidence, one hypothesis that remains a possibility is that the R768G mutation is not sufficiently disruptive to human ZNRF3 function to cause a DSD in the individuals identified. In this case, we would conclude that the causative mutation or mutations are yet to be identified.

The *in vitro* data appear to contradict this hypothesis. The R768G mutation significantly disrupts the ability of ZNRF3 to antagonise WNT/β-catenin signalling (S. Corrochano, unpublished data). However, *in vitro* assays such as these must be interpreted carefully. The

Super Top-flash (STF) assay was carried out in a human carcinoma cell line (HEK293T cells) and recapitulated in KGN cells, a human granulosa-like tumour cell line (A. Bashamboo, Pers. Comm.). The STF assay relies on overexpression of ZNRF3 at physiologically irrelevant levels. Furthermore, the physiological context in which mutant ZNRF3 acts *in vivo*, at approximately 6 weeks of age in the developing human gonad, may differ significantly from that of a heterologous cell line cultured in vitro. For example, human gonadal cells may express a second WNT-antagonist, which could compensate for the loss of ZNRF3 function *in vivo,* but which is not expressed *in vitro*. Finally, even if this mutation is disruptive *in vivo,* in the context of the human gonad, we cannot determine whether the extent of loss of function is sufficient to cause a phenotype. Overall, given that one should question, or at least be open-minded about, the significance of cell line assay data, these experiments do not definitively prove that the R768G mutation is causative in the two DSD individuals. This hypothesis is further supported by the fact that the R768G mutation has been identified in apparently unaffected individuals, which suggests that in some human genetic backgrounds, this mutation is not pathogenic. This will be discussed further below (see section **Genetic Background**).

6.3.2 ZNRF3 evolutionary conservation: the 29nt deletion allele

Intriguingly, a second allele (*Znrf3*^{del29nt}) generated as a by-product was also not sufficiently damaging to the protein product to cause any observable phenotype. This mutation caused a frame-shift and a premature stop codon, which removes amino acids 738-913 of mZNRF3. This suggests that a significant portion of the C-terminus of the protein is not necessary for the role of ZNRF3 in testis determination or any major developmental process in the

embryo, including eye development. It is also interesting that the residue mutated in the R749G mice is contained within this region.

Little is known about the structure and function of intracellular regions of ZNRF3 and RNF43, apart from the well characterised ring finger domain. However, in the mouse protein, there are over 580 amino acids downstream of the ring finger, which represents more than half the length of the protein. Furthermore, this region is maintained through evolution, even in non-mammals such as Zebrafish and Coelacanths. However, sequence identity in this region is very low with only short sections of this large region showing conservation. Despite the low homology, the maintenance of this large internal domain hints at possible conserved roles in a range of organisms. It is therefore intriguing that the deletion of such a large region of ZNRF3 can have little effect on the embryo or the adult.

One possible explanation is that this domain is required for a process in the adult. Adult homozygote animals were not examined closely, due to time constraints, and therefore an adult phenotype may have been missed. On the other hand, this region may not be required for gonadal or eye development, and may be compensated for by another protein in other tissues or contexts. For example, although *Rnf43* does not appear to compensate for the loss of *Znrf3* function in the gonad, it may do so elsewhere when they are co-expressed. Finally, this part of the protein may be critical in other organisms but may be redundant in mammals or specifically in mice, but has not been lost simply due to a lack of selective pressure.

6.3.4 The unfolded protein response

One question which also remains is whether R749G/R768G mutated ZNRF3 proteins are stable in the cell, or whether they are degraded via the Unfolded Protein Response (UPR).

The UPR is activated to prevent the build-up of toxic aggregates of misfolded proteins, when the cell senses endoplasmic reticulum (ER) stress. Protein aggregation can be induced by cellular conditions such as hypoxia or oxidative stress, but can also be due to a mutation causing misfolding of a specific protein (Koumenis et al. 2007; Kupsco and Schlenk 2015). Initially, activation of UPR causes a global decrease in protein synthesis, followed by upregulation of chaperone proteins to assist in correctly folding proteins being synthesised (Rao and Bredesen 2004). Subsequently, the misfolded proteins are degraded via ER-associated degradation (ERAD) (Y. C. Tsai and Weissman 2010).

There is good evidence that the human R768G protein is still present and stable in the cell. Analysis of GFP-tagged hZNRF3, showed that R768G-hZNRF3 was detectable in HEK293T cells, and appear to be similarly distributed (S. Corrochano, Pers. Comm.). However, in this experiment wild-type and mutant ZNRF3 was overexpressed by transient transfection. The large quantities of the protein may have simple overwhelmed the UPR, and therefore it is difficult to draw any firm conclusions. Furthermore, without a working antibody against mouse ZNRF3, it is not possible to determine whether the R749G-ZNRF3 protein is stable in the cell. Therefore, as previously described, the development of an antibody which can detect endogenous ZNRF3 is critical to understanding the effect of R749G on mouse ZNRF3.

6.3.5 Genetic Background

As previously described, the severity and nature of a DSD is highly dependent on the genetic background of an individual. Understanding the genomic context of the mutations found in ZNRF3 is particularly important in interpreting the role as the R768G mutation in humans, as it is a known polymorphism which has also been identified in apparently non-affected individuals. Screening the whole genome of the sisters, who carry the R749G mutation, may

help to identify any secondary mutations that may be contributing to their sensitivity to sex reversal. However, this process would be by no means simple. Mutations could be located in putative regulatory regions that have thus far not been associated with a function, let alone a function in sex development. Furthermore, causative SNPs may be numerous and may individually only have a subtle effect on the protein function or expression, which could make them impossible to identify with current screening methods.

The implications of differences in genetic background of individuals and of mice will be discussed in further depth in Chapter 7.

6.3.6 Limitations of CRISPR/Cas9

The CRISPR/Cas9 system is becoming increasingly popular for studying the role of point mutations *in vitro* and *in vivo*. Undoubtedly, it has revolutionised our ability to generate point mutations precisely, and with minimal risk of off-target mutations. However, the technology does have some disadvantages, particularly when using it *in vivo*, which have been highlighted during this project.

First, the Cas9 enzyme remains in the cell after the first division (Sung et al. 2014; Burger et al. 2016; H. Wang et al. 2013; Yen et al. 2014). Therefore, the DNA can be cut multiple times, over multiple cell divisions, which can generate multiple alleles at the target site. Furthermore, particularly in the case of the generation of point mutations, the repair process is not always accurate and therefore small deletions or insertions may arise, as exemplified by the generation of the *Znrf3*^{del29nt} allele exemplified in this thesis. However, these alternative alleles generated as a by-product can also yield interesting and unexpected results. Second, transmission of a correct allele to the next generation is not guaranteed. Founders are often mosaic, and therefore must carry the mutated allele in their germline

for transmission to occur. During this project, multiple founders were identified to carry the correct allele, using a genomic DNA sample from the ear. However, only two of these mice generated offspring carrying the correct mutation. Furthermore, by chance, these founders were female which resulted in a delay in establishing a colony. Finally, although the CRISPR/Cas9 system has evolved to be highly accurate, there is still a possibility of off-target effects, elsewhere in the genome (Cho et al. 2014; X.-H. Zhang et al. 2015). Without carrying out a whole genome sequence on the resulting mice, it is impossible to exclude this possibility. It is likely that some of these issues will be resolved as the technology is developed and optimised in future.

6.3.7 Summary: The R749G mutation does not cause a phenotype in mice

In summary, the absence of phenotype seen when the human R768G mutation was recapitulated in mice might be explained by multiple hypotheses detailed above. We have little evidence to indicate how the R749G mutation may affect mouse ZNRF3 function, or stability, and therefore it is difficult to conclude anything concrete from these results. Moreover, the mouse data do not allow us to infer anything definitive about the impact of the human R768G mutation *in vivo*. Nevertheless, perhaps the simplest explanation is that R749G does not disrupt mZNRF3, unlike the human equivalent. It is possible to directly test any hypothesis concerning the disruptive effects of R749G, by performing an STF assay with mZNRF3 and mouse cell lines. This could provide data, albeit with all the caveats discussed above, on whether the R749G mutation is able to disrupt ZNRF3 protein function *in vitro*.

Chapter 7: Discussion

7.0 Overview

Data in this thesis demonstrate that *Znrf3* is a novel testis-determining gene in mice. The thesis has described its role in mouse gonad development, and has examined two disruptive mutations in *ZNRF3* identified in human DSD patients. This is a noteworthy discovery because ZNRF3 is the first WNT-signalling antagonist reported to play significant a role in primary sex determination, despite the growing literature surrounding the importance of mutual antagonism of the pro-testis and pro-ovary pathways in the gonad, and the known role of *Wnt4* in the mammalian gonad. As previously described, deletion of other WNT-signalling antagonists, such as *Dkk1*, have previously been shown to have no impact on testis development (Combes et al. 2009). In addition, this thesis provides evidence that two human *ZNRF3* mutations, identified in an exome screen of 46,XY DSD patients, are causative, and has expanded our current knowledge of the role of WNT-signalling and its modulators in testis determination.

7.1 ZNRF3 and the testis-determining pathway

This thesis has demonstrated that ZNRF3 is a core component of the testis-determining pathway and suggests answers to some important questions that remain in the field:

1) How do FGF9 and WNT4 interact to mutually antagonise each other?
2) What is the mechanism which allows RSPO1 activity to upregulate WNT/β-catenin signalling in the context of the embryonic gonad?

7.1.1 ZNRF3 regulates mutually antagonistic relationships in the embryonic gonad

Mutual antagonism between the ovarian and testis-determining pathways is crucial for ensuring a robust switch in gonadal fate. Some interactions between pairs of genes in the testis and ovarian pathways are now well characterised genetically, such as that between *Fgf9* and *Wnt4* (Kim et al. 2006; S. Jameson, Lin, and Capel 2012), which is described in full in Chapter 1. Briefly, it has been demonstrated that the primary role of FGF9 in the gonad is to downregulate *Wnt4* expression (S. Jameson, Lin, and Capel 2012). Furthermore, the interaction is reciprocal, with WNT4 also acting to inhibit FGF9 in the gonad (Kim et al. 2006). However, a molecular mechanism which explains how two extracellular signalling molecules could antagonise each other is not available. This thesis offers a possible mechanism.

As previously described, organ culture experiments show that FGF9 protein can directly upregulate *Znrf3* expression in an XX gonad cultured *ex vivo* (P. Siggers, pers. comm.). FGFs are extracellular growth factors which regulate multiple important signalling pathways and result in transcriptional changes in the cell. Pathways controlling cell proliferation (RAS/RAF/MAPK), cell survival (PI3K/PDK/AK) and cell motility (PKC/NFAT) are all regulated by FGF signalling (Goetz and Mohammadi 2013). Therefore, it is feasible that one of these signalling cascades stimulated by FGF9 binding could lead to transcriptional upregulation of *Znrf3* in the mouse embryonic gonad. However, this upregulation could also be a secondary effect of the XX gonad assuming a more testicular fate in the presence of FGF9. Regardless of whether the impact of FGF9 on *Znrf3* expression is direct or indirect, ZNRF3 offers a

molecular link between FGF9 signalling and its suppression of WNT/β-catenin signalling in the developing XY gonad.

Interestingly, ZNRF3 may also impact *Fgf9* expression. Loss of *Znrf3* led to a decrease in *Fgf9* expression at 11.5 dpc. Although no significant difference was detected at this time-point between XY wild-type and XY *Znrf3*$^{-/-}$ gonads, and any conclusions are therefore speculative, a trend was seen, with XY *Znrf3*-null gonads expressing an intermediate level of *Znrf3* compared to XX and XY wild-type. Therefore, there is some evidence that ZNRF3 may also be promoting *Fgf9* expression. ZNRF3 antagonises WNT/β-catenin signalling which in turn may be antagonising FGF9 through a yet unknown molecular mechanism, though presumably through its inhibitory effect on *Sox9* expression.

7.1.2 RSPO1 regulates WNT-signalling in the developing gonad through ZNRF3

RSPO1 plays a significant role in the ovarian pathway: its removal from the XX mouse gonad causes partial female-to-male sex reversal. RSPO1 has been shown to upregulate WNT/β-catenin signalling in the ovary (A. Chassot et al. 2008). However, there are no reports in the literature that describe a molecular mechanism by which RSPO1 achieves this in the context of the gonad. Data presented in this thesis show that ZNRF3 acts to downregulate canonical WNT-signalling in the context of the developing XY gonad; when ZNRF3 is removed from the testis, WNT/β-catenin signalling dominates in the XY gonad, and somatic cells adopt an ovarian fate. Other studies reveal a role for RSPO1 in removal of ZNRF3/RNF43 from the cell membrane (Koo et al. 2012; Hao et al. 2012). The data reported in this thesis therefore suggest that one way in which RSPO1 is likely to be responsible for determining the female fate is through the inhibition of ZNRF3. In short, RSPO1 could promote the ovarian fate

through the repression of a repressor (ZNRF3) of ovary-specific WNT/β-catenin signalling. Such a double-negative interaction is a familiar one in the literature on sex determination: based on genetic considerations, SRY was described as a repressor of a repressor of testis development back in 1993 (McElreavey et al. 1993).

7.1.3 Summary: a model for the function of ZNRF3 in the testis-determining pathway

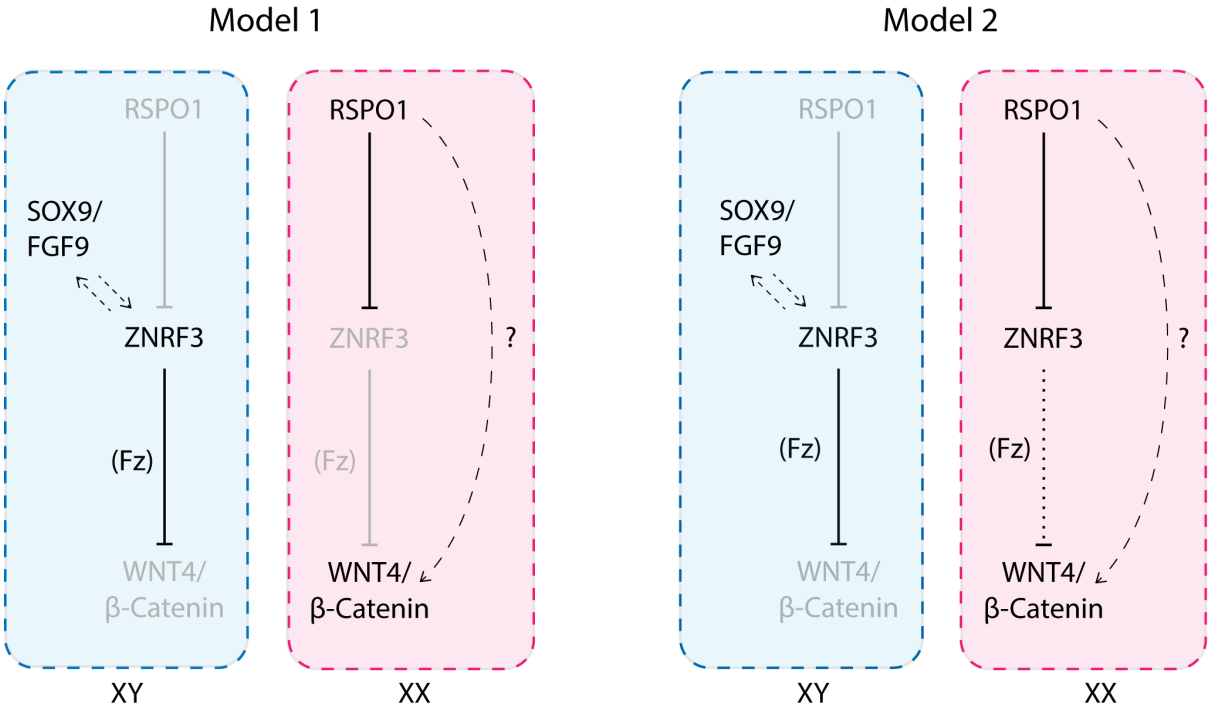

Figure 7.1 Models for the function of ZNRF3 in the sex determining pathway. In both models, RSPO1 removes ZNRF3 from the plasma membrane thereby inhibiting its function, and ZNRF3 inhibits WNT/β-catenin signalling by removing Frizzled Receptors (Fz) from the plasma membrane. In the developing XY gonad (blue), SOX9/FGF9 may also promote *Znrf3* expression in supporting cells. RSPO1 may also regulate WNT/β-catenin signalling through one or more ZNRF3-independent mechanisms (dotted arrow). **(1)** models the case where both *Znrf3* and *Rspo1* are differentially transcribed in the XY and XX (pink) gonadal supporting cells. ZNRF3 levels are lower in the XX gonad, reducing even further its ability to inhibit WNT/β-catenin signalling. **(2)** models the case where *Znrf3* is not sexually dimorphic, but where the higher levels of *Rspo1* in the XX gonad are sufficient alone to result in ZNRF3's removal from the plasma membrane, such that it is unable to efficiently suppress WNT/β-catenin signalling.

In conclusion, two models, summarised **Fig 7.1**, are consistent with the data reported in this thesis, and with published data. Both models place ZNRF3 at the centre of the positive interaction between RSPO1 and WNT/β-catenin signalling. In the XX gonad, ZNRF3 activity is low enough to allow ovary-promoting WNT/β-catenin signalling; however, this is supressed in the developing XY gonad, where ZNRF3 activity is high. When ZNRF3 is not present to repress WNT/β-catenin signalling in the developing XY gonad, the ovarian pathway can dominate, and partial or complete male-to-female sex reversal occurs.

The two models suggest different but related explanations for the differential activity of ZNRF3 in the developing XX and XY gonad. In model 1 (**Fig 7.1**), *Znrf3* transcripts are less abundant in the XX compared to XY supporting cell lineage, leading to reduced numbers of ZNRF3 receptors on the cell surface and efficient removal by RSPO1. This permits increased WNT/β-catenin signalling, to promote ovary development. In model 2 (**Fig 1.7**), *Znrf3* is expressed equally in both XX and XY gonads, and instead, differential expression of *Rspo1* is solely responsible for the increased activity of ZNRF3 in the XY gonad. In the XX gonad, RSPO1 inhibits ZNRF3 by removing it from the plasma membrane allowing WNT/β-catenin signalling (Hao et al. 2012). In contrast, in the context of the XY gonad, where *Rspo1* transcription is relatively low(Parma et al. 2006; S. A. Jameson et al. 2012), ZNRF3 activity is minimally repressed, and is therefore able to antagonise WNT/β-catenin signalling. These two models are not mutually exclusive. It is possible that both transcriptional regulation of *Znrf3* directly, and its differential activity imposed by RSPO1, contribute to the dominance of WNT//β-catenin signalling in the XX gonad and, in contrast, the WNT-antagonising activity of ZNRF3 in the developing XY gonad. Furthermore, other transcriptional and post-translational regulatory mechanisms may exist which could also regulate ZNRF3 activity.

7.2 WNT/β-catenin signalling and SOX9

There is good evidence that *Sox9* and WNT/β-catenin signalling mutually antagonise each other. Inhibition of *Sox9* by WNT/β-catenin signalling has been demonstrated specifically in the gonad (Freland and Beaulieu 2012; Bernard et al. 2012a). Multiple mechanisms for the inverse interaction, namely inhibition of WNT/β-catenin signalling by SOX9 have also been elucidated (Akiyama et al. 2004; Topol et al. 2009b), although not in the context of the gonad. Therefore, the direct impact of ZNRF3 on WNT/β-catenin signalling (Hao et al. 2012; Koo et al. 2012) may not only be regulating FGF9 activity, as described above, but may also directly impact the activity of SOX9.

WNT/β-catenin signalling has been shown to directly inhibit *Sox9* expression, specifically in the context of the gonad. Lithium Chloride (LiCl) stabilises β-catenin through the inhibition of GSK3β, which is part of the destruction complex (Freland and Beaulieu 2012). Bernard et al. (2012) show that cultured XX gonads treated with LiCl downregulate SOX9 and AMH, causing female-to-male sex reversal. Furthermore, *ex vivo* culture of transgenic gonads which exhibit *LacZ* under the control of TESCO, results in decreased reporter gene activity when β-catenin stabilisation is promoted. The ability of both SF1/SOX9 and SF1/SRY to activate *LacZ* expression is supressed, suggesting that SF1 is the target of this inhibition. In summary, β-catenin is capable of directly inhibiting *Sox9* expression in the gonad, by blocking the activity of SF1 on the TESCO enhancer (Bernard et al. 2012a).

Other reports exist linking SOX9 and inhibition of WNT/β-catenin signalling outside of the gonad. Chondrocytes are cells found in cartilage which rely on SOX9 for their specification (Ng et al. 1997; Q. Zhao et al. 1997; Akiyama et al. 2002). TOPFlash activity is decreased in

HEK293T cells upon transfection of *SOX9*, and increased in primary chondrocytes upon *SOX9* knockdown (Akiyama et al. 2004; Topol et al. 2009a). SOX9 appears to achieve this through two independent mechanisms: it can physically interact with the C-terminus of β-catenin, competing with TCF/LEF to inhibit the transcriptional activity of β-catenin (Akiyama et al. 2004); or it can act indirectly, via phosphorylation of β-catenin (Topol et al. 2009a). Both mechanisms, and others, may also be active in the context of the gonad. Therefore, ZNRF3 also has an impact on a second mutually antagonistic interaction in the gonad. In the testis, ZNRF3 acts to antagonise WNT/β-catenin signalling, releasing the repression on TESCO, and therefore allowing high *Sox9* expression level.

7.3 Genetic background

The mouse data reported here suggests that the sex reversal phenotype caused by a loss of *Znrf3* is genetic background dependent. The gonadal phenotype described increased in severity over successive generations of backcrossing to C57BL6/J (B6), which is sensitised to male-to-female sex reversal (Correa et al. 2012). This background effect may also play a role in the variability of the phenotype (see below). Furthermore, on the further sensitised background, B6.Y^{AKR} , full sex reversal was observed. It is likely that the genetic background of human individuals also plays a critical role in the severity of DSDs which may be caused by mutations in *ZNRF3.* This has the profound implication that a mutation in *ZNRF3* which is causative in one individual may not be pathogenic in another. As previously described, this could explain the identification of the R768G in apparently unaffected individuals.

7.4 Variability of gonadal phenotypes

A common theme in this thesis has been the range of different phenotypes seen between instances of the same genotype. This variability was seen when analysing both embryonic and adult gonads. At 14.5 dpc on B6, the extent of sex reversal in XY *Znrf3*-null gonads ranges from gonads where testicular tissue of variable morphology was present throughout, to full sex reversal where gonads were indistinguishable from ovaries. In adults, some B6.Y^{AKR} *Znrf3*$^{+/-}$ animals are phenotypically female, whilst others are fertile males. This phenomenon also extends to other phenotypes such as the failure to form a lens which was seen sporadically in *Znrf3*$^{+/-}$ embryos. This variability in gonadal phenotype could be determined either by the genetic background, or by the inherent stochasticity of primary sex determination.

Interestingly, the variability in phenotype only appears to be detectable downstream of WNT/β-catenin signalling. In XY *Znrf3*$^{-/-}$ gonads, marker genes of the canonical pathway such as *Lef1,* appear to be upregulated to the same extent in all gonads, and throughout the gonad, at both 11.5 dpc and 12.5 dpc. This is in contrast to the considerable variability seen in the expression of *Sox9* and *Wnt4* at 11.5 dpc and 12.5 dpc. On the other hand, WMISH is a semi-quantitative method, and therefore may have been insufficiently sensitive to detect variability in *Lef1* expression.

As previously described, the genetic background of an individual has a large effect on gonadal phenotype, both in humans and in mice. Therefore, the range of phenotypes seen may be due to subtle genetic differences between embryos, despite the near inbred nature of the C57BL6/J (B6) background. However, even within a single embryo, pairs of XY *Znrf3*$^{-/-}$ gonads were sometimes scored differently upon dissection. For example, XY *Znrf3* null

embryos were identified to have one gonad scored as an ovary, and another with a clear ovo-testicular morphology (data not shown). This suggests that it is not only the genomic context which influences the gonadal phenotype. Stochasticity in gene expression, discussed below, may therefore also play a role. WMISH hybridisation studies of attached pairs of 14.5 dpc gonads could help to further assess this.

The bipotential gonad is initially poised to develop into either an ovary or a testis. This equilibrium is perturbed one way or the other by inputs into the system, such as the presence or absence of SRY (Gubbay et al. 1990; Sinclair et al. 1990). Importantly, this process plays out in each individual supporting cell precursor in the gonad. This initial switch is then canalised through the mutually antagonistic interactions detailed previously. Small differences in the transcriptomes of an individual cells can therefore have large effects on their fates (Fig. 7.2). In this way, initial small disparities in gene expression between cells in the *Znrf3*-null gonad could lead to the variability in phenotype seen. This initial variability may have been caused by variability of the genetic background as described above. Alternatively, it could have also have been set up by stochastic processes.

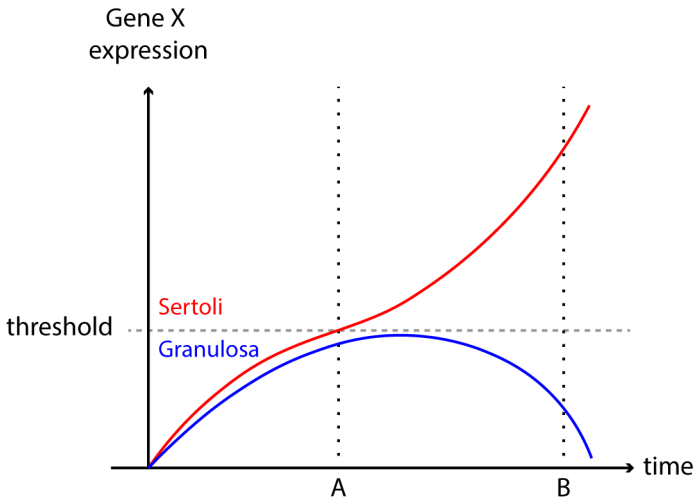

Figure 7.2 Reinforcement of cell fate in the gonad. A small initial difference in the expression of Gene X at time **A**, can lead to a large difference in expression at time **B**, due to canalisation of the Sertoli and granulosa cell fate.

Stochasticity describes the property of a state in which the outcomes of a process cannot be easily predicted from the inputs. In the context of the gonad, the initial transcriptome of an individual cell will be influenced by a plethora of internal or external signals, and this in turn will impact the development of the gonad. One hypothesis therefore is that loss of *Znrf3* on average upregulates WNT/β-catenin signalling to approximately a yet undetermined threshold level in the gonad. Small random, or stochastic, differences between *Znrf3*-null cells can then perturb the system either way, and in this way, the extent of sex reversal varies between embryos and within the same gonad.

7.5 A role for ZNRF3 in germ cells?

As previously described, *Stra8* levels appeared significantly reduced in both XY and XX *Znrf3*$^{-/-}$ gonads compared to wild-type controls. The fact that XX *Znrf3* null gonads are also affected suggests that it is not a consequence of the male-to-female sex reversal phenotype seen in *Znrf3* null gonads. Therefore, this reduction in *Stra8* expression could be due to fewer PGCs

being specified or entering the gonad, reduced proliferation or increased apoptosis, fewer germ cells entering meiosis, or a global delay in gonadal development.

PGCs appear to be specified normally in the *Znrf3* null gonad, and enter the gonad by migration. *Oct4* expression quantified by qRT-PCR (**Chapter 5**) suggests that at 12.5 dpc, there is no difference in the number of PGCs at this time-point. Furthermore, Immunohistochemical analysis of the expression of Pecam, which is expressed in PGCs and endothelial cells (Wakayama et al. 2003), was carried out on 13.5 dpc gonads (**Fig. S9**). This analysis showed the presence of PGCs in both XX and XY *Znrf3* null gonads. However, only a single sample of each sex was analysed due to time constraints, and therefore further analyses and quantification are required before a firm conclusion can be drawn. Furthermore, there does not appear to be a developmental delay at 11.5 or 12.5 dpc when comparing the tail-somite number of wild-type and $Znrf3^{-/-}$ gonads (**Fig. S10**). However, this does not preclude a delay having developed by 14.5dpc.

The canonical WNT-signalling pathway has been implicated in the specification and proliferation germ cells, in several studies. RSPO1-driven upregulation of WNT/β-catenin signalling has been shown to be required for XX PCG proliferation (Chassot et al. 2011). Various models have also demonstrated that ablation of β-catenin in XY germ cells leads to loss of germ cells in the embryo or in the adult (Takase and Nusse 2016; Rivas, Huang, and Agoulnik 2014; Y.-F. Chang et al. 2011; Kerr et al. 2014). Most importantly for this thesis, over-activation of the canonical pathway can also lead to defects in germ cell development (Chassot et al. 2017). Chassot et al. used a germ cell specific Cre, *Ddx4-Cre* (Gallardo et al. 2007), to drive recombination of the $Ctnnb1^{+/LoxP(ex3)}$ transgene (Harada et al. 1999). As previously described in the context of Maatouk et al. (2008), upon recombination exon 3 is

deleted, which contains residues which are normally phosphorylated to target β-catenin for degradation. Therefore, deletion of exon 3 results in a stabilised protein (Harada et al. 1999). When β-catenin expression is forced in germ cells of the gonad from 15.5 dpc onwards, neonatal testes appeared normal and initial testis development is not affected. Initially, at 15 *dpp*, there are also a similar number of germ cells in testes where β-catenin has been stabilised compared to wild-type controls. However, by 30 d*pp,* numbers are significantly lower in the mutant testes, and a significant number of testis cords are abnormal. Spermatogonia, in which β-catenin expression is forced, proliferate at a higher rate than controls, and this triggers germ cell apoptosis (Chassot et al. 2017). This study may partially explain why there are apparently fewer germ cells in *Znrf3* null gonads. However, Chassot et al. (2017) found that testes were normal at birth, whereas *Stra8* appears to be reduced in the *Znrf3* null gonad as early as 14.5 dpc. Furthermore, this study did not investigate the effect on XX germ cells (oogonia), which have a different developmental pathway to spermatogonia. Therefore, although this study implicates ectopic WNT/β-catenin expression in germ cell development, it is in a context quite distinct from the phenotype of the *Znrf3* null gonads at 14.5 dpc.

7.6 Gonadal ridge growth

One interesting observation made during WMISH experiments at 11.5 dpc, is that the *Znrf3*-null gonads look slightly thinner than the XY wild-type controls. XY *Sf1* positive cells undergo a sex-specific wave of proliferation between 11.2-11.8 dpc at the onset of *Sry* expression (J. Schmahl et al. 2000). Treatment of gonads with inhibitors of proliferation before this time cause defects in testicular-fate specification. However, if proliferation is inhibited after *Sry*

expression is initiated, gonads are able to specify the testicular fate (Jennifer Schmahl and Capel 2003). These data indicate that this male-specific proliferation is *Sry* expression-dependent, and does not play a role testis determination. *Rspo1* and *Wnt4,* which are both affected by the loss of *Znrf3*, have both been shown to be crucial for the initial grown of the primordial gonad. Simultaneous ablation of both genes results in fewer pre-Sertoli cells and the development of small testes with few testis cords (Chassot et al. 2012). However, testis determination was still initiated and no evidence of ovarian markers was seen in the XY gonads.

Therefore, there is strong evidence that altered WNT/β-catenin signalling could result in differential rates of proliferation in the *Znrf3*$^{-/-}$ gonad. However, if *Znrf3*-null gonads do show a proliferation phenotype, this defect probably does not contribute to the sex development phenotype seen at 14.5 dpc. Furthermore, evidence so far only points towards reduced WNT-signalling causing low proliferation rates in the gonad. Whether elevated levels could have the same impact is not understood. 5-ethynyl-2'-deoxyuridine (EDU) will be used to quantify the number of proliferating cells in gonads between 10.5 and 11.5 dpc, particularly focussing on early time-points when proliferation is crucial.

7.7 Alternative mechanisms of ZNRF3/RNF43 and RSPO1 function?

This thesis has relied on data suggesting that the mechanism of RSPO1/ZNRF3/β-catenin signalling relies on the availability of WNT-receptors (Frizzled) on the cell surface membrane, namely the elevated levels of WNT/β-catenin target gene expression in the XY *Znrf3*-null gonad. However, recent evidence describes alternative molecular mechanisms by

which RSPO1 or RNF43 may be able to regulate WNT-signalling. These mechanisms could have implications for the interpretation of some of the data in the literature and in this thesis, and are detailed below.

7.7.1 *Rnf43* can suppress WNT/β-catenin signalling downstream of β-catenin

There is some conflicting evidence within the literature which suggests that ZNRF3/RNF43 may work through multiple mechanisms to antagonise WNT-signalling. The first mechanism is that described in **Chapter 1** (Hao et al. 2012; Koo et al. 2012). Briefly, ZNRF3/RNF43 are both E3 ubiquitin ligases which poly-ubiquitinate the frizzled receptor, and target it for degradation. This results in the assembly of the destruction complex and therefore β-catenin degradation. This was independently demonstrated for both ZNRF3 (Hao et al. 2012) and RNF43 (Koo et al. 2012).

New data suggests that RNF43 is still able to supress canonical WNT-signalling *in vitro* when β-catenin is stabilised (Loregger et al. 2015). This data is not consistent with the hypothesis that the role of RNF43 is solely to remove frizzled receptors from the cell surface membrane, and suggests that RNF43 may be acting downstream of β-catenin in the molecular pathway. Furthermore, high levels of RNF43 are detected in the nucleus by cellular fractionation studies and immunohistochemistry on endogenous protein. Consistent with this subcellular location, RNF43 physically interacts with TCF4, a transcription factor which binds with β-catenin to activate the downstream effectors of canonical WNT-signalling, in coimmunoprecipitation studies. When RNF43 is overexpressed *in vitro*, TCF4 moves from the nucleoplasm to the nuclear envelope, and is sequestered here (Loregger et al. 2015). Taken together, this evidence suggests that RNF43 can antagonise WNT/β-catenin signalling

downstream of β-catenin, at the level of the chromatin. One question that remains, is whether ZNRF3 may also have a similar function. However, thus far, no evidence to support this has been reported.

7.7.2 The role of Rspondins

There is also some conflicting evidence concerning the role of R-spondins in the regulation of WNT/β-catenin signalling. Xie et al. (2013) propose that RSPO1 signals primarily through the downregulation of ZNRF3/RNF43. Briefly, they demonstrate that a ZNRF3 mutant, which is unable to bind RSPO2, can still function to downregulate WNT/β-catenin signalling *in vitro*. This mutant ZNRF3 is simply resistant to inhibition by RSPO2. This supports the argument that RSPO2 functions primarily through its interaction with ZNRF3. On the other hand, (Carmon et al. 2014) showed that RSPO1 was more effective at stimulating WNT-signalling when ZNRF3 was knocked down using siRNA, in HEK293T cells. They propose that there is an alternative molecular mechanism which allows R-spondins to upregulate WNT/β-catenin signalling, that is independent of ZNRF3/RNF43.

The possibility of an independent role for RSPOs is further supported by studies which show that human RSPO1 has a high affinity for LRP6, a WNT ligand co-receptor (K_d = 1.2nM) (Wei et al. 2007), which is comparatively stronger than the interaction between RNF43 and a pre-assembled complex of RSPO1/LGR5 (K_d = 0.5uM (P.-H. P. H. Chen et al. 2013)). This evidence suggests that the interaction between RSPOs and ZNRF3/RNF43 is weak and may not be physiologically relevant and RSPOs may instead interact with LRP6 to carry out its function. R-spondins phosphorylate LRP6 *in vitro* (Wei et al. 2007) and this phosphorylation is both necessary and sufficient to promote WNT/β-catenin signalling (Tamai et al. 2004). Carmon et al. (2014) propose that this mechanism is mediated by a protein, IQGAP1, which when

knocked down *in vitro* reduces the sensitivity of cells to RSPO-induced WNT/β-catenin signalling.

A secondary role for R-spondin proteins, which is independent of ZNRF3/RNF43, therefore seems likely. However, these studies do not offer convincing evidence against R-spondins also working through ZNRF3/RNF43. Although potentiation of WNT/β-catenin signalling by RSPO1 appeared greater in the context of a ZNRF3 knock-down (Carmon et al. 2014), no analysis of the level of knockdown was carried out. Furthermore, no investigation was carried out into the potential compensatory role of RNF43 in this context. Therefore, from this evidence, particularly in light of the convincing evidence presented in (Hao et al. 2012; Koo et al. 2012), a role for ZNRF3/RNF43 in the upregulation of WNT/β-catenin signalling by R-spondins appears to be established.

Above (section 7.1.2), it was proposed that RSPO1 upregulates WNT/β-catenin signalling in the gonad through the inhibition of ZNRF3. Evidence suggests that RPSO1 is also able to achieve this upregulation by an alternative mechanism. If this is the case, we may expect that removing *Rspo1* from the *Znrf3* null gonad, by generating a double knockout, we may be able to partially rescue the XY *Znrf3*$^{-/-}$ sex reversal phenotype. Analysis of *Rspo1*$^{-/-}$, *Znrf3*$^{-/-}$ gonads may help to elucidate the genetic relationship between *Rspo1* and *Znrf3*. Further understanding of this relationship will also help our understanding of the regulation of ZNRF3 activity. One hypothesis is that ZNRF3 activity is not regulated at the transcriptional level, but instead is regulated solely through the differential activity and expression of *Rspo1* in the developing testis and the ovary. If *Rspo1* does not signal primarily through ZNRF3/RNF43, ZNRF3 must be regulated by an alternative means.

7.8 Differing roles of ZNRF3 and RNF43

At the beginning of this project, we hypothesised that ZNRF3 and RNF43, due to high structural conservation between the two proteins, would play similar roles in development. However, this thesis, and recent evidence from the literature, seem to suggest more divergent functions despite a conserved mechanism for antagonising WNT-signalling (Hao et al. 2012; Koo et al. 2012). These differences could in part be due to patterns of expression of the two genes. It is interesting to question whether RNF43 would be able to supress WNT/β-catenin signalling in the testis, in a similar fashion to ZNRF3.

Further evidence for this divergence in role is highlighted by studies of the role of ZNRF3 and RNF43 in cancer. WNT-signalling has been tightly associated with cancer for many years, and there is a vast literature which identifies its importance in key aspects such as maintenance of cancer stem cells, and the role of non-canonical WNT-signalling in metastasis. Recently, mutations in *RNF43* have been identified in a plethora of different cancers, including pancreatic cancer, gastric cancer, colorectal adenocarcinomas amongst others (Witkiewicz et al. 2015; K. Wang et al. 2014; Giannakis et al. 2014). Mutations in *ZNRF3*, on the other hand, have only been identified thus far in Adrenocortical Carcinoma (ACC), where it is in fact, the most commonly mutated gene (Assié et al. 2014). These data could imply that RNF43 and ZNRF3 may play differing roles in cancer, and that these two homologous proteins may have more divergent functions than first thought. However, this differing distribution of mutations in *ZNRF3* compared to *RNF43* may stem from differences in how mutations can cause them to malfunction, and this may not reflect back on their wild-type function.

7.9 Genomic Context: *Kremen1*

Kremen1 encodes a transmembrane co-receptor for *Dkk1*. KREMEN1 and DKK1 cooperate to antagonise WNT/β-catenin signalling (B. Mao et al. 2002) and *Kremen1* is located adjacent to *Znrf3* on mouse chromosome 11. This genomic proximity is conserved in many organisms, including humans and zebrafish. This could indicate that *Znrf3* and *Kremen1* are co-regulated, and importantly for this thesis, may work together in the testis to downregulate ovary-specific WNT-signalling. Studies in zebrafish and other organisms indicate that neighbouring genes are more likely to be co-expressed than randomly chosen pairs of genes (Tsai et al. 2009). Co-regulation of neighbouring genes can be due to a whole range of factors, which will not be discussed here due to space constraint, but are reviewed in (Michalak 2008).

Despite the physical proximity of the two genes, several online tools failed to find a significant correlation in co-expression between *Znrf3* and *Kremen1*. For example, COXPRESdb calculated a correlation coefficient of 0.24 when comparing human *ZNRF3* and *KREMEN1* expression, where 1 is perfect correlation and 0 is a random association (Okamura et al. 2015). Low incidence of co-expression suggests that, despite their proximity, they are regulated independently. Furthermore, there is little evidence that *Kremen1*, or its homologue *Kremen2*, play a role in gonad development. *Kremen1*$^{-/-}$, *Kremen2*$^{-/-}$ double knockout mice are both viable and fertile, indicating that testis development is not severely disrupted (Ellwanger et al. 2008).

7.10 The use of mice in the study of human disease

Mice are an excellent model of human disease, and furthermore, have been critical in elucidating the role of key genes such as *Sox9* and *Sry* in mammalian sex development. There are many advantages of using mice as model organisms. Their physiology and genome is highly similar to humans, and we have a sophisticated genetic tool-kit available to manipulate and study the effects of disease phenotypes. Furthermore, their small size and high breeding rate is advantageous in carrying out large-scale genetic studies, and makes them relatively cheap to breed and house compared to other larger mammals. Furthermore, we can study the effect of drugs and other interventions in mouse disease models, which may be impossible or unethical to do on a large scale in humans (Rosenthal and Brown 2007).

However, this thesis has highlighted some of the issues arising from using mice as models of human disease. The fact that *Znrf3*$^{R749G/R749G}$ CRISPR/Cas9-generated mice do not show a sex reversal phenotype demonstrates that careful analysis is required when comparing data from mouse models to human disease phenotypes. If the *Znrf3*-null model had not also been analysed, we may have concluded that *Znrf3* does not play a role in sex determination. On the other hand, this thesis has succeeded in using mice to model a human DSD using a null-allele. Particularly interesting was our ability to use a sensitised genetic background, the B6.Y^{AKR} strain, to model the phenotype of individuals with 46, XY DSD harbouring just a single mutated copy of *ZNRF3*.

In summary, the data in this thesis represents a cautionary tale. It demonstrates that, despite the revolution that is occurring because of the wide-spread use of the CRISPR/Cas9 system, it is not sufficient to only analyse the effects of a given point mutation *in vivo*, in the

mouse. Null alleles are a critical tool for determining the role of genes in a developmental process, and can facilitate the modelling of numerous aspects of human disease, including genetic background effects.

7.11 Future work

This thesis has thoroughly assessed the sex reversal phenotype seen in XY *Znrf3*-null mice, in both embryos and adults. It has analysed the effect of downstream genes to gain insight into the relationship between *Znrf3* and the known testis-determining pathway. However, many questions remain which, due to time constraints, this thesis has not been able to analyse.

7.11.1 Further assessing expression of *Znrf3*: single cell transcriptomics

One unresolved question is whether there is true sexual dimorphism in the expression pattern of *Znrf3*. Conflicting results from the work in this thesis, and from the literature, make it difficult to fully understand the transcriptional regulation of ZNRF3. New technologies are now available for single-cell analysis of gene expression, which may improve our ability to obtain useful results from the limiting number of cells obtained from the gonad. Furthermore, new computational methods are being employed which allow mapping of lineages over "pseudotime". The algorithm groups cells based on their transcriptomes, in a similar way to assembling phylogenetic trees, by ensuring the minimal change to expression in every step through pseudotime (Reid and Wernisch 2016; Z. Liu et al. 2017). Indeed, these technologies are beginning to be used in the gonad, and similar methods were used to generate the single-cell transcriptomic data shown in Chapter 3

(Serge Nef, Isabel Stevant – pers. comm.)(Stevant et al. 2017). This will allow us to define cell types in the gonad more precisely and, in the case of analysing *Znrf3* expression, compare expression more precisely between the supporting cell populations in XX and XY gonads. Datasets such as these would allow for analysis of *Znrf3* expression over time. Single cell data could also be collected from XY *Znrf3*$^{-/-}$ gonads and transcriptomes analysed in each of the cell lineages of the gonad. This would not only confirm the results presented in this thesis, but may allow us to delve deeper into the mechanistic consequences of the loss of *Znrf3* in multiple cell types.

7.11.2 A role for *Znrf3* in adults

The results of deleting *Znrf3* in the adult gonad was described in **Chapter 4.** When *Znrf3*$^{flox.flox}$ *ERT2-Ubiq-Cre* mice were treated with tamoxifen, no gonadal phenotype was seen. However, this conclusion was made using only H&E histological sections. Previous studies of transdifferentiation of adult gonads have used antibodies against FOXL2 to identify individual cells (Lindeman et al. 2015). Although these studies show significant morphological changes in the gonad which could be identified in histological sections, a sex reversal phenotype caused by loss of *Znrf3* may be less obvious. Therefore, analysis of male and female markers of sexual fate could be crucial in ascertaining whether *Znrf3* plays a minor role in maintaining the fate of the adult testis.

ZNRF3 and *RNF43* have been shown to compensate for each other in adult tissues, for example in the context of adult intestinal crypt cells (Koo et al. 2012). Therefore, despite the minimal role of *Rnf43* in the mouse embryonic gonad, its presence in the adult testis may be compensating for the loss of *Znrf3*. The generation of *Znrf3*$^{flox/flox}$*, Rnf43*$^{flox/flox}$*, ERT2-Ubiq-Cre* XY mice could yield greater insight into the role of these two genes in maintaining

testicular fate. However, the breeding scheme and number of mice required for such an experiment would be very large, and time consuming.

7.11.4 The role of other WNT-ligands in the gonad

Hao et al. (2012) demonstrated that, at a minimum, *Znrf3* can regulate the presence of FZD4, 5, 6 and 8 on the cell surface membrane. This suggests that *Znrf3* has a wide-ranging effect on WNT-signalling in the cell. Therefore, it is possible that the target of ZNRF3 in the testis is not only *Wnt4*. Thus far, there is little evidence in the literature for a substantial role of WNT-molecules, other than *Wnt4*, in the gonad. There is good evidence that other WNT-ligands, including WNT3 and WNT5A, play a major role in PGC specification and migration (Cantú, Altshuler-Keylin, and Laird 2016; Ohinata et al. 2009; Chawengsaksophak et al. 2012). However, when these WNT-ligands, such as WNT5A, are lost from the mammalian gonad, primary sex determination is not affected (Chawengsaksophak et al. 2012). Nevertheless, the role of many WNT-ligands in the gonad, and in sex determination, remains to be elucidated.

One interesting comparison to make is between the gonadal phenotype of XY *Znrf3* nulls and a mouse model where human *WNT4* is overexpressed (B. K. Jordan et al. 2003). Significant upregulation of *Wnt4* detected in *Znrf3* null gonads (Chapter 5), and therefore we may expect a similar phenotype in the overexpression model. However, the adult gonadal phenotype of *WNT*4-overexpressing mouse, described fully in Chapter 1, is significantly less severe than XY *Znrf3*$^{-/-}$ embryonic gonads (B. K. Jordan et al. 2003). This could suggest that loss of ZNRF3 is leading to the upregulation of WNTs other than *Wnt4* in the mouse gonad. However, Jordan et al. did not examine embryonic gonads, and did not measure the extent to which *WNT4* was overexpressed in this mouse model.

Therefore, despite the current lack of evidence, other WNT-ligands may still play a significant role in primary sex determination. Compensation between multiple WNT-signalling molecules may mean that knocking out a single WNT-molecule is not sufficient to result in a phenotype. Furthermore, despite the significant role that *Wnt4* plays in the ovary, *Wnt4*-null gonads only show partial sex reversal, suggesting possible functional redundancy of *Wnt4* with other WNT-signalling molecules (Jeays-Ward, Dandonneau, and Swain 2004).

7.11.5 Investigating non-canonical WNT signalling

ZNRF3 has been shown to regulate both canonical (or β-catenin-dependent) and non-canonical (or β-catenin-independent) signalling in the context of the Zebrafish (Hao et al. 2012). This thesis, however, has focused on the effects of the loss of *Znrf3* on canonical signalling in the gonad. This focus was mainly due to the known role of β-catenin in the gonad, and the sex reversal phenotype seen when β-catenin is artificially stabilised (Maatouk et al. 2008). *Wnt4,* which plays a crucial role in ovarian development, is classically categorised as a non-canonical WNT molecule. However, evidence suggests that it is able to stabilise β-catenin in some contexts (Lyons et al. 2004; Bernardi et al. 2011), but not in others (Tanigawa et al. 2011; Shimizu et al. 1997). In some cases, *Wnt4* has even been shown to inhibit canonical WNT-signalling (Bernard et al. 2008).

There is no evidence that non-canonical WNT pathways play a critical role in primary sex determination. On the other hand, several so called non-canonical WNTs have been implicated in primary sex determination. A previously described, the loss of *Wnt5a* from the early mouse gonad does not result in a sex reversal phenotype, but results in small, abnormally located testes (Warr et al. 2008). *Wnt11* has also been implicated in maintaining

the polarity and epithelial characteristics of adult Sertoli cells which, in turn, is crucial for maintenance of germ cells (X. N. Wang et al. 2013).

Non-canonical WNT signalling also plays a role in migrating cells. For example, blocking *Wnt11* activity is sufficient to prevent the migration of neural crest cells in Zebrafish, and this can be rescued by activating the non-canonical WNT-signalling pathway (De Calisto et al. 2005). There are several examples of aspects of gonadal development which rely on cell migration. For example, the formation of testis cords requires migration of endothelial cells from the mesonephros (Combes et al. 2009). Furthermore, PGCs migrate into the gonad, a process which has been demonstrated to rely on non-canonical WNT-signalling (Chawengsaksophak et al. 2012; Laird et al. 2011). Therefore, measuring the impact of *Znrf3* on non-canonical pathways *in vitro* and *in vivo* is important to fully understand all the potential roles of *Znrf3* in the developing gonad.

Measuring changes in non-canonical pathways, particularly the Planar Cell Polarity (PCP) pathway, can be significantly more difficult than the simple read-outs available for assessing WNT/β-catenin signalling. Methods often rely on observations of cell morphology and behaviours, which are often difficult to quantify. One robust method would be to use immunohistochemistry to assess asymmetric localisation of proteins on the cell surface membrane.

7.11.6 Frizzled Receptors

As previously described, ZNRF3 has been shown to downregulate several Frizzled receptors *in vitro* (Hao et al. 2012). However, ZNRF3 may act through different receptors dependent on the context. It is therefore important to assess this in the context of the gonad. Coimmunoprecipitation studies allow us to study interactions between proteins *in vivo*. In

this way, ZNRF3 could be pulled down and probed with antibodies against Frizzled receptors or the products examined by mass spectrometry. However, this would require an antibody which could be used to immunoprecipitate endogenous ZNRF3. Furthermore, the process could be further complicated by the small amount of tissue that can be obtained from a pair of gonads. Generating a mouse line carrying a tagged version of ZNRF3 at the endogenous locus, could solve this problem. However, the tag used to pull the protein down may disrupt interactions between proteins seen in endogenous conditions. Finally, a cellular model of the developing embryonic Sertoli cell might be used, but no such stably reprogrammed line is available despite recent efforts (Buganim et al. 2012).

7.12 Closing Remarks

This thesis has presented evidence for the role of a new testis-determining gene, *ZNRF3,* in humans and mice. The data strongly suggest that the primary role for ZNRF3 in the testis is the downregulation of the canonical WNT-signalling pathway, usually active in the developing ovary. Therefore, when ZNRF3 function is disrupted, ectopic WNT/β-catenin signalling in the supporting cells of the testis causes at least some of them to assume a pre-granulosa cell fate over a pre-Sertoli fate. In this way, ZNRF3 is likely a new bridge which mediates the mutually antagonistic interaction between the canonical WNT-signalling pathway in the ovary, and the FGF9/SOX9 testis-determining pathway. Furthermore, this thesis has presented a model of human DSDs whereby loss of one allele of *Znrf3* is sufficient to cause full male-to-female sex reversal, on a sensitised genetic background (B6.Y^{AKR}).

The discovery of this new link between the ovary- and testis-determining pathways exemplifies the critical importance of mutually antagonistic interactions in the gonad, and

has demonstrated that the suppression of the ovarian pathway in the XY gonad is absolutely required for normal testis development. It is also an example of how exome screening of patients, despite only covering a fraction of the genome, can be very valuable in identifying new candidate genes in disease pathogenesis. It has shown the value of using null-alleles to probe the role of such genes, and cautions against the use of CRISPR/Cas9 generated point mutation alleles in isolation.

References

Adams, Ian R, and Anne McLaren. 2002. “Sexually Dimorphic Development of Mouse Primordial Germ Cells: Switching from Oogenesis to Spermatogenesis.” *Development (Cambridge, England)* 129 (5):1155–64. http://www.ncbi.nlm.nih.gov/pubmed/11874911.

Akiyama, Haruhiko, Marie-Christine Chaboissier, James F Martin, Andreas Schedl, and Benoit de Crombrugghe. 2002. “The Transcription Factor Sox9 Has Essential Roles in Successive Steps of the Chondrocyte Differentiation Pathway and Is Required for Expression of Sox5 and Sox6.” *Genes & Development* 16 (21). Cold Spring Harbor Laboratory Press:2813–28. https://doi.org/10.1101/gad.1017802.

Akiyama, Haruhiko, Jon P Lyons, Yuko Mori-Akiyama, Xiaohong Yang, Ren Zhang, Zhaoping Zhang, Jian Min Deng, et al. 2004. “Interactions between Sox9 and Beta-Catenin Control Chondrocyte Differentiation.” *Genes & Development* 18 (9). Cold Spring Harbor Laboratory Press:1072–87. https://doi.org/10.1101/gad.1171104.

Albrecht, Kenneth H, and Eva M Eicher. 2001. “Evidence That Sry Is Expressed in Pre-Sertoli Cells and Sertoli and Granulosa Cells Have a Common Precursor.” *Developmental Biology* 240 (1):92–107. https://doi.org/10.1006/dbio.2001.0438.

Assié, Guillaume, Eric Letouzé, Martin Fassnacht, Anne Jouinot, Windy Luscap, Olivia Barreau, Hanin Omeiri, et al. 2014. “Integrated Genomic Characterization of Adrenocortical Carcinoma.” *Nature Genetics* 46 (6):607–12. https://doi.org/10.1038/ng.2953.

Auguste, A, A-A Chassot, E P Grégoire, L Renault, M Pannetier, M Treier, Eric Pailhoux, and M-C Chaboissier. 2011. “Loss of R-spondin1 and Foxl2 Amplifies Female-to-Male Sex Reversal in XX Mice.” *Sexual Development : Genetics, Molecular Biology, Evolution, Endocrinology, Embryology, and Pathology of Sex Determination and Differentiation* 5 (6). Karger Publishers:304–17. https://doi.org/10.1159/000334517.

Bagheri-Fam, Stefan, Makoto Ono, Li Li, Liang Zhao, Janelle Ryan, Raymond Lai, Yukako Katsura, et al. 2015. “*FGFR2* Mutation in 46,XY Sex Reversal with Craniosynostosis.” *Human Molecular Genetics* 24 (23):6699–6710. https://doi.org/10.1093/hmg/ddv374.

Bamshad, Michael J., Sarah B. Ng, Abigail W. Bigham, Holly K. Tabor, Mary J. Emond, Deborah A. Nickerson, and Jay Shendure. 2011. “Exome Sequencing as a Tool for Mendelian Disease Gene Discovery.” *Nature Reviews Genetics* 12 (11):745–55. https://doi.org/10.1038/nrg3031.

Bardoni, B., E. Zanaria, S. Guioli, G. Floridia, K. C. Worley, G. Tonini, E. Ferrante, et al. 1994. “A Dosage Sensitive Locus at Chromosome Xp21 Is Involved in Male to Female Sex Reversal.” *Nature Genetics* 7 (4):497–501. https://doi.org/10.1038/ng0894-497.

Barrangou, R., C. Fremaux, H. Deveau, M. Richards, P. Boyaval, S. Moineau, D. A. Romero, and P. Horvath. 2007. “CRISPR Provides Acquired Resistance Against Viruses in Prokaryotes.” *Science* 315 (5819):1709–12. https://doi.org/10.1126/science.1138140.

Barrionuevo, Francisco, Stefan Bagheri-Fam, Jü Rgen Klattig, Ralf Kist, Makoto M Taketo, Christoph Englert, and Gerd Scherer. 2006. “Homozygous Inactivation of Sox9 Causes Complete XY Sex Reversal in Mice 1.” *BIOLOGY OF REPRODUCTION* 74:195–201. https://doi.org/10.1095/biolreprod.105.045930.

Barrionuevo, Francisco J, Alicia Hurtado, Gwang-Jin Kim, Francisca M Real, Mohammed Bakkali, Janel L Kopp, Maike Sander, Gerd Scherer, Miguel Burgos, and Rafael Jiménez. 2016. "*Sox9* and *Sox8* Protect the Adult Testis from Male-to-Female Genetic Reprogramming and Complete Degeneration." *eLife* 5 (June). https://doi.org/10.7554/eLife.15635.

Barsoum, Ivraym B., Nathan C. Bingham, Keith L. Parker, Joan S. Jorgensen, and Humphrey H.-C. Yao. 2009. "Activation of the Hedgehog Pathway in the Mouse Fetal Ovary Leads to Ectopic Appearance of Fetal Leydig Cells and Female Pseudohermaphroditism." *Developmental Biology* 329 (1):96–103. https://doi.org/10.1016/j.ydbio.2009.02.025.

Bassing, Craig H., and Frederick W. Alt. 2004. "The Cellular Response to General and Programmed DNA Double Strand Breaks." *DNA Repair* 3 (8–9):781–96. https://doi.org/10.1016/j.dnarep.2004.06.001.

Beaulieu, Chandree L., Jacek Majewski, Jeremy Schwartzentruber, Mark E. Samuels, Bridget A. Fernandez, Francois P. Bernier, Michael Brudno, et al. 2014. "FORGE Canada Consortium: Outcomes of a 2-Year National Rare-Disease Gene-Discovery Project." *The American Journal of Human Genetics* 94 (6):809–17. https://doi.org/10.1016/j.ajhg.2014.05.003.

Bernard, Pascal, Alice Fleming, Arnaud Lacombe, Vincent R Harley, and Eric Vilain. 2008. "Wnt4 Inhibits Beta-catenin/TCF Signalling by Redirecting Beta-Catenin to the Cell Membrane." *Biology of the Cell* 100 (3). NIH Public Access:167–77. https://doi.org/10.1042/BC20070072.

Bernard, Pascal, Janelle Ryan, Helena Sim, Daniel P. Czech, Andrew H. Sinclair, Peter Koopman, and Vincent R. Harley. 2012a. "Wnt Signaling in Ovarian Development Inhibits Sf1 Activation of *Sox9* via the *Tesco* Enhancer." *Endocrinology* 153 (2):901–12. https://doi.org/10.1210/en.2011-1347.

Bernard, Pascal, Janelle Ryan, Helena Sim, Daniel P Czech, Andrew H Sinclair, Peter Koopman, and Vincent R Harley. 2012b. "Wnt Signaling in Ovarian Development Inhibits Sf1 Activation of Sox9 via the Tesco Enhancer." *Endocrinology* 153 (2):901–12. https://doi.org/10.1210/en.2011-1347.

Bernardi, Henri, Stephanie Gay, Yann Fedon, Barbara Vernus, Anne Bonnieu, and Francis Bacou. 2011. "Wnt4 Activates the Canonical β-Catenin Pathway and Regulates Negatively Myostatin: Functional Implication in Myogenesis." *American Journal of Physiology - Cell Physiology* 300 (5). http://ajpcell.physiology.org/content/300/5/C1122.

Beverdam, Annemiek, and Peter Koopman. 2006. "Expression Profiling of Purified Mouse Gonadal Somatic Cells during the Critical Time Window of Sex Determination Reveals Novel Candidate Genes for Human Sexual Dysgenesis Syndromes." *Human Molecular Genetics* 15 (3):417–31. https://doi.org/10.1093/hmg/ddi463.

Bingham, Nathan C., Sunita Verma-Kurvari, Luis F. Parada, and Keith L. Parker. 2006. "Development of a Steroidogenic Factor 1/Cre Transgenic Mouse Line." *Genesis* 44 (9):419–24. https://doi.org/10.1002/dvg.20231.

Bogani, Debora, Pam Siggers, Rachel Brixey, Nick Warr, Sarah Beddow, Jessica Edwards, Debbie Williams, et al. 2009. "Loss of Mitogen-Activated Protein Kinase Kinase Kinase 4 (MAP3K4) Reveals a Requirement for MAPK Signalling in Mouse Sex Determination." Edited by Robin Lovell-Badge. *PLoS Biology* 7 (9):e1000196. https://doi.org/10.1371/journal.pbio.1000196.

Bolotin, Alexander, Benoit Quinquis, Alexei Sorokin, and S Dusko Ehrlich. 2005. "Clustered

Regularly Interspaced Short Palindrome Repeats (CRISPRs) Have Spacers of Extrachromosomal Origin." *Microbiology* 151 (8):2551–61. https://doi.org/10.1099/mic.0.28048-0.

Bouma, G. J., L. L. Washburn, K. H. Albrecht, and E. M. Eicher. 2007. "Correct Dosage of Fog2 and Gata4 Transcription Factors Is Critical for Fetal Testis Development in Mice." *Proceedings of the National Academy of Sciences* 104 (38):14994–99. https://doi.org/10.1073/pnas.0701677104.

Bowles, J. 2006. "Retinoid Signaling Determines Germ Cell Fate in Mice." *Science* 312 (5773):596–600. https://doi.org/10.1126/science.1125691.

Bowles, Josephine, M Bullejos, and Peter Koopman. 2000. "A Subtractive Gene Expression Screen Suggests a Role for Vanin-1 in Testis Development in Mice." *Genesis (New York, N.Y. : 2000)* 27 (3):124–35. https://doi.org/10.1002/1526-968X(200007)27:3<124::AID-GENE50>3.0.CO;2-E [pii].

Buehr, Mia, Anne McLaren, Aine Bartley, and Susan Darling. 1993. "Proliferation and Migration of Primordial Germ Cells in We/We Mouse Embryos." *Developmental Dynamics* 198 (3):182–89. https://doi.org/10.1002/aja.1001980304.

Buganim, Yosef, Elena Itskovich, Yueh-Chiang Hu, Albert W. Cheng, Kibibi Ganz, Sovan Sarkar, Dongdong Fu, G. Grant Welstead, David C. Page, and Rudolf Jaenisch. 2012. "Direct Reprogramming of Fibroblasts into Embryonic Sertoli-like Cells by Defined Factors." *Cell Stem Cell* 11 (3):373–86. https://doi.org/10.1016/j.stem.2012.07.019.

Bullejos, Monica, and Peter Koopman. 2005. "Delayed Sry and Sox9 Expression in Developing Mouse Gonads Underlies B6-YDOM Sex Reversal." *Developmental Biology* 278 (2):473–81. https://doi.org/10.1016/j.ydbio.2004.11.030.

Burger, Alexa, Helen Lindsay, Anastasia Felker, Christopher Hess, Carolin Anders, Elena Chiavacci, Jonas Zaugg, et al. 2016. "Maximizing Mutagenesis with Solubilized CRISPR-Cas9 Ribonucleoprotein Complexes." *Development* 143 (11):2025–37. https://doi.org/10.1242/dev.134809.

Burgoyne, P S, M Buehr, P Koopman, J Rossant, and A McLaren. 1988. "Cell-Autonomous Action of the Testis-Determining Gene: Sertoli Cells Are Exclusively XY in XX----XY Chimaeric Mouse Testes." *Development (Cambridge, England)* 102 (2):443–50. http://www.ncbi.nlm.nih.gov/pubmed/3166423.

Burgoyne, P S, M Buehr, and A McLaren. 1988. "XY Follicle Cells in Ovaries of XX----XY Female Mouse Chimaeras." *Development (Cambridge, England)* 104 (4):683–88. http://www.ncbi.nlm.nih.gov/pubmed/3268409.

Calisto, Jaime De, Claudio Araya, Lorena Marchant, Chaudhary F. Riaz, and Roberto Mayor. 2005. "Essential Role of Non-Canonical Wnt Signalling in Neural Crest Migration." *Development* 132 (11). http://dev.biologists.org/content/132/11/2587.

Cantú, Andrea V, Svetlana Altshuler-Keylin, and Diana J Laird. 2016. "Discrete Somatic Niches Coordinate Proliferation and Migration of Primordial Germ Cells via Wnt Signaling." *The Journal of Cell Biology* 214 (2). Rockefeller University Press:215–29. https://doi.org/10.1083/jcb.201511061.

Carmon, Kendra S, Xing Gong, Jing Yi, Anthony Thomas, and Qingyun Liu. 2014. "RSPO-LGR4 Functions via IQGAP1 to Potentiate Wnt Signaling." *Proceedings of the National Academy of Sciences of the United States of America* 111 (13):E1221-9. https://doi.org/10.1073/pnas.1323106111.

Chaboissier, Marie-Christine, Akio Kobayashi, Valerie I. P. Vidal, Susanne Lützkendorf, Henk J. G. van de Kant, Michael Wegner, Dirk G. de Rooij, Richard R. Behringer, and Andreas

Schedl. 2004. “Functional Analysis of Sox8 and Sox9 during Sex Determination in the Mouse.” *Development* 131 (9). http://dev.biologists.org/content/131/9/1891.

Chamorro, Mario N, Donald R Schwartz, Alin Vonica, Ali H Brivanlou, Kathleen R Cho, and Harold E Varmus. 2005. “FGF-20 and DKK1 Are Transcriptional Targets of Beta-Catenin and FGF-20 Is Implicated in Cancer and Development.” *The EMBO Journal* 24 (1):73–84. https://doi.org/10.1038/sj.emboj.7600460.

Chang, Hao, Fei Gao, Florian Guillou, Makoto M Taketo, Vicki Huff, and Richard R Behringer. 2008. “Wt1 Negatively Regulates Beta-Catenin Signaling during Testis Development.” *Development (Cambridge, England)* 135 (10). The Company of Biologists Ltd:1875–85. https://doi.org/10.1242/dev.018572.

Chang, Yao-Fu, Jennifer S. Lee-Chang, Krystle Y. Harris, Amiya P. Sinha-Hikim, and Manjeet K. Rao. 2011. “Role of β-Catenin in Post-Meiotic Male Germ Cell Differentiation.” Edited by Cara Gottardi. *PLoS ONE* 6 (11). Public Library of Science:e28039. https://doi.org/10.1371/journal.pone.0028039.

Chassot, A.-A., F. Ranc, E. P. Gregoire, H. L. Roepers-Gajadien, M. M. Taketo, G. Camerino, D. G. de Rooij, A. Schedl, and M.-C. Chaboissier. 2008. “Activation of -Catenin Signaling by Rspo1 Controls Differentiation of the Mammalian Ovary.” *Human Molecular Genetics* 17 (9). Oxford University Press:1264–77. https://doi.org/10.1093/hmg/ddn016.

Chassot, Anne-Amandine, Stephen T Bradford, Aurélie Auguste, Elodie P Gregoire, Eric Pailhoux, Dirk G de Rooij, Andreas Schedl, et al. 2012. “WNT4 and RSPO1 Together Are Required for Cell Proliferation in the Early Mouse Gonad.” *Development (Cambridge, England)* 139 (23). Oxford University Press for The Company of Biologists Limited:4461–72. https://doi.org/10.1242/dev.078972.

Chassot, Anne-Amandine, Elodie P. Gregoire, Rowena Lavery, Makoto M. Taketo, Dirk G. de Rooij, Ian R. Adams, and Marie-Christine Chaboissier. 2011. “RSPO1/β-Catenin Signaling Pathway Regulates Oogonia Differentiation and Entry into Meiosis in the Mouse Fetal Ovary.” Edited by Reiner Albert Veitia. *PLoS ONE* 6 (10). Public Library of Science:e25641. https://doi.org/10.1371/journal.pone.0025641.

Chassot, Anne-Amandine, Morgane Le Rolle, Maxime Jourden, Maketo M. Taketo, Norbert B. Ghyselinck, and Marie-Christine Chaboissier. 2017. “Constitutive WNT/CTNNB1 Activation Triggers Spermatogonial Stem Cell Proliferation and Germ Cell Depletion.” *Developmental Biology* 426 (1):17–27. https://doi.org/10.1016/j.ydbio.2017.04.010.

Chassot, Anne, Fariba Ranc, Elodie P. Gregoire, Hermien L. Roepers-Gajadien, Makoto M. Taketo, Giovanna Camerino, Dirk G. de Rooij, Andreas Schedl, and Marie Christine M.-C. Chaboissier. 2008. “Activation of Beta-Catenin Signaling by Rspo1 Controls Differentiation of the Mammalian Ovary.” *Human Molecular Genetics* 17 (9). Oxford University Press:1264–77. https://doi.org/10.1093/hmg/ddn016.

Chawengsaksophak, Kallayanee, Terje Svingen, Ee Ting Ng, Trevor Epp, Cassy M. Spiller, Charlotte Clark, Helen Cooper, and Peter Koopman. 2012. “Loss of Wnt5a Disrupts Primordial Germ Cell Migration and Male Sexual Development in Mice1.” *Biology of Reproduction* 86 (1):1–12. https://doi.org/10.1095/biolreprod.111.095232.

Chen, P.-H. Po Han, Xiaoyan Chen, Zhenghong Lin, Deyu Fang, and Xiaolin He. 2013. “The Structural Basis of R-Spondin Recognition by LGR5 and RNF43” 27 (12):1345–50. https://doi.org/10.1101/gad.219915.113.

Chen, Yen-Shan, Joseph D Racca, Paul W Sequeira, and Michael A Weiss. 2015. “Inherited Sex-Reversal Mutations in SRY Define a Functional Threshold of Gonadogenesis :

Biochemical and Evolutionary Implications of a Rare Monogenic Syndrome" 2015 (216):1–12. https://doi.org/10.21767/2380-7245.100020.

Cho, Seung Woo, Sojung Kim, Yongsub Kim, Jiyeon Kweon, Heon Seok Kim, Sangsu Bae, and Jin Soo Kim. 2014. "Analysis of off-Target Effects of CRISPR/Cas-Derived RNA-Guided Endonucleases and Nickases." *Genome Research* 24 (1). Cold Spring Harbor Laboratory Press:132–41. https://doi.org/10.1101/gr.162339.113.

Chuma, Shinichiro, and Norio Nakatsuji. 2001. "Autonomous Transition into Meiosis of Mouse Fetal Germ Cells in Vitro and Its Inhibition by gp130-Mediated Signaling." *Developmental Biology* 229 (2):468–79. https://doi.org/10.1006/dbio.2000.9989.

Clépet, C, A J Schafer, A H Sinclair, M S Palmer, R Lovell-Badge, and P N Goodfellow. 1993. "The Human SRY Transcript." *Human Molecular Genetics* 2 (12):2007–12. http://www.ncbi.nlm.nih.gov/pubmed/8111368.

Colvin, J S, R P Green, J Schmahl, B Capel, D M Ornitz, D.M. Ornitz, P. Leder, et al. 2001. "Male-to-Female Sex Reversal in Mice Lacking Fibroblast Growth Factor 9." *Cell* 104 (6). Oxford University Press, Oxford:875–89. https://doi.org/10.1016/S0092-8674(01)00284-7.

Combes, Alexander N., Dagmar Wilhelm, Tara Davidson, Elisabetta Dejana, Vincent Harley, Andrew Sinclair, and Peter Koopman. 2009. "Endothelial Cell Migration Directs Testis Cord Formation." *Developmental Biology* 326 (1):112–20. https://doi.org/10.1016/j.ydbio.2008.10.040.

Correa, Stephanie M., Linda L. Washburn, Ravi S. Kahlon, Michelle C. Musson, Gerrit J. Bouma, Eva M. Eicher, and Kenneth H. Albrecht. 2012. "Sex Reversal in C57BL/6J XY Mice Caused by Increased Expression of Ovarian Genes and Insufficient Activation of the Testis Determining Pathway." *PLoS Genetics* 8 (4). https://doi.org/10.1371/journal.pgen.1002569.

Dann, Charles E., Jen-Chih Hsieh, Amir Rattner, Divya Sharma, Jeremy Nathans, and Daniel J. Leahy. 2001. "Insights into Wnt Binding and Signalling from the Structures of Two Frizzled Cysteine-Rich Domains." *Nature* 412 (6842):86–90. https://doi.org/10.1038/35083601.

Deltcheva, Elitza, Krzysztof Chylinski, Cynthia M Sharma, Karine Gonzales, Yanjie Chao, Zaid A Pirzada, Maria R Eckert, Jörg Vogel, and Emmanuelle Charpentier. 2011. "CRISPR RNA Maturation by Trans-Encoded Small RNA and Host Factor RNase III." *Nature* 471 (7340). Europe PMC Funders:602–7. https://doi.org/10.1038/nature09886.

Deveau, H., R. Barrangou, J. E. Garneau, J. Labonte, C. Fremaux, P. Boyaval, D. A. Romero, P. Horvath, and S. Moineau. 2008. "Phage Response to CRISPR-Encoded Resistance in Streptococcus Thermophilus." *Journal of Bacteriology* 190 (4):1390–1400. https://doi.org/10.1128/JB.01412-07.

Edson, Mark A., Ankur K. Nagaraja, and Martin M. Matzuk. 2009. "The Mammalian Ovary from Genesis to Revelation." *Endocrine Reviews* 30 (6):624–712. https://doi.org/10.1210/er.2009-0012.

Eicher, E M, L L Washburn, J B Whitney 3rd, and K E Morrow. 1982. "Mus Poschiavinus Y Chromosome in the C57BL/6J Murine Genome Causes Sex Reversal." *Science* 217 (4559):535–37. https://doi.org/10.1126/science.7089579.

Elejalde, B. Rafael, John M. Opitz, Maria Mercedes de Elejalde, Enid F. Gilbert, Mario Abellera, Lorraine Meisner, Robert R. Lebel, J. Michael Hartigan, and W. Roy Breg. 1984. "Tandem dup(1p) within the Short Arm of Chromosome 1 in a Child with Ambiguous Genitalia and Multiple Congenital Anomalies." *American Journal of Medical Genetics*

17 (4):723–30. https://doi.org/10.1002/ajmg.1320170403.
Ellwanger, Kristina, Hiroaki Saito, Philippe Clément-Lacroix, Nicole Maltry, Joachim Niedermeyer, Woon Kyu Lee, Roland Baron, Georges Rawadi, Heiner Westphal, and Christof Niehrs. 2008. "Targeted Disruption of the Wnt Regulator Kremen Induces Limb Defects and High Bone Density." *Molecular and Cellular Biology* 28 (15). American Society for Microbiology:4875–82. https://doi.org/10.1128/MCB.00222-08.
Feil, R, J Brocard, B Mascrez, M LeMeur, D Metzger, and P Chambon. 1996. "Ligand-Activated Site-Specific Recombination in Mice." *Proceedings of the National Academy of Sciences of the United States of America* 93 (20). National Academy of Sciences:10887–90. https://doi.org/10.1073/pnas.93.20.10887.
Feil, Robert, Jürgen Wagner, Daniel Metzger, and Pierre Chambon. 1997. "Regulation of Cre Recombinase Activity by Mutated Estrogen Receptor Ligand-Binding Domains." *Biochemical and Biophysical Research Communications* 237 (3):752–57. https://doi.org/10.1006/bbrc.1997.7124.
Filali, Mohammed, Ningli Cheng, Duane Abbott, Vladimir Leontiev, and John F Engelhardt. 2002. "Wnt-3A/beta-Catenin Signaling Induces Transcription from the LEF-1 Promoter." *The Journal of Biological Chemistry* 277 (36). American Society for Biochemistry and Molecular Biology:33398–410. https://doi.org/10.1074/jbc.M107977200.
Fleming, Nicholas I., Kevin C. Knower, Kyren A. Lazarus, Peter J. Fuller, Evan R. Simpson, and Colin D. Clyne. 2010. "Aromatase Is a Direct Target of FOXL2: C134W in Granulosa Cell Tumors via a Single Highly Conserved Binding Site in the Ovarian Specific Promoter." Edited by Sudhansu Kumar Dey. *PLoS ONE* 5 (12). Public Library of Science:e14389. https://doi.org/10.1371/journal.pone.0014389.
Foster, Jamie W., Marina A. Dominguez-Steglich, Silvana Guioli, Cheni Kwok, Polly A. Weller, Milena Stevanović, Jean Weissenbach, et al. 1994. "Campomelic Dysplasia and Autosomal Sex Reversal Caused by Mutations in an SRY-Related Gene." *Nature* 372 (6506). Nature Publishing Group:525–30. https://doi.org/10.1038/372525a0.
Freland, Laure, and Jean-Martin Beaulieu. 2012. "Inhibition of GSK3 by Lithium, from Single Molecules to Signaling Networks." *Frontiers in Molecular Neuroscience* 5 (January). Frontiers Media SA:14. https://doi.org/10.3389/fnmol.2012.00014.
Friedel, Roland H., Wolfgang Wurst, Benedikt Wefers, and Ralf Kühn. 2011. "Generating Conditional Knockout Mice." *Methods in Molecular Biology (Clifton, N.J.)* 693:205–31. https://doi.org/10.1007/978-1-60761-974-1_12.
Gallardo, Teresa, Lane Shirley, George B. John, and Diego H. Castrillon. 2007. "Generation of a Germ Cell-Specific Mouse Transgenic Cre line,Vasa-Cre." *Genesis* 45 (6):413–17. https://doi.org/10.1002/dvg.20310.
Garneau, Josiane E., Marie-Ève Dupuis, Manuela Villion, Dennis A. Romero, Rodolphe Barrangou, Patrick Boyaval, Christophe Fremaux, Philippe Horvath, Alfonso H. Magadán, and Sylvain Moineau. 2010. "The CRISPR/Cas Bacterial Immune System Cleaves Bacteriophage and Plasmid DNA." *Nature* 468 (7320):67–71. https://doi.org/10.1038/nature09523.
Garzo, V G, and J H Dorrington. 1984. "Aromatase Activity in Human Granulosa Cells during Follicular Development and the Modulation by Follicle-Stimulating Hormone and Insulin." *American Journal of Obstetrics and Gynecology* 148 (5):657–62. http://www.ncbi.nlm.nih.gov/pubmed/6422764.
Gasiunas, Giedrius, Rodolphe Barrangou, Philippe Horvath, and Virginijus Siksnys. 2012.

"Cas9-crRNA Ribonucleoprotein Complex Mediates Specific DNA Cleavage for Adaptive Immunity in Bacteria." *Proceedings of the National Academy of Sciences of the United States of America* 109 (39). National Academy of Sciences:E2579-86. https://doi.org/10.1073/pnas.1208507109.

Georgi, Benjamin, Benjamin F. Voight, and Maja Bućan. 2013. "From Mouse to Human: Evolutionary Genomics Analysis of Human Orthologs of Essential Genes." Edited by Jonathan Flint. *PLoS Genetics* 9 (5). Public Library of Science:e1003484. https://doi.org/10.1371/journal.pgen.1003484.

Giannakis, Marios, Eran Hodis, Xinmeng Jasmine Mu, Mai Yamauchi, Joseph Rosenbluh, Kristian Cibulskis, Gordon Saksena, et al. 2014. "RNF43 Is Frequently Mutated in Colorectal and Endometrial Cancers." *Nature Genetics* 46 (12):1264–66. https://doi.org/10.1038/ng.3127.

Gierl, Mathias S., Wolfram H. Gruhn, Annika von Seggern, Nicole Maltry, and Christof Niehrs. 2012. "GADD45G Functions in Male Sex Determination by Promoting p38 Signaling and Sry Expression." *Developmental Cell* 23 (5):1032–42. https://doi.org/10.1016/j.devcel.2012.09.014.

Ginsburg, M, M H Snow, and A McLaren. 1990. "Primordial Germ Cells in the Mouse Embryo during Gastrulation." *Development (Cambridge, England)* 110 (2):521–28. http://www.ncbi.nlm.nih.gov/pubmed/2133553.

Goetz, Regina, and Moosa Mohammadi. 2013. "Exploring Mechanisms of FGF Signalling through the Lens of Structural Biology." *Nature Reviews Molecular Cell Biology* 14 (3):166–80. https://doi.org/10.1038/nrm3528.

Griffiths, Anthony J. F. 2000. *An Introduction to Genetic Analysis*. W.H. Freeman.

Griswold, Michael D. 1998. "The Central Role of Sertoli Cells in Spermatogenesis." *Seminars in Cell & Developmental Biology* 9 (4):411–16. https://doi.org/10.1006/scdb.1998.0203.

Griswold, S L, and R R Behringer. 2009. "Fetal Leydig Cell Origin and Development." *Sexual Development : Genetics, Molecular Biology, Evolution, Endocrinology, Embryology, and Pathology of Sex Determination and Differentiation* 3 (1). NIH Public Access:1–15. https://doi.org/10.1159/000200077.

Gubb, D, and A García-Bellido. 1982. "A Genetic Analysis of the Determination of Cuticular Polarity during Development in Drosophila Melanogaster." *Journal of Embryology and Experimental Morphology* 68 (April):37–57. http://www.ncbi.nlm.nih.gov/pubmed/6809878.

Gubbay, John, Jérôme Collignon, Peter Koopman, Blanche Capel, Androulla Economou, Andrea Münsterberg, Nigel Vivian, Peter Goodfellow, and Robin Lovell-Badge. 1990. "A Gene Mapping to the Sex-Determining Region of the Mouse Y Chromosome Is a Member of a Novel Family of Embryonically Expressed Genes." *Nature* 346 (6281). Nature Publishing Group:245–50. https://doi.org/10.1038/346245a0.

Habas, Raymond, and Igor B Dawid. 2005. "Dishevelled and Wnt Signaling: Is the Nucleus the Final Frontier?" *Journal of Biology* 4 (1). BioMed Central:2. https://doi.org/10.1186/jbiol22.

Hacker, A, B Capel, P Goodfellow, and R Lovell-Badge. 1995. "Expression of Sry, the Mouse Sex Determining Gene." *Development (Cambridge, England)* 121 (6):1603–14. http://www.ncbi.nlm.nih.gov/pubmed/7600978.

Hao, Huai-Xiang, Yang Xie, Yue Zhang, Olga Charlat, Emma Oster, Monika Avello, Hong Lei, et al. 2012. "ZNRF3 Promotes Wnt Receptor Turnover in an R-Spondin-Sensitive

Manner." *Nature* 485. https://doi.org/10.1038/nature11019.

Harada, N., Y Tamai, T Ishikawa, B Sauer, K Takaku, M Oshima, and M M Taketo. 1999. "Intestinal Polyposis in Mice with a Dominant Stable Mutation of the Beta -Catenin Gene." *The EMBO Journal* 18 (21):5931–42. https://doi.org/10.1093/emboj/18.21.5931.

Harnden, D G, and J S Stewart. 1959. "The Chromosomes in a Case of Pure Gonadal Dysgenesis." *British Medical Journal* 2 (5162):1285–87. http://www.ncbi.nlm.nih.gov/pubmed/14399877.

Hawley, R. Scott., and Michelle Y. Walker. 2003. *Advanced Genetic Analysis : Finding Meaning in a Genome*. Blackwell Pub. https://books.google.co.uk/books?id=OycrbQJKhxIC&pg=PA14&lpg=PA14&dq=neomorphic+alleles&source=bl&ots=xQigP7G_qg&sig=byRFFLnbFVqtg2brqCuBedrxRHI&hl=en&sa=X&ved=0ahUKEwjti5u6o7HWAhVYGsAKHRM-ClEQ6AEIbzAK#v=onepage&q=neomorphic alleles&f=false.

Herskowitz, Ira. 1987. "Functional Inactivation of Genes by Dominant Negative Mutations." *Nature* 329 (6136):219–22. https://doi.org/10.1038/329219a0.

Hiramatsu, Ryuji, Shogo Matoba, Masami Kanai-Azuma, Naoki Tsunekawa, Yuko Katoh-Fukui, Masamichi Kurohmaru, Ken-ichirou Morohashi, Dagmar Wilhelm, Peter Koopman, and Yoshiakira Kanai. 2008. "A Critical Time Window of Sry Action in Gonadal Sex Determination in Mice." *Development* 136 (1). http://dev.biologists.org/content/136/1/129.long.

Hoffmeyer, Angelika, Roland Piekorz, Richard Moriggl, and James N Ihle. 2001. "Gadd45⁄ Is Dispensable for Normal Mouse Development and T-Cell Proliferation" 21 (9):3137–43. https://doi.org/10.1128/MCB.21.9.3137–3143.2001.

Hu, Yueh-Chiang, Leah M Okumura, and David C Page. 2013. "Gata4 Is Required for Formation of the Genital Ridge in Mice." *PLoS Genet* 9 (7). http://journals.plos.org/plosgenetics/article/file?id=10.1371/journal.pgen.1003629&type=printable.

Huang, B, S Wang, Y Ning, A N Lamb, and J Bartley. 1999. "Autosomal XX Sex Reversal Caused by Duplication of SOX9." *American Journal of Medical Genetics* 87 (4):349–53. http://www.ncbi.nlm.nih.gov/pubmed/10588843.

Hughes, I. A., C. Houk, S. F. Ahmed, and P. A. Lee. 2006. "Consensus Statement on Management of Intersex Disorders." *Journal of Pediatric Urology* 2 (3):148–62. https://doi.org/10.1016/j.jpurol.2006.03.004.

Ikeda, Y, W H Shen, H A Ingraham, and K L Parker. 1994. "Developmental Expression of Mouse Steroidogenic Factor-1, an Essential Regulator of the Steroid Hydroxylases." *Molecular Endocrinology (Baltimore, Md.)* 8 (5):654–62. https://doi.org/10.1210/mend.8.5.8058073.

Ishino, Y, H Shinagawa, K Makino, M Amemura, and A Nakata. 1987. "Nucleotide Sequence of the Iap Gene, Responsible for Alkaline Phosphatase Isozyme Conversion in Escherichia Coli, and Identification of the Gene Product." *Journal of Bacteriology* 169 (12):5429–33. http://www.ncbi.nlm.nih.gov/pubmed/3316184.

Ishitani, Tohru, Satoshi Kishida, Junko Hyodo-Miura, Naoto Ueno, Jun Yasuda, Marian Waterman, Hiroshi Shibuya, Randall T Moon, Jun Ninomiya-Tsuji, and Kunihiro Matsumoto. 2003. "The TAK1-NLK Mitogen-Activated Protein Kinase Cascade Functions in the Wnt-5a/Ca(2+) Pathway to Antagonize Wnt/beta-Catenin Signaling." *Molecular and Cellular Biology* 23 (1):131–39.

http://www.ncbi.nlm.nih.gov/pubmed/12482967.
Jacobs, Patricia., and J. A. Strong. 1959. “A Case of Human Intersexuality Having a Possible XXY Sex-Determining Mechanism.” *Nature* 183 (4657):302–3. https://doi.org/10.1038/183302a0.
Jameson, Samantha A., Anirudh Natarajan, Jonah Cool, Tony DeFalco, Danielle M. Maatouk, Lindsey Mork, Steven C. Munger, and Blanche Capel. 2012. “Temporal Transcriptional Profiling of Somatic and Germ Cells Reveals Biased Lineage Priming of Sexual Fate in the Fetal Mouse Gonad.” Edited by Gregory S. Barsh. *PLoS Genetics* 8 (3). Public Library of Science:e1002575. https://doi.org/10.1371/journal.pgen.1002575.
Jameson, Samantha, Yi-Tzu Lin, and Blanche Capel. 2012. “Testis Development Requires the Repression of Wnt4 by Fgf Signaling.” *Developmental Biology* 370 (1):24–32. https://doi.org/10.1016/j.ydbio.2012.06.009.
Jeays-Ward, Katherine, Mathieu Dandonneau, and Amanda Swain. 2004. “Wnt4 Is Required for Proper Male as Well as Female Sexual Development.” https://doi.org/10.1016/j.ydbio.2004.08.049.
Jenny, Andreas, Jessica Reynolds-Kenneally, Gishnu Das, Micheal Burnett, and Marek Mlodzik. 2005. “Diego and Prickle Regulate Frizzled Planar Cell Polarity Signalling by Competing for Dishevelled Binding.” *Nature Cell Biology* 7 (7):691–97. https://doi.org/10.1038/ncb1271.
Jho, Eek-hoon, Tong Zhang, Claire Domon, Choun-Ki Joo, Jean-Noel Freund, and Frank Costantini. 2002. “Wnt/beta-catenin/Tcf Signaling Induces the Transcription of Axin2, a Negative Regulator of the Signaling Pathway.” *Molecular and Cellular Biology* 22 (4). American Society for Microbiology:1172–83. https://doi.org/10.1128/MCB.22.4.1172.
Jiang, Wenyan, David Bikard, David Cox, Feng Zhang, and Luciano A Marraffini. 2013. “RNA-Guided Editing of Bacterial Genomes Using CRISPR-Cas Systems.” *Nature Biotechnology* 31 (3):233–39. https://doi.org/10.1038/nbt.2508.
Jinek, M., K. Chylinski, I. Fonfara, M. Hauer, J. A. Doudna, and E. Charpentier. 2012. “A Programmable Dual-RNA-Guided DNA Endonuclease in Adaptive Bacterial Immunity.” *Science* 337 (6096):816–21. https://doi.org/10.1126/science.1225829.
Johnen, Heiko, Laura Gonzá lez-Silva, Laura Carramolino, Juana Maria Flores, Miguel Torres, and Jesú M Salvador. 2013. “Gadd45g Is Essential for Primary Sex Determination, Male Fertility and Testis Development.” *PLoS ONE* 8 (3). https://doi.org/10.1371/journal.pone.0058751.
Jones, Steve E., and Catherine Jomary. 2002. “Secreted Frizzled-Related Proteins: Searching for Relationships and Patterns.” *BioEssays* 24 (9):811–20. https://doi.org/10.1002/bies.10136.
Jordan, B. K., J. H.- C. Shen, R. Olaso, H. A. Ingraham, and E. Vilain. 2003. “Wnt4 Overexpression Disrupts Normal Testicular Vasculature and Inhibits Testosterone Synthesis by Repressing Steroidogenic Factor 1/ -Catenin Synergy.” *Proceedings of the National Academy of Sciences* 100 (19):10866–71. https://doi.org/10.1073/pnas.1834480100.
Jordan, Brian K., Mansoor Mohammed, Saunders T. Ching, Emmanuèle Délot, Xiao-Ning Chen, Phoebe Dewing, Amanda Swain, P. Nagesh Rao, B. Rafael Elejalde, and Eric Vilain. 2001. “Up-Regulation of WNT-4 Signaling and Dosage-Sensitive Sex Reversal in Humans.” *The American Journal of Human Genetics* 68 (5):1102–9. https://doi.org/10.1086/320125.
Jordan, Daniel M., Stephan G. Frangakis, Christelle Golzio, Christopher A. Cassa, Joanne

Kurtzberg, Erica E. Davis, Shamil R. Sunyaev, Nicholas Katsanis, and Nicholas Katsanis. 2015. “Identification of Cis-Suppression of Human Disease Mutations by Comparative Genomics.” *Nature* 524 (7564):225–29. https://doi.org/10.1038/nature14497.

Karl, Jeannie, and Blanche Capel. 1998. “Sertoli Cells of the Mouse Testis Originate from the Coelomic Epithelium.” *Developmental Biology* 203 (2):323–33. https://doi.org/10.1006/dbio.1998.9068.

Katoh-Fukui, Yuko, Kanako Miyabayashi, Tomoko Komatsu, Akiko Owaki, Takashi Baba, Yuichi Shima, Tomohide Kidokoro, et al. 2012. “*Cbx2* , a Polycomb Group Gene, Is Required for *Sry* Gene Expression in Mice.” *Endocrinology* 153 (2). Oxford University Press:913–24. https://doi.org/10.1210/en.2011-1055.

Katoh-Fukui, Yuko, Reiko Tsuchiya, Toshihiko Shiroishi, Yoko Nakahara, Naoko Hashimoto, Kousei Noguchi, and Toru Higashinakagawa. 1998. “Male-to-Female Sex Reversal in M33 Mutant Mice.” *Nature* 393 (6686):688–92. https://doi.org/10.1038/31482.

Katoh, M. 2001. “Molecular Cloning and Characterization of Human WNT3.” *International Journal of Oncology* 19 (5):977–82. http://www.ncbi.nlm.nih.gov/pubmed/11604997.

Kawano, Y., and Robert Kypta. 2003. “Secreted Antagonists of the Wnt Signalling Pathway.” *Journal of Cell Science* 116 (13):2627–34. https://doi.org/10.1242/jcs.00623.

Kent, J, S C Wheatley, J E Andrews, A H Sinclair, and P Koopman. 1996. “A Male-Specific Role for SOX9 in Vertebrate Sex Determination.” *Development (Cambridge, England)* 122 (9):2813–22. http://www.ncbi.nlm.nih.gov/pubmed/8787755.

Kerr, Genevieve E., Julia C. Young, Katja Horvay, Helen E. Abud, and Kate L. Loveland. 2014. “Regulated Wnt/Beta-Catenin Signaling Sustains Adult Spermatogenesis in Mice1.” *Biology of Reproduction* 90 (1). Cache River Press, Clearwater, FL:381–86. https://doi.org/10.1095/biolreprod.112.105809.

Kim, Yuna, Akio Kobayashi, Ryohei Sekido, Leo DiNapoli, Jennifer Brennan, Marie-Christine Chaboissier, Francis Poulat, Richard R Behringer, Robin Lovell-Badge, and Blanche Capel. 2006. “Fgf9 and Wnt4 Act as Antagonistic Signals to Regulate Mammalian Sex Determination.” Edited by Hiroshi Hamada. *PLoS Biology* 4 (6). Public Library of Science:e187. https://doi.org/10.1371/journal.pbio.0040187.

Kimelman, D, and W Xu. 2006. “B-Catenin Destruction Complex: Insights and Questions from a Structural Perspective.” *Oncogene* 25:7482–91. https://doi.org/10.1038/sj.onc.1210055.

Kimura, Tohru, Toshinobu Nakamura, Kazushige Murayama, Hiroki Umehara, Noriko Yamano, Shoko Watanabe, Makoto M. Taketo, and Toru Nakano. 2006. “The Stabilization of β-Catenin Leads to Impaired Primordial Germ Cell Development via Aberrant Cell Cycle Progression.” *Developmental Biology* 300 (2):545–53. https://doi.org/10.1016/j.ydbio.2006.06.038.

Klonisch, Thomas, Paul A Fowler, and Sabine Hombach-Klonisch. 2004. “Molecular and Genetic Regulation of Testis Descent and External Genitalia Development.” *Developmental Biology* 270 (1):1–18. https://doi.org/10.1016/j.ydbio.2004.02.018.

Kohn, Aimee D., and Randall T. Moon. 2005. “Wnt and Calcium Signaling: Beta-Catenin-Independent Pathways.” *Cell Calcium* 38 (3–4):439–46. https://doi.org/10.1016/j.ceca.2005.06.022.

Koo, Bon-Kyoung, Maureen Spit, Ingrid Jordens, Teck Y. Low, Daniel E. Stange, Marc van de Wetering, Johan H. van Es, et al. 2012. “Tumour Suppressor RNF43 Is a Stem-Cell E3 Ligase That Induces Endocytosis of Wnt Receptors.” *Nature* 488 (7413):665–69. https://doi.org/10.1038/nature11308.

Koopman, Peter, John Gubbay, Nigel Vivian, Peter Goodfellow, and Robin Lovell-Badge. 1991. “Male Development of Chromosomally Female Mice Transgenic for Sry.” *Nature* 351 (6322). Nature Publishing Group:117–21. https://doi.org/10.1038/351117a0.

Koubova, Jana, Douglas B Menke, Qing Zhou, Blanche Capel, Michael D Griswold, and David C Page. 2006. “Retinoic Acid Regulates Sex-Specific Timing of Meiotic Initiation in Mice.” *Proceedings of the National Academy of Sciences* 103 (8). National Academy of Sciences:2474–79. https://doi.org/10.1073/pnas.0510813103.

Koumenis, Constantinos, Meixia Bi, Jiangbin Ye, Douglas Feldman, and Albert C. Koong. 2007. “Hypoxia and the Unfolded Protein Response.” In *Methods in Enzymology*, 435:275–93. https://doi.org/10.1016/S0076-6879(07)35014-3.

Kreidberg, Jordan A., Hannu Sariola, Janet M. Loring, Masahiro Maeda, Jerry Pelletier, David Housman, and Rudolf Jaenisch. 1993. “WT-1 Is Required for Early Kidney Development.” *Cell* 74 (4):679–91. https://doi.org/10.1016/0092-8674(93)90515-R.

Kumar, Sandeep, Christina Chatzi, Thomas Brade, Thomas J. Cunningham, Xianling Zhao, and Gregg Duester. 2011. “Sex-Specific Timing of Meiotic Initiation Is Regulated by Cyp26b1 Independent of Retinoic Acid Signalling.” *Nature Communications* 2 (1):151. https://doi.org/10.1038/ncomms1136.

Kupsco, Allison, and Daniel Schlenk. 2015. “Oxidative Stress, Unfolded Protein Response, and Apoptosis in Developmental Toxicity.” *International Review of Cell and Molecular Biology* 317. NIH Public Access:1–66. https://doi.org/10.1016/bs.ircmb.2015.02.002.

Laino, Luigi, Silvia Majore, Nicoletta Preziosi, Barbara Grammatico, Carmelilia De Bernardo, Salvatore Scommegna, Anna Maria Rapone, Giacinto Marrocco, Irene Bottillo, and Paola Grammatico. 2014. “Disorders of Sex Development: A Genetic Study of Patients in a Multidisciplinary Clinic.” *Endocrine Connections* 3 (4). Bioscientifica Ltd.:180–92. https://doi.org/10.1530/EC-14-0085.

Laird, Diana J., Svetlana Altshuler-Keylin, Michael D. Kissner, Xin Zhou, and Kathryn V. Anderson. 2011. “Ror2 Enhances Polarity and Directional Migration of Primordial Germ Cells.” Edited by Patrick P. L. Tam. *PLoS Genetics* 7 (12). Cold Spring Harbor Laboratory Press:e1002428. https://doi.org/10.1371/journal.pgen.1002428.

Leung, Janet Y., Frank T. Kolligs, Rong Wu, Yali Zhai, Rork Kuick, Samir Hanash, Kathleen R. Cho, and Eric R. Fearon. 2002. “Activation of AXIN2 Expression by β-Catenin-T Cell Factor.” *Journal of Biological Chemistry* 277 (24):21657–65. https://doi.org/10.1074/jbc.M200139200.

Lewandoski, M. 2001. “Conditional Control of Gene Expression in the Mouse.” *Nature Reviews. Genetics* 2 (10):743–55. https://doi.org/10.1038/35093537.

Leyns, L, T Bouwmeester, S H Kim, S Piccolo, and E M De Robertis. 1997. “Frzb-1 Is a Secreted Antagonist of Wnt Signaling Expressed in the Spemann Organizer.” *Cell* 88 (6):747–56. http://www.ncbi.nlm.nih.gov/pubmed/9118218.

Lieber, Michael R. 2010. “The Mechanism of Double-Strand DNA Break Repair by the Nonhomologous DNA End-Joining Pathway.” *Annual Review of Biochemistry* 79 (1):181–211. https://doi.org/10.1146/annurev.biochem.052308.093131.

Lindeman, Robin E., Micah D. Gearhart, Anna Minkina, Anthony D. Krentz, Vivian J. Bardwell, and David Zarkower. 2015. “Sexual Cell-Fate Reprogramming in the Ovary by DMRT1.” *Current Biology*. Vol. 25. https://doi.org/10.1016/j.cub.2015.01.034.

Liu, Chang, Jia Peng, Martin M Matzuk, & Humphrey, and H-C Yao. 2015. “ARTICLE Lineage Specification of Ovarian Theca Cells Requires Multicellular Interactions via Oocyte and Granulosa Cells.” *Nature Communications*. https://doi.org/10.1038/ncomms7934.

Liu, Chia-Feng, Nathan Bingham, Keith Parker, and Humphrey H-C Yao. 2009. “Sex-Specific Roles of Beta-Catenin in Mouse Gonadal Development.” *Human Molecular Genetics* 18 (3). Oxford University Press:405–17. https://doi.org/10.1093/hmg/ddn362.

Liu, Zehua, Huazhe Lou, Kaikun Xie, Hao Wang, Ning Chen, Oscar M. Aparicio, Michael Q. Zhang, Rui Jiang, and Ting Chen. 2017. “Reconstructing Cell Cycle Pseudo Time-Series via Single-Cell Transcriptome Data.” *Nature Communications* 8 (1). Nature Publishing Group:22. https://doi.org/10.1038/s41467-017-00039-z.

Logan, Catriona Y., and Roel Nusse. 2004. “THE WNT SIGNALING PATHWAY IN DEVELOPMENT AND DISEASE” 20 (1):781–810. https://doi.org/10.1146/annurev.cellbio.20.010403.113126.

Loregger, Anke, Martina Grandl, Raquel Mejías-Luque, Michael Allgäuer, Kathrin Degenhart, Verena Haselmann, Christina Oikonomou, et al. 2015. “The E3 Ligase RNF43 Inhibits Wnt Signaling Downstream of Mutated β-Catenin by Sequestering TCF4 to the Nuclear Membrane.” *Science Signaling* 8 (393):ra90-ra90. https://doi.org/10.1126/scisignal.aac6757.

Ludbrook, Louisa M., Pascal Bernard, Stefan Bagheri-Fam, Janelle Ryan, Ryohei Sekido, Dagmar Wilhelm, Robin Lovell-Badge, and Vincent R. Harley. 2012. “Excess DAX1 Leads to XY Ovotesticular Disorder of Sex Development (DSD) in Mice by Inhibiting Steroidogenic Factor-1 (SF1) Activation of the Testis Enhancer of SRY-Box-9 (Sox9).” *Endocrinology* 153 (4). Cold Spring Harbor Laboratory Press, Cold Spring Harbor, NY:1948–58. https://doi.org/10.1210/en.2011-1428.

Luo, X, Y Ikeda, and K L Parker. 1994. “A Cell-Specific Nuclear Receptor Is Essential for Adrenal and Gonadal Development and Sexual Differentiation.” *Cell* 77 (4):481–90. http://www.ncbi.nlm.nih.gov/pubmed/8187173.

Luo, Xinmei, and Kay Hofmann. 2001. “The Protease-Associated Domain: A Homology Domain Associated with Multiple Classes of Proteases.” *Trends in Biochemical Sciences* 26 (3):147–48. https://doi.org/10.1016/S0968-0004(00)01768-0.

Lyons, Jon P, Ulrich W Mueller, Hong Ji, Christopher Everett, Xiang Fang, Jen-Chih Hsieh, AngelaI.M Barth, and Pierre D McCrea. 2004. “Wnt-4 Activates the Canonical β-Catenin-Mediated Wnt Pathway and Binds Frizzled-6 CRD: Functional Implications of Wnt/β-Catenin Activity in Kidney Epithelial Cells.” *Experimental Cell Research* 298 (2):369–87. https://doi.org/10.1016/j.yexcr.2004.04.036.

Ma, Hanhui, Ardalan Naseri, Pablo Reyes-Gutierrez, Scot A Wolfe, Shaojie Zhang, and Thoru Pederson. 2015. “Multicolor CRISPR Labeling of Chromosomal Loci in Human Cells.” *Proceedings of the National Academy of Sciences of the United States of America* 112 (10). National Academy of Sciences:3002–7. https://doi.org/10.1073/pnas.1420024112.

Maatouk, Danielle M., Lindsey Mork, Ashley Hinson, Akio Kobayashi, Andrew P. McMahon, and Blanche Capel. 2012. “Germ Cells Are Not Required to Establish the Female Pathway in Mouse Fetal Gonads.” Edited by Hugh Clarke. *PLoS ONE* 7 (10). Public Library of Science:e47238. https://doi.org/10.1371/journal.pone.0047238.

Maatouk, Danielle M, Leo Dinapoli, Ashley Alvers, Keith L Parker, Makoto M Taketo, and Blanche Capel. 2008. “Stabilization of β-Catenin in XY Gonads Causes Male-to-Female Sex-Reversal.” *Human Molecular Genetics* 17 (19):2949–55. https://doi.org/10.1093/hmg/ddn193.

Mahon, Piers, and Alex Bateman. 2000. “The PA Domain: A Protease-Associated Domain.” *Protein Science* 9 (10). Cold Spring Harbor Laboratory Press:1930–34.

https://doi.org/10.1110/ps.9.10.1930.
Mandel, Hannah, Revital Shemer, Zvi U Borochowitz, Marina Okopnik, Carlos Knopf, Margarita Indelman, Arie Drugan, et al. 2008. “SERKAL Syndrome: An Autosomal-Recessive Disorder Caused by a Loss-of-Function Mutation in WNT4.” *American Journal of Human Genetics* 82 (1). Elsevier:39–47. https://doi.org/10.1016/j.ajhg.2007.08.005.
Mao, Bingyu, Wei Wu, Gary Davidson, Joachim Marhold, Mingfa Li, Bernard M Mechler, Hajo Delius, et al. 2002. “Kremen Proteins Are Dickkopf Receptors That Regulate Wnt/beta-Catenin Signalling.” *Nature* 417 (6889):664–67. https://doi.org/10.1038/nature756.
Mao, Zhiyong, Michael Bozzella, Andrei Seluanov, and Vera Gorbunova. 2008. “DNA Repair by Nonhomologous End Joining and Homologous Recombination during Cell Cycle in Human Cells.” *Cell Cycle (Georgetown, Tex.)* 7 (18). NIH Public Access:2902–6. https://doi.org/10.4161/cc.7.18.6679.
Matson, Clinton K, Mark W Murphy, Aaron L Sarver, Michael D Griswold, Vivian J Bardwell, and David Zarkower. 2011. “DMRT1 Prevents Female Reprogramming in the Postnatal Mammalian Testis.” https://doi.org/10.1038/nature10239.
McClelland, Kathryn S., Katrina Bell, Christian Larney, Vincent R. Harley, Andrew H. Sinclair, Alicia Oshlack, Peter Koopman, and Josephine Bowles. 2015. “Purification and Transcriptomic Analysis of Mouse Fetal Leydig Cells Reveals Candidate Genes for Specification of Gonadal Steroidogenic Cells1.” *Biology of Reproduction* 92 (6). https://doi.org/10.1095/biolreprod.115.128918.
McElreavey, K, E Vilain, N Abbas, I Herskowitz, and M Fellous. 1993. “A Regulatory Cascade Hypothesis for Mammalian Sex Determination: SRY Represses a Negative Regulator of Male Development.” *Proceedings of the National Academy of Sciences of the United States of America* 90 (8). National Academy of Sciences:3368–72. https://doi.org/10.1073/PNAS.90.8.3368.
McLaren, A., and D. Southee. 1997. “Entry of Mouse Embryonic Germ Cells into Meiosis.” *Developmental Biology* 187 (1):107–13. https://doi.org/10.1006/dbio.1997.8584.
McLaren, Anne. 2000. “Establishment of the Germ Cell Lineage in Mammals.” *Journal of Cellular Physiology* 182 (2). John Wiley & Sons, Inc.:141–43. https://doi.org/10.1002/(SICI)1097-4652(200002)182:2<141::AID-JCP1>3.0.CO;2-I.
McMahon, Andrew P., and Brian A. Parr. 1998. “Sexually Dimorphic Development of the Mammalian Reproductive Tract Requires Wnt-7a.” *Nature* 395 (6703). Nature Publishing Group:707–10. https://doi.org/10.1038/27221.
Menke, Douglas B, and David C Page. 2002. “Sexually Dimorphic Gene Expression in the Developing Mouse Gonad.” *Gene Expression Patterns : GEP* 2 (3–4):359–67. http://www.ncbi.nlm.nih.gov/pubmed/12617826.
Metzger, D, J Clifford, H Chiba, and P Chambon. 1995. “Conditional Site-Specific Recombination in Mammalian Cells Using a Ligand-Dependent Chimeric Cre Recombinase.” *Proc Natl Acad Sci U S A* 92 (15):6991–95. https://doi.org/10.1073/pnas.92.15.6991.
Michalak, Pawel. 2008. “Coexpression, Coregulation, and Cofunctionality of Neighboring Genes in Eukaryotic Genomes.” *Genomics* 91 (3):243–48. https://doi.org/10.1016/j.ygeno.2007.11.002.
Miyamoto, Yoko, Hiroaki Taniguchi, Frédéric Hamel, David W Silversides, and Robert S Viger. 2008. “A GATA4/WT1 Cooperation Regulates Transcription of Genes Required for Mammalian Sex Determination and Differentiation.” *BMC Molecular Biology* 9 (1):44. https://doi.org/10.1186/1471-2199-9-44.

Mojica, F J, C Díez-Villaseñor, E Soria, and G Juez. 2000. “Biological Significance of a Family of Regularly Spaced Repeats in the Genomes of Archaea, Bacteria and Mitochondria.” *Molecular Microbiology* 36 (1):244–46. http://www.ncbi.nlm.nih.gov/pubmed/10760181.

Mullen, Rachel D, and Richard R Behringer. 2014. “Molecular Genetics of Müllerian Duct Formation, Regression and Differentiation.” *Sexual Development : Genetics, Molecular Biology, Evolution, Endocrinology, Embryology, and Pathology of Sex Determination and Differentiation* 8 (5). NIH Public Access:281–96. https://doi.org/10.1159/000364935.

Munger, Steven C., David L. Aylor, Haider Ali Syed, Paul M. Magwene, David W. Threadgill, and Blanche Capel. 2009. “Elucidation of the Transcription Network Governing Mammalian Sex Determination by Exploiting Strain-Specific Susceptibility to Sex Reversal.” *Genes and Development* 23 (21). Cold Spring Harbor Laboratory Press:2521–36. https://doi.org/10.1101/gad.1835809.

Munger, Steven C., Anirudh Natarajan, Loren L. Looger, Uwe Ohler, and Blanche Capel. 2013. “Fine Time Course Expression Analysis Identifies Cascades of Activation and Repression and Maps a Putative Regulator of Mammalian Sex Determination.” Edited by David R. Beier. *PLoS Genetics* 9 (7):e1003630. https://doi.org/10.1371/journal.pgen.1003630.

Nef, Serge, Olivier Schaad, Nancy R. Stallings, Christopher R. Cederroth, Jean-Luc Pitetti, Guillaume Schaer, Safia Malki, et al. 2005. “Gene Expression during Sex Determination Reveals a Robust Female Genetic Program at the Onset of Ovarian Development.” *Developmental Biology* 287 (2):361–77. https://doi.org/10.1016/j.ydbio.2005.09.008.

Nef, Serge, and Jean-Dominique Vassalli. 2009. “Complementary Pathways in Mammalian Female Sex Determination.” *Journal of Biology* 8 (8):74. https://doi.org/10.1186/jbiol173.

Ng, L J, Susan Wheatley, George E.O Muscat, John Conway-Campbell, Jo Bowles, Edwina Wright, Donald M Bell, Patrick P.L Tam, Kathryn S.E Cheah, and Peter Koopman. 1997. “Sox9 Binds DNA, Activates Transcription, and Coexpresses with Type II Collagen during Chondrogenesis in the Mouse.” *Developmental Biology* 183 (1):108–21. https://doi.org/10.1006/dbio.1996.8487.

Niida, Atsushi, Takatoshi Hiroko, Mana Kasai, Yoichi Furukawa, Yusuke Nakamura, Yutaka Suzuki, Sumio Sugano, and Tetsu Akiyama. 2004. “DKK1, a Negative Regulator of Wnt Signaling, Is a Target of the Beta-catenin/TCF Pathway.” *Oncogene* 23 (52):8520–26. https://doi.org/10.1038/sj.onc.1207892.

Ohinata, Yasuhide, Hiroshi Ohta, Mayo Shigeta, Kaori Yamanaka, Teruhiko Wakayama, and Mitinori Saitou. 2009. “A Signaling Principle for the Specification of the Germ Cell Lineage in Mice.” *Cell* 137 (3):571–84. https://doi.org/10.1016/j.cell.2009.03.014.

Oishi, Isao, Hiroaki Suzuki, Nobuyuki Onishi, Ritsuko Takada, Shuichi Kani, Bisei Ohkawara, Ikue Koshida, et al. 2003. “The Receptor Tyrosine Kinase Ror2 Is Involved in Non-Canonical Wnt5a/JNK Signalling Pathway.” *Genes to Cells : Devoted to Molecular & Cellular Mechanisms* 8 (7):645–54. http://www.ncbi.nlm.nih.gov/pubmed/12839624.

Okamura, Y., Y. Aoki, T. Obayashi, S. Tadaka, S. Ito, T. Narise, and K. Kinoshita. 2015. “COXPRESdb in 2015: Coexpression Database for Animal Species by DNA-Microarray and RNAseq-Based Expression Data with Multiple Quality Assessment Systems.” *Nucleic Acids Research* 43 (D1):D82–86. https://doi.org/10.1093/nar/gku1163.

Orban, P C, D Chui, and J D Marth. 1992. “Tissue- and Site-Specific DNA Recombination in

Transgenic Mice." *Proceedings of the National Academy of Sciences of the United States of America* 89 (15). National Academy of Sciences:6861–65. https://doi.org/10.1073/pnas.89.15.6861.

Ostrer, Harry. 2014. "Disorders of Sex Development (DSDs): An Update." *The Journal of Clinical Endocrinology & Metabolism* 99 (5). Oxford University Press:1503–9. https://doi.org/10.1210/jc.2013-3690.

Ottolenghi, C., Shakib Omari, J Elias Garcia-Ortiz, Manuela Uda, Laura Crisponi, Antonino Forabosco, Giuseppe Pilia, and David Schlessinger. 2005. "Foxl2 Is Required for Commitment to Ovary Differentiation." *Human Molecular Genetics* 14 (14):2053–62. https://doi.org/10.1093/hmg/ddi210.

Palmer, S J, and P S Burgoyne. 1991. "In Situ Analysis of Fetal, Prepuberal and Adult XX----XY Chimaeric Mouse Testes: Sertoli Cells Are Predominantly, but Not Exclusively, XY." *Development (Cambridge, England)* 112 (1):265–68. http://www.ncbi.nlm.nih.gov/pubmed/1769333.

Pannetier, M., Stéphane Fabre, Frank Batista, Ayhan Kocer, Lauriane Renault, Geneviève Jolivet, Béatrice Mandon-Pépin, Corinne Cotinot, Reiner Veitia, and Eric Pailhoux. 2006. "FOXL2 Activates P450 Aromatase Gene Transcription: Towards a Better Characterization of the Early Steps of Mammalian Ovarian Development." *Journal of Molecular Endocrinology* 36 (3):399–413. https://doi.org/10.1677/jme.1.01947.

Parma, Pietro, Orietta Radi, Valerie Vidal, Marie Christine Chaboissier, Elena Dellambra, Stella Valentini, Liliana Guerra, Andreas Schedl, and Giovanna Camerino. 2006. "R-spondin1 Is Essential in Sex Determination, Skin Differentiation and Malignancy." *Nature Genetics* 38 (11). Nature Publishing Group:1304–9. https://doi.org/10.1038/ng1907.

Pearlman, Alexander, Johnny Loke, Cedric Le Caignec, Stefan White, Lisa Chin, Andrew Friedman, Nicholas Warr, et al. 2010. "Mutations in MAP3K1 Cause 46,XY Disorders of Sex Development and Implicate a Common Signal Transduction Pathway in Human Testis Determination." *The American Journal of Human Genetics* 87 (6):898–904. https://doi.org/10.1016/j.ajhg.2010.11.003.

Peng, Weng Chuan, Wim De Lau, Pramod K Madoori, Federico Forneris, Joke C M Granneman, Hans Clevers, and Piet Gros. 2013. "Structures of Wnt-Antagonist ZNRF3 and Its Complex with R-Spondin 1 and Implications for Signaling." https://doi.org/10.1371/journal.pone.0083110.

Peters, Hannah. 1970. "Migration of Gonocytes Into the Mammalian Gonad and Their Differentiation." *Philosophical Transactions of the Royal Society of London B: Biological Sciences* 259 (828). http://rstb.royalsocietypublishing.org/content/259/828/91.long.

Pourcel, C, G Salvignol, and G Vergnaud. 2005. "CRISPR Elements in Yersinia Pestis Acquire New Repeats by Preferential Uptake of Bacteriophage DNA, and Provide Additional Tools for Evolutionary Studies." *Microbiology* 151 (3):653–63. https://doi.org/10.1099/mic.0.27437-0.

Rahmoun, Massilva, Rowena Lavery, Sabine Laurent-Chaballier, Nicolas Bellora, Gayle K. Philip, Moïra Rossitto, Aleisha Symon, et al. 2017. "In Mammalian Foetal Testes, SOX9 Regulates Expression of Its Target Genes by Binding to Genomic Regions with Conserved Signatures." *Nucleic Acids Research* 16 (May):119–34. https://doi.org/10.1093/nar/gkx328.

Rao, Rammohan V, and Dale E Bredesen. 2004. "Misfolded Proteins, Endoplasmic Reticulum Stress and Neurodegeneration." *Current Opinion in Cell Biology* 16 (6). NIH Public

Access:653–62. https://doi.org/10.1016/j.ceb.2004.09.012.
Raymond, Christopher S, Mark W Murphy, M Gerard O'Sullivan, Vivian J Bardwell, and David Zarkower. 2000. "Dmrt1, a Gene Related to Worm and Fly Sexual Regulators, Is Required for Mammalian Testis Differentiation." *Genes and Development* 14 (20). Cold Spring Harbor Laboratory Press:2587–95. https://doi.org/10.1101/gad.834100.
Reid, John E., and Lorenz Wernisch. 2016. "Pseudotime Estimation: Deconfounding Single Cell Time Series." *Bioinformatics* 32 (19). Oxford University Press:2973–80. https://doi.org/10.1093/bioinformatics/btw372.
Rivas, Bryan, Zaohua Huang, and Alexander I. Agoulnik. 2014. "Normal Fertility in Male Mice with Deletion of β-Catenin Gene in Germ Cells." *Genesis* 52 (4):328–32. https://doi.org/10.1002/dvg.22742.
Roosen-Runge, Edward C., and Doris Anderson. 1959. "The Development of the Interstitial Cells in the Testis of the Albino Rat." *Cells Tissues Organs* 37 (1–2):125–37. https://doi.org/10.1159/000141460.
Rosenthal, Nadia, and Steve Brown. 2007. "The Mouse Ascending: Perspectives for Human-Disease Models." *Nature Cell Biology* 9 (9):993–99. https://doi.org/10.1038/ncb437.
Rosner, Mitchell H., M. Alessandra Vigano, Keiko Ozato, Paula M. Timmons, Francoise Poirie, Peter W. J. Rigby, and Louis M. Staudt. 1990. "A POU-Domain Transcription Factor in Early Stem Cells and Germ Cells of the Mammalian Embryo." *Nature* 345 (6277). Nature Publishing Group:686–92. https://doi.org/10.1038/345686a0.
Ruzankina, Yaroslava, Carolina Pinzon-Guzman, Amma Asare, Tony Ong, Laura Pontano, George Cotsarelis, Valerie P. Zediak, Marielena Velez, Avinash Bhandoola, and Eric J. Brown. 2007. "Deletion of the Developmentally Essential Gene ATR in Adult Mice Leads to Age-Related Phenotypes and Stem Cell Loss." *Cell Stem Cell* 1 (1):113–26. https://doi.org/10.1016/j.stem.2007.03.002.
Sauer, B. 1987. "Functional Expression of the Cre-Lox Site-Specific Recombination System in the Yeast Saccharomyces Cerevisiae." *Molecular and Cellular Biology* 7 (6). American Society for Microbiology (ASM):2087–96. https://doi.org/10.1128/MCB.7.6.2087.Updated.
Sauer, B, and N Henderson. 1988. "Site-Specific DNA Recombination in Mammalian Cells by the Cre Recombinase of Bacteriophage P1." *Proceedings of the National Academy of Sciences of the United States of America* 85 (14). National Academy of Sciences:5166–70. http://www.ncbi.nlm.nih.gov/pubmed/2839833.
Schambony, Alexandra, and Doris Wedlich. 2007. "Wnt-5A/Ror2 Regulate Expression of XPAPC through an Alternative Noncanonical Signaling Pathway." *Developmental Cell* 12 (5):779–92. https://doi.org/10.1016/j.devcel.2007.02.016.
Schepers, Goslik, Megan Wilson, Dagmar Wilhelm, and Peter Koopman. 2003. "SOX8 Is Expressed during Testis Differentiation in Mice and Synergizes with SF1 to Activate the Amh Promoter in Vitro." *The Journal of Biological Chemistry* 278 (30). American Society for Biochemistry and Molecular Biology:28101–8. https://doi.org/10.1074/jbc.M304067200.
Schlessinger, Karni, Alan Hall, and Nicholas Tolwinski. 2009. "Wnt Signaling Pathways Meet Rho GTPases." *Genes & Development* 23 (3). Cold Spring Harbor Laboratory Press:265–77. https://doi.org/10.1101/gad.1760809.
Schmahl, J., E M Eicher, L L Washburn, and B. Capel. 2000. "Sry Induces Cell Proliferation in the Mouse Gonad." *Development (Cambridge, England)* 127 (1):65–73. http://dev.biologists.org/content/127/1/65.

Schmahl, Jennifer, and Blanche Capel. 2003. “Cell Proliferation Is Necessary for the Determination of Male Fate in the Gonad.” *Developmental Biology* 258 (2):264–76. https://doi.org/10.1016/S0012-1606(03)00122-2.

Schmidt, Dirk, Catherine E. Ovitt, Katrin Anlag, Sandra Fehsenfeld, Lars Gredsted, Anna-Corina Treier, and Mathias Treier. 2004. “The Murine Winged-Helix Transcription Factor Foxl2 Is Required for Granulosa Cell Differentiation and Ovary Maintenance.” *Development* 131 (4). http://dev.biologists.org/content/131/4/933.long.

Schöler, H R, G R Dressler, R Balling, H Rohdewohld, and P Gruss. 1990. “Oct-4: A Germline-Specific Transcription Factor Mapping to the Mouse T-Complex.” *The EMBO Journal* 9 (7):2185–95. http://www.ncbi.nlm.nih.gov/pubmed/2357966.

Sekido, Ryohei, and Robin Lovell-Badge. 2008. “Sex Determination Involves Synergistic Action of SRY and SF1 on a Specific Sox9 Enhancer.” *Nature* 453 (7197):930–34. https://doi.org/10.1038/nature06944.

Shackleford, G M, and H E Varmus. 1987. “Expression of the Proto-Oncogene Int-1 Is Restricted to Postmeiotic Male Germ Cells and the Neural Tube of Mid-Gestational Embryos.” *Cell* 50 (1):89–95. http://www.ncbi.nlm.nih.gov/pubmed/3594566.

Shalem, Ophir, Neville E. Sanjana, Ella Hartenian, Xi Shi, David A. Scott, Tarjei S. Mikkelsen, Dirk Heckl, et al. 2014. “Genome-Scale CRISPR-Cas9 Knockout Screening in Human Cells.” *Science* 343 (6166):84–87. https://doi.org/10.1126/science.1247005.

Sheldahl, Laird C., Diane C. Slusarski, Petra Pandur, Jeffrey R. Miller, Michael Kühl, and Randall T. Moon. 2003. “Dishevelled Activates Ca $^{2+}$ Flux, PKC, and CamKII in Vertebrate Embryos.” *The Journal of Cell Biology* 161 (4):769–77. https://doi.org/10.1083/jcb.200211094.

Shimizu, H, M A Julius, M Giarré, Z Zheng, A M Brown, and J Kitajewski. 1997. “Transformation by Wnt Family Proteins Correlates with Regulation of Beta-Catenin.” *Cell Growth & Differentiation : The Molecular Biology Journal of the American Association for Cancer Research* 8 (12):1349–58. http://www.ncbi.nlm.nih.gov/pubmed/9419423.

Siggers, Pam, Gwenn-Aël Carré, Debora Bogani, Nick Warr, Sara Wells, Helen Hilton, Chris Esapa, Mohammad K. Hajihosseini, and Andy Greenfield. 2014. “A Novel Mouse Fgfr2 Mutant, Hobbyhorse (Hob), Exhibits Complete XY Gonadal Sex Reversal.” Edited by Andrew Wolfe. *PLoS ONE* 9 (6). Public Library of Science:e100447. https://doi.org/10.1371/journal.pone.0100447.

Silva, Sara Morais da, Adam Hacker, Vince Harley, Peter Goodfellow, Amanda Swain, and Robin Lovell-Badge. 1996. “Sox9 Expression during Gonadal Development Implies a Conserved Role for the Gene in Testis Differentiation in Mammals and Birds.” *Nature Genetics* 14 (1):62–68. https://doi.org/10.1038/ng0996-62.

Sinclair, Andrew H., Philippe Berta, Mark S. Palmer, J. Ross Hawkins, Beatrice L. Griffiths, Matthijs J. Smith, Jamie W. Foster, Anna-Maria Frischauf, Robin Lovell-Badge, and Peter N. Goodfellow. 1990. “A Gene from the Human Sex-Determining Region Encodes a Protein with Homology to a Conserved DNA-Binding Motif.” *Nature* 346 (6281). Nature Publishing Group:240–44. https://doi.org/10.1038/346240a0.

Slater, Guy, Ewan Birney, Wolfgang Huber, B Bolstad, M Dettling, S Dudoit, B Ellis, et al. 2005. “In Situ Analysis of Cross-Hybridisation on Microarrays and the Inference of Expression Correlation.” *BMC Bioinformatics* 6 (1). BioMed Central:31. https://doi.org/10.1186/1471-2105-6-31.

Song, Fei, and Knut Stieger. 2017. “Optimizing the DNA Donor Template for Homology-

Directed Repair of Double-Strand Breaks." *Molecular Therapy. Nucleic Acids* 7 (June). American Society of Gene & Cell Therapy:53–60. https://doi.org/10.1016/j.omtn.2017.02.006.

Stevant, Isabelle, Yasmine Neirijnck, Christelle Borel, Jessica Escoffier, Lee B Smith, Stylianos E Antonarakis, Emmanouil T Dermitzakis, and Serge Nef. 2017. "Deciphering Cell Lineage Specification during Male Sex Determination with Single-Cell RNA Sequencing." *Doi.org*, September. Cold Spring Harbor Laboratory, 190264. https://doi.org/10.1101/190264.

Sugimura, Ryohichi, and Linheng Li. 2010. "Noncanonical Wnt Signaling in Vertebrate Development, Stem Cells, and Diseases." *Birth Defects Research Part C: Embryo Today: Reviews* 90 (4). Wiley Subscription Services, Inc., A Wiley Company:243–56. https://doi.org/10.1002/bdrc.20195.

Sung, Young Hoon, Jong Min Kim, Hyun Taek Kim, Jaehoon Lee, Jisun Jeon, Young Jin, Jung Hwa Choi, et al. 2014. "Highly Efficient Gene Knockout in Mice and Zebrafish with RNA-Guided Endonucleases." *Genome Research* 24 (1). Cold Spring Harbor Laboratory Press:125–31. https://doi.org/10.1101/gr.163394.113.

Svingen, Terje, and Peter Koopman. 2013. "Building the Mammalian Testis: Origins, Differentiation, and Assembly of the Component Cell Populations." https://doi.org/10.1101/gad.228080.113.

Swain, A, and R Lovell-Badge. 1999. "Mammalian Sex Determination: A Molecular Drama." *Genes & Development* 13 (7):755–67. http://www.ncbi.nlm.nih.gov/pubmed/10197976.

Swain, Amanda, Veronica Narvaez, Paul Burgoyne, Giovanna Camerino, and Robin Lovell-Badge. 1998. "Dax1 Antagonizes Sry Action in Mammalian Sex Determination." *Nature* 391 (6669). Nature Publishing Group:761–67. https://doi.org/10.1038/35799.

Takase, Hinako M, and Roeland Nusse. 2016. "Paracrine Wnt/β-Catenin Signaling Mediates Proliferation of Undifferentiated Spermatogonia in the Adult Mouse Testis." *Proceedings of the National Academy of Sciences of the United States of America* 113 (11). National Academy of Sciences:E1489-97. https://doi.org/10.1073/pnas.1601461113.

Tam, P. P. L. 1981. "The Control of Somitogenesis in Mouse Embryos." *Development* 65 (Supplement). http://dev.biologists.org/content/65/Supplement/103.short.

Tamai, Keiko, Xin Zeng, Chunming Liu, Xinjun Zhang, Yuko Harada, Zhijie Chang, and Xi He. 2004. "A Mechanism for Wnt Coreceptor Activation." *Molecular Cell* 13 (1):149–56. http://www.ncbi.nlm.nih.gov/pubmed/14731402.

Tanigawa, Shunsuke, Honghe Wang, Yili Yang, Nirmala Sharma, Nadya Tarasova, Rieko Ajima, Terry P. Yamaguchi, Luis G. Rodriguez, and Alan O. Perantoni. 2011. "Wnt4 Induces Nephronic Tubules in Metanephric Mesenchyme by a Non-Canonical Mechanism." *Developmental Biology* 352 (1):58–69. https://doi.org/10.1016/j.ydbio.2011.01.012.

Thyen, Ute, Kathrin Lanz, Paul-Martin Holterhus, and Olaf Hiort. 2006. "Epidemiology and Initial Management of Ambiguous Genitalia at Birth in Germany." *Hormone Research in Paediatrics* 66 (4):195–203. https://doi.org/10.1159/000094782.

Topol, Lilia, Wen Chen, Hai Song, Timothy F. Day, and Yingzi Yang. 2009a. "Sox9 Inhibits Wnt Signaling by Promoting β-Catenin Phosphorylation in the Nucleus." *Journal of Biological Chemistry* 284 (5):3323–33. https://doi.org/10.1074/jbc.M808048200.

Topol, Lilia, Wen Chen, Hai Song, Timothy F Day, and Yingzi Yang. 2009b. "Sox9 Inhibits Wnt

Signaling by Promoting Beta-Catenin Phosphorylation in the Nucleus." *The Journal of Biological Chemistry* 284 (5). American Society for Biochemistry and Molecular Biology:3323–33. https://doi.org/10.1074/jbc.M808048200.

Tsai, Huai-Kuang, Pei-Ying Huang, Cheng-Yan Kao, and Daryi Wang. 2009. "Co-Expression of Neighboring Genes in the Zebrafish (Danio Rerio) Genome." *International Journal of Molecular Sciences* 10 (8). Multidisciplinary Digital Publishing Institute (MDPI):3658–70. https://doi.org/10.3390/ijms10083658.

Tsai, Yien Che, and Allan M Weissman. 2010. "The Unfolded Protein Response, Degradation from Endoplasmic Reticulum and Cancer." *Genes & Cancer* 1 (7). Impact Journals, LLC:764–78. https://doi.org/10.1177/1947601910383011.

Uhlenhaut, N Henriette, Susanne Jakob, Katrin Anlag, Tobias Eisenberger, Ryohei Sekido, Jana Kress, Anna Corina Treier, et al. 2009. "Somatic Sex Reprogramming of Adult Ovaries to Testes by FOXL2 Ablation." *Cell* 139 (6):1130–42. https://doi.org/10.1016/j.cell.2009.11.021.

Unger, Sheila, Gerd Scherer, and Andrea Superti-Furga. 1993. *Campomelic Dysplasia*. *GeneReviews(®)*. University of Washington, Seattle. http://www.ncbi.nlm.nih.gov/pubmed/20301724.

Vainio, Seppo, Minna Heikkila, Andreas Kispert, Norman Chin, and Andrew P McMahon. 1999. "Female Development in Mammals Is Regulated by Wnt-4 Signalling" 397 (February). Nature Publishing Group:405–9. https://doi.org/10.1038/17068.

Vergnaud, G, D C Page, M C Simmler, L Brown, F Rouyer, B Noel, D Botstein, A de la Chapelle, and J Weissenbach. 1986. "A Deletion Map of the Human Y Chromosome Based on DNA Hybridization." *American Journal of Human Genetics* 38 (2). Elsevier:109–24. http://www.ncbi.nlm.nih.gov/pubmed/3004206.

Vidal, Valerie P.I., Marie-Christine Chaboissier, Dirk G. de Rooij, and Andreas Schedl. 2001. "Sox9 Induces Testis Development in XX Transgenic Mice." *Nature Genetics* 28 (3):216–17. https://doi.org/10.1038/90046.

Wakayama, Tomohiko, Koichi Hamada, Miyuki Yamamoto, Toshio Suda, and Shoichi Iseki. 2003. "The Expression of Platelet Endothelial Cell Adhesion Molecule-1 in Mouse Primordial Germ Cells during Their Migration and Early Gonadal Formation." *Histochemistry and Cell Biology* 119 (5):355–62. https://doi.org/10.1007/s00418-003-0528-1.

Walck-Shannon, Elise, and Jeff Hardin. 2013. "Cell Intercalation from Top to Bottom." *Nature Reviews Molecular Cell Biology* 15 (1):34–48. https://doi.org/10.1038/nrm3723.

Wang, Haoyi, Hui Yang, Chikdu S. Shivalila, Meelad M. Dawlaty, Albert W. Cheng, Feng Zhang, and Rudolf Jaenisch. 2013. "One-Step Generation of Mice Carrying Mutations in Multiple Genes by CRISPR/cas-Mediated Genome Engineering." *Cell* 153 (4):910–18. https://doi.org/10.1016/j.cell.2013.04.025.

Wang, Kai, Siu Tsan Yuen, Jiangchun Xu, Siu Po Lee, Helen H N Yan, Stephanie T Shi, Hoi Cheong Siu, et al. 2014. "Whole-Genome Sequencing and Comprehensive Molecular Profiling Identify New Driver Mutations in Gastric Cancer." *Nature Genetics* 46 (6):573–82. https://doi.org/10.1038/ng.2983.

Wang, S, M Krinks, K Lin, F P Luyten, and M Moos. 1997. "Frzb, a Secreted Protein Expressed in the Spemann Organizer, Binds and Inhibits Wnt-8." *Cell* 88 (6):757–66. http://www.ncbi.nlm.nih.gov/pubmed/9118219.

Wang, Xiao Na, Ze Song Li, Yu Ren, Tao Jiang, Ya Qing Wang, Min Chen, Jun Zhang, et al.

2013. “The Wilms Tumor Gene, Wt1, Is Critical for Mouse Spermatogenesis via Regulation of Sertoli Cell Polarity and Is Associated with Non-Obstructive Azoospermia in Humans.” Edited by Nicholas Hastie. *PLoS Genetics* 9 (8). Public Library of Science:e1003645. https://doi.org/10.1371/journal.pgen.1003645.

Warr, Nick, Debora Bogani, Pam Siggers, Rachel Brixey, Hilda Tateossian, Asha Dopplapudi, Sara Wells, et al. 2011. “Minor Abnormalities of Testis Development in Mice Lacking the Gene Encoding the MAPK Signalling Component, MAP3K1.” *PloS One* 6 (5). Public Library of Science:e19572. https://doi.org/10.1371/journal.pone.0019572.

Warr, Nick, Gwenn-Aël Carre, Pam Siggers, Jessica Vitos Faleato, Rachel Brixey, Madeleine Pope, Debora Bogani, et al. 2012. “Gadd45γ and Map3k4 Interactions Regulate Mouse Testis Determination via p38 MAPK-Mediated Control of Sry Expression.” *Developmental Cell* 23 (5). Elsevier:1020–31. https://doi.org/10.1016/j.devcel.2012.09.016.

Warr, Nick, Pam Siggers, Debora Bogani, Rachel Brixey, Laura Pastorelli, Laura Yates, Charlotte H Dean, et al. 2008. “Sfrp1 and Sfrp2 Are Required for Normal Male Sexual Development in Mice.” *Developmental Biology* 326:273–84. https://doi.org/10.1016/j.ydbio.2008.11.023.

Washburn, Linda L, and Eva M Eicher. 1989. “Normal Testis Determination in the Mouse Depends on Genetic Interaction of a Locus on Chromosome 17 and the Y Chromosome.” *Genetics* 123 (1):173–79. https://www.ncbi.nlm.nih.gov/pmc/articles/PMC1203780/pdf/ge1231173.pdf.

Wei, Qiou, Chika Yokota, Mikhail V Semenov, Brad Doble, Jim Woodgett, and Xi He. 2007. “R-spondin1 Is a High Affinity Ligand for LRP6 and Induces LRP6 Phosphorylation and Beta-Catenin Signaling.” *The Journal of Biological Chemistry* 282 (21). American Society for Biochemistry and Molecular Biology:15903–11. https://doi.org/10.1074/jbc.M701927200.

Wen, Qing, C.Yan Cheng, and Yi-Xun Liu. 2016. “Development, Function and Fate of Fetal Leydig Cells.” *Seminars in Cell & Developmental Biology* 59 (November):89–98. https://doi.org/10.1016/j.semcdb.2016.03.003.

Westphal, Heiner, Ohad S. Birk, Delane E. Casiano, Christopher A. Wassif, Tiziana Cogliati, Liping Zhao, Yangu Zhao, et al. 2000. “The LIM Homeobox Gene Lhx9 Is Essential for Mouse Gonad Formation.” *Nature* 403 (6772). Nature Publishing Group:909–13. https://doi.org/10.1038/35002622.

Wieacker, P, D Missbach, S Jakubiczka, S Borgmann, and N Albers. 1996. “Sex Reversal in a Child with the Karyotype 46,XY, Dup (1) (p22.3p32.3).” *Clinical Genetics* 49 (5):271–73. http://www.ncbi.nlm.nih.gov/pubmed/8832137.

Wilhelm, D., and Christoph Englert. 2002. “The Wilms Tumor Suppressor WT1 Regulates Early Gonad Development by Activation of Sf1.” *Genes & Development* 16 (14):1839–51. https://doi.org/10.1101/gad.220102.

Witkiewicz, Agnieszka K., Elizabeth A. McMillan, Uthra Balaji, GuemHee Baek, Wan-Chi Lin, John Mansour, Mehri Mollaee, et al. 2015. “Whole-Exome Sequencing of Pancreatic Cancer Defines Genetic Diversity and Therapeutic Targets.” *Nature Communications* 6 (April):6744. https://doi.org/10.1038/ncomms7744.

Wong, L L, and P N Adler. 1993. “Tissue Polarity Genes of Drosophila Regulate the Subcellular Location for Prehair Initiation in Pupal Wing Cells.” *The Journal of Cell Biology* 123 (1):209–21. http://www.ncbi.nlm.nih.gov/pubmed/8408199.

Wong, Michael D., Jun Dazai, Johnathon R. Walls, Nicholas W. Gale, and R. Mark Henkelman.

2013. “Design and Implementation of a Custom Built Optical Projection Tomography System.” Edited by James P. Brody. *PLoS ONE* 8 (9). Public Library of Science:e73491. https://doi.org/10.1371/journal.pone.0073491.

Xie, Yang, Raffaella Zamponi, Olga Charlat, Melissa Ramones, Susanne Swalley, Xiaomo Jiang, Daniel Rivera, et al. 2013. “Interaction with Both ZNRF3 and LGR4 Is Required for the Signalling Activity of R-Spondin.” *EMBO Reports* 14. https://doi.org/10.1038/embor.2013.167.

Yang, Yaping, Donna M. Muzny, Jeffrey G. Reid, Matthew N. Bainbridge, Alecia Willis, Patricia A. Ward, Alicia Braxton, et al. 2013. “Clinical Whole-Exome Sequencing for the Diagnosis of Mendelian Disorders.” *New England Journal of Medicine* 369 (16):1502–11. https://doi.org/10.1056/NEJMoa1306555.

Yao, Humphrey H C, Martin M Matzuk, Carolina J Jorgez, Douglas B Menke, David C Page, Amanda Swain, and Blanche Capel. 2004. “Follistatin Operates Downstream of Wnt4 in Mammalian Ovary Organogenesis.” *Developmental Dynamics : An Official Publication of the American Association of Anatomists* 230 (2). NIH Public Access:210–15. https://doi.org/10.1002/dvdy.20042.

Yao, Humphrey Hung-Chang, Wendy Whoriskey, and Blanche Capel. 2002. “Desert Hedgehog/Patched 1 Signaling Specifies Fetal Leydig Cell Fate in Testis Organogenesis.” *Genes & Development* 16 (11). Cold Spring Harbor Laboratory Press:1433–40. https://doi.org/10.1101/gad.981202.

Yen, Shuo-Ting, Min Zhang, Jian Min Deng, Shireen J. Usman, Chad N. Smith, Jan Parker-Thornburg, Paul G. Swinton, James F. Martin, and Richard R. Behringer. 2014. “Somatic Mosaicism and Allele Complexity Induced by CRISPR/Cas9 RNA Injections in Mouse Zygotes.” *Developmental Biology* 393 (1):3–9. https://doi.org/10.1016/j.ydbio.2014.06.017.

Zanaria, Elena, Françoise Muscatelli, Barbara Bardoni, Tim M. Strom, Silvana Guioli, Weiwen Guo, Enzo Lalli, et al. 1994. “An Unusual Member of the Nuclear Hormone Receptor Superfamily Responsible for X-Linked Adrenal Hypoplasia Congenita.” *Nature* 372 (6507). Nature Publishing Group:635–41. https://doi.org/10.1038/372635a0.

Zebisch, Matthias, and E. Yvonne Jones. 2015. “Crystal Structure of R-Spondin 2 in Complex with the Ectodomains of Its Receptors LGR5 and ZNRF3.” *Journal of Structural Biology* 191 (2):149–55. https://doi.org/10.1016/j.jsb.2015.05.008.

Zeng, Yi A., and Esther M Verheyen. 2004. “Nemo Is an Inducible Antagonist of Wingless Signaling during Drosophila Wing Development.” *Development (Cambridge, England)* 131 (12):2911–20. https://doi.org/10.1242/dev.01177.

Zhang, Xiao-Hui, Louis Y Tee, Xiao-Gang Wang, Qun-Shan Huang, and Shi-Hua Yang. 2015. “Off-Target Effects in CRISPR/Cas9-Mediated Genome Engineering.” *Molecular Therapy - Nucleic Acids* 4 (January). Cell Press:e264. https://doi.org/10.1038/mtna.2015.37.

Zhang, Yong, Christa Riesterer, Anne Marie Ayrall, Fred Sablitzky, Trevor D Littlewood, and Michael Reth. 1996. “Inducible Site-Directed Recombination in Mouse Embryonic Stem Cells.” *Nucleic Acids Research* 24 (4):543–48. https://doi.org/10.1093/nar/24.4.543.

Zhao, Fei, Heather L. Franco, Karina F. Rodriguez, Paula R. Brown, Ming-Jer Tsai, Sophia Y. Tsai, and Humphrey H.-C. Yao. 2017. “Elimination of the Male Reproductive Tract in the Female Embryo Is Promoted by COUP-TFII in Mice.” *Science* 357 (6352). http://science.sciencemag.org/content/357/6352/717/tab-pdf.

Zhao, L., T. Svingen, E. T. Ng, and P. Koopman. 2015. “Female-to-Male Sex Reversal in Mice

Caused by Transgenic Overexpression of Dmrt1." *Development* 142 (6):1083–88. https://doi.org/10.1242/dev.122184.

Zhao, Q, H Eberspaecher, V Lefebvre, and B De Crombrugghe. 1997. "Parallel Expression of Sox9 and Col2a1 in Cells Undergoing Chondrogenesis." *Developmental Dynamics : An Official Publication of the American Association of Anatomists* 209 (4):377–86. https://doi.org/10.1002/(SICI)1097-0177(199708)209:4<377::AID-AJA5>3.0.CO;2-F.

Zhao, Shanrong, Wai-Ping Fung-Leung, Anton Bittner, Karen Ngo, Xuejun Liu, Fung-Leung W-p, and Authors Shanrong Zhao. 2014. "Comparison of RNA-Seq and Microarray in Transcriptome Profiling of Activated T Cells." https://doi.org/10.1371/journal.pone.0078644.

Appendix

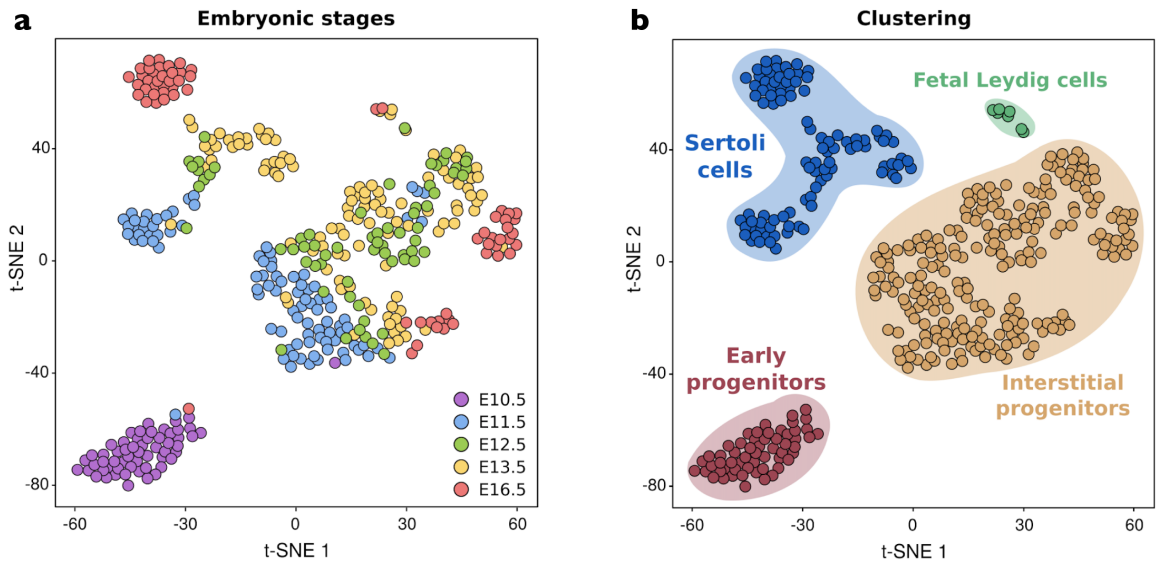

Figure S1. Cell lineage map of Single Cell Transcriptomic data. Figure provided by Isabel Stevant and Serge Nef (Pers. Comms.). Each circle on the plots represents an individual sequenced cell. **(a)** shows the predicted age in embryonic days (E) of each cell. **(b)** shows the cell type of each cell as determined by their transcriptomic profiles.

Age (dpc) XY vs. XX	P=	
11.5	0.2181	ns
12.5	0.1699	ns
13.5	0.6202	ns

Table S1. List of P-values: *Znrf3* expression. (With reference to **Fig 3.4b**: qRT-PCR was performed on B6 11.5 dpc (17-18ts), 12.5 dpc (27-28ts) and 13.5 dpc sub-dissected gonads.)

Transcript	Weight (kDa)	Detected by	
		peptide #1	peptide #2
001 WT	99	Y	Y
001 Del	36	Y	Y
002 WT	88	Y	Y
002 Del	25	Y	Y
003 WT *not affected by deletion	26	Y	N

Table S2. Predicted weights of mutant and wild-type ZNRF3. Table shows predicted molecular weights in kilodaltons (kDa) of transcript 1 (001), transcript 2 (002) and transcript (003) ZNRF3, for both the wild-type (WT) and mutant (Del) proteins. Table also shows whether antibodies raised again peptide 1, or against peptide 2, can recognise the protein product. An antibody raised against peptide 1 can detect all mutant and wild-type isoforms. An antibody raised against peptide 2 can detect all mutant and wild-type isoforms, except for transcript 3 (003). Transcript 3 does not contain the deleted exon, and therefore is not altered in the mutant.

Gene	Age ()	Sex	P-value (*Gadd45g*$^{-/-}$ vs *Gadd45g*$^{+/+}$)	
Znrf3-all	11.5	XX	0.4405	ns
	11.5	XY	0.6811	ns
	12.5	XX	0.5996	ns
	12.5	XY	0.0074	**
Gadd45g	11.5	XX	0.0836	ns
	11.5	XY	0.0019	**
	12.5	XX	0.0036	**
	12.5	XY	0.0114	*
Znrf3 transcript 1	11.5	XX	0.3870	ns
	11.5	XY	0.1918	ns
	12.5	XX	0.7650	ns
	12.5	XY	0.3937	ns
Znrf3 transcript 2	11.5	XX	0.3207	ns
	11.5	XY	0.3298	ns
	12.5	XX	0.7518	ns
	12.5	XY	0.7030	ns
Znrf3 transcript 3	11.5	XX	0.1640	ns
	11.5	XY	0.4292	ns
	12.5	XX	0.3971	ns
	12.5	XY	0.5486	ns

Table S3. List of P-values: *Gadd45g* null tissue. (With reference to **Fig 3.6**: qRT-PCR was performed on wildtype and *Gadd45*$^{-/-}$ subdissected gonads at 11.5 and 12.5 dpc.)

```
ZNRF3   1    MRPRSGGRPGAPGRRRRRLRRGPRGRRLPPPPPLPLLL-----------GLLLAAAGPGA  49
             M   SGG                   +L      P LL           G +LAAA
RNF43   1    M---SGGH-----------------QLQLAVLWPWLLMATLHAGFGHTGRVLAAAVESE  39

ZNRF3   50   ARAKETAFVEVVLFESSPSGDYTTHTTGLTGRFSRAGAMLSAEGEIVQMHPLGLCNNNDE  109
               A++ A + V+  +  P+G        L G F+    +  AEG+++Q HPL LCN +D+
RNF43   40   RSAEQKAVIRVIPLKMDPTGKLNLT---LEGVFAGVAEVTPAEGKLMQSHPLYLCNASDD  96

ZNRF3   110  EDLYEYGWVGVVKLEQPELDPKPCLTVLGKAKRAVQRGATAVIFDVSENPEAIDQLNQGS  169
             ++L E G++ +VKLE P   P+PCL++  KA+ A +RGA AV+FD++E+  A +QL Q
RNF43   97   DNL-EPGFISIVKLESPRRAPRPCLSLASKARMAGERGANAVLFDITEDRSAAEQLQQPL  155

ZNRF3   170  EDPLKRPVVYVKGADAIKLMNIVNKQKVARARIQHLPPRQPTEYFDMGIFLAFFVVVSLV  229
               L +PVV + G+DA KLM  V K + A   I+   P     Y D+ I L     V ++
RNF43   156  G--LTKPVVLIWGSDAAKLMEFVYKNRKAYVWIELKEPPAGANY-DVWILLTVVGTVFVI  212

ZNRF3   230  CLILLVKIKLKQRRSQ-NSMNRLAVQALEKMETRKFNSKSKGRREGSCGALDTLSS-GST  287
              L  +++I+ +   S+ + + +   +A+ ++ TR++ +   G R       D+ SS  ST
RNF43   213  ILASVLRIRCRPHHSRPDPLQQRTARAISQLATRRYQA---GCRRARAEWPDSGSSCSST  269

ZNRF3   288  SDCAICLEKYIDGEELRVIPCTHRFHRKCVDPWLLQHHTCPHCRHNIIEQKGNPGAVCVE  347
               CAICLE++ +G+ELRVI C H FHR CVDPWL QH TCP C  NI+E      A
RNF43   270  PVCAICLEEFSEGQELRVISCLHEFHRTCVDPWLYQHRTCPLCMFNIVEGDSFSQAPAAS  329

ZNRF3   348  TSNLTRGRQPRVTLPVHYPGRVHR--TNAIPAYPTRTSMDSHGNPVTLLTMDRH--GEQN  403
              S    GR  R+ L   +PG  H    +A    P+RTS+     P   L       G ++
RNF43   330  PSYQEPGR--RLHLIRQHPGHAHYHLPSAYLLGPSRTSVARTPRPRPFLPSQEPSMGSRH  387

ZNRF3   404  LYSPQTPTYVRGYPPLHLDHTLAPHRCSLEHRAYSPAHPFRRPKFSSRSFSKAACFSQYE  463
               P+T             H  AP     +H A SP HP+ +        ++  C SQ+
RNF43   388  QRLPRT------------SHLRAPEE--QQHLAVSP-HPYAQ----GWGLNRLRCTSQH-  427

ZNRF3   464  TMYQHYYFQGLSYPEQEGQTIPSVTPRGQSRAFPPSGASSLLFPTMVHVAPPTHVESGST  523
                                P+  P    RA P                   H  SGS
RNF43   428  ----------------------PAACPVALRRARP-------------------HESSGSG  447

ZNRF3   524  SSFSCYHGHRSVCSGYLADCPGSDSSSNSSGQCRCSSSDSVVDCTEVSNQGVYGSCSTFR  583
              S+          SGYLAD P SDSSS   G C  SSSDSVV+CT+VS QG++GS STFR
RNF43   448  ESYCTER------SGYLADGPASDSSS---GPCHGSSSDSVVNCTDVSLQGIHGSSSTFR  498

ZNRF3   584  SSLSSDYDPFIYRSRGPAVHLEGSPPPEELPAGHSQSAGRGEPWLGPASPSGDQLSTCSL  643
             SSLSSD+DP +Y S               P G  Q  G     + P+  S  +
RNF43   499  SSLSSDFDPLVYCS----------------PEGDLQGKG-----IQPSVTSRPR------  531
```

```
ZNRF3   644  EMNYSSNSSLEPRGPNSSTSEVGLEVSPGAALDLRRTWKGGPEGPSCACCFEPQPFPPGS  703
                  S  S+ PRG    +S +            +  W G   GP       PQ  P  S
RNF43   532  -----SLDSVVPRGETQVSSHIHYHRHRHHHYKRQFQWHGRKPGPETGI---PQSMPAAS  583

ZNRF3   704  G--IETSAGGSSLFLGPRLLEDCNPPSGEPQLGSSQGLYGLHSDHYPR-TDGVKYEGLPC  760
               +E S     L + P        P+ +     ++   GL     P  +      GL
RNF43   584  HTQLEPSLPDQQL-ITPNPTASSMLPNPQRPRALTEPAPGLAEASSPSPSPKPNPSGLLN  642

ZNRF3   761  CFYEEKQVAHSAGRGNGCYTEDYSVSVQYTLTEEPPPSCYAGPRDLSQRIPIIPEDVDCD  820
                     V H   +  G  +E    S+   LT     +C   P   S R+
RNF43   643  LQKSSLTVRHPHRKRRGGPSEPLPTSLPPDLTVHT--ACPVFPH-YSPRLAY--------  691

ZNRF3   821  LGLPQDCHGMHNHSPWGGALSLDVPRLHWSLGTTREEEQAPCYQAE---------VQP--  869
               P + H +    P       D   LH        E   PCY +           QP
RNF43   692  -PWPPEVHPLMFRPP-----GPDRRLLH--------EVPGPCYSSSQPVWLYLNPCQPLG  737

ZNRF3   870  GCSPEEAGASRASLSSAPQDTQESHALAAEASGPGSGPGIGT----GA  913
              C P E  +     S   +    SH     A  PGS   +
RNF43   738  PCLPGEGHSKWTFDSPEGRRCPYSHCQVLPAQ-PGSEEELEELCEQAV  78
```

NW Score	Identities
580	271/948(29%)

Figure S2. Needleman-Wunsch alignment of mouse ZNRF3 and RNF43. Using NCBI National Library of Medicine Basic Local Alignment Search Tool (BLAST). Mouse ZNRF3 ("ZNRF3") and mouse RNF43 ("RNF43") amino acid sequence is shown. Conserved amino acids are shown as letters (green). Similar amino acids are shown as a "+" (green) **(a).** The Needleman-Wunsch (NW) score and % identity are shown **(b)**.

	XX	XY
Znrf3$^{+/+}$	164	180
Znrf3$^{+/-}$	316	330
Znrf3$^{-/-}$	122	157

Table S4. Total numbers of *Znrf3*$^{-/-}$, *Znrf3*$^{+/-}$ and *Znrf3*$^{+/+}$ embryos. Embryos between 11.5 and 16.5 dpc were included. A comparison is made between the number of XX and XY embryos.

Comparison	P= (Anogenital Distance)		P= (testis weights)	
XX *Znrf3*$^{+/+}$ vs XY^{AKR} *Znrf3*$^{+/+}$	<0.0001	****	-	-
XX *Znrf3*$^{+/+}$ vs XY^{AKR} *Znrf3*$^{+/-}$	0.0651	ns	-	-
XY^{AKR} *Znrf3*$^{+/+}$ vs XY^{AKR} *Znrf3*$^{+/-}$	0.0031	**	0.0004	***

Table S5. List of P-values: Adult *Znrf3*$^{+/-}$ B6.Y^{AKR} anogenital distance and testis weights. (With reference to **Fig 4.6c, d**: Anogenital distances **(c)** and testis weights **(d)** were measured.)

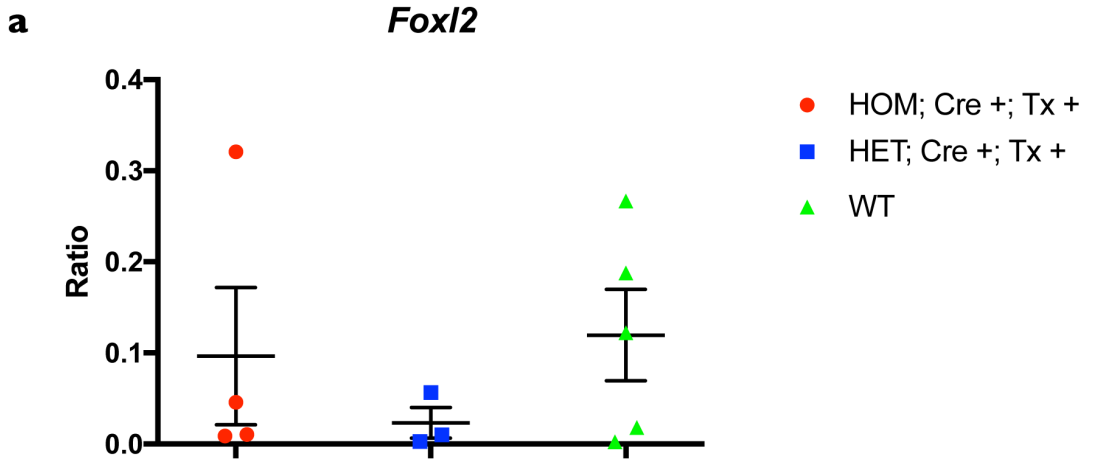

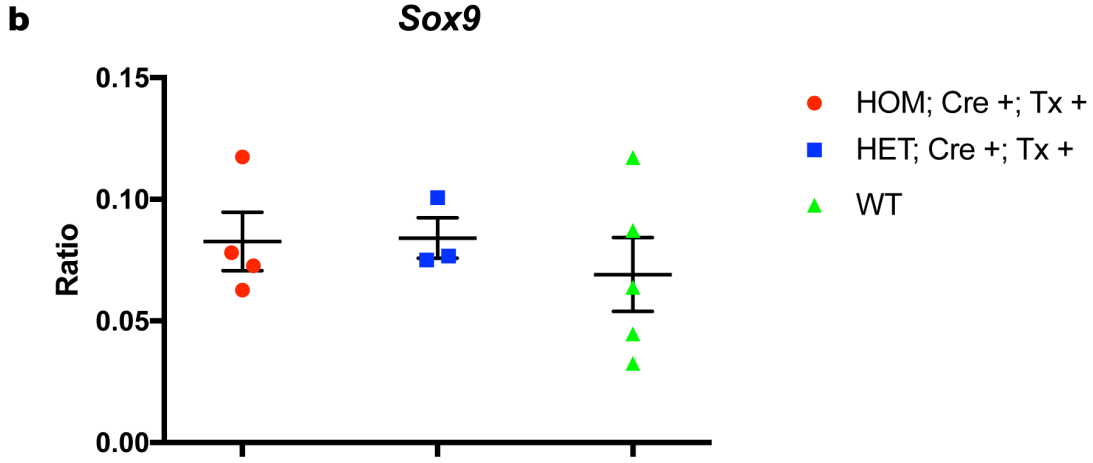

c

	WT vs. Hom Cre+ Tx+		Hom Cre+ Tx+ vs. Het Cre+ Tx+		Het Cre+ Tx+ vs. WT	
Sox9	0.5045	ns	0.9276	ns	0.4199	ns
Foxl2	0.808	ns	0.4067	ns	0.1304	ns

Figure S3. *Sox9* and *Foxl2* expression in adult *Znrf3*$^{flox/flox}$, *Ubiq-ERT2-Cre* mice. qRT-PCR was performed on adult testes (20 weeks) (n=2-6, each genotype) using primers specific for *Foxl2* **(a)** and for *Sox9* **(b)**. Genotypes tested: XY *Znrf3*$^{+/+}$, carrying or not carrying ERT2-Ubiq-Cre, and not treated with tamoxifen (WT); *Znrf3*$^{+/flox}$ carrying ERT2-Ubiq-Cre, treated with tamoxifen (HET, Cre +; Tx +); and *Znrf3*$^{flox/flox}$ carrying ERT2-Ubiq-Cre, treated with tamoxifen (HOM, Cre +; Tx +). Relative expression was calculated relative to *Hprt1* (ratio). Error bars show SEM. T-tests (two-tailed) were performed with Welch's correction. Significant results are signified by * = P<0.05, ** = P<0.01, *** = P<0.001. Non-significant differences are signified by NS. Exact P values are shown in table **(c).**

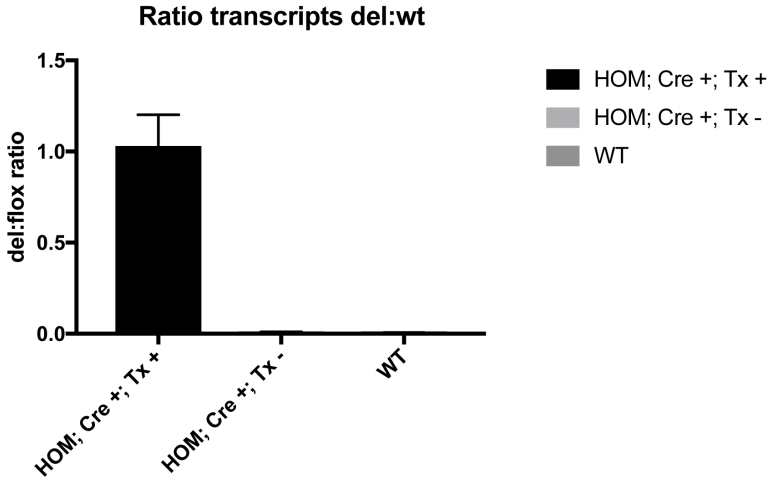

Figure S4. Ratio of *Znrf3*^{flox} and *Znrf3*^{del} alleles in tamoxifen treated adult *Znrf3*$^{flox/flox}$, *Ubiq-ERT2-Cre* mice. qRT-PCR was performed on adult testes (20 weeks) (n=2-6, each genotype. Genotypes tested: XY *Znrf3*$^{+/+}$, carrying or not carrying ERT2-Ubiq-Cre, and not treated with tamoxifen (WT); *Znrf3*$^{flox/flox}$ carrying ERT2-Ubiq-Cre, not treated with tamoxifen (HOM, Cre +; Tx -); and *Znrf3*$^{flox/flox}$ carrying ERT2-Ubiq-Cre, treated with tamoxifen (HOM, Cre +; Tx +).

Primer assay	Comparison		P =	
Znrf3-del allele	HOM; Cre +; Tx +	WT	0.0035	**
	HOM; Cre +; Tx +	HOM; Cre +; Tx -	0.0029	**
	WT	HOM; Cre +; Tx -	0.7190	ns
Znrf3-WT/flox allele	HOM; Cre +; Tx +	WT	0.0004	***
	HOM; Cre +; Tx +	HOM; Cre +; Tx -	0.0471	*
	WT	HOM; Cre +; Tx -	0.0223	*

Table S6. List of P-values: Adult *Znrf3*$^{flox/flox}$, *Ubiq-ERT2-Cre* mice. (With reference to **Fig 4.13a, b:** qRT-PCR was performed on adult testes (20 weeks) (n=2-6, each genotype) using primers specific for the recombined allele (*Znrf3*-del) **(a)** and for the wildtype or flox allele (*Znrf3*-WT/flox) **(b)**.)

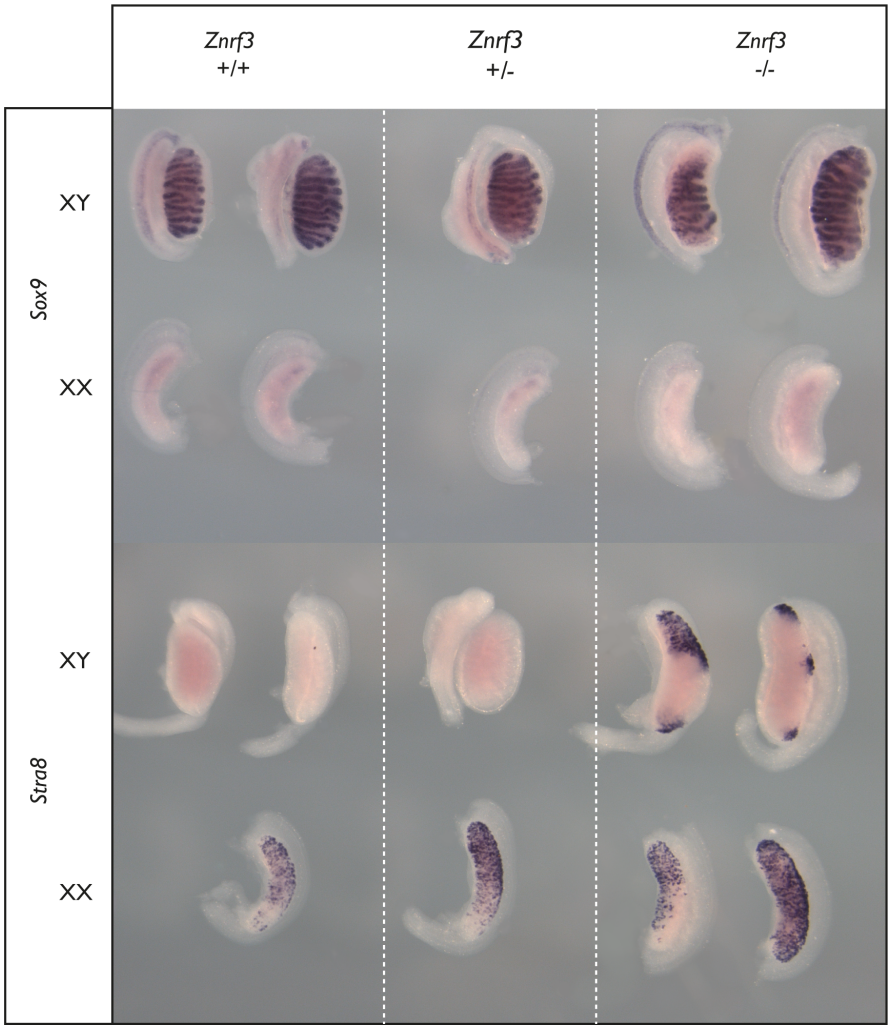

Figure S5. Sex reversal phenotype in XY *Znrf3*$^{-/-}$ gonads (early backcross). WMISH was carried out on 14.5 dpc gonads. The top row shows expression of *Sox9* and the bottom row shows expression of *Stra8*.

	Age (dpc)	XX WT vs XY WT		XX WT vs XY Hom		XY WT vs XY Hom	
Axin2	11.5	0.3671	ns	0.0663	ns	0.0116	*
"	12.5	<0.0001	****	<0.0001	****	0.0002	***
Znrf3	11.5	0.6532	ns	0.0085	**	0.0077	**
"	12.5	0.479	ns	0.0019	**	0.0776	ns
Lef1	11.5	0.0078	**	0.3691	ns	0.023	*
"	12.5	0.0005	***	0.0014	**	0.0062	**
Sox9	11.5	0.0027	**	0.1624	ns	0.0085	**
"	12.5	0.009	**	0.002	**	0.0326	*
Wnt4	11.5	0.1742	ns	0.8374	ns	0.0425	*
"	12.5	0.003	**	0.0036	**	0.0057	**
Rspo1	11.5	0.2549	ns	0.4509	ns	0.8913	ns
"	12.5	0.003	**	0.0031	**	0.0143	*
Sf1	11.5	0.7852	ns	0.6884	ns	0.6106	ns
"	12.5	0.0941	ns	0.2457	ns	0.1733	ns
Oct4	11.5	0.7206	ns	0.2028	ns	0.0034	**
"	12.5	0.1986	ns	0.2831	ns	0.3207	ns
Wt1	11.5	0.0088	**	0.032	*	0.2298	ns
"	12.5	0.0422	*	0.5428	ns	0.0518	ns
Foxl2	12.5	0.0045	**	0.0018	**	0.0055	**
Sry	11.5	0.005	**	0.0065	**	0.3514	ns
Fgf9 (17ts)	11.5	0.4194	ns	0.4634	ns	0.794	ns
Sox9 (17ts)	11.5	0.0264	*	0.0374	*	0.1363	ns

Table S7. List of P-values: 11.5 dpc and 12.5 dpc XY and XX *Znrf3*$^{+/+}$, and XY *Znrf3*$^{-/-}$ gonads. (With reference to **Fig. 5.1b; 5.2b, c; Fig. 5.3b, c, e, f; 5.4a, a'; Fig. 5.5 a, a', b; Fig. 5.7a-c, a'-c'; Fig. 5.8a, a'; Fig. 5.6**). List of P-values and corresponding star symbols for two-tailed T-tests with Welch's correction, comparing qRT-PCR quantified gene expression in XX *Znrf3*$^{+/+}$ (XX WT), XY *Znrf3*$^{+/+}$ (XY WT) and XY *Znrf3*$^{-/-}$ (XY Hom) gonads. Results for 11.5 dpc gonads (white) and 12.5 gonads (blue) are shown. Results from a separate experiment (corresponding to results in **Fig 5.6.**) are shown in green.

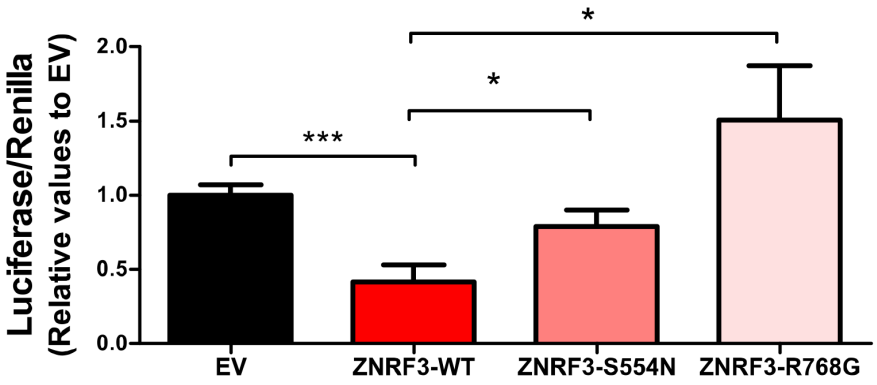

Figure S6. Super Top-flash (STF) assay in HEK293T cells. Figure and the following figure legend were provided by S. Corrochano (Pers. Comms.). The effect of overexpressing ZNRF3 and the different mutant forms on Wnt/β-catenin signalling was tested in STF-luciferase reporter assay in the absence or presence of Wnt3a in HEK293T cell line. The Overexpression of ZNRF3-WT inhibits STF-luciferase activity, specially observed upon Wnt3a treatment. This inhibitory effect is significantly compromised, although not totally supressed, when overexpressing the mutant forms of ZNRF3-S554N and ZNRF3-R768G. EV= empty vector. Data are expressed as mean ± s.e.m (n=5 independent experiments; each experimental assay was done in triplicates). Welch's test comparison between ZNRF3-WT and all the other groups.* = *P*< 0.05; *** = *P*< 0.001. ns= non-significant.

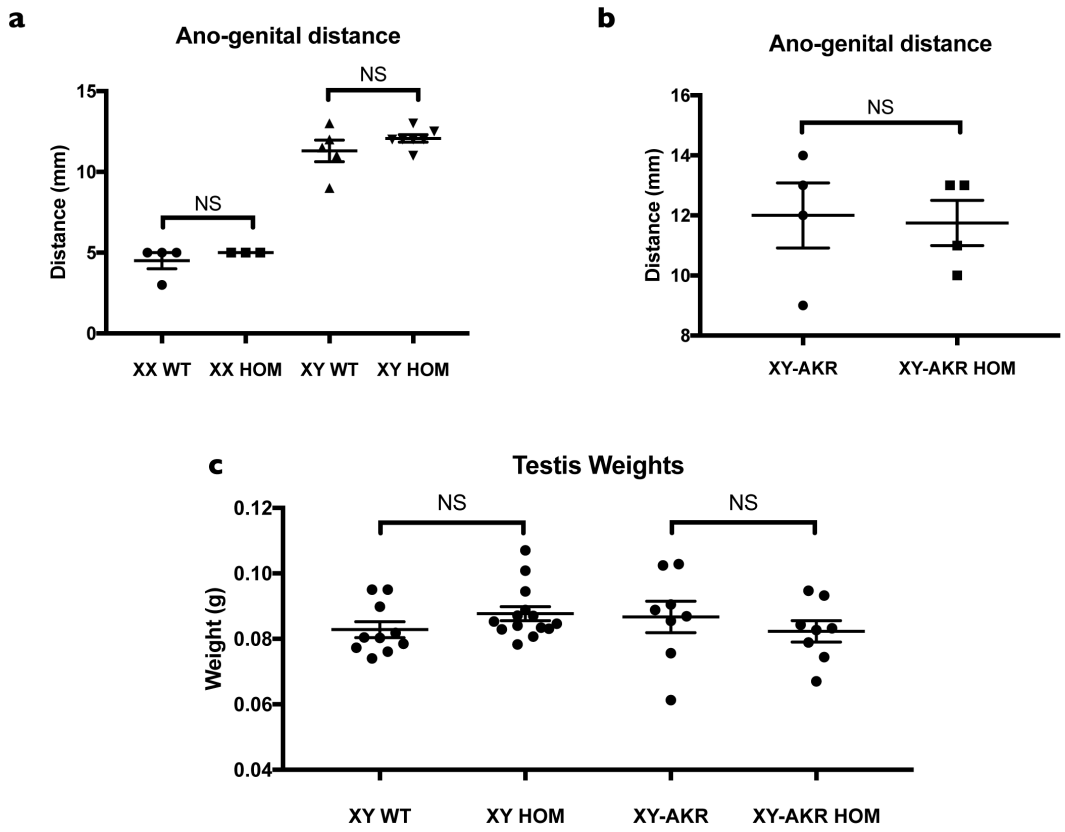

Figure S7. Anogenital distances and testis weights of *Znrf3*$^{R749G/R749G}$ B6 and B6.Y^{AKR} mice. Anogenital distances (mm) of XX *Znrf3*$^{+/+}$ (XX WT), XX *Znrf3*$^{R749G/R749G}$ (XX HOM), XY *Znrf3*$^{+/+}$ (XY WT), and XY *Znrf3*$^{R749G/R749G}$ (XY HOM) adults **(a)**. Anogenital distances (mm) of XY^{AKR} *Znrf3*$^{+/+}$ (XY-AKR), and XY^{AKR} *Znrf3*$^{R749G/R749G}$ (XY-AKR HOM) adults **(b)**. Testis weights (g) of XY *Znrf3*$^{+/+}$ (XY WT), XY *Znrf3*$^{R749G/R749G}$ (XY HOM), XY^{AKR} *Znrf3*$^{+/+}$ (XY-AKR), and XY^{AKR} *Znrf3*$^{R749G/R749G}$ (XY-AKR HOM) adult testes **(c)**.

Comparison		P= (AG distance)		P= (testis weight)	
XX WT	XY WT	<0.0001	****	-	-
XY WT	XY HOM	0.3221	ns	0.1478	ns
XY-AKR	XY-AKR HOM	0.8562	ns	0.4595	ns
XX WT	XX HOM	0.3910	ns	-	-

Table S8. List of P-values: Anogenital distances and testis weights of *Znrf3*$^{R749G/R749G}$ B6 and B6.Y^{AKR} mice. (With reference to **Fig. S7**).

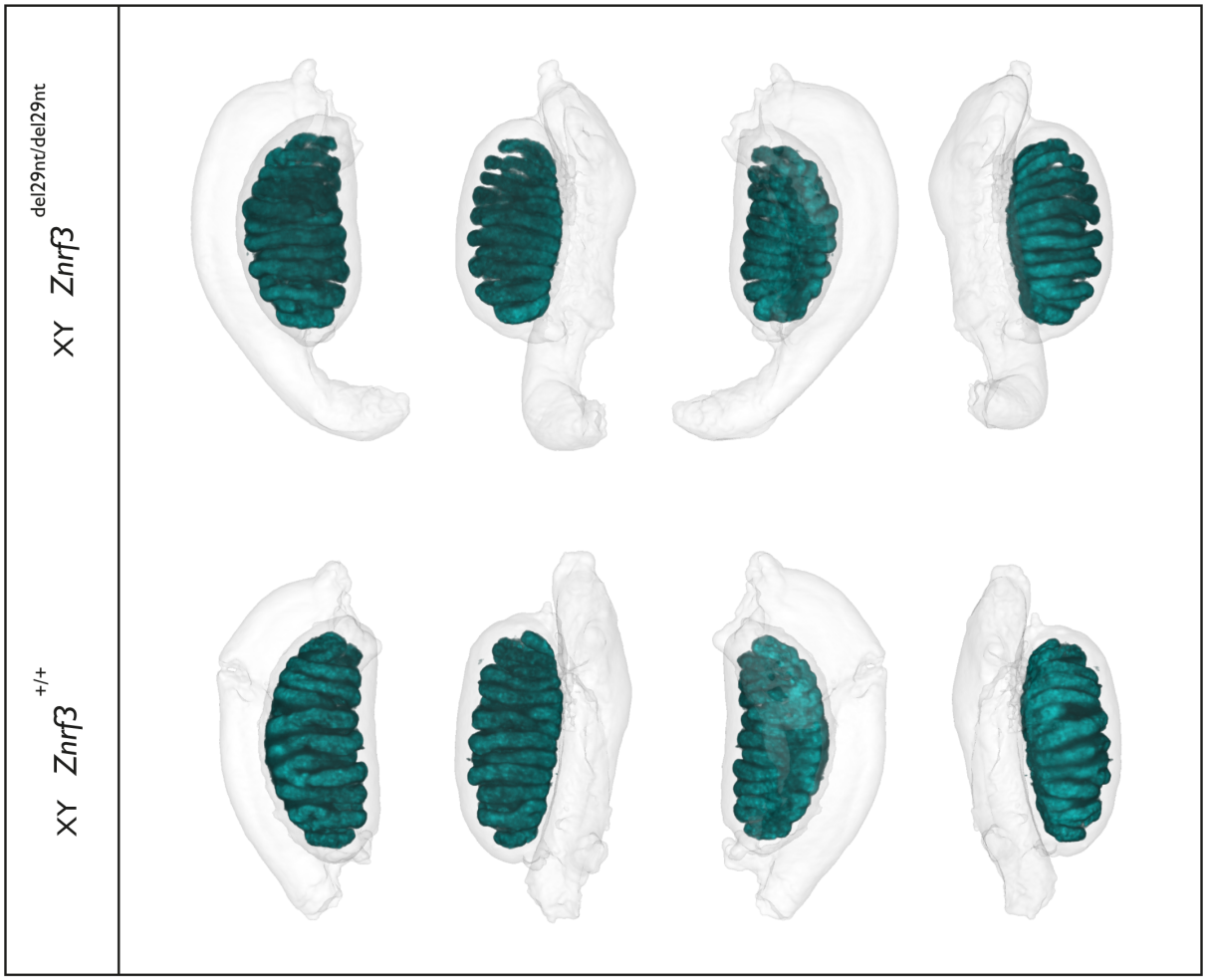

Figure S8. Alternative views of OPT visualisation of WMISH gonads showing *Sox9* expression. 14.5 dpc XY wild-type and *Znrf3*$^{del29nt/del29nt}$ gonads. Images of 3D scans rotated 90° for each view. (With reference to **Figure 6.5** Optical Project Tomography (OPT) scans of *Sox9* expression)

Wild-type (*Znrf3*$^{+/+}$) movie:
https://www.dropbox.com/s/1iesvafsd6p6ft0/2SMALLreslisox9_crispr29nt_WT_1_movie_-2.gif?dl=0
Homozygote (*Znrf3*$^{del29nt/del29nt}$) movie:
https://www.dropbox.com/s/zormzdu2p1bcum0/2SMALLsox9_crispr29nt_HOM_1_movie_-2.gif?dl=0

Please download the file, if required drag file into the search bar of a web-browser to view the animated movie. Alternatively, view in image J and use arrow keys to move between images in the stack.

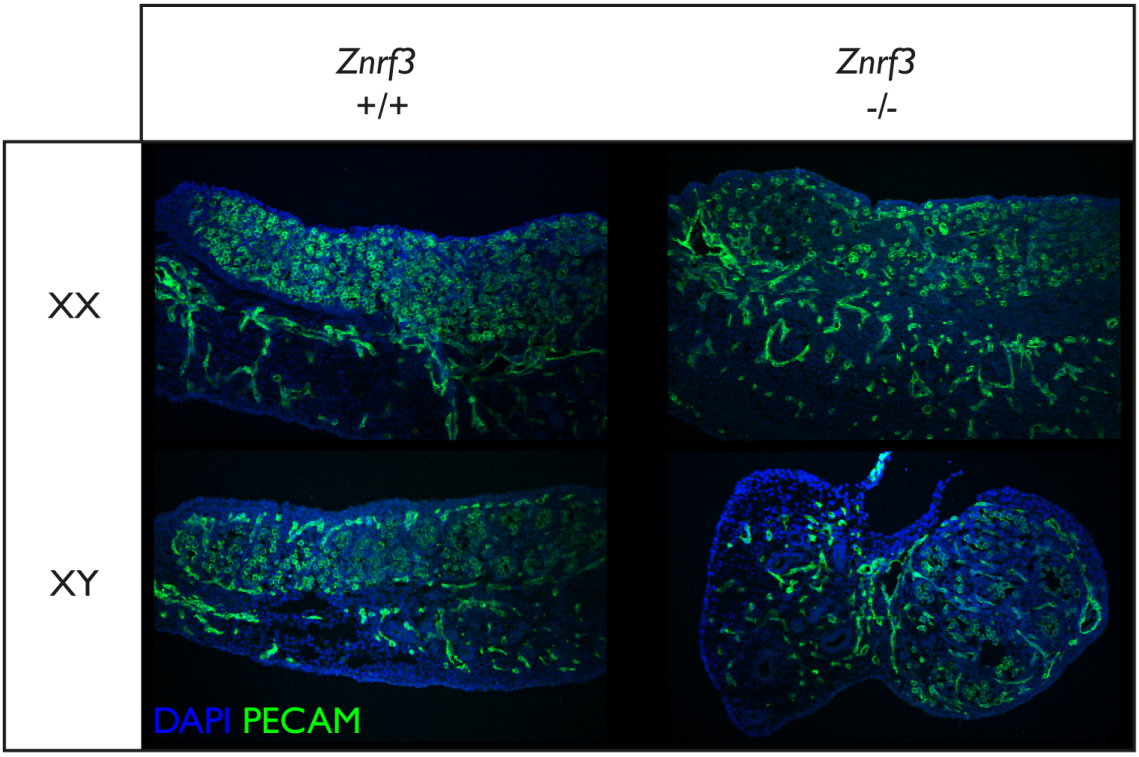

Figure S9. Immunohistochemical analysis of expression of PECAM. Frozen sections of 13.5 dpc XX and XY, wild-type (*Znrf3*$^{+/+}$) and *Znrf3*$^{-/-}$ B6 gonads were analysed for PECAM (green) expression. DAPI (blue) highlights nuclei. (n=1 for each sex and genotype).

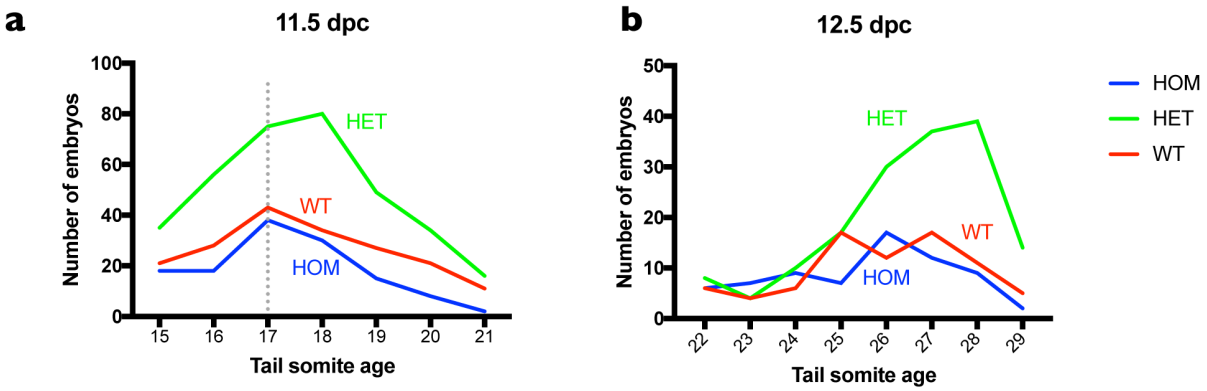

Figure S10. Total number of each age in tail somites (ts). Counts of 11.5 dpc **(a)** and 12.5 dpc **(b)** embryos of each genotype: *Znrf3*$^{+/+}$ (WT), *Znrf3*$^{+/-}$ (HET) and *Znrf3*$^{-/-}$ (HOM). Dotted grey line shows peak at 11.5 dpc. No clear peak can be identified at 12.5 dpc for wild-types.